

Supplementary Information

Au(III)-Aryl Intermediates in Oxidant-Free C-N and C-O Cross-Coupling Catalysis

Jordi Serra,^a Teodor Parella,^b Xavi Ribas^{a,*}

^a QBIS Group, Institut de Química Computacional i Catàlisi (IQCC) and Departament de Química, Universitat de Girona, Campus Montilivi, Girona, E-17071, Catalonia, Spain.

^b Servei de RMN, Facultat de Ciències, Universitat Autònoma de Barcelona, Campus UAB, Bellaterra E08193, Catalonia, Spain.

Email: xavi.ribas@udg.edu

CONTENTS

1. Materials and Methods	S2
1.1. Materials, methods and instrumentation.....	S2
1.2. Synthesis of substrates and catalysts	S2
1.3. Synthesis of gold(III) complexes 3a and 3b	S3
1.4. General procedure for the coupling of <i>p</i> -chlorophenolate and sodium alkoxides to substrates 1a-Br and 2a-Br	S4
1.5. General procedure for the C-N bond formation with aryl iodides 1a-I and 2a-I	S6
1.6. Reactivity of 1a-I and AuI in the presence of bases and <i>p</i> -chlorophenolate.....	S10
2. Supplementary Figures	S12
3. X-Ray Crystallography Data	S113
4. References	S117

1. Materials and methods

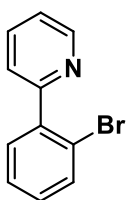
1.1. Materials and Instrumentation

Reagents and solvents used were commercially available reagent quality unless indicated otherwise. Solvents were purchased from SDS-Carlo Erba and Scharlab and were purified and dried by passing through an activated alumina purification system (MBraun SPS-800). Preparation and handling of air-sensitive materials was carried out in a N₂ drybox (JACOMEX) with O₂ and H₂O concentrations < 1.0 ppm. NMR data were collected on a BRUKER 400 or 300 AVANCE spectrometer in the corresponding deuterated solvent, and ¹H and ¹³C{¹H} experiments were recorded under routine conditions. ESI-MS experiments were collected and analyzed on a Bruker Daltonics Esquire 6000 spectrometer with acetonitrile or acetonitrile/water (80:20) as solvent. High resolution mass spectra (HRMS) were recorded on a Bruker MicrOTOF-Q II TM instrument using ESI or Cryospray ionization sources with acetonitrile as solvent by Dr. Laura Gómez of Serveis Tècnics of the University of Girona.

1.2. Synthesis of substrates and catalysts

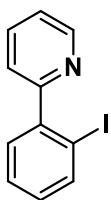
The cationic NHC-Au(I) catalyst [Au(NCMe)IPr]SbF₆ was prepared following a literature procedure.^[1]

2-(2-bromophenyl)-pyridine (**1a-Br**) was synthesized as previously described by Pd-catalyzed cross-coupling of 2-bromopyridine and 2-bromophenylboronic acid.^[2] Derivative 2-(2-iodophenyl)-pyridine (**1a-I**) was prepared following a procedure found in the literature.^[3]



1a-Br: Spectral data are in accordance with those reported in the literature. ¹H-NMR (CDCl₃, 400 MHz) δ, ppm: 8.71 (dq, *J* = 4.8, 2.0, 0.8 Hz, 1H, H^a), 7.76 (td, *J* = 7.6, 1.6 Hz, 1H, H^c), 7.67 (dd, *J* = 8.0, 1.2 Hz, 1H, H^h), 7.60 (dt, *J* = 8.0, 1.2 Hz, 1H, H^d), 7.54 (dd, *J* = 8.0, 1.6 Hz, 1H, H^e), 7.41 (td, *J* = 7.6, 1.2 Hz, 1H, H^g), 7.27 (m, 2H, H^b, H^f); **HRMS (ESI)** (CH₃CN, *m/z*): calcd for C₁₁H₈BrN [M + H⁺]

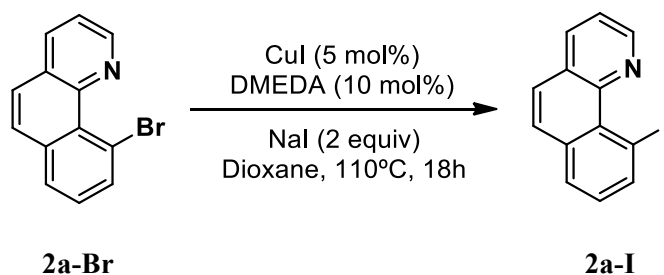
233.9913, found: 233.9918.



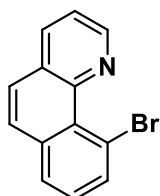
1a-I: Spectral data are in accordance with those reported in the literature.^[4] ¹H-NMR (CDCl₃, 400 MHz) δ, ppm: 8.71 (dq, *J* = 4.8, 2.0, 1.2 Hz, 1H, H^a), 7.97 (ddd, *J* = 8.0, 0.8, 0.4 Hz, 1H, H^e), 7.77 (td, *J* = 7.6, 1.6 Hz, 1H, H^c), 7.51 (dt, *J* = 8.0, 0.8 Hz, 1H, H^d), 7.44 (m, 2H, H^g and H^h), 7.31 (ddd, *J* = 4.8, 2.8, 1.2 Hz, 1H, H^b), 7.09 (ddd, *J* = 8.0, 2.4, 1.2 Hz, 1H, H^f); **HRMS (ESI)** (CH₃CN, *m/z*): calcd for C₁₁H₈NI [M + H⁺]

281.9774, found: 281.9776.

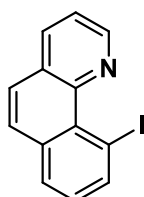
10-Bromobenzo[*h*]quinolone (**2a-Br**) was prepared according to the literature procedure starting from benzo[*h*]quinolone.^[5] Derivative 10-Iodobenzo[*h*]quinolone (**2a-I**) was synthesized from **2a-Br** following Buchwald's copper-catalyzed iodination of aryl bromides.^[2]



A vial was charged with **2a-Br** (516 mg, 2 mmol) and NaI (600 mg, 4 mmol) and entered in an inert-atmosphere glovebox. There CuI (19.0 mg, 0.1 mmol, 5 mol%), *N,N'*-Dimethylethylenediamine (22 μ L, 0.2 mmol) and dry dioxane (1 mL) were added. The vial was capped and the reaction mixture was stirred at 110 $^{\circ}$ C for 18h. The resulting mixture was purified by column chromatography on silica using a solvent mixture of hexane-ethyl acetate 9:1. The desired product was obtained as a white solid (407 mg, 67% isolated yield).

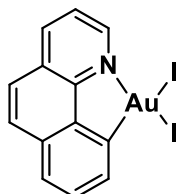


2a-Br: Spectral data are in accordance with those reported in the literature. $^1\text{H-NMR}$ (CDCl_3 , 400 MHz) δ , ppm: 9.11 (dd, $J = 4.4, 2.0$ Hz, 1H, H^a), 8.18 (dd, $J = 8.0, 2.0$ Hz, 1H, H^c), 8.10 (dd, $J = 7.6, 1.2$ Hz, 1H, H^h), 7.88 (dd, $J = 8.0, 0.8$ Hz, 1H, H^f), 7.75 (dd, $J = 8.8$ Hz, 2H, H^d+H^e), 7.57 (dd, $J = 8.0, 4.4$ Hz, 1H, H^b), 7.47 (t, $J = 8.0$ Hz, 1H, H^g); **HRMS (ESI)** (CH_3CN , m/z): calcd for $\text{C}_{13}\text{H}_8\text{BrN}$ [$\text{M} + \text{H}^+$] 257.9913, found: 257.9910.

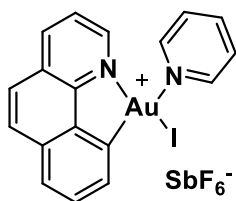


2a-I: $^1\text{H-NMR}$ (CDCl_3 , 400 MHz) δ , ppm: 9.11 (dd, $J = 4.4, 2.0$ Hz, 1H, H^a), 8.55 (dd, $J = 7.6, 1.2$ Hz, 1H, H^h), 8.17 (dd, $J = 8.0, 2.0$ Hz, 1H, H^c), 7.92 (dd, $J = 8.0, 1.2$ Hz, 1H, H^f), 7.74 (dd, $J = 8.8$ Hz, 2H, H^d+H^e), 7.58 (dd, $J = 8.0, 4.4$ Hz, 1H, H^b), 7.28 (t, $J = 8.0$ Hz, 1H, H^g); $^{13}\text{C}\{^1\text{H}\}$ -NMR (CDCl_3 , 100 MHz) δ , ppm: 145.85 (C1), 144.52 (C13), 143.41 (C10), 135.58 (C3), 135.20 (C7), 129.22 (C8), 129.14 (C12), 128.45 (C9), 128.15 (C6), 126.80 (C4), 126.18 (C5), 122.17 (C2), 88.85 (C11); **HRMS (ESI)** (CH_3CN , m/z): calcd for $\text{C}_{13}\text{H}_8\text{IN}$ [$\text{M} + \text{H}^+$] 305.9774, found: 305.9771.

1.3. Synthesis of the Gold(III) complexes **3a** and **3b**



To a mixture of gold iodide (65.2 mg, 0.2 mmol) and 10-Iodobenzo[*h*]quinolone (**2a-I**) was added toluene (1 mL) at room temperature and stirred at 60 $^{\circ}$ C for 18h. The resulting suspension was then dried under vacuum and washed with cold DCM to yield **3a** as a red powder (120.8 mg, 96%). $^1\text{H-NMR}$ (CDCl_3 , 400 MHz, 323K) δ , ppm: 10.36 (dd, $J = 5.6, 1.2$ Hz, 1H, H^a), 8.93 (dd, $J = 8.0, 0.8$ Hz, 1H, H^h), 8.55 (dd, $J = 8.0, 0.4$ Hz, 1H, H^c), 7.88 (d, $J = 8.8$ Hz, 1H, H^e), 7.87 (d, $J = 8.0$ Hz, 1H, H^f), 7.79 (dd, $J = 8.0, 5.6$ Hz, 1H, H^b), 7.71 (d, $J = 8.7$ Hz, 1H, H^d), 7.59 (t, $J = 8.0$ Hz, 1H, H^g); $^{13}\text{C}\{^1\text{H}\}$ -NMR (CDCl_3 , 100 MHz, 323K) δ , ppm: 154.81 (C13), 153.63 (C11), 150.00 (C1), 140.64 (C12), 140.26 (C3), 135.88 (C7), 134.52 (C10), 131.44 (C9), 130.38 (C6), 129.22 (C4), 126.33 (C8), 124.06 (C5), 122.60 (C2).

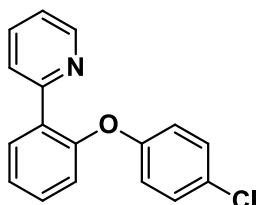


3b: Complex **3a** (25.2 mg, 0.04 mmol) and AgSbF₆ (13.9 mg, 0.04 mmol) were suspended in acetonitrile (1 mL) and pyridine (3.5 mg, 0.044 mmol) was added at room temperature. After stirring for <1 min at room temperature, the resulting orange mixture was filtered through *Celite*®, dried under vacuum and washed with hexanes (3 x 2 mL) to give the desired complex as a yellow solid (29.7 mg, 91%). **¹H-NMR** (CD₃CN, 400 MHz, 248K) δ, ppm: 8.89 (m, 3H, H^h+Hⁱ), 8.82 (m, 1H, H^c), 8.33 (tt, *J* = 8.0, 1.6 Hz, 1H, H^k), 7.98 (m, 4H, H^f+H^e+H^j), 7.91 (d, *J* = 8.8 Hz, 1H, H^d), 7.75 (m, 2H, H^a+H^b), 7.49 (t, *J* = 8.0 Hz, 1H, H^g); **¹³C{¹H}-NMR** (CD₃CN, 100 MHz, 248K) δ, ppm: 152.23 (C13), 150.55 (C14), 145.66 (C1), 142.74 (C3), 142.62 (C16), 139.50 (C11), 139.33 (C12), 138.56 (C10), 136.21 (C7), 131.88 (C9), 130.32 (C6), 129.32 (C4), 128.80 (C15), 127.74 (C8), 125.29 (C5), 123.59 (C2); **HRMS (ESI)** (CH₃CN, *m/z*): calcd for C₁₈H₁₃AuIN₂ [M⁺] 580.9783, found: 580.9782.

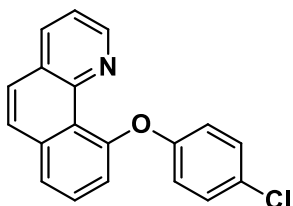
1.4. General procedure for the coupling of *p*-chlorophenolate and sodium alkoxides to substrates **1a-Br** and **2a-Br**

Substrates **1a-Br** or **2a-Br** (0.02 mmol), [Au(NCMe)IPr]SbF₆ (2 μmol, 10 mol%) and *p*-chlorophenolate or sodium alkoxide (2 equivalents, 0.04 mmol) were weighed using a precision balance (accuracy: +/-0.01 mg) into a glass vial, and dissolved in CD₃CN for *p*-chlorophenolate or the protic solvent of choice for the other alkoxides. The vial was sealed and the mixture stirred at 110°C. After the required reaction time, the crude was allowed to reach room temperature and, if needed, solvent evaporated under vacuum. The residue was re-dissolved in CDCl₃ and a standard solution of 1,3,5-trimethoxybenzene (20mM, 40 μL) was added. The products in the crude reaction mixture were identified by ¹H-NMR and ESI-HRMS.

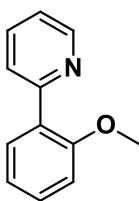
Product isolation: The same synthetic protocol was followed, in this case employing 0.2 mmol substrate **1a-Br** or **2a-Br**, 0.02 mmol [Au(NCMe)IPr]SbF₆ and 0.4 mmol alkoxide in 0.8 mL of solvent. After solvent evaporation the residue was subjected to column chromatography on silica gel (eluent: hexanes/EtOAc).



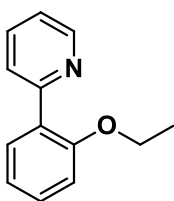
1aa: Column chromatography on silica gel (hexane-ethyl acetate 7:3) provided a colorless oil (41.0 mg, 73% isolated yield). Spectroscopic data are consistent with literature reports.^[4] **¹H-NMR** (CDCl₃, 400 MHz) δ, ppm: 8.67 (dq, *J* = 4.8, 2.0, 0.8 Hz, 1H, H^a), 7.90 (dd, *J* = 7.6, 1.6 Hz, 1H, H^c), 7.77 (dt, *J* = 8.0, 1.2 Hz, 1H, H^d), 7.65 (ddd, *J* = 8.0, 7.6, 2.0 Hz, 1H, H^e), 7.38 (ddd, *J* = 7.6, 7.4, 1.6 Hz, 1H, H^g), 7.29 (td, *J* = 8., 7.6, 1.2 Hz, 1H, H^f), 7.20 (m, 2H, H^b+Hⁱ), 7.01 (dd, *J* = 7.4, 1.2 Hz, 1H, H^h), 6.86 (d, *J* = 8.8 Hz, 2H, H^j); **HRMS (ESI)** (CH₃CN, *m/z*): calcd for C₁₇H₁₂NCIO [M + H⁺] 282.0680, found: 282.0682.



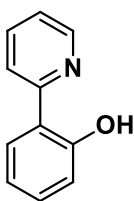
2aa: Column chromatography on silica gel (hexane-ethyl acetate 4:1) provided a pale yellow solid (47.6 mg, 78% isolated yield). **¹H-NMR** (CDCl₃, 400 MHz) δ, ppm: 8.80 (dd, *J* = 4.4, 2.0 Hz, 1H, H^a), 8.11 (dd, *J* = 8.0, 2.0 Hz, 1H, H^c), 7.84 (d, *J* = 8.8 Hz, 1H, H^e), 7.83 (dd, *J* = 8.0, 1.2 Hz, 1H, H^b), 7.70 (d, *J* = 8.8 Hz, 1H, H^d), 7.69 (t, *J* = 8.0 Hz, 1H, H^g), 7.43 (dd, *J* = 8.0, 1.6 Hz, 1H, H^f), 7.41 (dd, *J* = 8.0, 4.4 Hz, 1H, H^b), 7.15 (d, *J* = 9.2, 1.6 Hz, 2H, Hⁱ), 6.82 (d, *J* = 9.2 Hz, 2H, Hⁱ); **¹³C{¹H}-NMR** (CDCl₃, 100 MHz) δ, ppm: 158.49 (C14), 153.21 (C11), 148.84 (C1), 145.79 (C13), 136.60 (C7), 135.38 (C3), 129.09 (C16), 128.51 (C5), 127.94 (C6), 127.12 (C4), 126.67 (C9), 126.03 (C17), 125.80 (C10), 124.40 (C12), 122.31 (C8), 121.43 (C2), 117.65 (C15); **HRMS (ESI)** (CH₃CN, *m/z*): calcd for C₁₉H₁₂NOCl [*M* + H⁺] 306.0680, found: 306.0677.



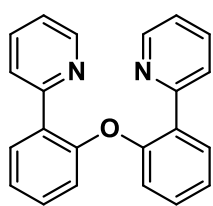
1ab: Column chromatography on silica gel (hexane-ethyl acetate 1:1) afforded a colorless oil (30.7 mg, 83% isolated yield). Spectral data match literature reports.^[6] **¹H-NMR** (CDCl₃, 400 MHz) δ, ppm: 8.70 (ddd, *J* = 4.8, 2.0, 1.2 Hz, 1H, H^a), 7.81 (dt, *J* = 8.0, 1.2 Hz, 1H, H^d), 7.76 (dd, *J* = 7.6, 2.0 Hz, 1H, H^c), 7.70 (td, *J* = 7.6, 2.0 Hz, 1H, H^c), 7.37 (ddd, *J* = 8.8, 7.6, 2.0 Hz, 1H, H^g), 7.20 (ddd, *J* = 7.6, 4.8, 1.2 Hz, 1H, H^b), 7.08 (td, *J* = 7.6, 1.2 Hz, 1H, H^f), 7.01 (dd, *J* = 8.4, 1.2 Hz, 1H, H^b), 3.86 (s, 3H, Hⁱ); **HRMS (ESI)** (CH₃CN, *m/z*): calcd for C₁₂H₁₁NO [*M* + H⁺] 186.0913, found: 186.0914.



1ac: Column chromatography on silica gel (hexane-ethyl acetate 3:1) gave a yellow oil (24.3 mg, 61% isolated yield). Spectral data match previously reported data.^[7] **¹H-NMR** (CDCl₃, 400 MHz) δ, ppm: 8.70 (ddd, *J* = 4.8, 2.0, 1.2 Hz, 1H, H^a), 7.90 (dt, *J* = 8.0, 1.2 Hz, 1H, H^c), 7.81 (dd, *J* = 7.6, 2.0 Hz, 1H, H^c), 7.69 (td, *J* = 8.0, 2.0 Hz, 1H, H^c), 7.34 (ddd, *J* = 8.4, 7.2, 1.6 Hz, 1H, H^g), 7.19 (ddd, *J* = 7.6, 4.8, 1.2 Hz, 1H, H^b), 7.07 (td, *J* = 7.6, 1.2 Hz, 1H, H^f), 7.01 (dd, *J* = 8.4, 1.2 Hz, 1H, H^b), 4.09 (q, *J* = 7.2 Hz, 2H, Hⁱ), 1.39 (t, *J* = 7.2 Hz, 3H, Hⁱ); **HRMS (ESI)** (CH₃CN, *m/z*): calcd for C₁₃H₁₃NO [*M* + H⁺] 200.1064, found: 200.1070.



1af: Column chromatography on silica gel (hexane-ethyl acetate 9:1) afforded a yellow oil (14.4 mg, 42% isolated yield). Spectral data match literature reports.^[8] **¹H-NMR** (CDCl₃, 400 MHz) δ, ppm: 14.36 (s, br, 1H, O-*H*), 8.52 (ddd, *J* = 4.8, 1.6, 0.8 Hz, 1H, H^a), 7.92 (d, *J* = 8.4 Hz, 1H, H^d), 7.84 (ddd, *J* = 8.4, 7.6, 1.6 Hz, 1H, H^c), 7.81 (dd, *J* = 8.0, 1.6 Hz, 1H, H^c), 7.31 (ddd, *J* = 8.4, 7.2, 1.6 Hz, 1H, H^g), 7.25 (ddd, *J* = 7.6, 4.8, 0.8 Hz, 1H, H^b), 7.03 (dd, *J* = 8.4, 1.2 Hz, 1H, H^b), 6.91 (ddd, *J* = 8.0, 7.2, 1.2 Hz, 1H, H^f); **HRMS (ESI)** (CH₃CN, *m/z*): calcd for C₁₁H₉NO [*M* + H⁺] 172.0757, found: 172.0763.



1ag: Column chromatography on silica gel (hexane-ethyl acetate 3:2) provided a white solid (13.0 mg, 20% isolated yield). $^1\text{H-NMR}$ (CDCl_3 , 400 MHz) δ , ppm: 8.67 (ddd, $J = 4.8, 2.0, 0.8$ Hz, 2H, H^a), 7.86 (dd, $J = 7.6, 2.0$ Hz, 2H, H^e), 7.72 (dt, $J = 8.0, 2.0$ Hz, 2H, H^d), 7.58 (td, $J = 7.6, 2.0$ Hz, 2H, H^c), 7.30 (ddd, $J = 8.0, 7.2, 2.0$ Hz, 2H, H^b), 7.21 (td, $J = 7.6, 1.2$ Hz, 2H, H^f), 7.17 (ddd, $J = 7.2, 4.8, 1.2$ Hz, 2H, H^b), 6.95 (dd, $J = 8.0, 1.2$ Hz, 2H, H^b); $^{13}\text{C}\{^1\text{H}\}$ -NMR (CDCl_3 , 100 MHz) δ , ppm: 155.15 (C5), 154.22 (C11), 149.52 (C1), 135.84 (C3), 131.56 (C6), 131.42 (C7), 130.03 (C9), 124.74 (C4), 123.89 (C8), 122.02 (C2), 119.05 (10); **HRMS (ESI)** (CH_3CN , m/z): calcd for $\text{C}_{22}\text{H}_{16}\text{N}_2\text{O}$ [$\text{M} + \text{H}^+$] 325.1335, found: 325.1318.

1.5. General procedure for the C-N bond formation with **1a-I** and **2a-I**

For the optimization of the reaction conditions with *p*-nitroaniline, a vial was charged with **1a-I** (0.02 mmol), $[\text{Au}(\text{NCMe})\text{IPr}]\text{SbF}_6$ (1.8mg, 0.002 mmol), *p*-nitroaniline and base, and 0.5 mL of deuterated solvent were added. The vial was capped and the mixture stirred at 110°C for 24h. The reaction crude was then allowed to reach room temperature and a standard solution of 1,3,5-trimethoxybenzene (20mM, 40 μL) was added. The resulting suspension was analyzed by $^1\text{H-NMR}$. The presence of the final C-N coupling product **1ah** was also confirmed by ESI-MS.

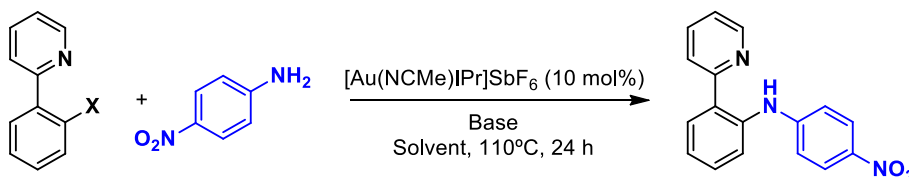


Table S1. Optimization of reaction conditions for the *p*-nitroaniline insertion reaction using 2-(2-bromophenyl)-pyridine (**1a-Br**) or 2-(2-iodophenyl)-pyridine (**1a-I**)

Entry	X	Solvent	Base	Yield 1a (%) ^a
1	Br	CH_3CN	K_3PO_4 (3)	0
2	Br	CH_3CN	CsF (3)	0
3	Br	CH_3CN	$\text{KO}t\text{-Bu}$ (3)	0
4	Br	CH_3CN	CsF (5)	0 ^b
5	Br	Toluene	CsF (5)	0 ^b
6	Br	Dioxane	CsF (5)	4 ^{b,c}
7	Br	DMSO	CsF (5)	24 ^b
8	Br	DMSO	$\text{KO}t\text{-Bu}$ (5)	39 ^b
9	I	DMSO	CsF (5)	44 ^b
10	I	DMSO	$\text{KO}t\text{-Bu}$ (5)	93 ^b
11	I	DMSO	$\text{KO}t\text{-Bu}$ (3)	95 (92) ^d

^aYields as determined by $^1\text{H-NMR}$ using 1,3,5-trimethoxybenzene as an internal standard. ^b[*p*- NO_2 aniline] = 100 mM; ^cAfter the required reaction time, solvent was removed under vacuum and CDCl_3 (0.6 mL) was added for $^1\text{H-NMR}$ analysis. ^dT = 100°C .

Following the optimized procedure described above (Table S1), different amines and amides were screened. General conditions: [2-(2-iodophenyl)pyridine] = 20 mM, [Au(I)] = 2 mM, [nucleophile] = 60 mM, [KO-*t*-Bu] = 60 mM, 0.5 mL DMSO-*d*₆, 110°C, 24h.

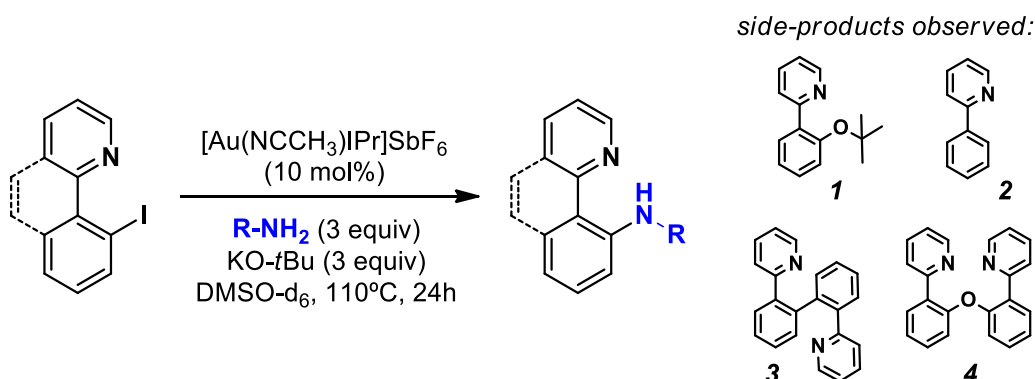
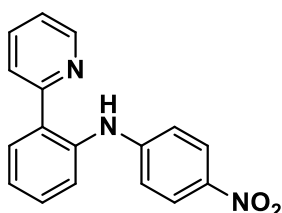


Table S2. Outcomes of the C-N cross-coupling reactions using **1a-I** and **2a-I**.

Entry	Nucleophile	T (°C)	Yield [%] ^a	Conversion [%] ^a	Side-products (% yield) ^a
1	<i>p</i> -Nitroaniline	100	92	100	1 (trace)
2 ^b	<i>p</i> -Nitroaniline	100	93	100	-
3	2-Hydroxypyridine	100	95	100	-
4	Imidazole	100	93	100	-
5	Benzamide	110	59	66	4 (trace)
6 ^c	Cyclohexylamine	110	72	81	3 (5)
7 ^c	Propylamine	110	79	84	4 (trace)
8 ^c	Piperidine	110	51	67	2 (4); 3 (6)
9	Aniline	110	50	100	2 (8); 3 (15); 4 (9)
10	<i>p</i> -Anisidine	110	17	44	1 (12); 3 (7)
11	Diethylamine	110	8	19	-

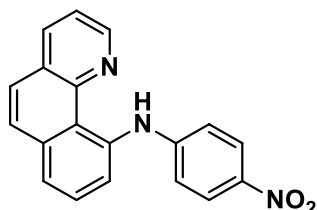
^aAverage yields and conversions of at least two experiments as determined by ¹H-NMR using 1,3,5-trimethoxybenzene as internal standard. ^b10-Iodobenzo[*h*]quinolone (**2a-I**) as substrate. ^cAverage GC and ¹H-NMR yields and conversions using 1,3,5-trimethoxybenzene as an internal standard.

Product isolation: A larger scale reaction was also performed: (0.2 mmol substrate **1a-I** or **2a-I**; 0.02 mmol [Au(NCMe)IPr]SbF₆; 0.6 mmol nucleophile; 0.6 mmol KO-*t*-Bu) in 0.8 mL of DMSO. After cooling down to room temperature the residue was subjected to column chromatography on silica gel (eluent: hexanes/EtOAc).

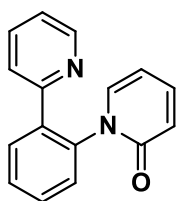


1ah: Column chromatography on silica gel (hexanes-ethyl acetate 3:2) provided a yellow solid (43.8 mg, 79% isolated yield). ¹H-NMR (CDCl₃, 400 MHz) δ, ppm: 10.89 (s, 1H, H¹), 8.66 (dq, *J* = 4.8, 2.0, 0.8

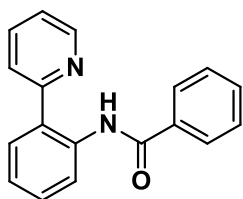
Hz, 1H, H^a), 8.11 (d, $J = 8.8$ Hz, 2H, H^k), 7.83 (ddd, $J = 8.0, 7.6, 2.0$ Hz, 1H, H^c), 7.72 (dt, $J = 8.0, 1.2$ Hz, 1H, H^d), 7.67 (dd, $J = 7.6, 1.2$ Hz, 1H, H^h), 7.60 (dd, $J = 8.0, 0.8$ Hz, 1H, H^e), 7.39 (td, $J = 7.6, 1.6$ Hz, 1H, H^g), 7.28 (ddd, $J = 7.6, 4.8, 1.2$ Hz, 1H, H^b), 7.15 (td, $J = 7.6, 1.2$ Hz, 1H, H^f), 7.11 (d, $J = 8.8$ Hz, 2H, Hⁱ); ¹³C{**1H**}-NMR (CDCl₃, 100 MHz) δ , ppm: 158.21 (C5), 149.41 (C12), 147.66 (C1), 139.76 (C15), 139.42 (C11), 137.56 (C3), 130.21 (C10), 129.69 (C9), 127.85 (C6), 126.10 (C14), 123.03 (C4), 122.82 (C8), 121.95 (C2), 119.97 (C17), 115.10 (C13); **HRMS (ESI)** (CH₃CN, m/z): calcd for C₁₇H₁₃N₃O₂ [M + H⁺] 291.1075, found: 291.1081.



2ah: Column chromatography on silica gel (hexane-ethyl acetate 3:2) afforded an orange solid (52.9 mg, 84% isolated yield). ¹H-NMR (CDCl₃, 400 MHz) δ , ppm: 13.65 (s, br, 1H, Hⁱ), 8.95 (dd, $J = 4.4, 2.0$ Hz, 1H, H^a), 8.26 (dd, $J = 8.0, 2.0$ Hz, 1H, H^c), 8.21 (d, $J = 9.2$ Hz, 2H, H^k), 7.84 (dd, $J = 8.0, 1.2$ Hz, 1H, H^h), 7.83 (d, $J = 8.8$ Hz, 1H, H^e), 7.69 (d, $J = 8.8$ Hz, 1H, H^d), 7.65 (t, $J = 8.0$ Hz, 1H, H^g), 7.57 (dd, $J = 8.0, 4.4$ Hz, 1H, H^b), 7.54 (dd, $J = 8.0, 0.8$ Hz, 1H, H^f), 7.45 (d, $J = 9.2$ Hz, 2H, Hⁱ); ¹³C{**1H**}-NMR (CDCl₃, 100 MHz) δ , ppm: 149.44 (C14), 148.18 (C13), 146.11 (C1), 141.88 (C11), 140.41 (C17), 136.35 (C3), 136.02 (C7), 129.29 (C6), 128.33 (C9), 127.47 (C4), 126.05 (C16), 125.64 (C5), 121.13 (C8), 120.79 (C2), 118.00 (C12), 116.72 (C15), 114.35 (C10); **HRMS (ESI)** (CH₃CN, m/z): calcd for C₁₉H₁₃N₃O₂ [M + H⁺] 316.1081, found: 316.1074

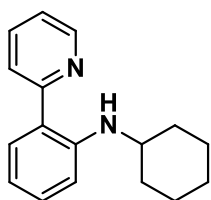


1ai: Column chromatography on silica gel (hexane-ethyl acetate 2:3) provided a colorless oil (37.2 mg, 75% isolated yield). ¹H-NMR (CDCl₃, 400 MHz) δ , ppm: 8.63 (dq, $J = 4.8, 2.0, 1.2$ Hz, 1H, H^a), 8.14 (dq, $J = 5.2, 2.0, 0.8$ Hz, 1H, Hⁱ), 7.89 (dd, $J = 8.0, 1.6$ Hz, 1H, H^e), 7.72 (dt, $J = 8.0, 1.2$ Hz, 1H, H^d), 7.59 (m, 2H, H^c+H^h), 7.44 (ddd, $J = 8.0, 7.6, 1.6$ Hz, 1H, H^g), 7.35 (td, $J = 7.6, 1.2$ Hz, 1H, H^f), 7.16 (dd, $J = 8.0, 1.2$ Hz, 1H, H^h), 7.13 (ddd, $J = 7.6, 4.8, 1.2$ Hz, 1H, H^b), 6.91 (ddd, $J = 7.2, 5.2, 1.2$ Hz, 1H, H^k), 6.77 (dt, $J = 8.4, 1.2$ Hz, 1H, Hⁱ); ¹³C{**1H**}-NMR (CDCl₃, 100 MHz) δ , ppm: 163.68 (C12), 155.35 (C5), 153.56 (C6), 149.54 (C1), 147.87 (C16), 139.33 (C3), 135.89 (C14), 133.19 (C11), 131.39 (C7), 129.96 (C9), 125.49 (C8), 124.48 (C4), 122.50 (C10), 121.95 (C2), 118.31 (C15), 111.10 (C13); **HRMS (ESI)** (CH₃CN, m/z): calcd for C₁₆H₁₂N₂O [M + H⁺] 249.1022, found: 249.1022.

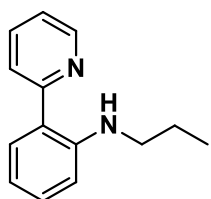


1aj: Column chromatography on silica gel (hexane-diethyl ether 50:50) afforded a white solid (24.7 mg, 45% isolated yield). ¹H-NMR (CDCl₃, 400 MHz) δ , ppm: 8.79 (dd, $J = 8.4, 1.2$ Hz, 1H, H^h), 8.69 (dq, $J = 4.8, 1.6, 0.8$ Hz, 1H, H^a), 8.04 (m, 2H, H^j), 7.87 (ddd, $J = 8.0, 7.2, 2.0$ Hz, 1H, H^c), 7.81 (dt, $J = 8.0, 1.2$ Hz, 1H, H^d), 7.74 (dd, $J = 8.0, 1.6$ Hz, 1H, H^e), 7.50 (m, 4H, H^k+H^l+H^g), 7.30 (ddd, $J = 7.2, 4.8, 1.2$ Hz, 1H, H^b), 7.21 (ddd, $J = 8.0, 7.2, 1.2$ Hz, 1H, H^f); ¹³C{**1H**}-NMR (CDCl₃, 100 MHz) δ , ppm: 165.58 (C12), 158.40 (C5), 147.33 (C1), 138.13

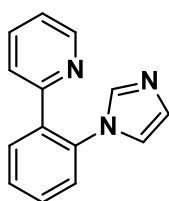
(C11), 137.87 (C3), 135.79 (C13), 131.50 (C16), 130.28 (C7), 128.77 (C9), 128.60 (C15), 127.39 (C14), 125.64 (C6), 123.56 (C8), 123.02 (C4), 121.98 (C10), 121.96 (C2); **HRMS (ESI)** (CH₃CN, m/z): calcd for C₁₈H₁₄N₂O [M + Na⁺] 297.0998, found: 297.1008.



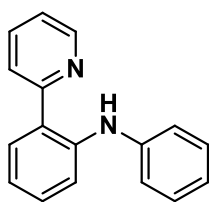
1ak: Column chromatography on silica gel (hexane-ethyl acetate 3:2) afforded a yellow oil (34.4 mg, 70% isolated yield). **¹H-NMR** (CDCl₃, 400 MHz) δ, ppm: 8.57 (dq, *J* = 4.8, 2.0, 0.8 Hz, 1H, H^a), 8.18 (s, 1H, Hⁱ), 7.73 (ddd, *J* = 8.0, 7.2, 2.0 Hz, 1H, H^c), 7.66 (dt, *J* = 8.0, 1.2 Hz, 1H, H^d), 7.52 (dd, *J* = 7.6, 1.6 Hz, 1H, H^e), 7.23 (ddd, *J* = 8.4, 7.2, 1.6 Hz, 1H, H^g), 7.14 (ddd, *J* = 7.2, 4.8, 1.2 Hz, 1H, H^b), 6.77 (d, *J* = 8.4 Hz, 1H, H^h), 6.66 (ddd, *J* = 7.6, 7.2, 0.4 Hz, 1H, H^f), 3.41 (m, 1H, H^j), 2.04 (m, 2H, H^k), 1.76 (m, 2H, H^m), 1.60 (m, 1H, H^o), 1.36 (m, 5H, H^l+Hⁿ+H^p); **¹³C{¹H}-NMR** (CDCl₃, 100 MHz) δ, ppm: 159.91 (C5), 147.32 (C1), 146.90 (C11), 136.73 (C3), 130.20 (C9), 129.69 (C7), 122.35 (C4), 121.04 (C6), 120.54 (C2), 115.03 (C8), 111.94 (C10), 50.80 (C12), 32.95 (C13), 26.11 (C15), 24.70 (C14); **HRMS (ESI)** (CH₃CN, m/z): calcd for C₁₇H₂₀N₂ [M + H⁺] 253.1699, found: 253.1696.



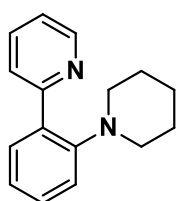
1al: Column chromatography on silica gel (hexane-ethyl acetate 3:2) gave a pale yellow oil (30.1 mg, 71% isolated yield). **¹H-NMR** (CDCl₃, 400 MHz) δ, ppm: 8.58 (dq, *J* = 4.8, 2.0, 1.2 Hz, 1H, H^a), 8.12 (s, br, 1H, Hⁱ), 7.74 (ddd, *J* = 8.4, 7.2, 2.0 Hz, 1H, H^c), 7.67 (dt, *J* = 8.4, 1.2 Hz, 1H, H^d), 7.53 (dd, *J* = 8.0, 1.6 Hz, 1H, H^e), 7.26 (ddd, *J* = 8.4, 7.6, 1.6 Hz, 1H, H^g), 7.15 (ddd, *J* = 7.2, 4.8, 1.2 Hz, 1H, H^b), 6.75 (dd, *J* = 8.4, 1.2 Hz, 1H, H^h), 6.70 (ddd, *J* = 8.0, 7.6, 1.2 Hz, 1H, H^f), 3.17 (t, *J* = 7.2 Hz, 2H, H^j), 1.71 (sext., *J* = 7.2 Hz, 2H, H^k), 1.03 (t, *J* = 7.2 Hz, 3H, H^l); **¹³C{¹H}-NMR** (CDCl₃, 100 MHz) δ, ppm: 159.86 (C5), 147.90 (C11), 147.38 (C1), 136.81 (C3), 130.32 (C9), 129.44 (C7), 122.34 (C4), 121.15 (C6), 120.65 (C2), 115.39 (C8), 111.35 (C10), 45.19 (C12), 22.53 (C13), 11.86 (C14); **HRMS (ESI)** (CH₃CN, m/z): calcd for C₁₄H₁₆N₂ [M + H⁺] 213.1386, found: 213.1381



1am: Column chromatography on silica gel (hexane-ethyl acetate 1:4) provided a colorless liquid, which was subsequently washed with brine (5 x 3mL) in order to remove residual DMSO. A white solid was obtained (33.6 mg, 76% isolated yield). **¹H-NMR** (CDCl₃, 400 MHz) δ, ppm: 8.65 (dq, *J* = 4.8, 2.0, 0.8 Hz, 1H, H^a), 7.79 (dd, *J* = 7.2, 2.0 Hz, 1H, H^e), 7.54 (m, 3H, H^c+H^g+H^f), 7.44 (s, br, 1H, H^k), 7.39 (dd, *J* = 7.2, 2.0 Hz, 1H, H^b), 7.20 (ddd, *J* = 7.6, 4.8, 1.2 Hz, 1H, H^b), 7.06 (s, br, 1H, Hⁱ), 6.89 (s, br, 1H, Hⁱ), 6.83 (dt, *J* = 8.0, 0.8 Hz, 1H, H^d); **¹³C{¹H}-NMR** (CDCl₃, 100 MHz) δ, ppm: 155.69 (C5), 149.93 (C1), 137.53 (C14), 136.52 (C6), 136.42 (C3), 135.20 (C11), 131.45 (C7), 129.65 (C13), 129.59 (C8), 128.92 (C9), 126.36 (C10), 123.13 (C4), 122.51 (C2), 120.61 (C12); **HRMS (ESI)** (CH₃CN, m/z): calcd for C₁₄H₁₁N₃ [M + H⁺] 222.1026, found: 222.1020.



1an: Column chromatography on silica gel (hexane-ethyl acetate 9:1) provided a yellow oil (20.2 mg, 41% isolated yield). Spectroscopic data are consistent with literature reports.^[9] $^1\text{H-NMR}$ (CDCl_3 , 400 MHz) δ , ppm: 10.22 (s, 1H, Hⁱ), 8.63 (dq, $J = 4.8, 1.6, 0.8$ Hz, 1H, H^a), 7.78 (ddd, $J = 8.0, 7.2, 2.0$ Hz, 1H, H^c), 7.70 (dt, $J = 8.0, 1.2$ Hz, 1H, H^d), 7.61 (dd, $J = 8.0, 1.6$ Hz, 1H, H^e or H^h), 7.47 (dd, $J = 8.4, 1.2$ Hz, 1H, H^e or H^h), 7.23 (m, 6H, Hⁱ+H^k+H^s+H^b or H^f), 6.92 (m, 2H, H^l+H^b or H^f); **HRMS (ESI)** (CH_3CN , m/z): calcd for $\text{C}_{17}\text{H}_{14}\text{N}_2$ [$\text{M} + \text{H}^+$] 247.1230, found: 247.1231.

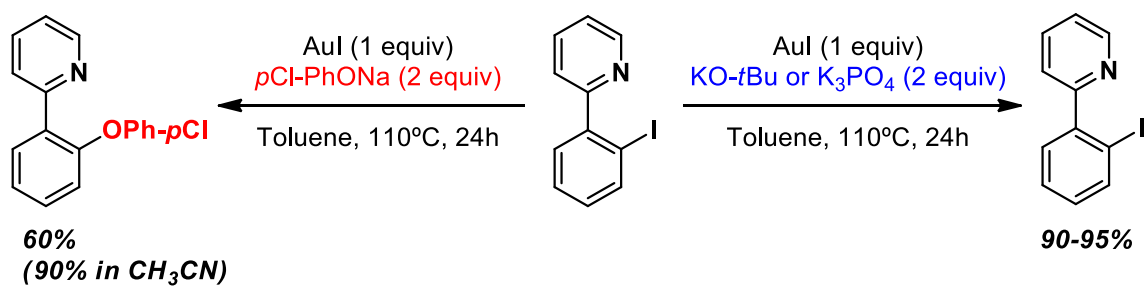


1ap: Column chromatography on silica gel (hexane-ethyl acetate 2:3) gave a colorless oil (19.0 mg, 40% isolated yield). Spectral data match literature reports.^[10] $^1\text{H-NMR}$ (CDCl_3 , 400 MHz) δ , ppm: 8.69 (dq, $J = 4.8, 2.0, 0.8$ Hz, 1H, H^a), 8.08 (dt, $J = 8.0, 1.2$ Hz, 1H, H^d), 7.65 (ddd, $J = 8.0, 7.6, 2.0$ Hz, 1H, H^s), 7.58 (dd, $J = 7.6, 2.0$ Hz, 1H, H^c), 7.31 (ddd, $J = 8.0, 7.6, 2.0$ Hz, 1H, H^c), 7.17 (ddd, $J = 7.6, 4.8, 1.2$ Hz, 1H, H^b), 7.09 (td, $J = 7.6, 1.2$ Hz, 1H, H^f), 7.05 (dd, $J = 8.0, 1.2$ Hz, 1H, H^h), 2.79 (m, 4H, CH_2), 1.49 (m, 6H, CH_2); **HRMS (ESI)** (CH_3CN , m/z): calcd for $\text{C}_{16}\text{H}_{18}\text{N}_2$ [$\text{M} + \text{H}^+$] 239.1543, found: 239.1541. .

1.6. Reactivity of **1a-I** and AuI in the presence of bases and *p*-chlorophenolate

Attempts to isolate a C-N cyclometalated gold(III) complex by reacting **1a-I** and AuI led in all cases to quantitative recovery of the starting substrate. We rationalize that, although the oxidative addition has an accessible barrier, as expected from the C-O and C-N coupling reactions, the ensuing complex $[\text{Au}(\mathbf{1a})\text{I}_2]$ is thermodynamically disfavored, pulling the equilibrium back towards the reagents. Aiming at supporting this proposal, we performed the reaction in the presence of a base or sodium *p*-chlorophenolate. Thus, **1a-I** (5.6 mg, 0.02 mmol), AuI (6.5, 0.02 mmol) and KO-*t*Bu (4.5 mg, 0.04 mmol) or K_3PO_4 (8.5 mg, 0.04 mmol) or sodium *p*-chlorophenolate (6.0 mg, 0.04 mmol) were weighed into a glass vial, and dissolved in toluene. The vial was capped and the mixture stirred at 110°C for 24h. $^1\text{H-NMR}$ analyses of the crude revealed presence of **1a-I** (90-95%) for potassium *tert*-butoxide and potassium phosphate, while in the presence of sodium *p*-chlorophenolate 60% of the **1aa** coupling product was observed. This yield could be increased up to 90% upon toluene replacement for acetonitrile (see Scheme S1).

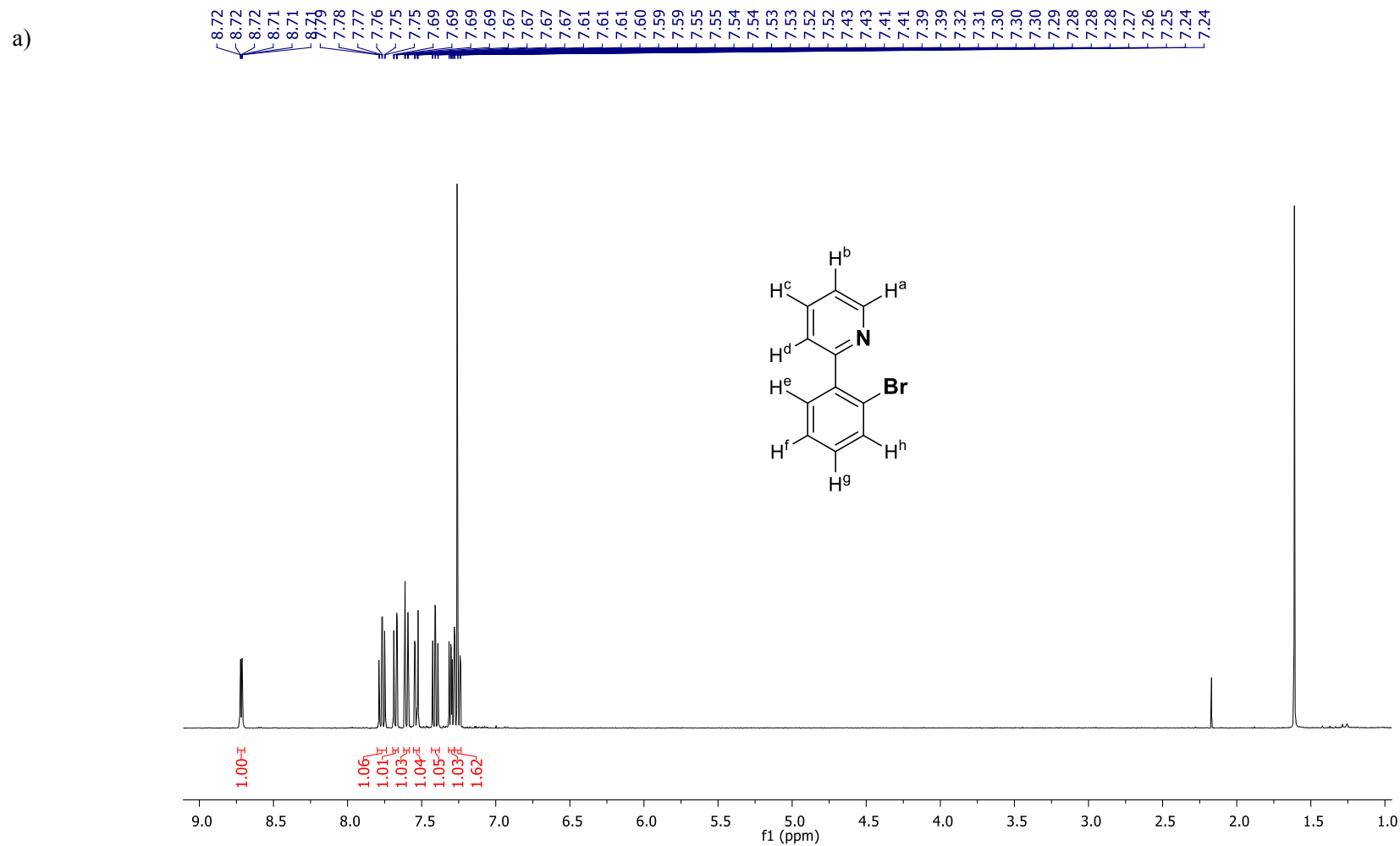
KO-*t*Bu and K_3PO_4 cannot displace the iodides in a putative $[\text{Au}(\mathbf{1a})\text{I}_2]$ complex, which would immediately lead to the reductive elimination and consumption of **1a-I**. On the other hand, however, the nucleophilic character of sodium *p*-chlorophenolate allows for this process occur. A catalytic performance can be likewise attained by adding IPr· carbene in the reaction mixture. Overall, this strongly suggests $\text{C}_{\text{sp}^2}\text{-I}$ bond activation by Au(I).



Scheme S1: Outcomes observed in the reaction between **1a-I** and AuI, when potassium *tert*-butoxide, potassium phosphate or sodium *p*-chlorophenolate are added.

2. Supplementary figures

Figure S1. a) ^1H -NMR spectrum of compound **1a-Br** in CDCl_3 , 400 MHz, at 298 K; b) HRMS (ESI-MS) spectrum (m/z). Observed HRMS (left) with the theoretical isotope prediction (right).



b)

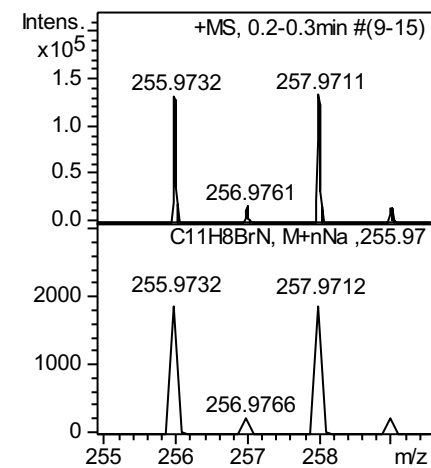
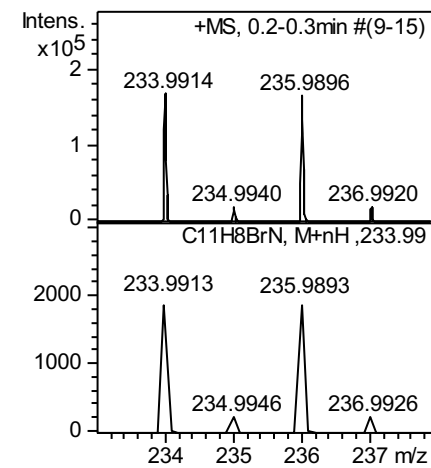
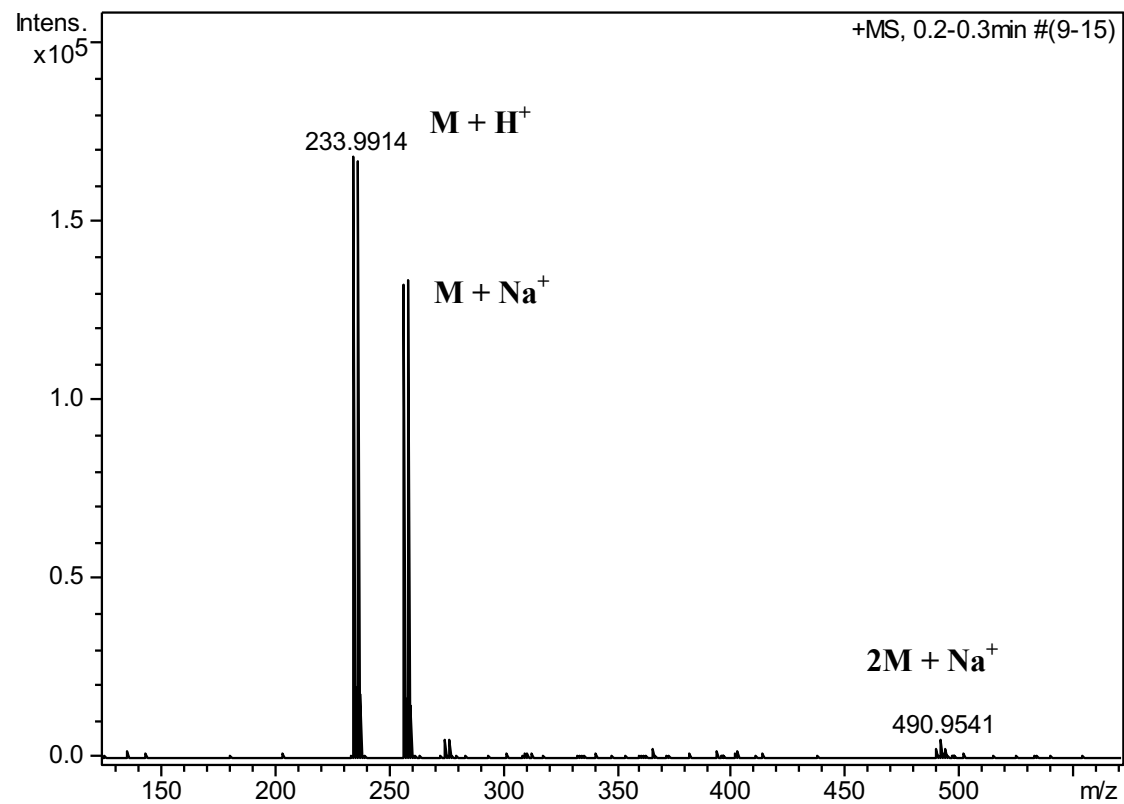
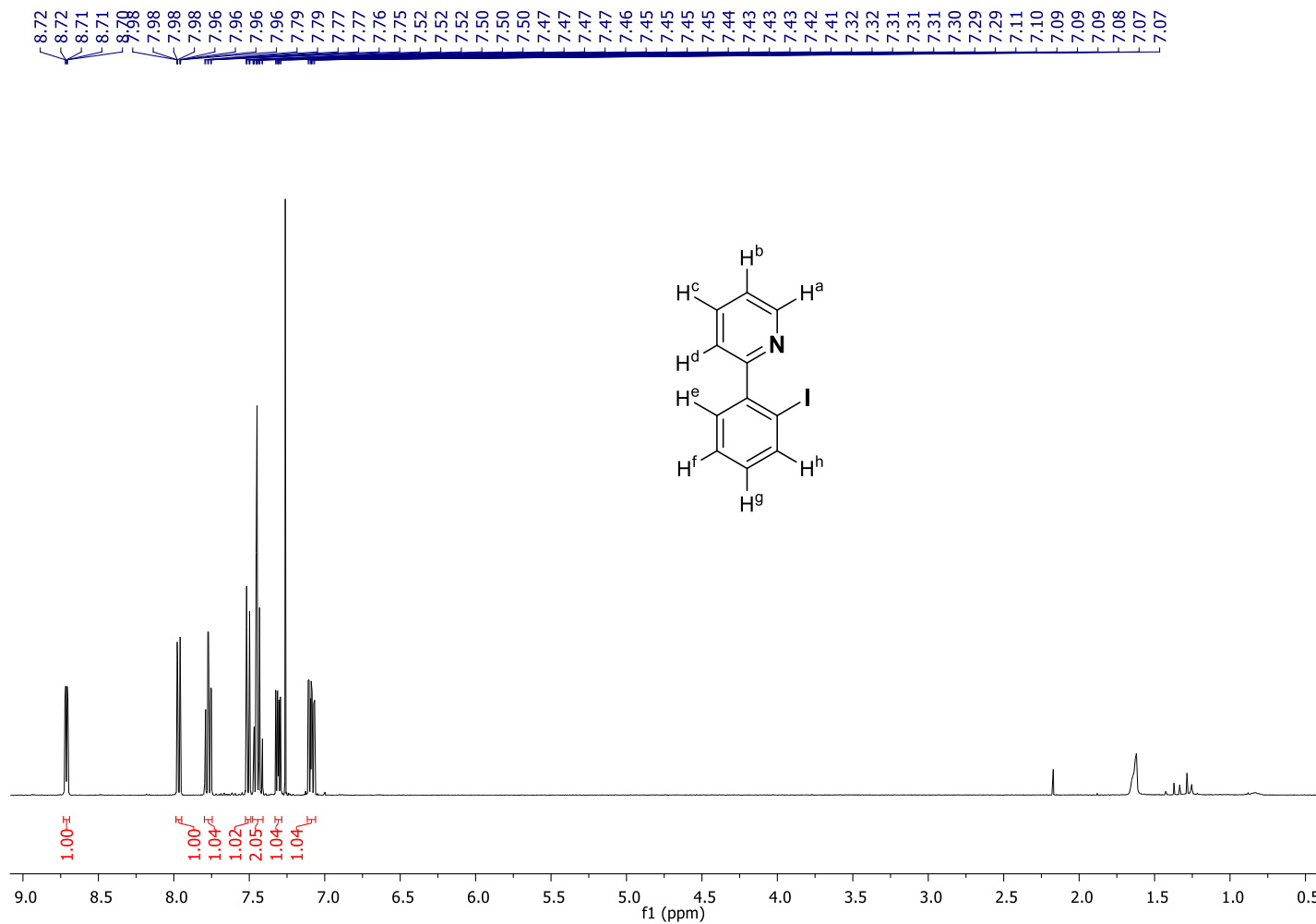


Figure S2. a) $^1\text{H-NMR}$ spectrum of compound **1a-I** in CDCl_3 , 400 MHz, at 298 K; b) HRMS (ESI-MS) spectrum (m/z). Observed HRMS (left) with the theoretical isotope prediction (right).

a)



b)

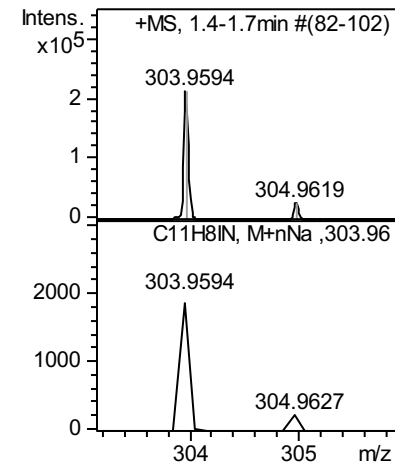
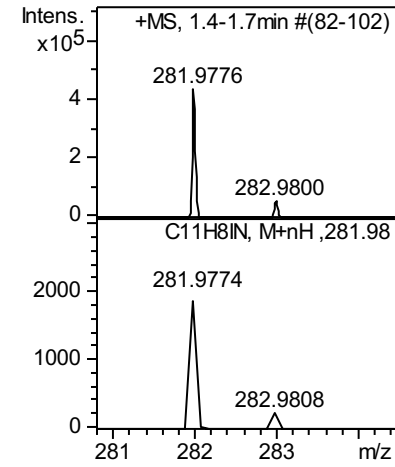
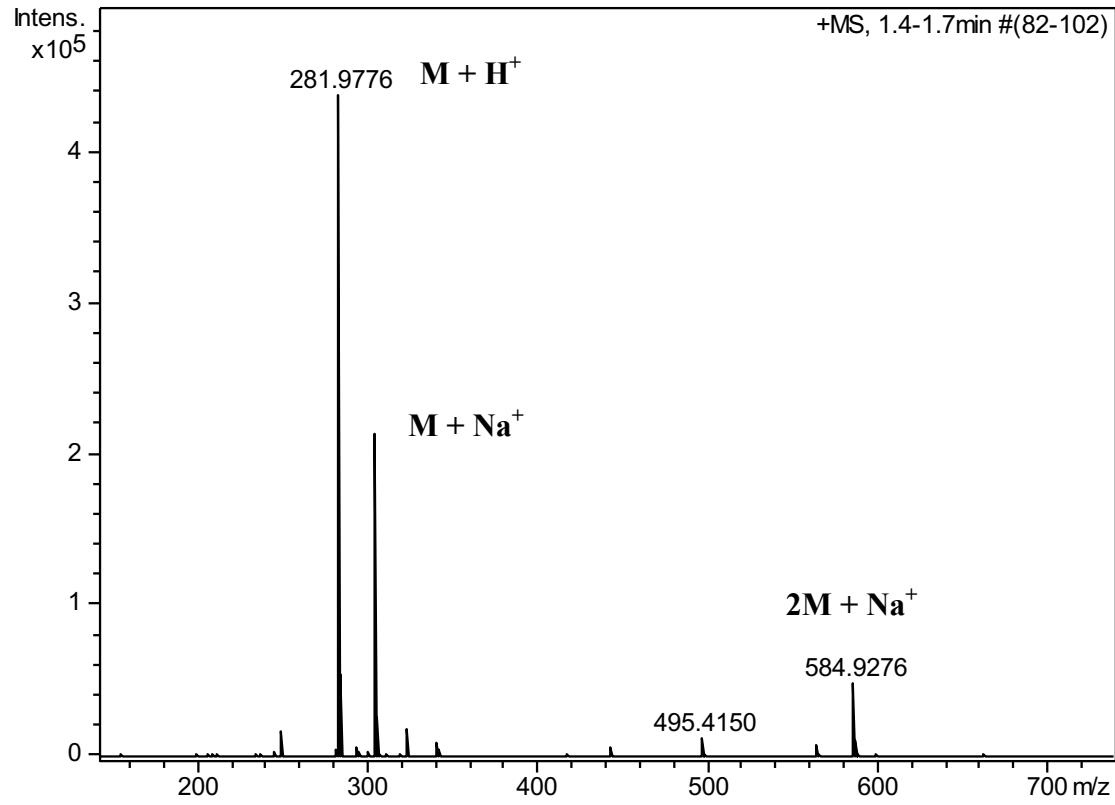
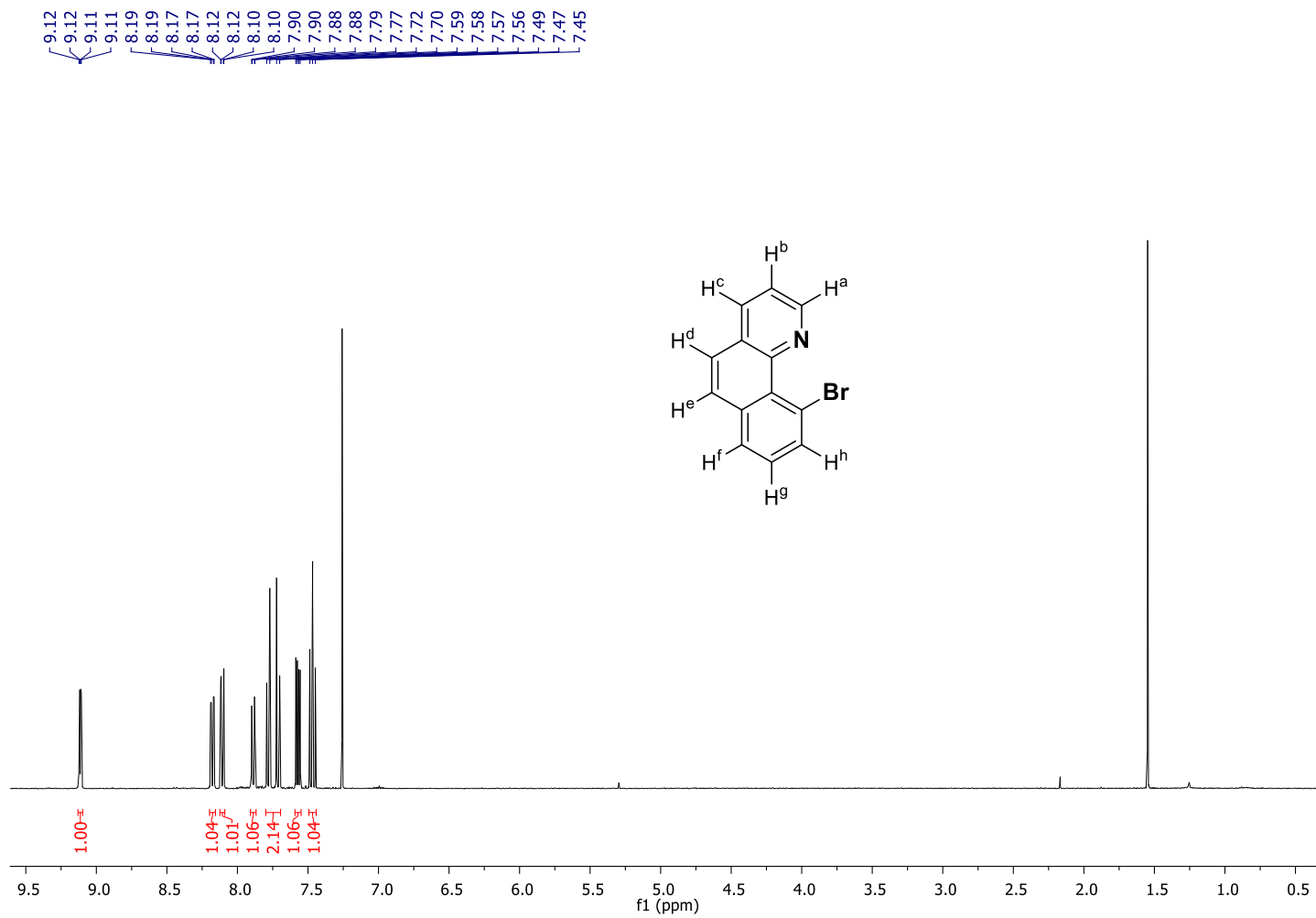


Figure S3. a) $^1\text{H-NMR}$ spectrum of compound **2a-Br** in CDCl_3 , 400 MHz, at 298 K; b) HRMS (ESI-MS) spectrum (m/z). Observed HRMS (left) with the theoretical isotope prediction (right).

a)



b)

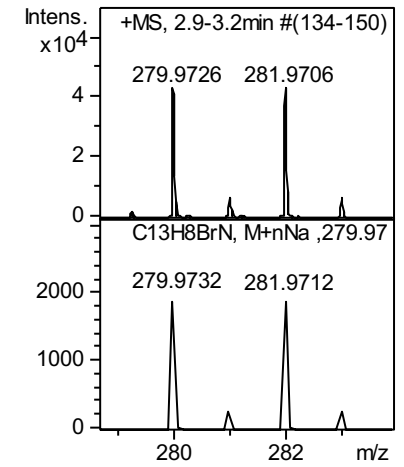
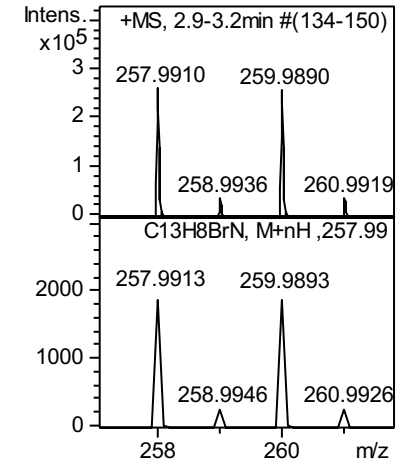
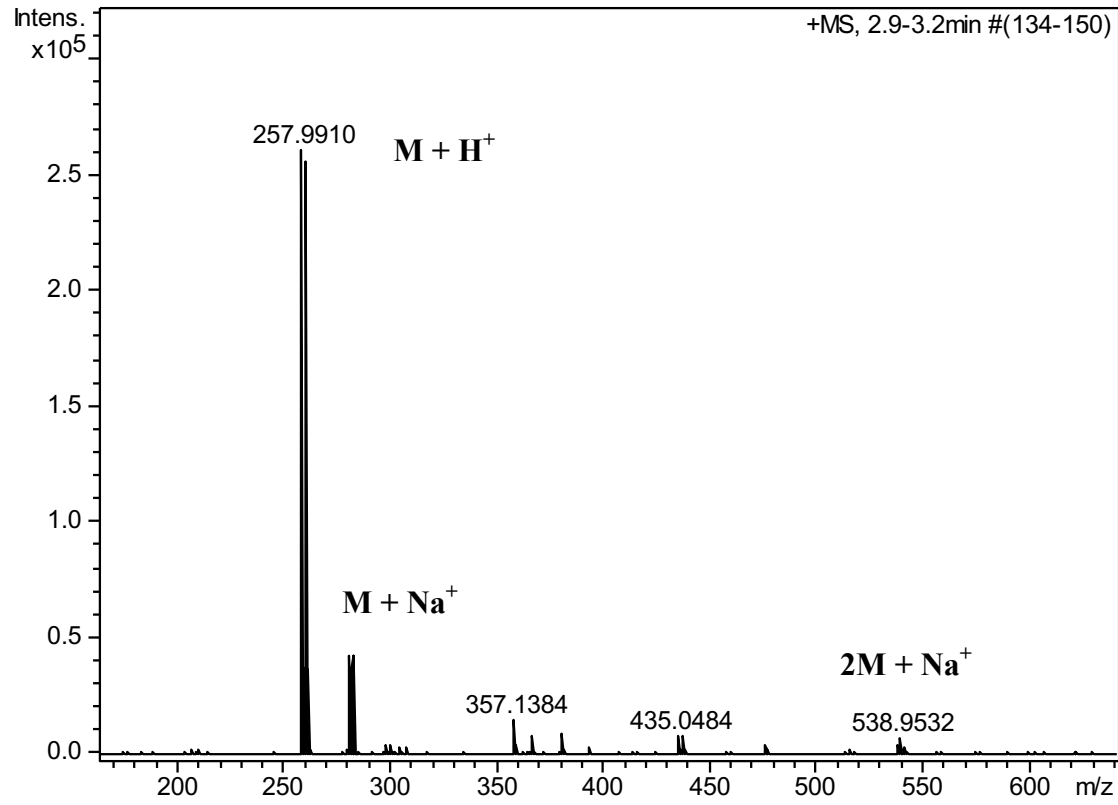
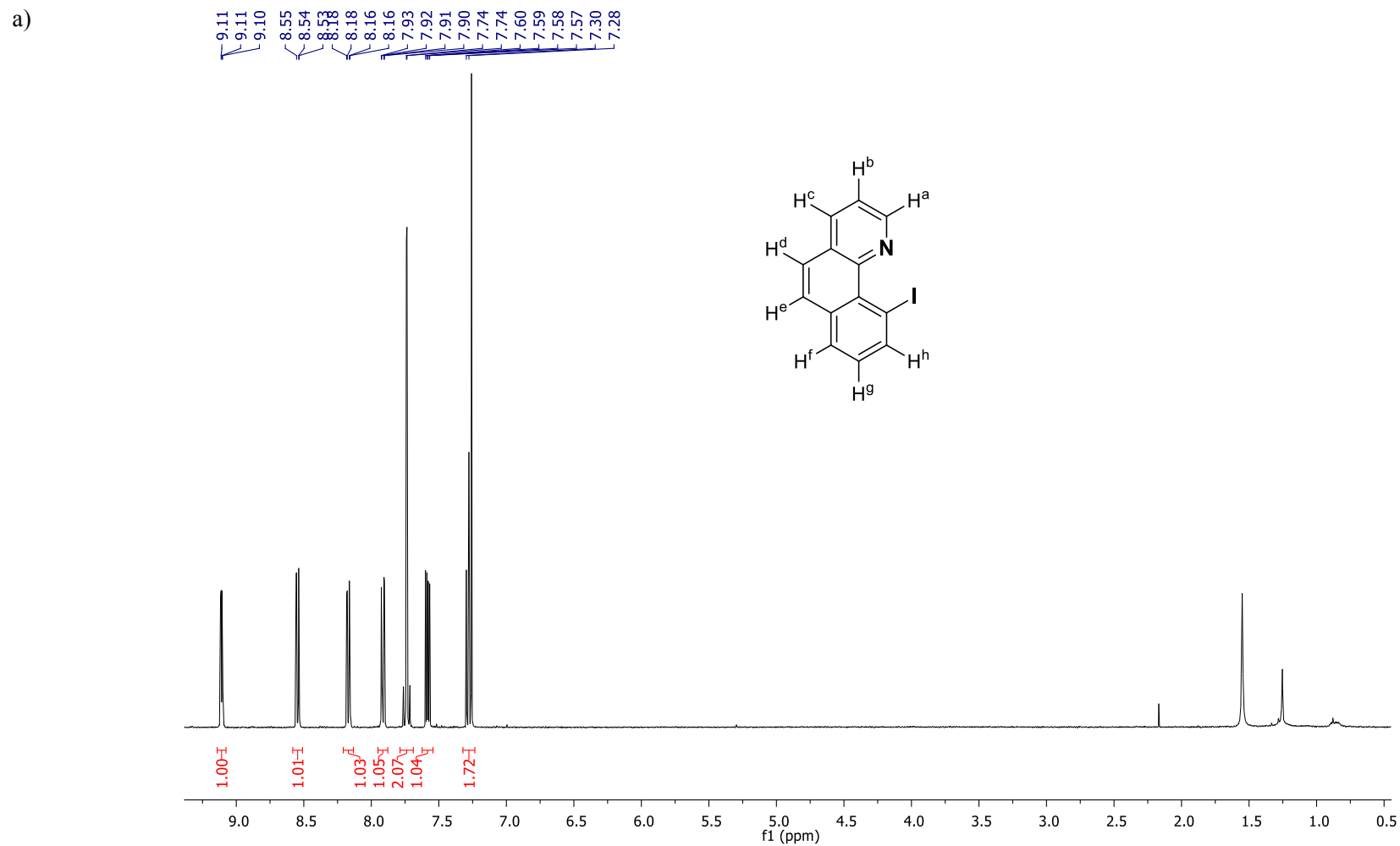
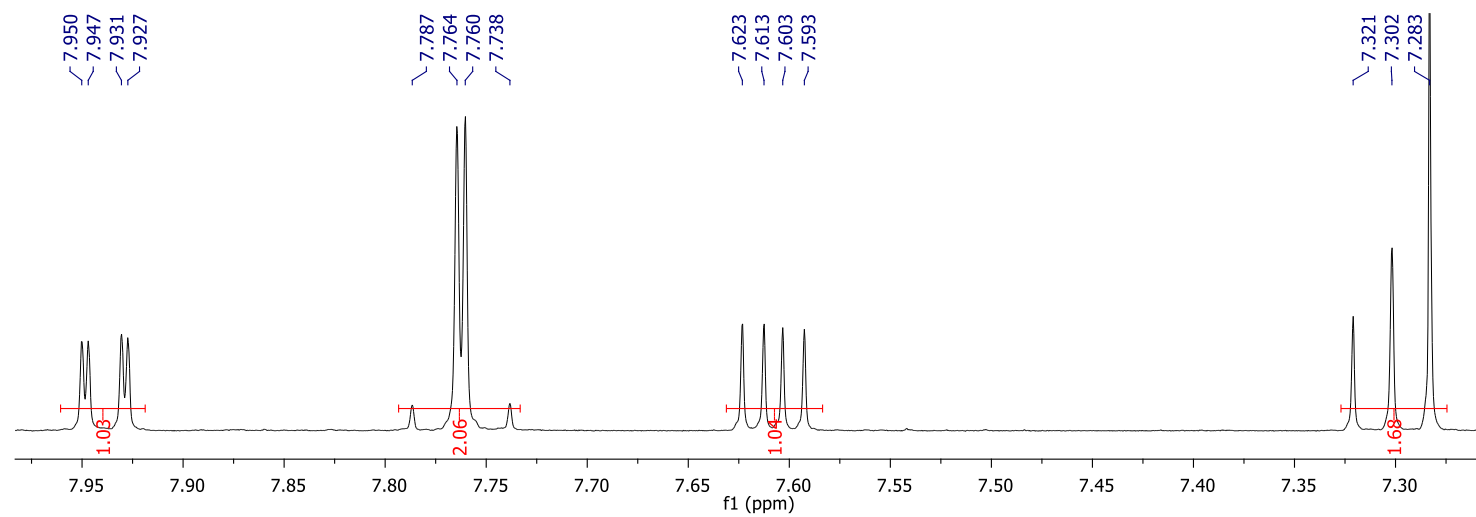
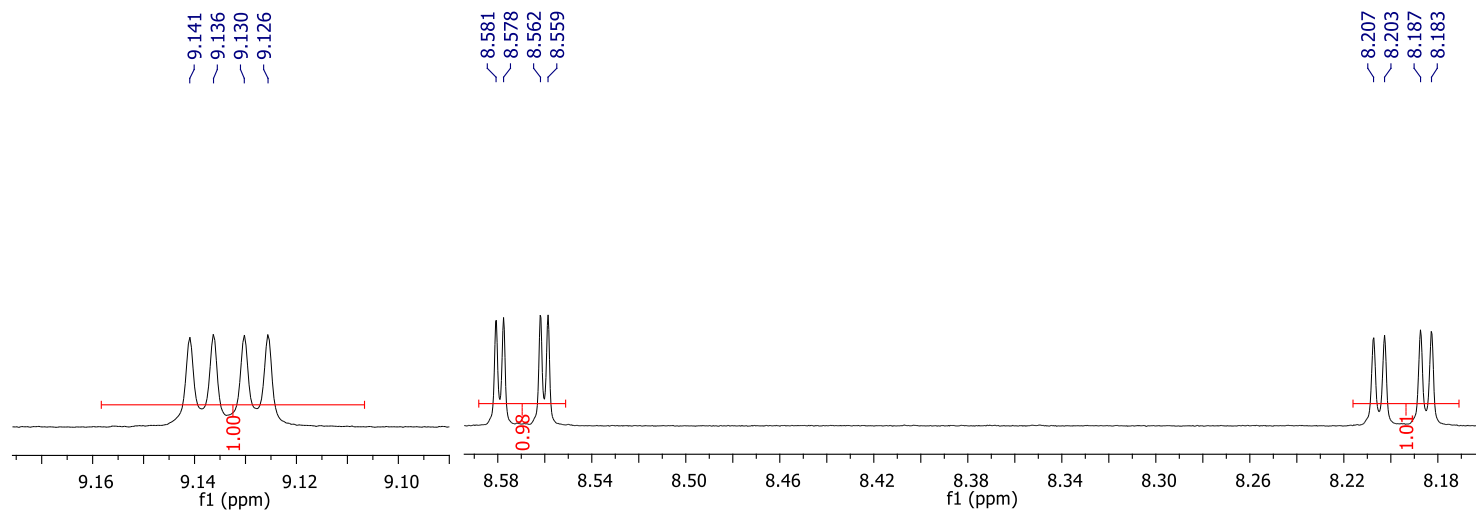


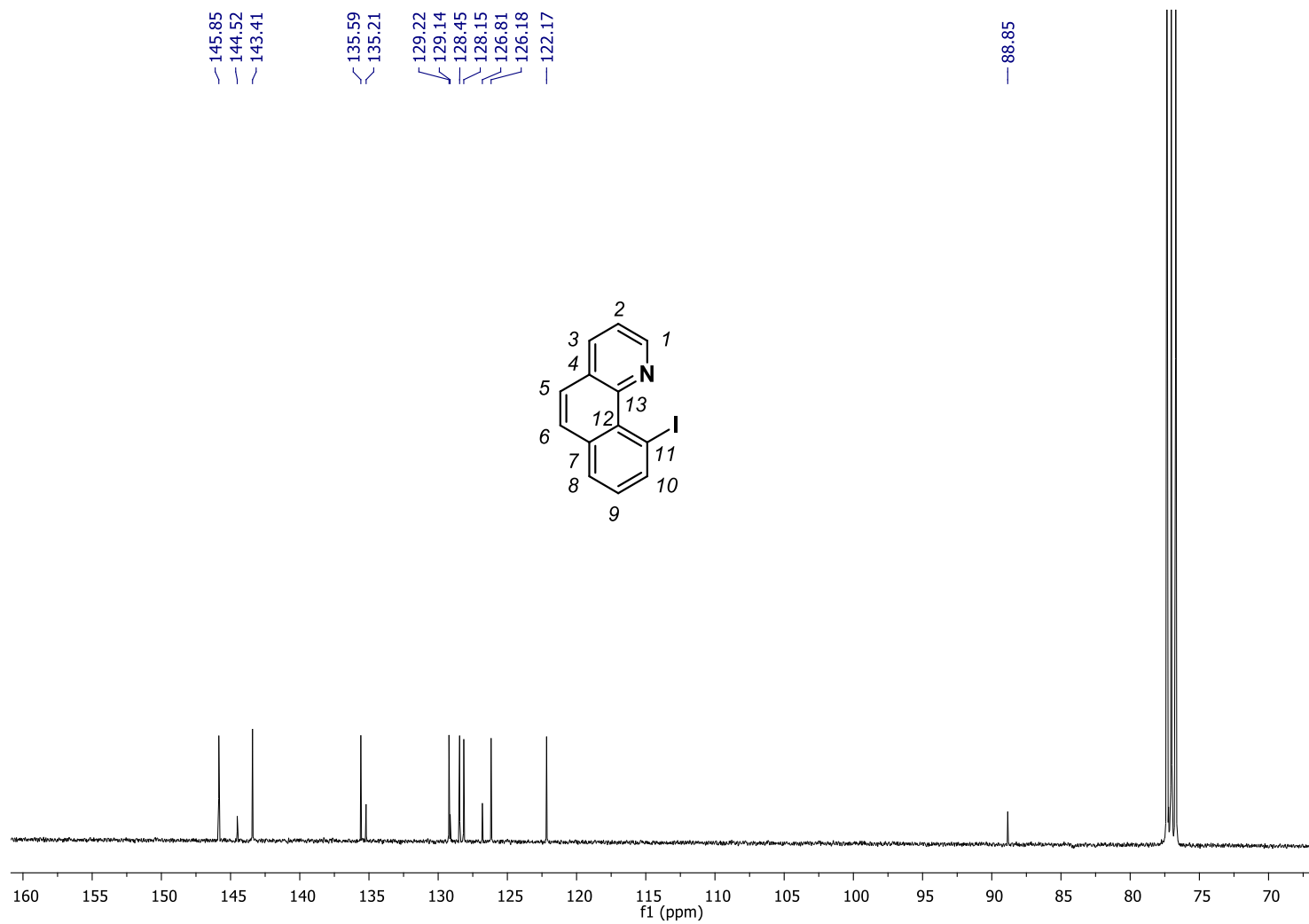
Figure S4. a) ^1H -NMR spectrum of compound **2a-I** in CDCl_3 , 400 MHz, at 298 K; b) $^{13}\text{C}\{^1\text{H}\}$ -NMR spectrum (CDCl_3 , 100 MHz, 298 K); c) ^1H - ^1H COSY spectrum (CDCl_3 , 100 MHz, 298 K); d) ^1H - ^{13}C HSQCed spectrum (CDCl_3 , 400 MHz, 298 K); e) ^1H - ^{13}C HMBC spectrum (CDCl_3 , 400 MHz, 298 K); f) HRMS (ESI-MS) spectrum (m/z). Observed HRMS (left) with the theoretical isotope prediction (right).



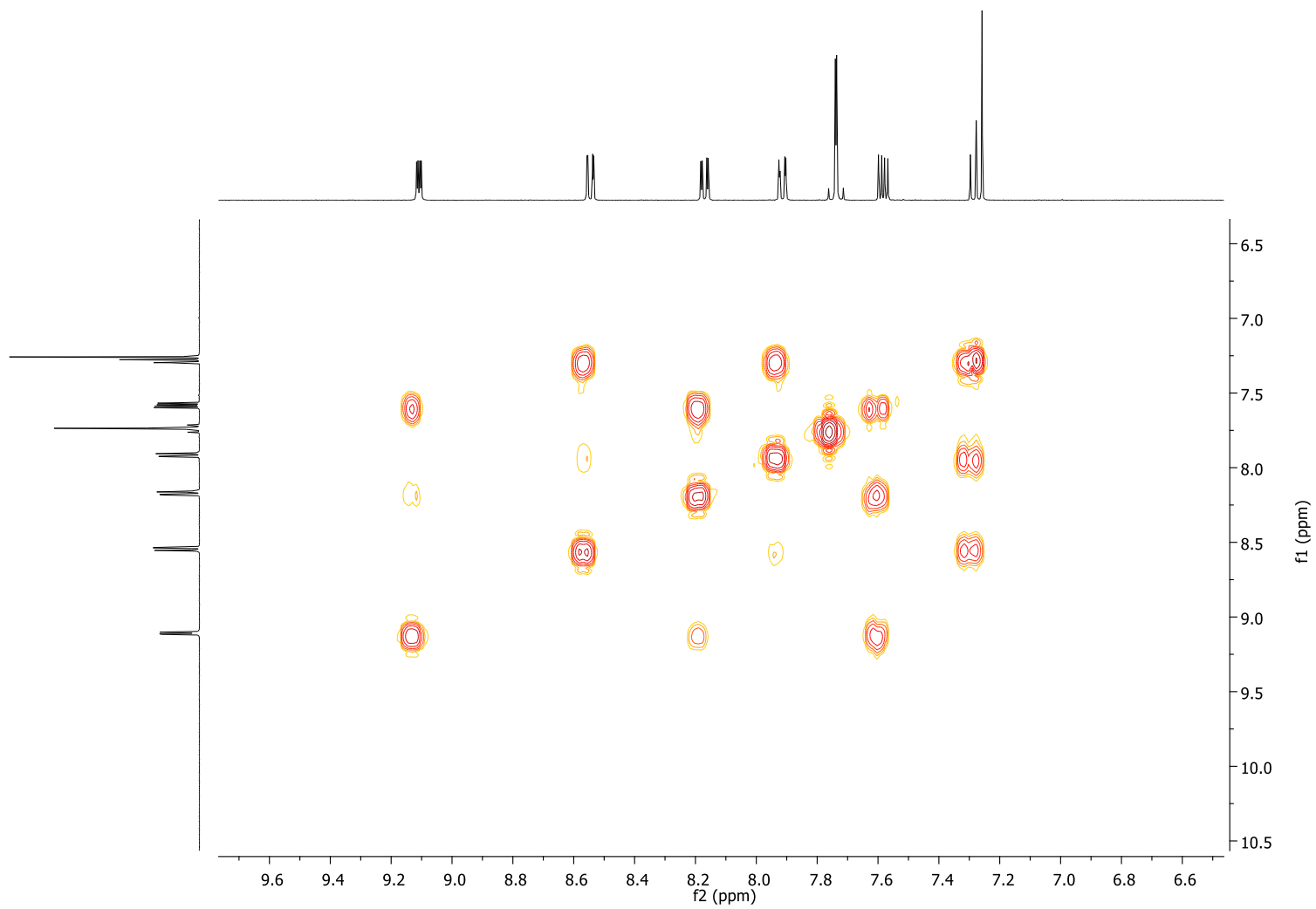


Selected aromatic region

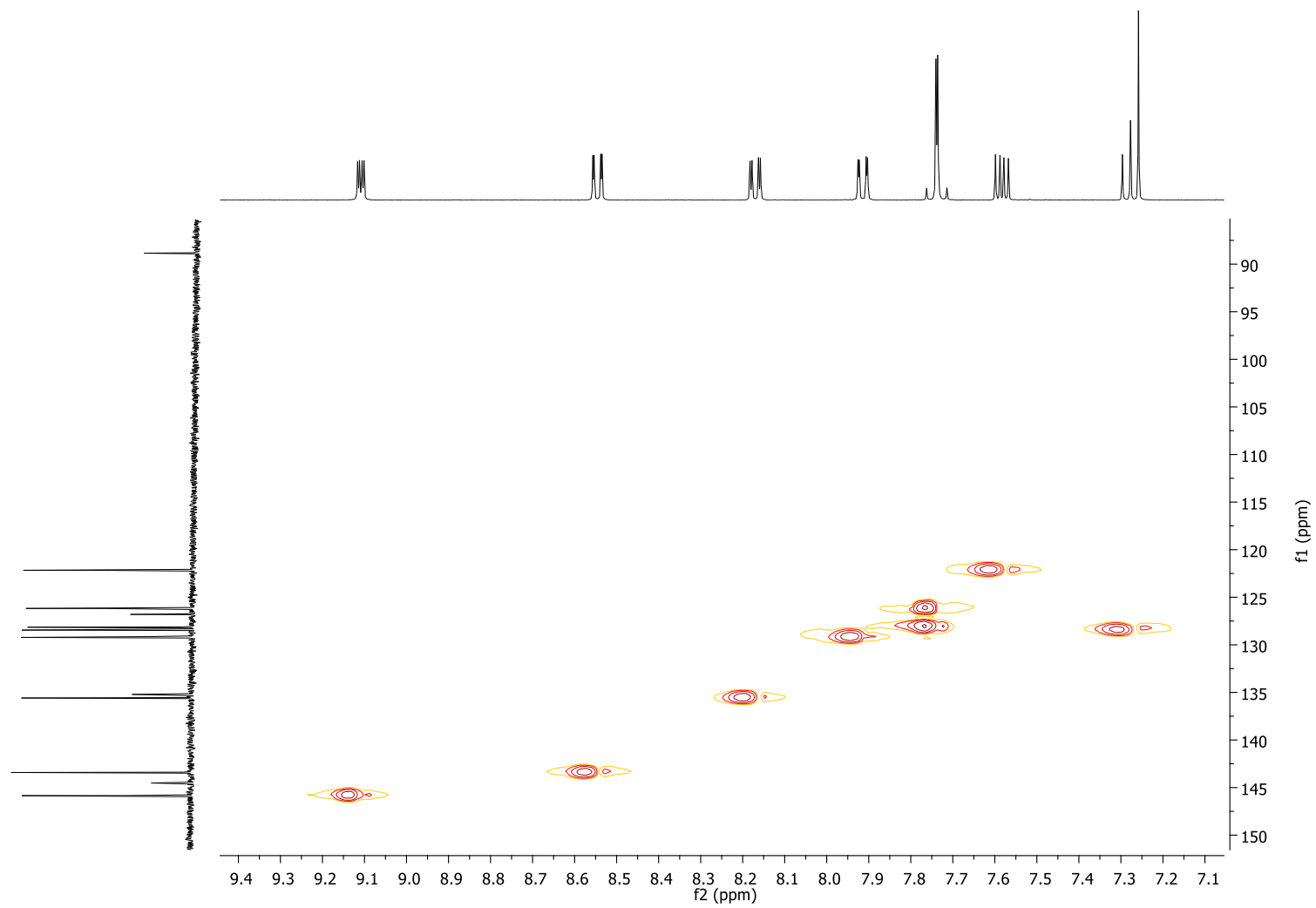
b)



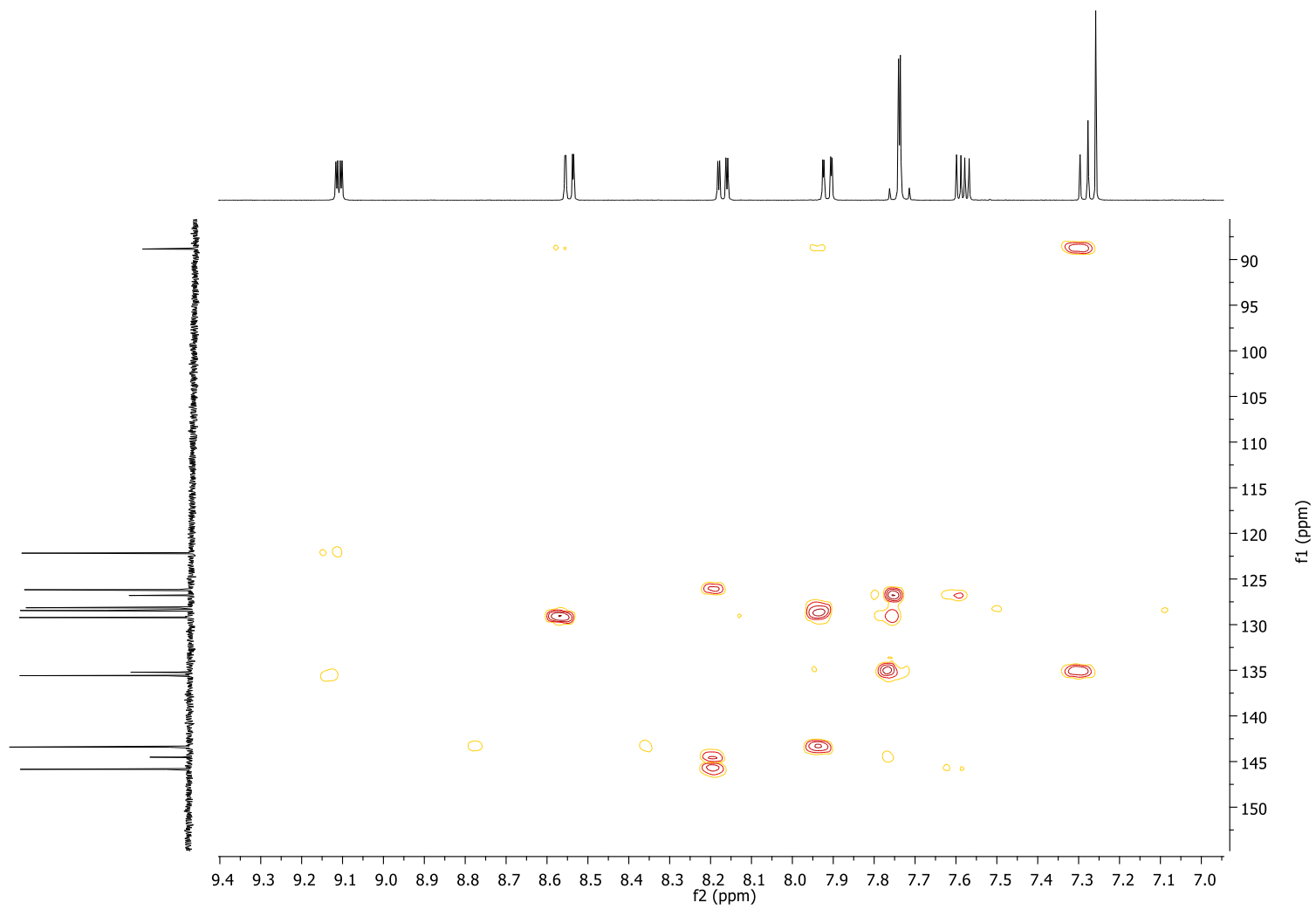
c)



d)



e)



f)

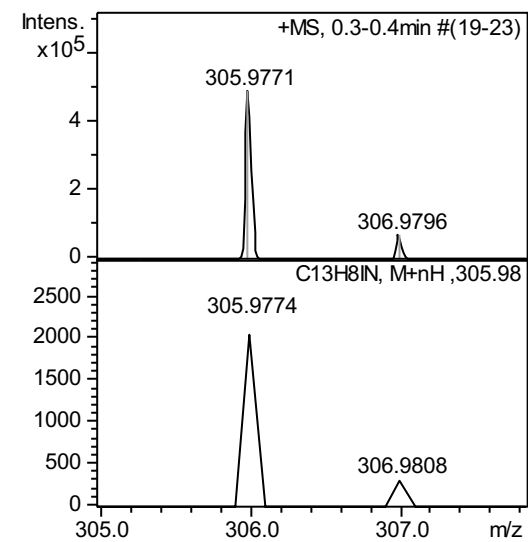
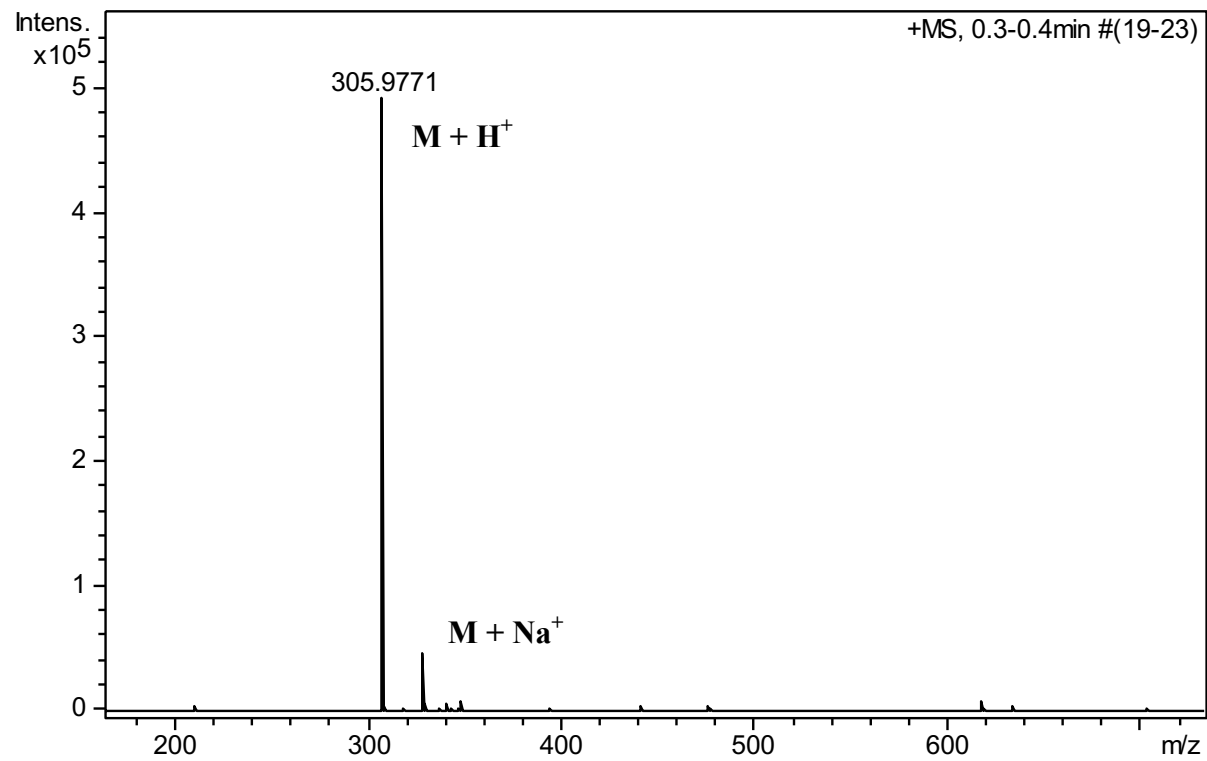
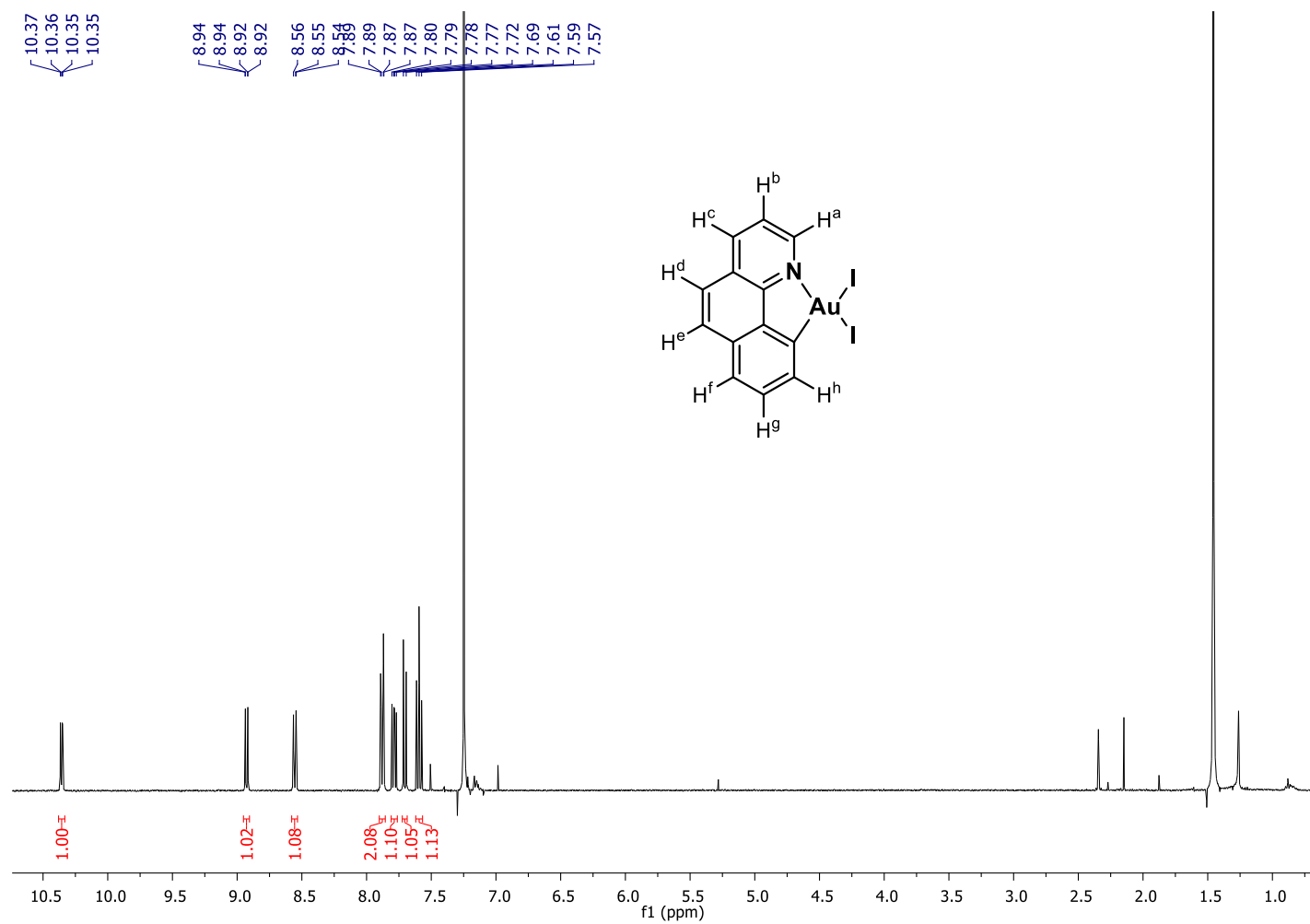
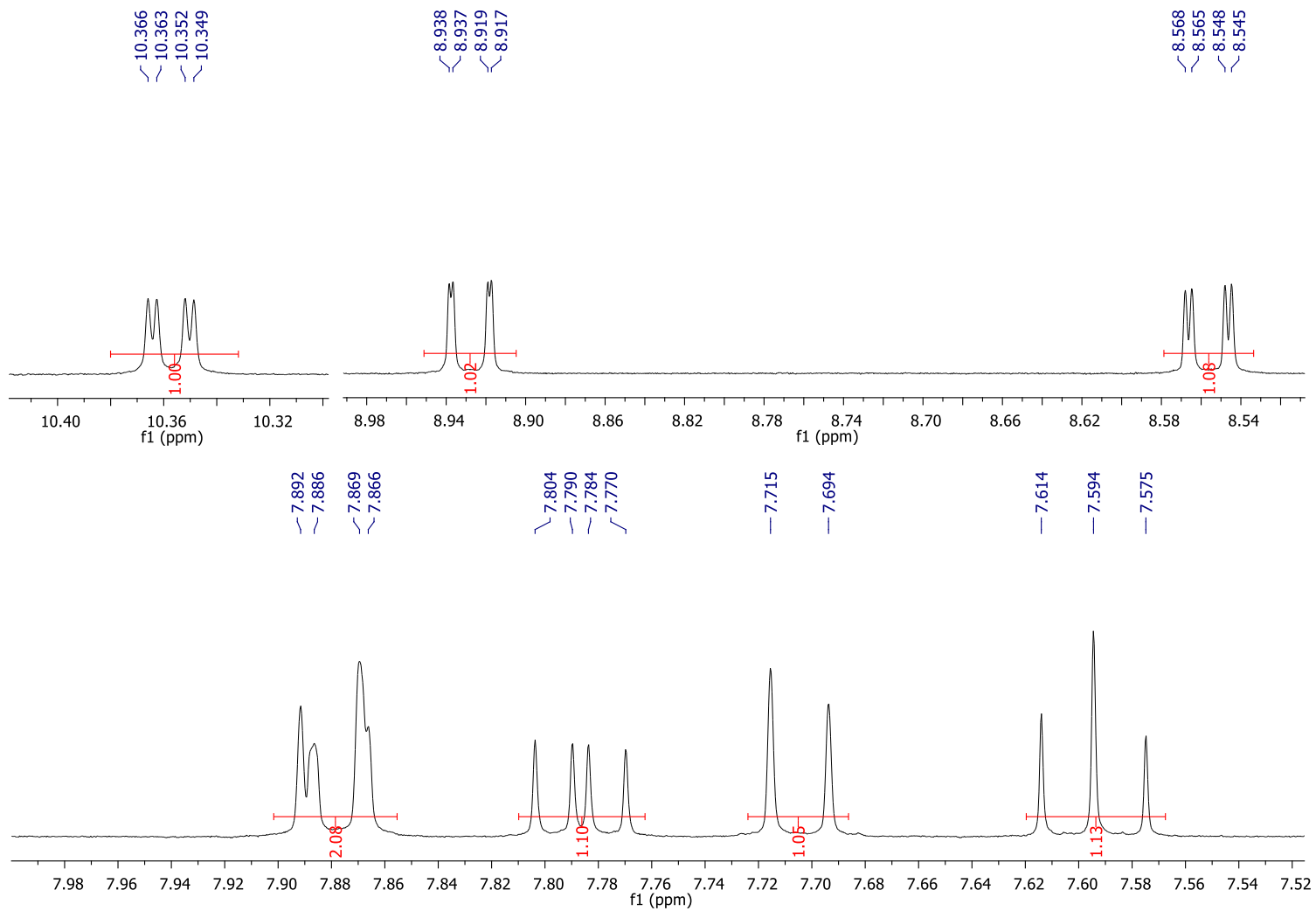


Figure S5. a) ^1H -NMR spectrum of complex **3a** in CDCl_3 , 400 MHz, at 323 K; b) $^{13}\text{C}\{^1\text{H}\}$ -NMR spectrum (CDCl_3 , 100 MHz, 323 K); c) ^1H - ^1H COSY spectrum (CDCl_3 , 100 MHz, 323 K); d) ^1H - ^{13}C HSQCed spectrum (CDCl_3 , 400 MHz, 323 K).

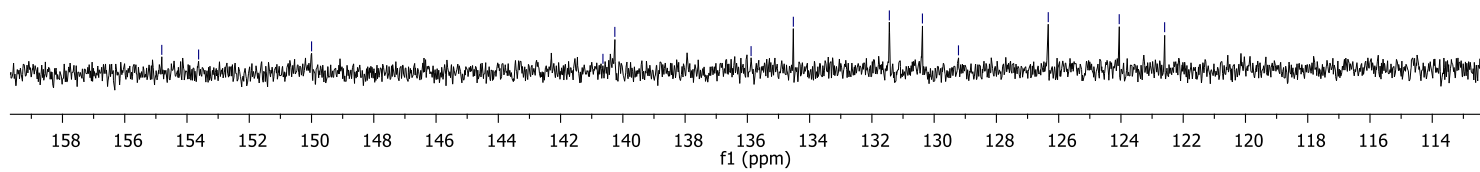
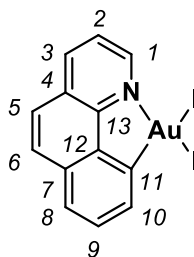
a)



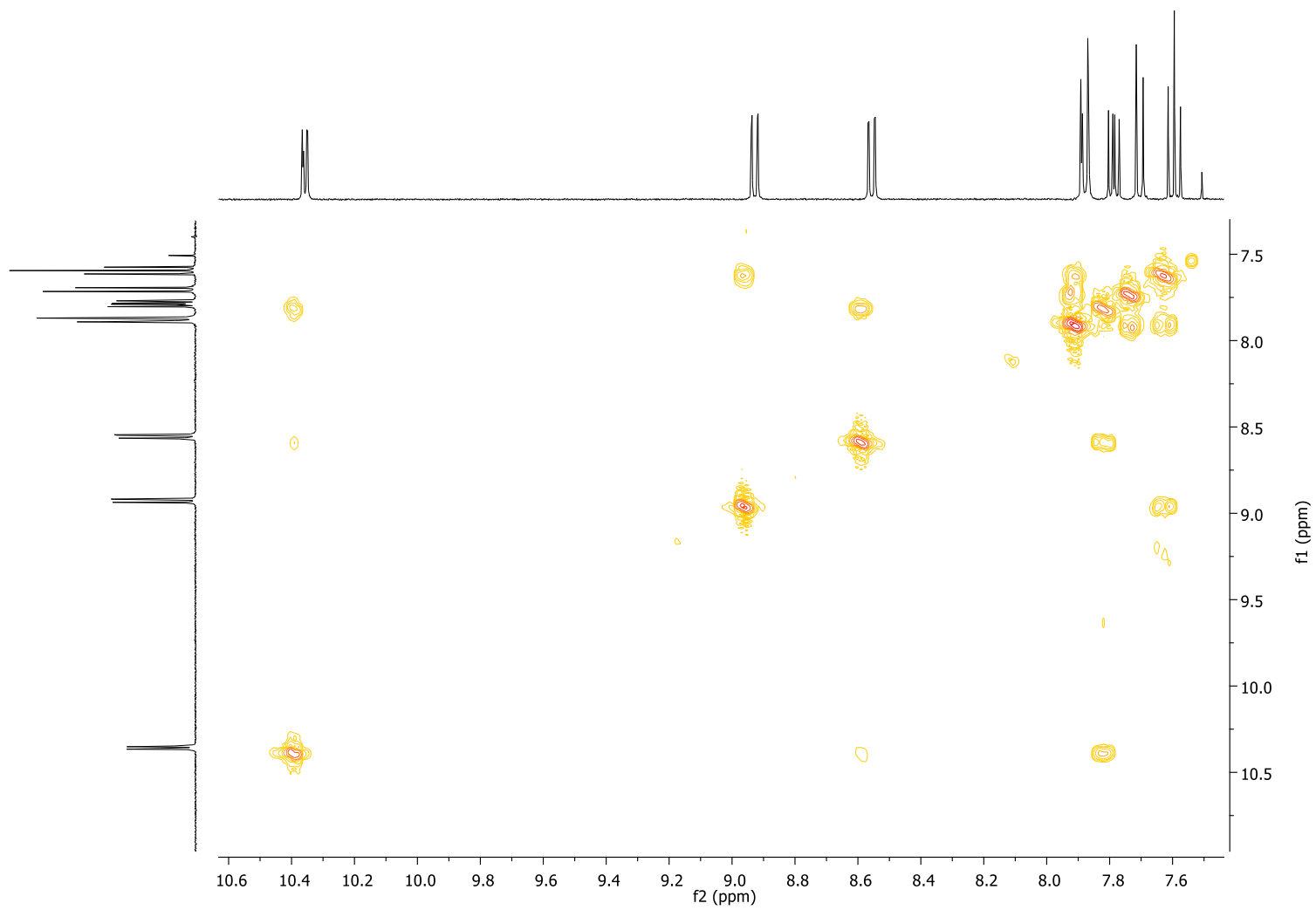


Selected aromatic region

b)



c)



d)

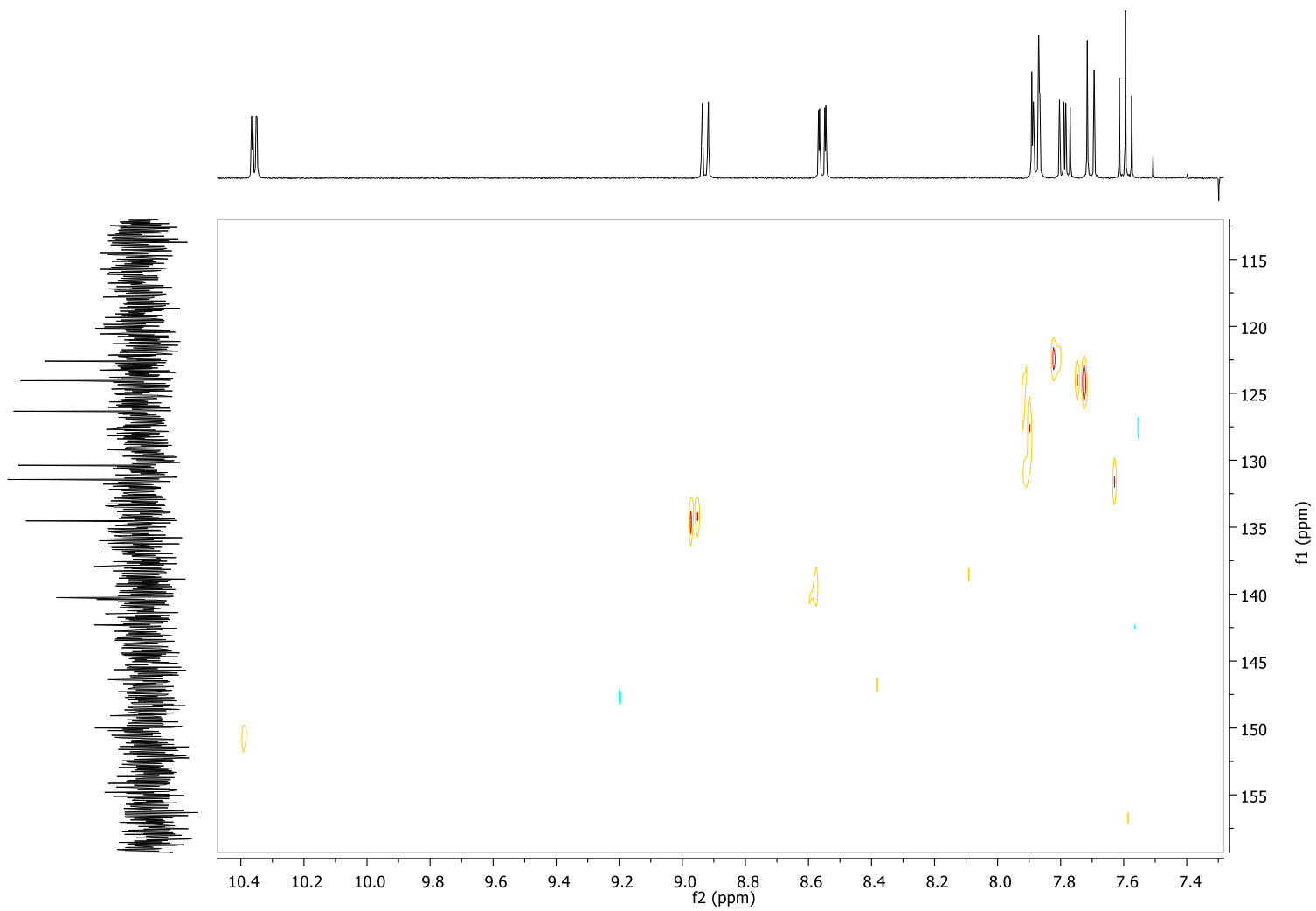
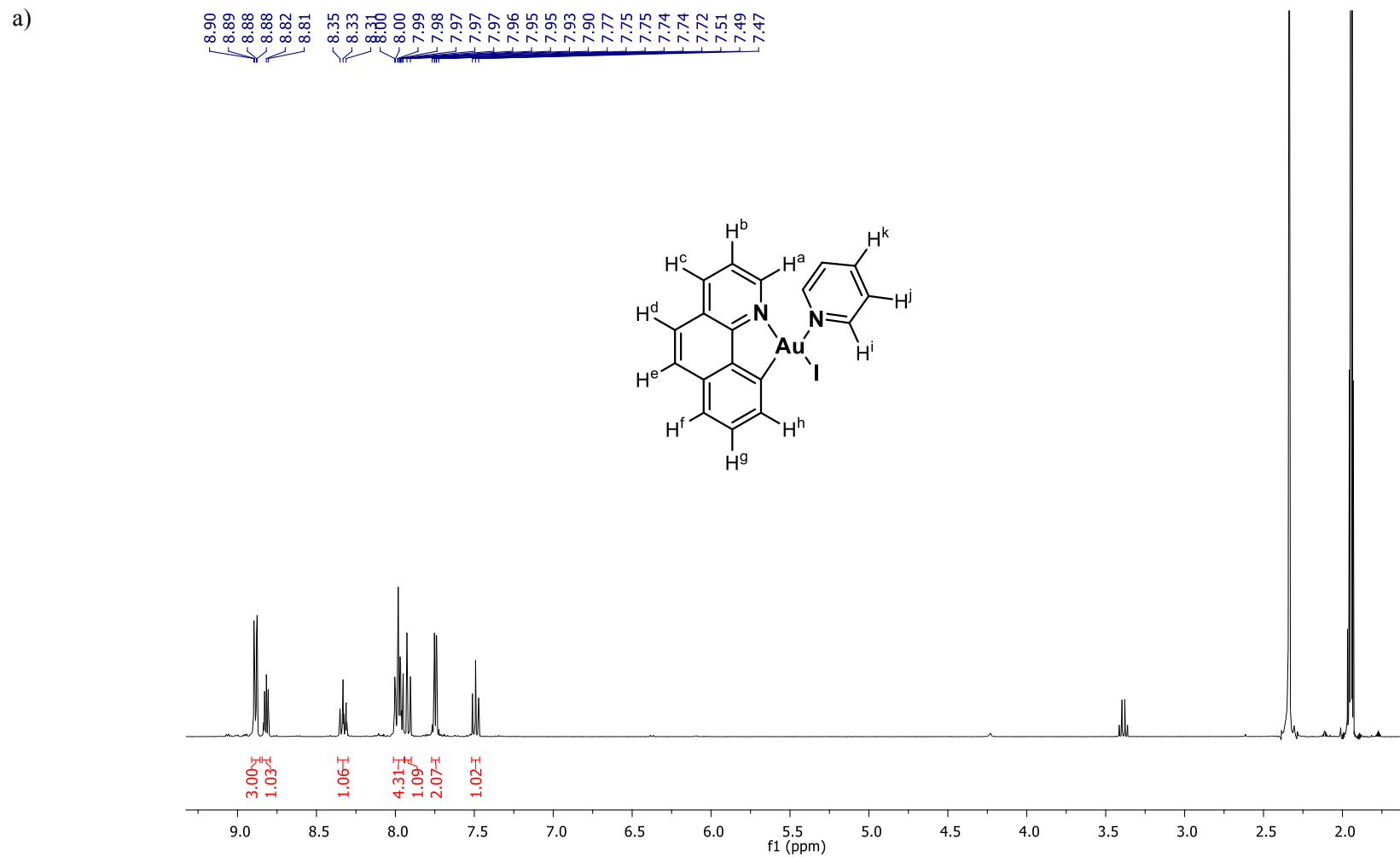
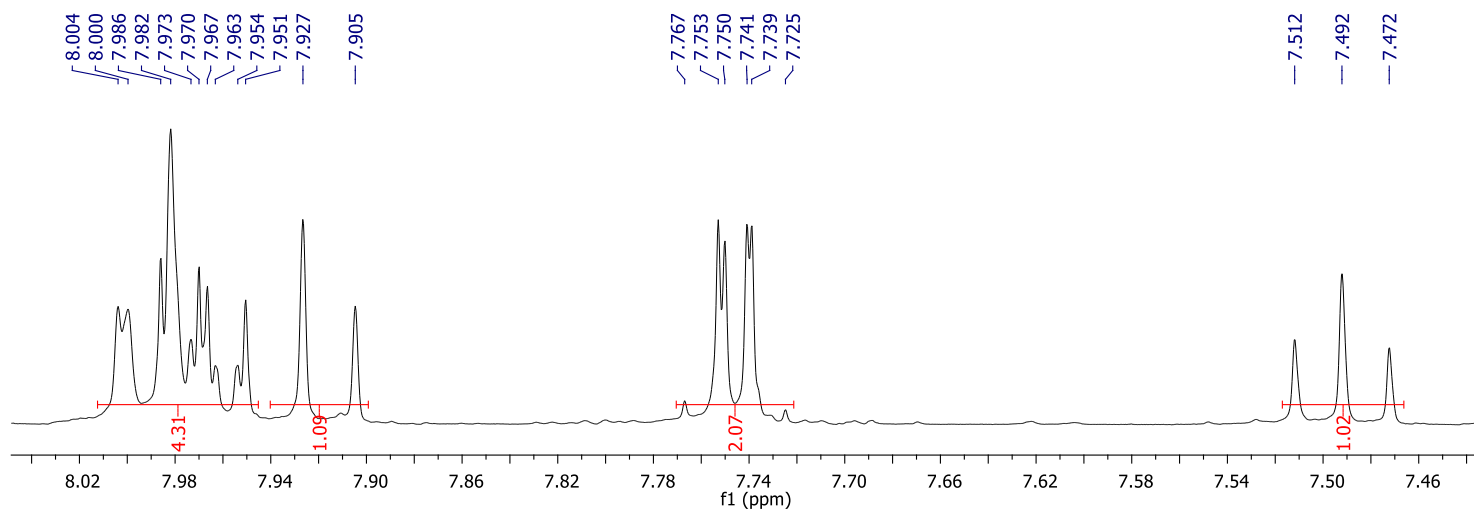
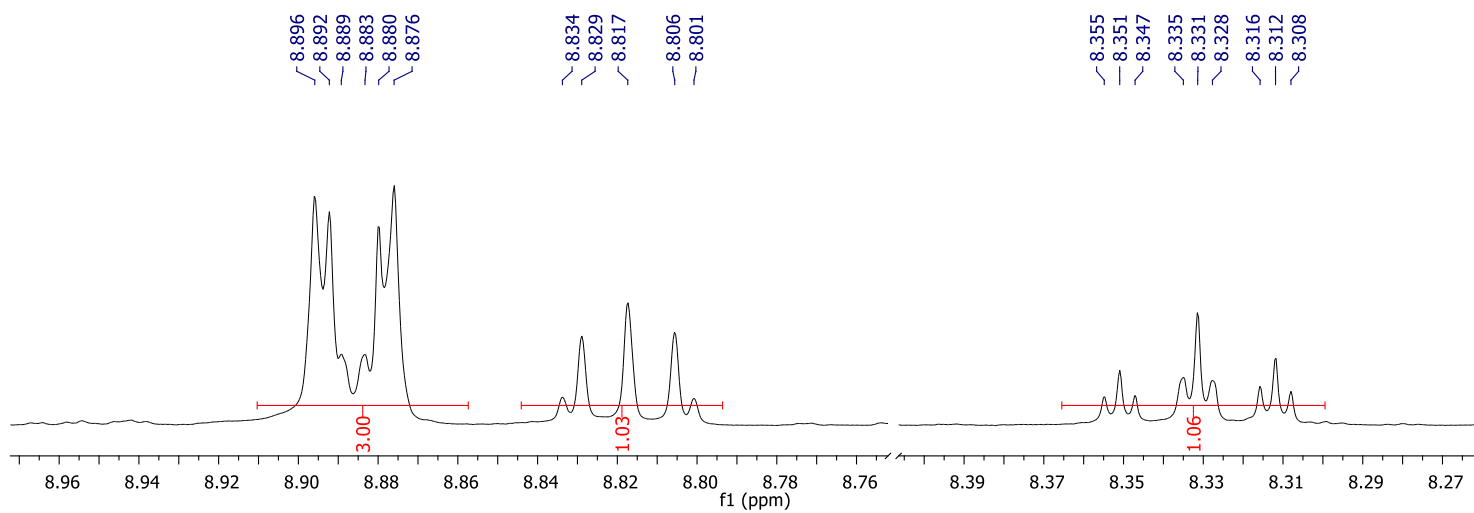


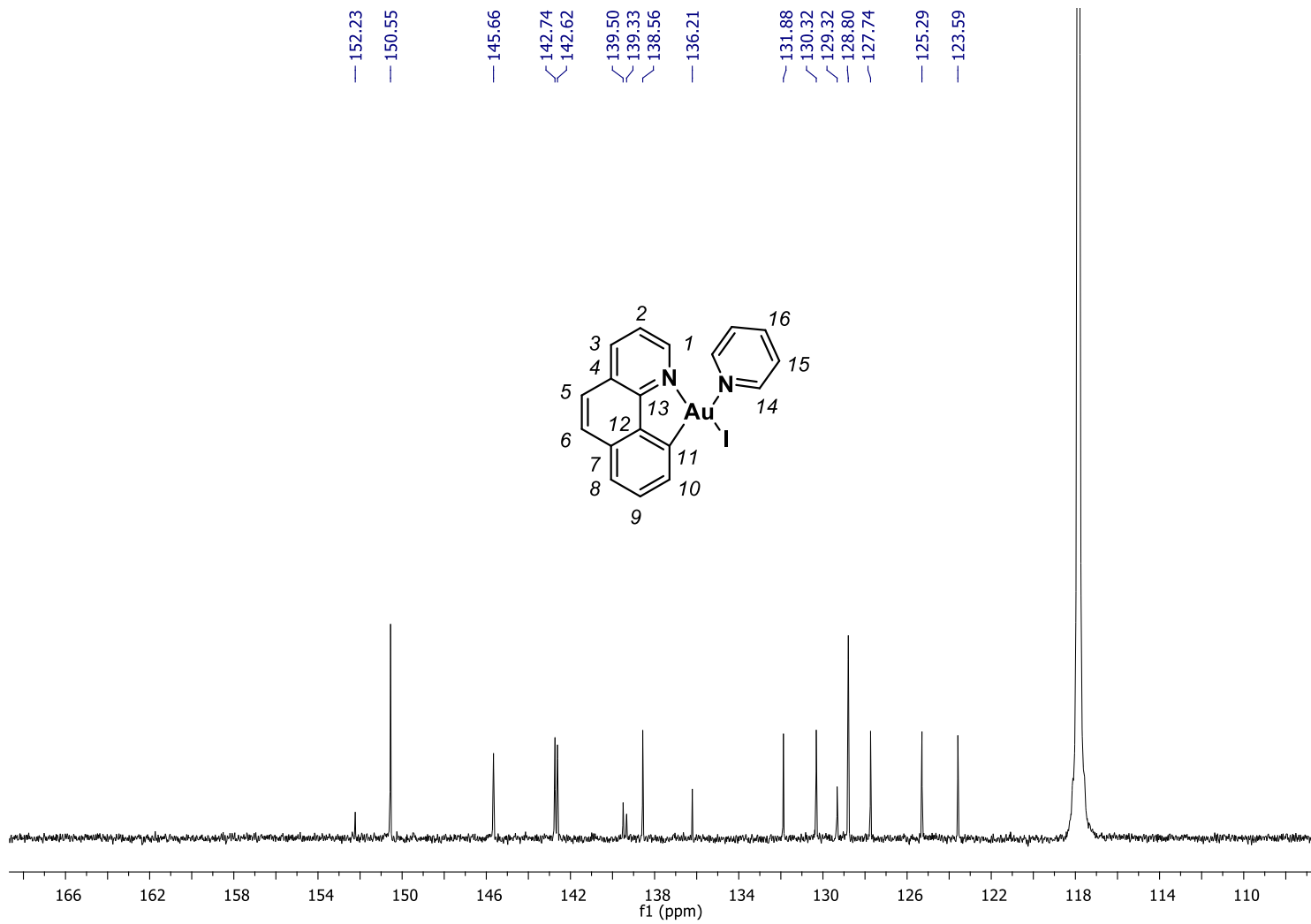
Figure S6. a) ^1H -NMR spectrum of complex **3b** in CDCl_3 , 400 MHz, at 248 K; b) $^{13}\text{C}\{^1\text{H}\}$ -NMR spectrum (CDCl_3 , 100 MHz, 248 K); c) ^1H - ^1H COSY spectrum (CDCl_3 , 100 MHz, 248 K); d) ^1H - ^{13}C HSQCed spectrum (CDCl_3 , 400 MHz, 248 K); e) ^1H - ^{13}C HMBC spectrum (CDCl_3 , 400 MHz, 248 K); f) HRMS (ESI-MS) spectrum (m/z). Observed HRMS (top) with the theoretical isotope prediction (bottom).



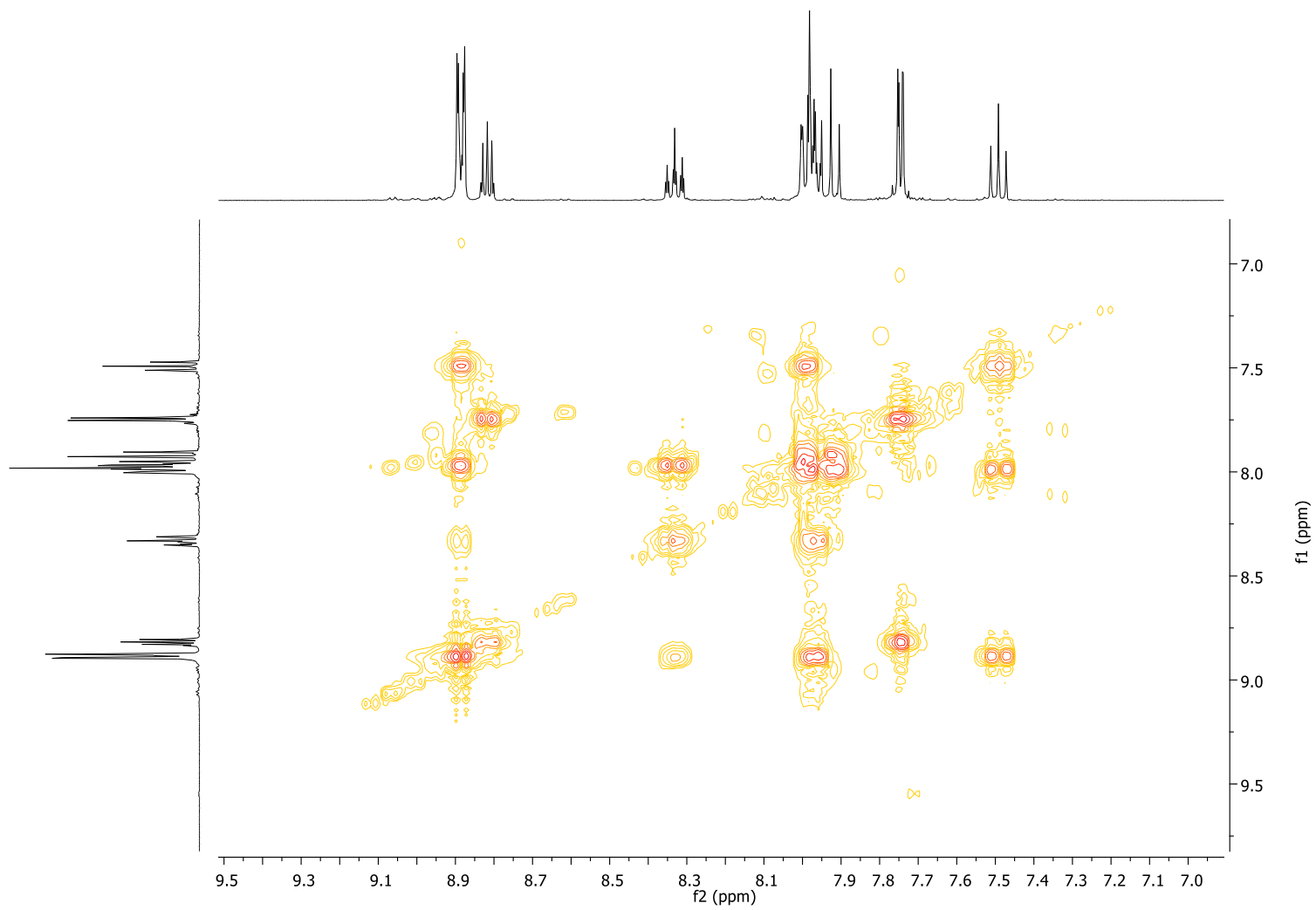


Selected aromatic region

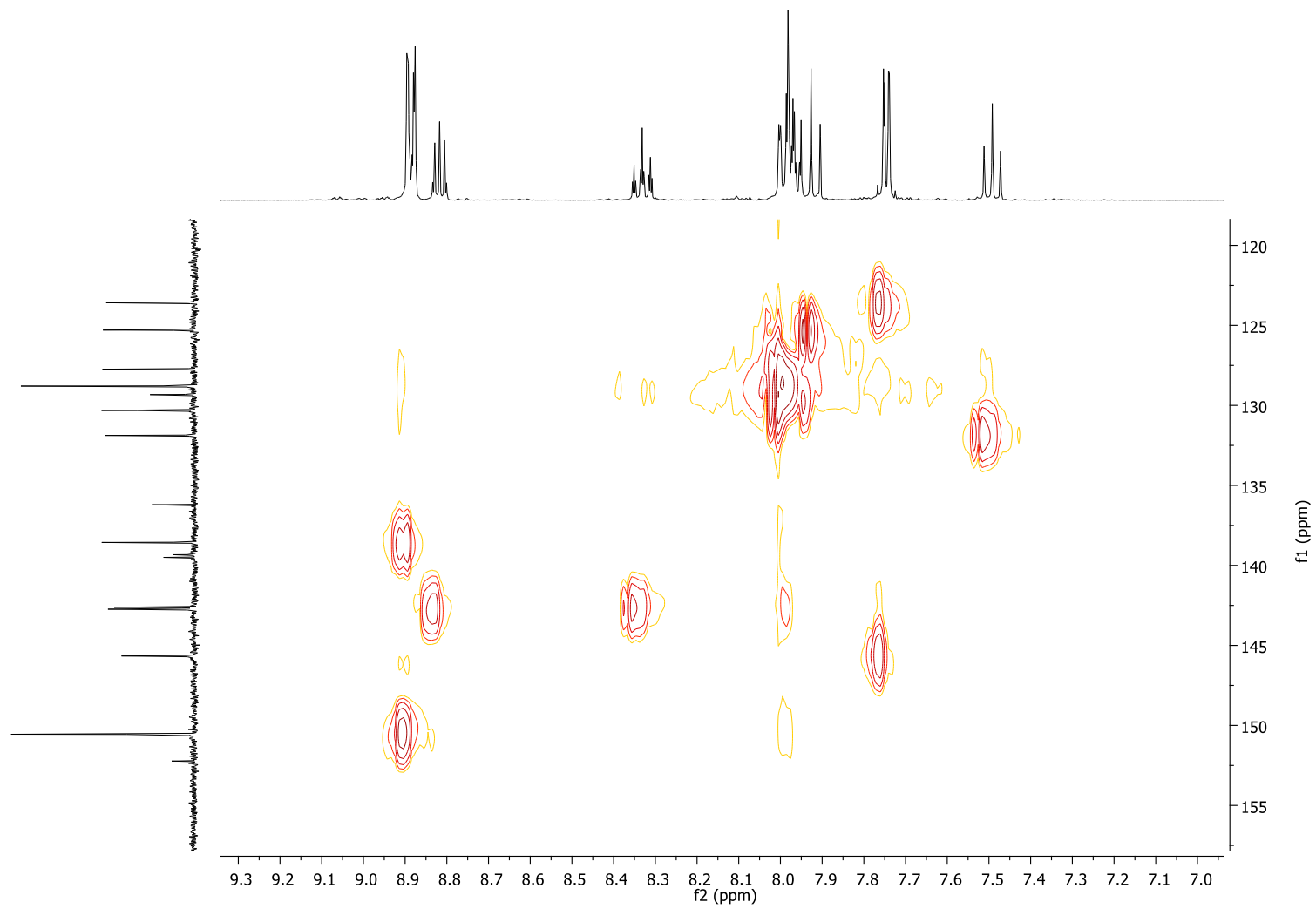
b)



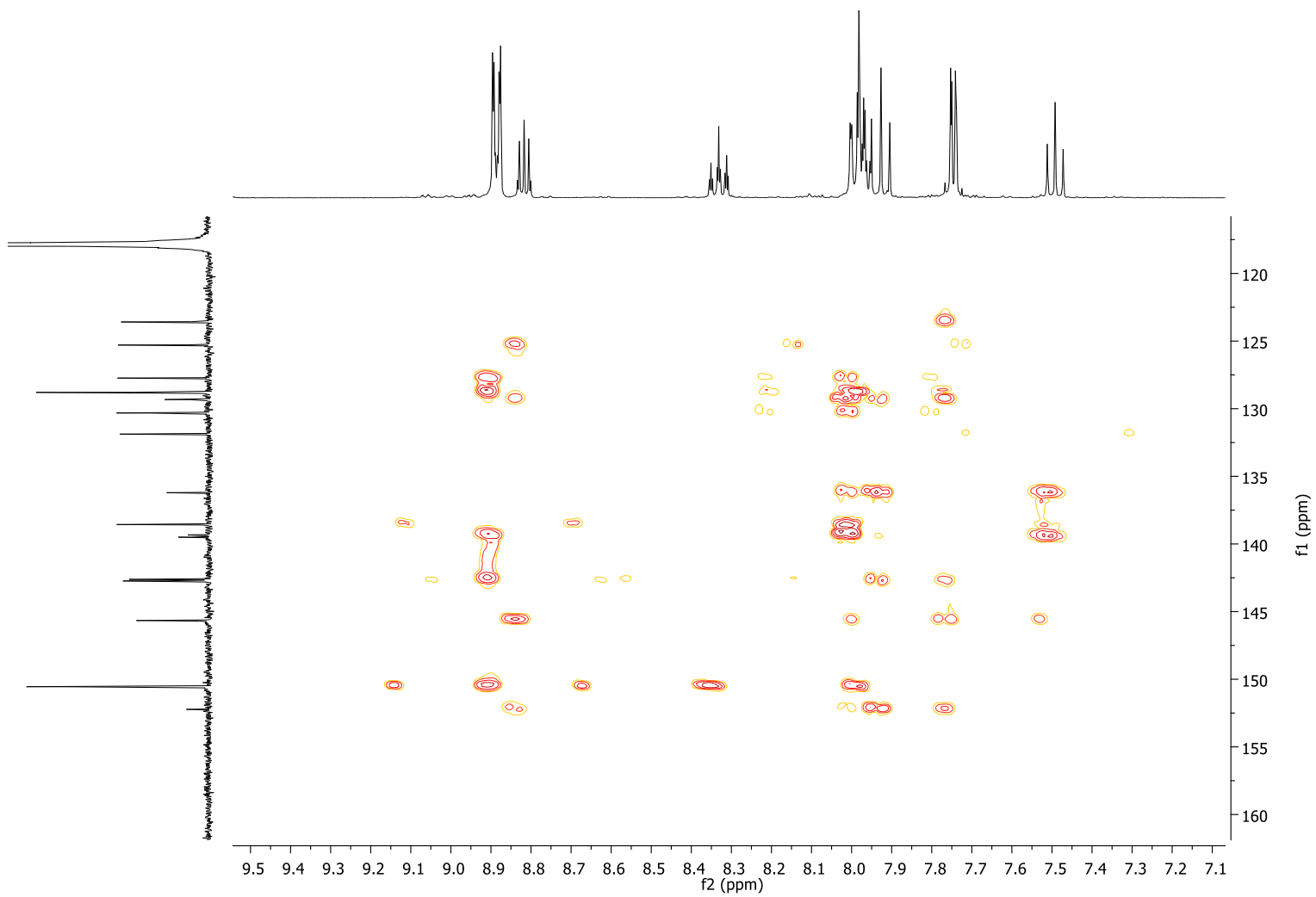
c)



d)



e)



f)

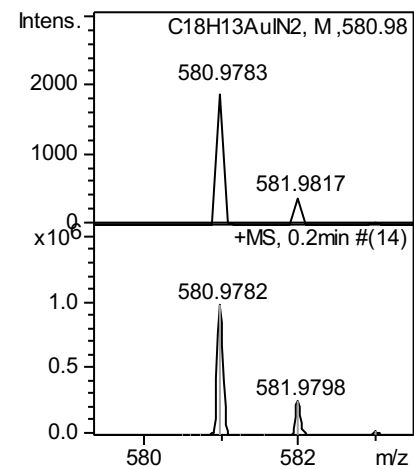
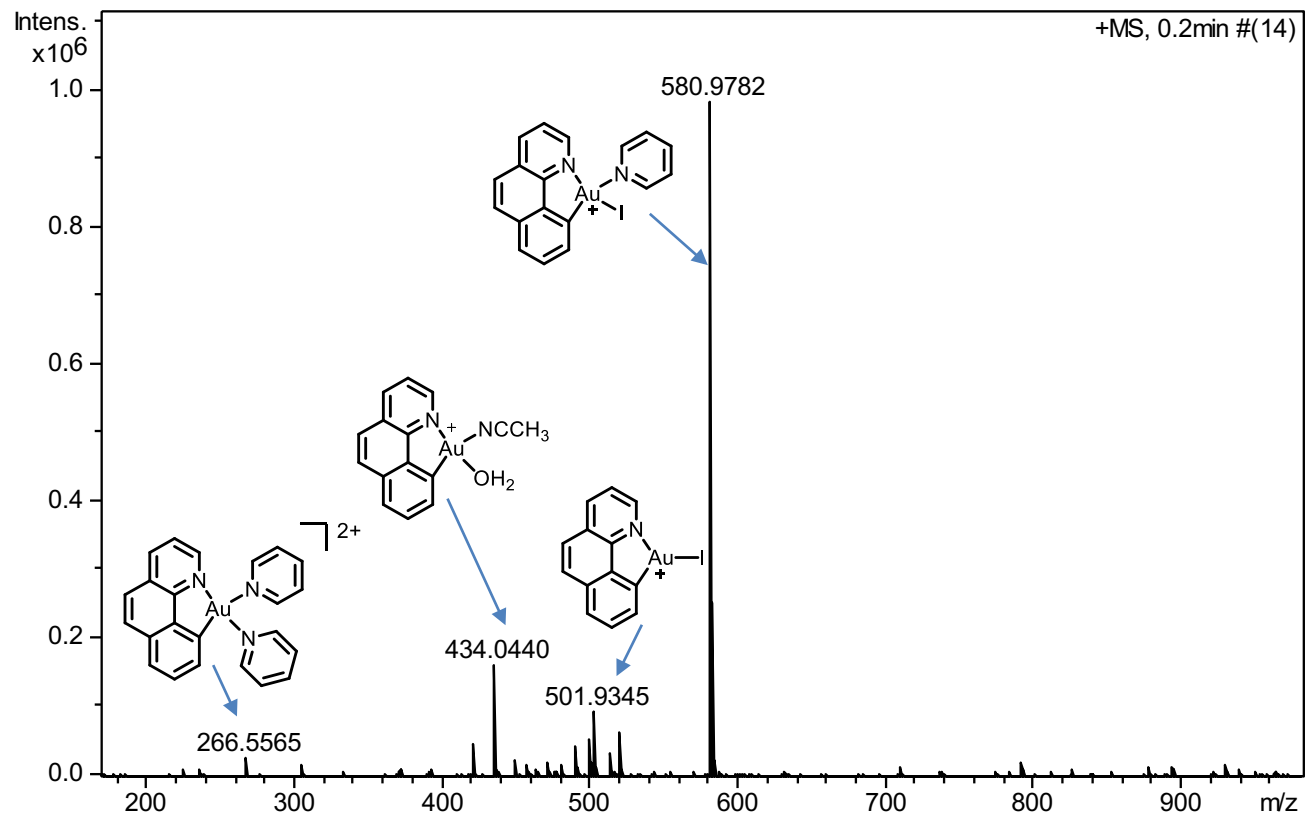
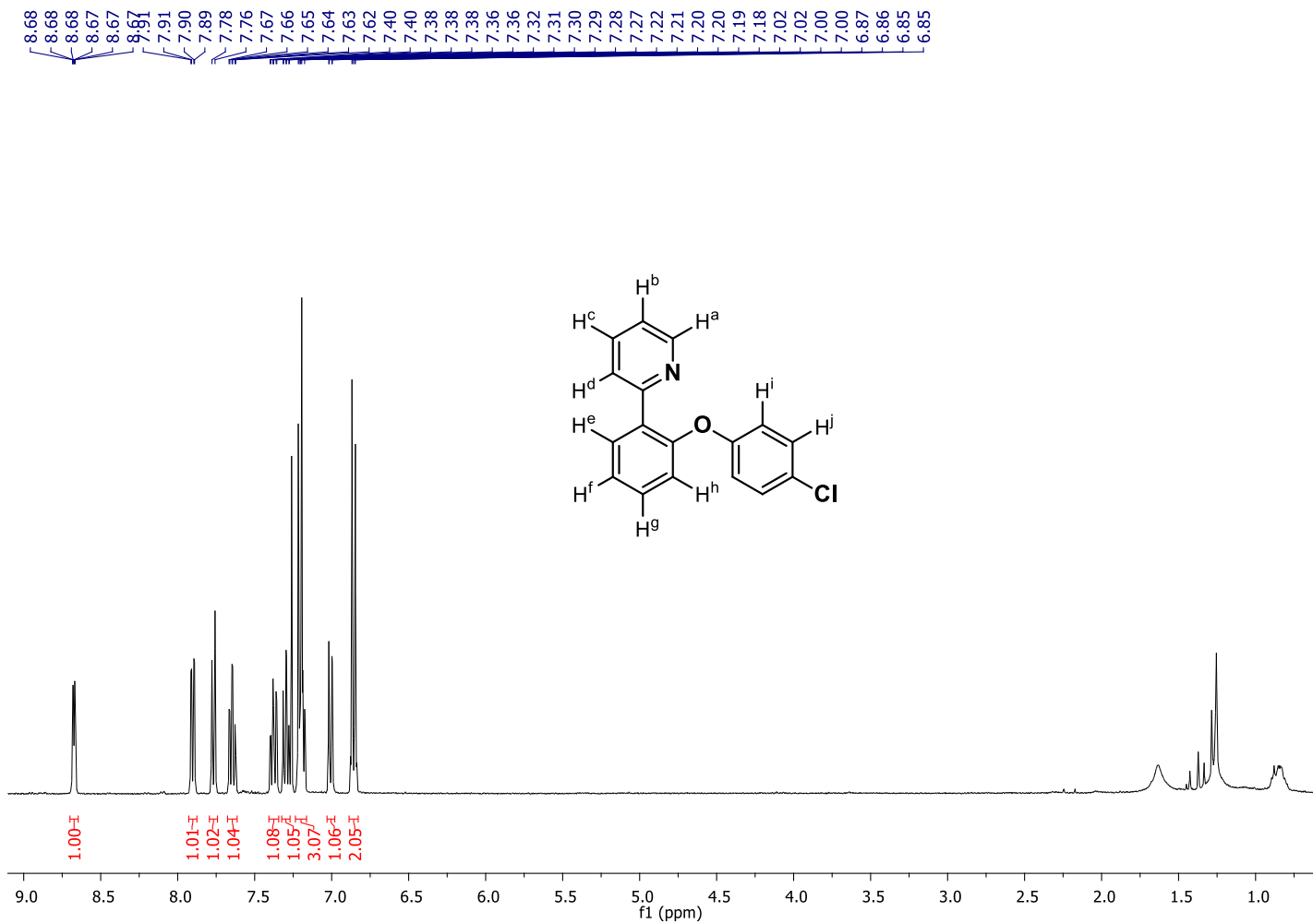


Figure S7. a) $^1\text{H-NMR}$ spectrum of compound **1aa** in CDCl_3 , 400 MHz, at 298 K; b) HRMS (ESI-MS) spectrum (m/z). Observed HRMS (left) with the theoretical isotope prediction (right).

a)



b)

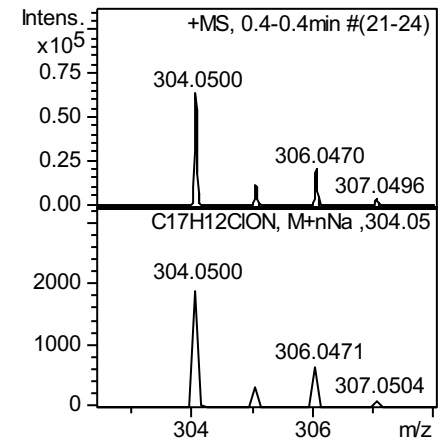
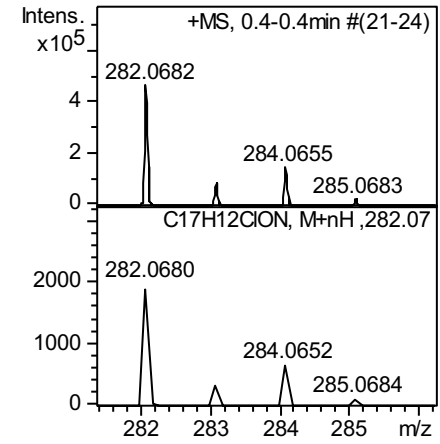
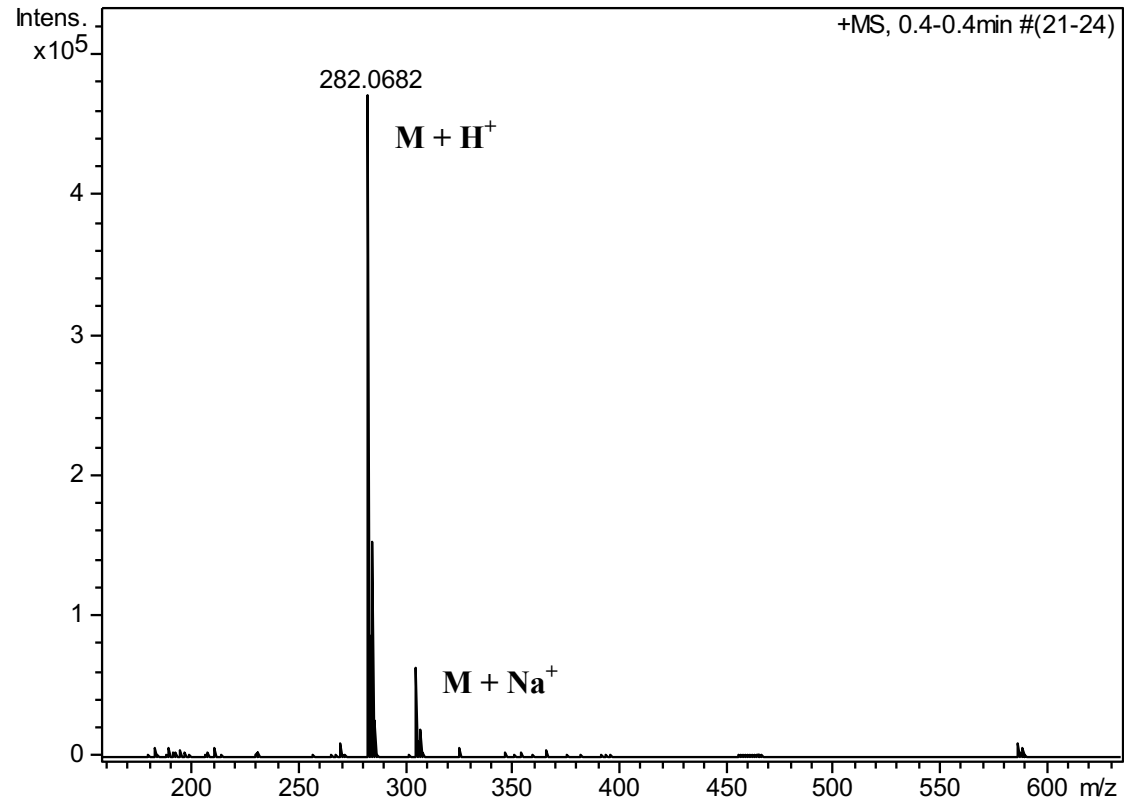
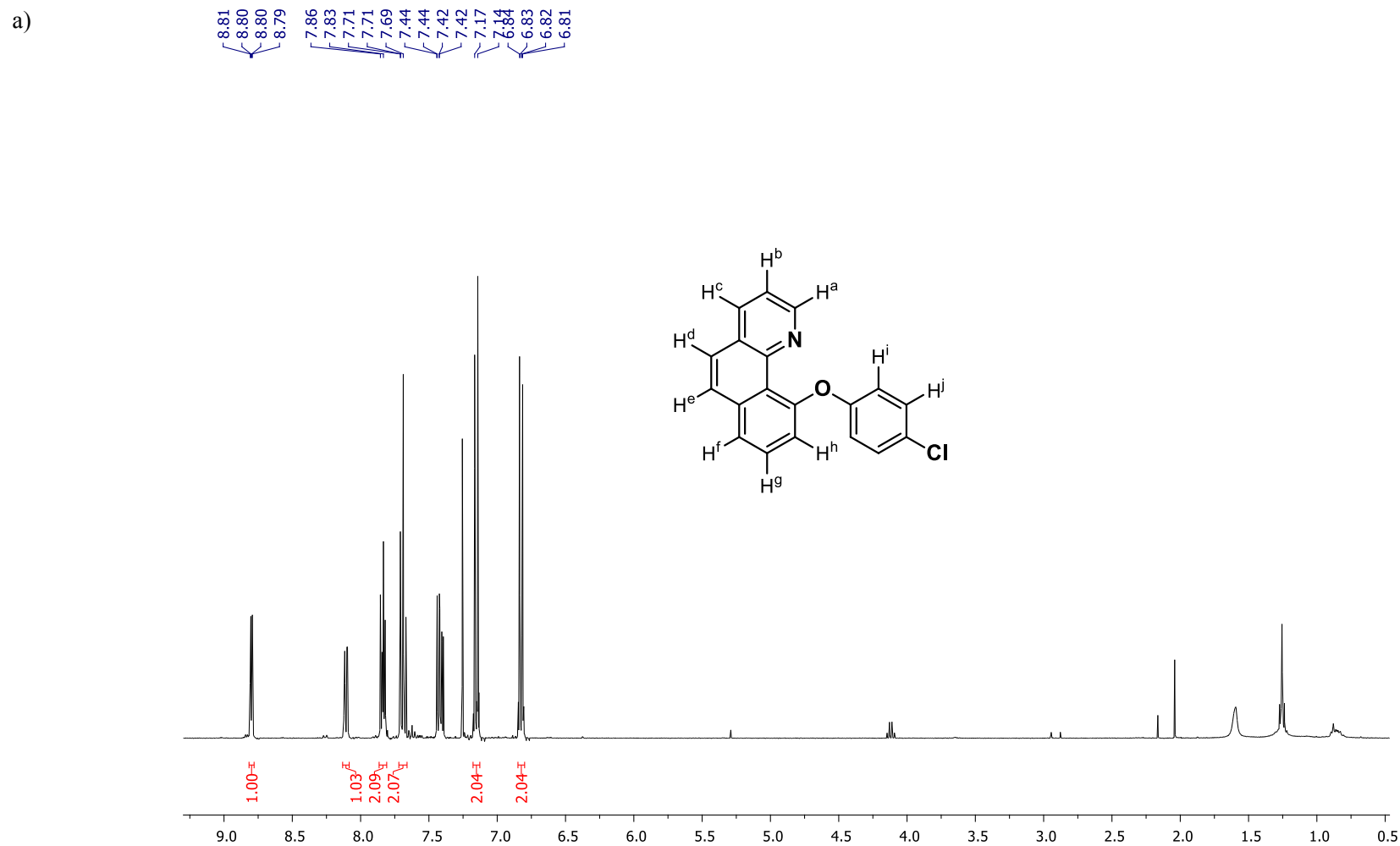
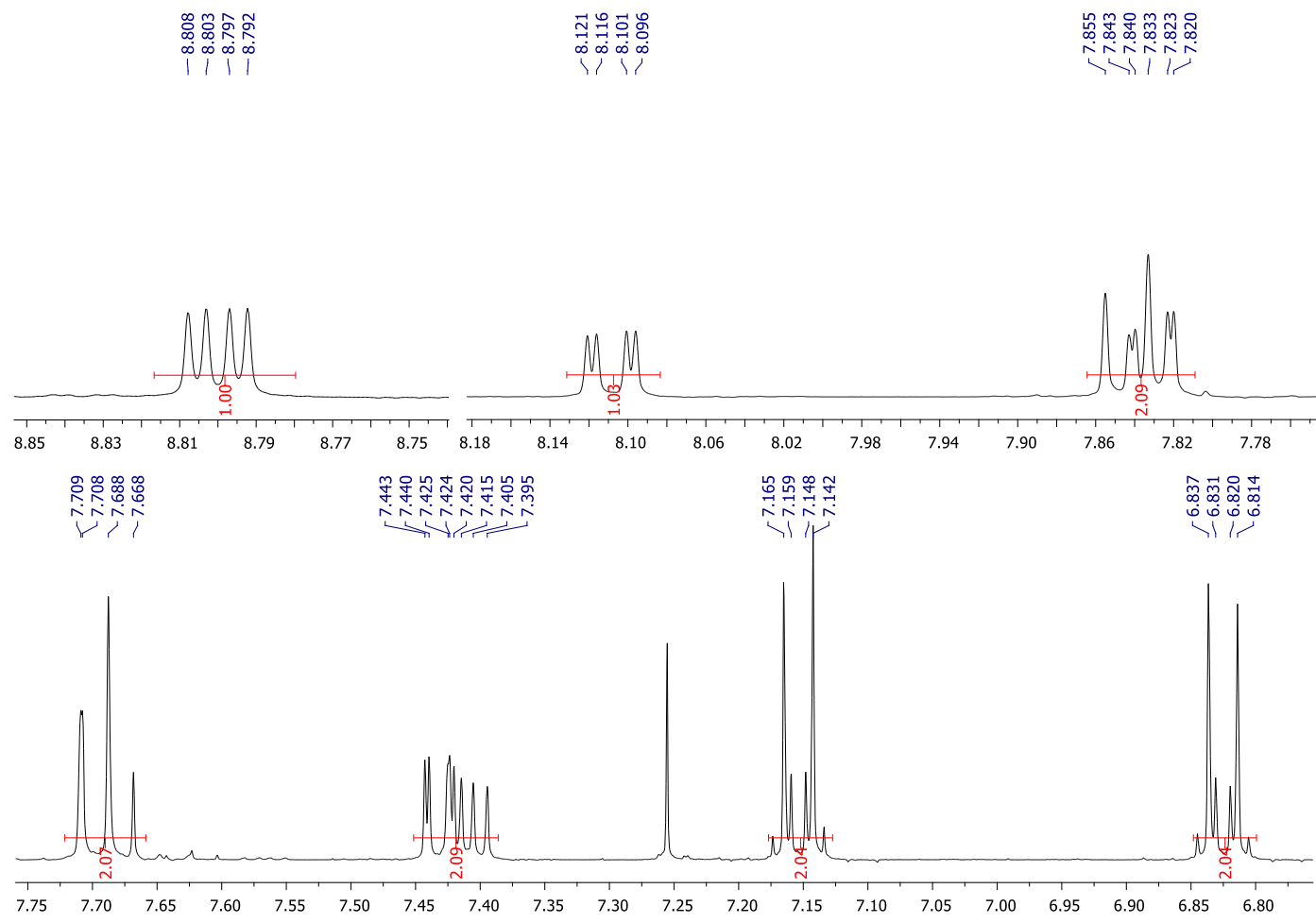


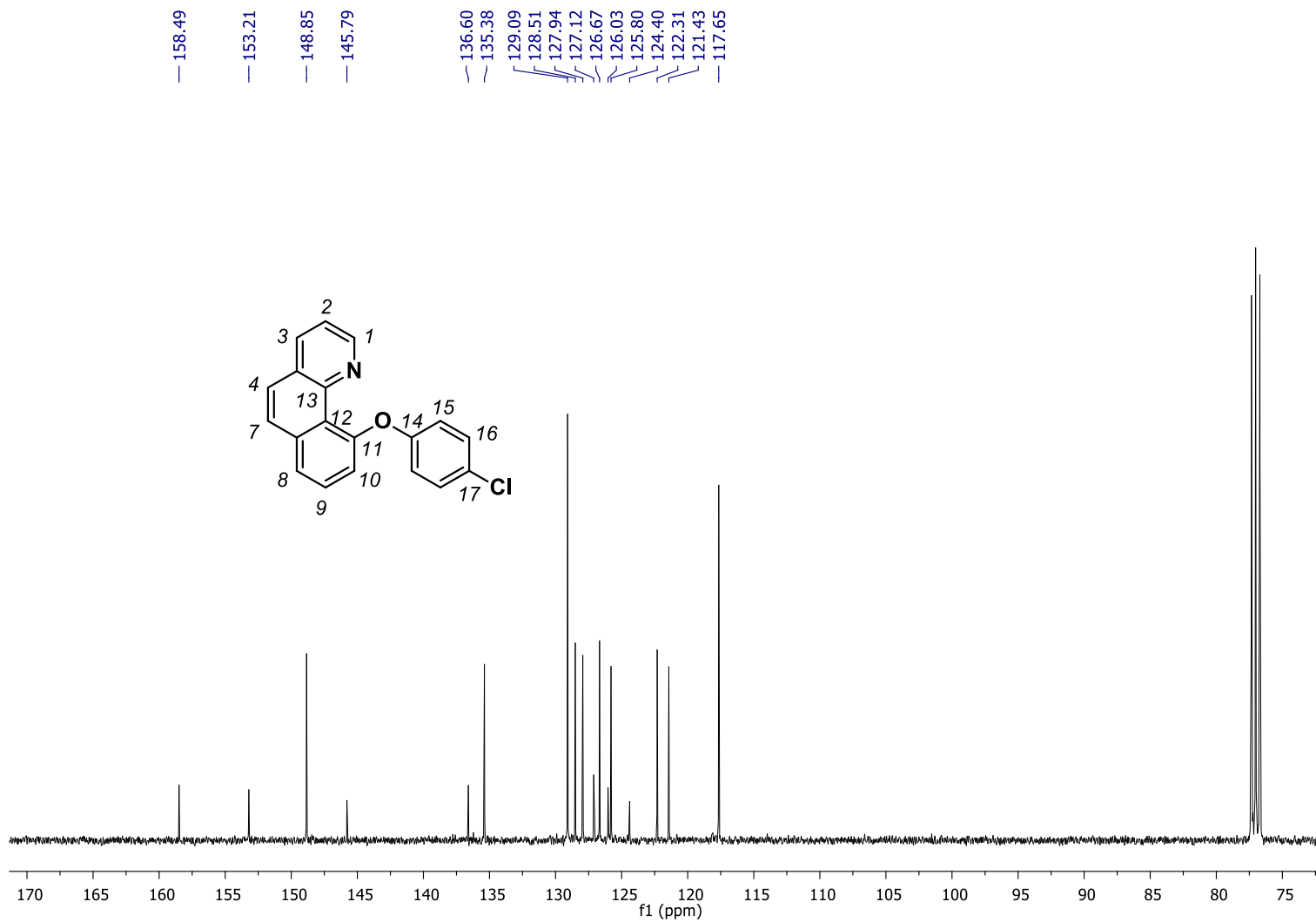
Figure S8. a) ^1H -NMR spectrum of compound **2aa** in CDCl_3 , 400 MHz, at 298 K; b) $^{13}\text{C}\{^1\text{H}\}$ -NMR spectrum (CDCl_3 , 100 MHz, 298 K); c) ^1H - ^1H COSY spectrum (CDCl_3 , 100 MHz, 298 K); d) ^1H - ^{13}C HSQCed spectrum (CDCl_3 , 400 MHz, 298 K); e) ^1H - ^{13}C HMBC spectrum (CDCl_3 , 400 MHz, 298 K); f) HRMS (ESI-MS) spectrum (m/z). Observed HRMS (left) with the theoretical isotope prediction (right).



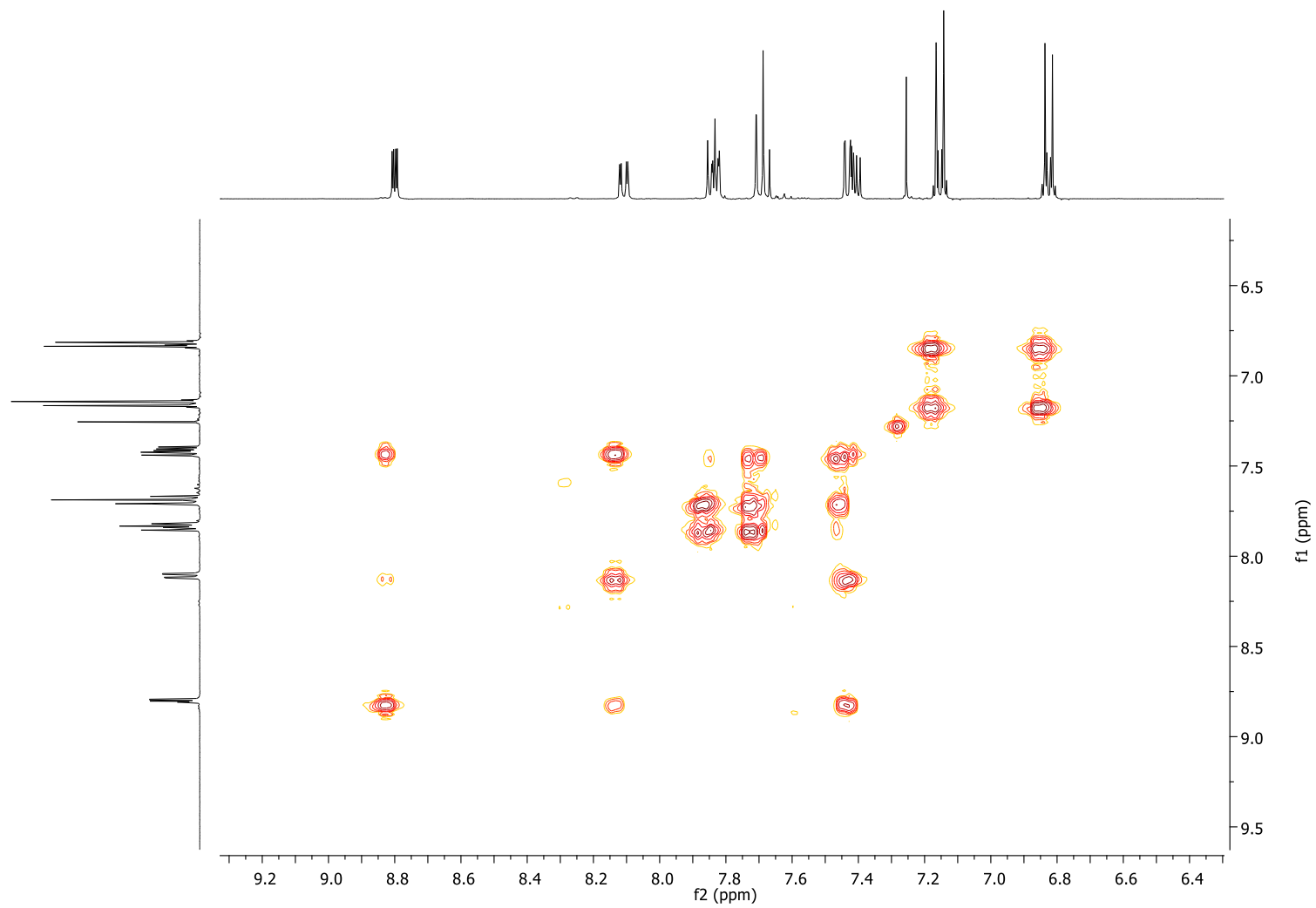


Selected aromatic region

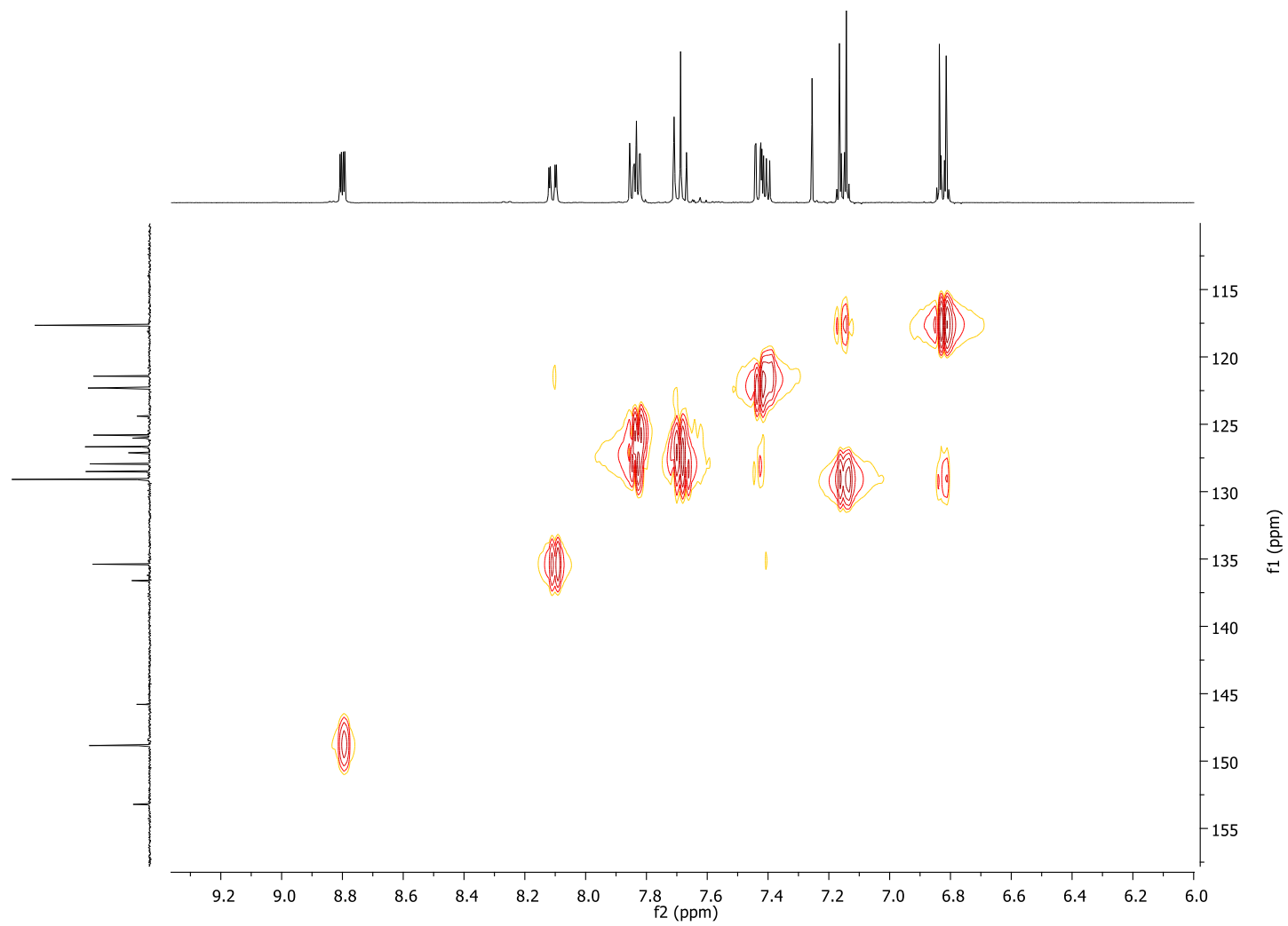
b)



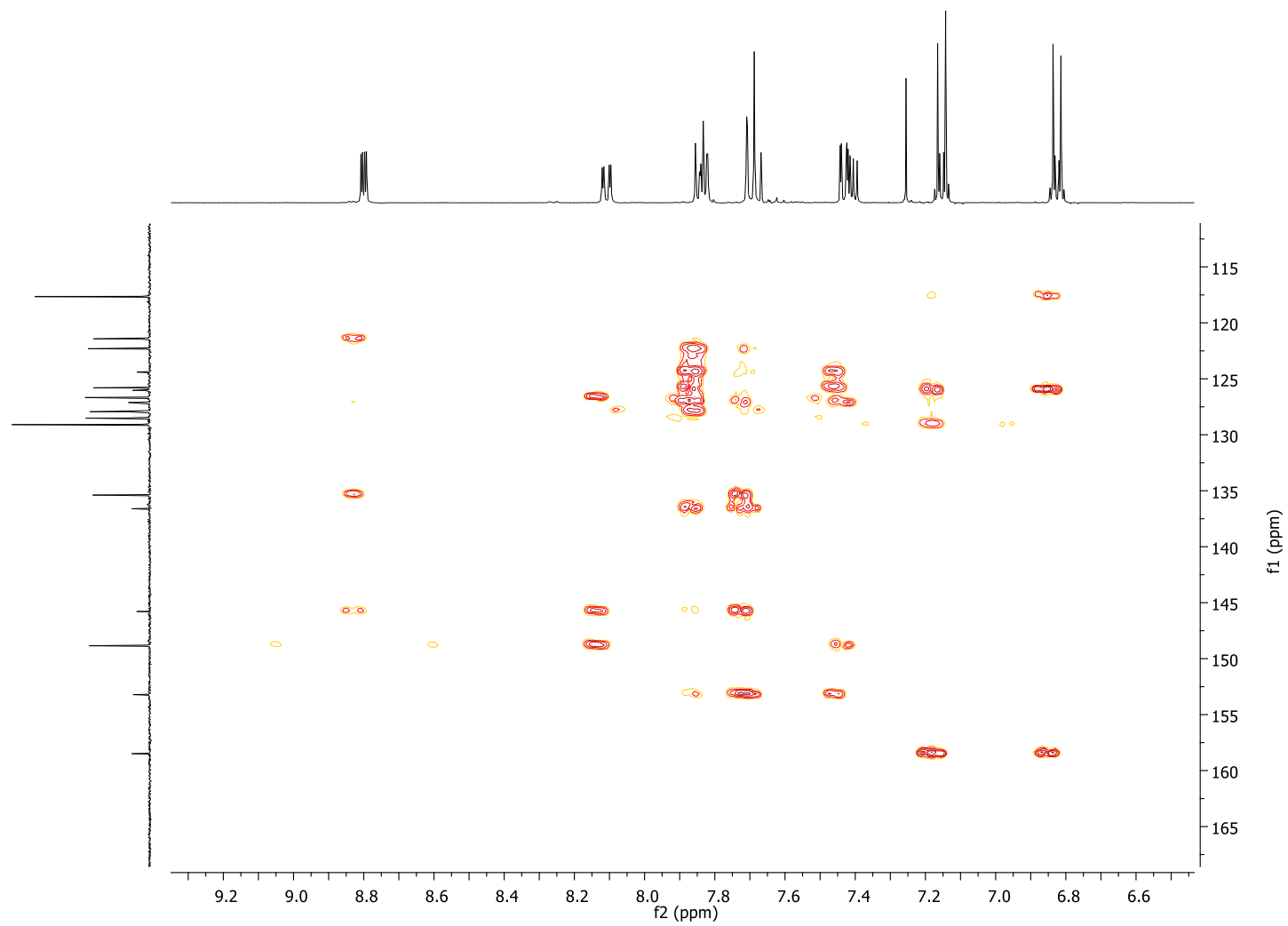
c)



d)



e)



e)

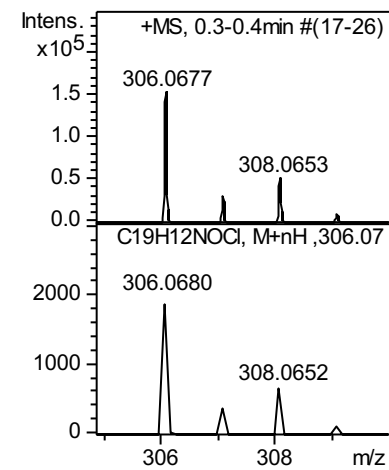
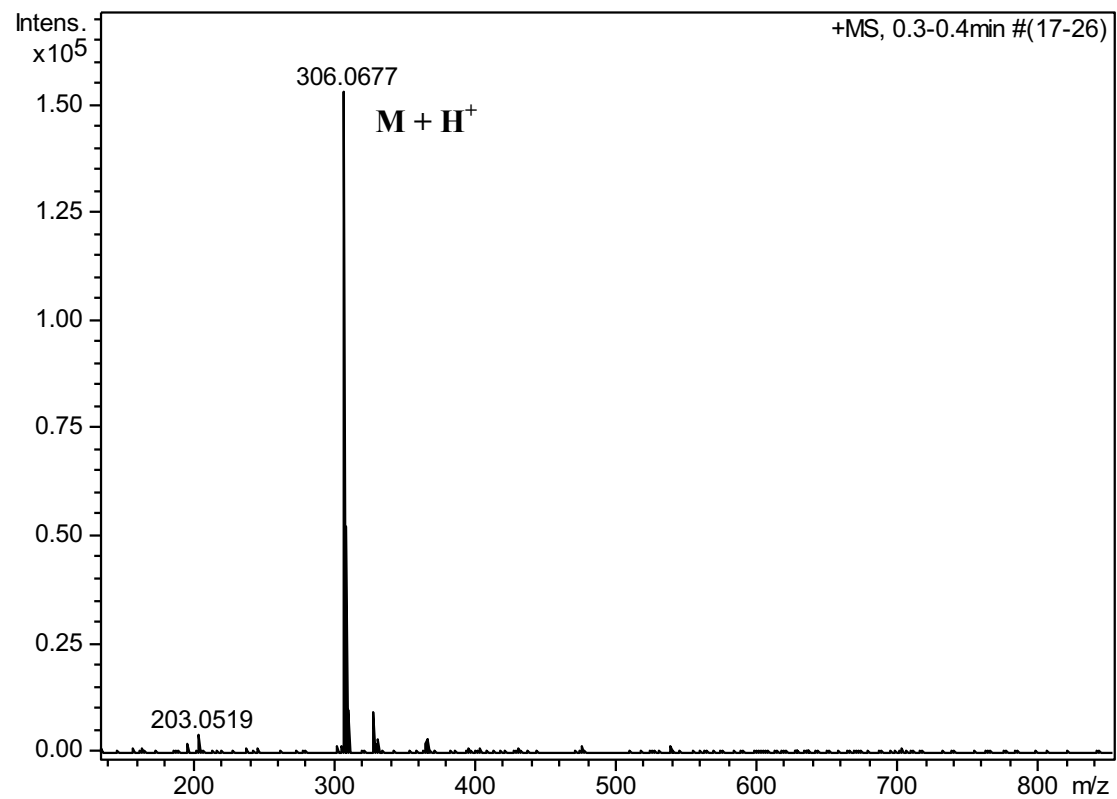
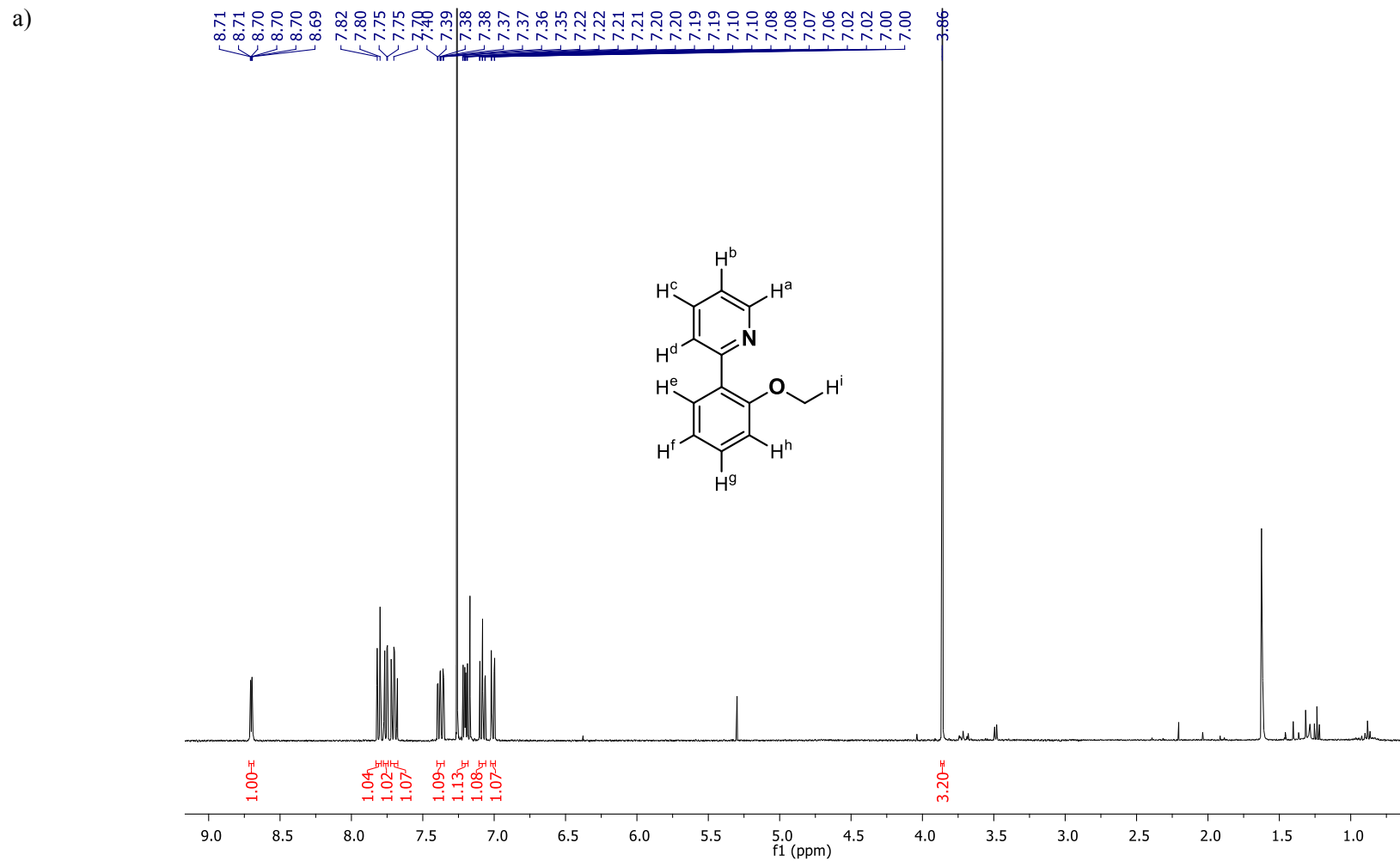


Figure S9. a) $^1\text{H-NMR}$ spectrum of compound **1ab** in CDCl_3 , 400 MHz, at 298 K; b) HRMS (ESI-MS) spectrum (m/z). Observed HRMS (left) with the theoretical isotope prediction (right).



b)

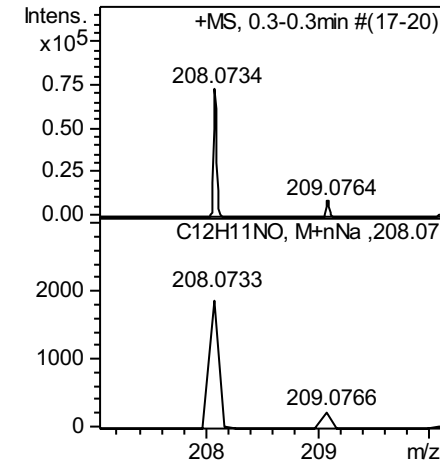
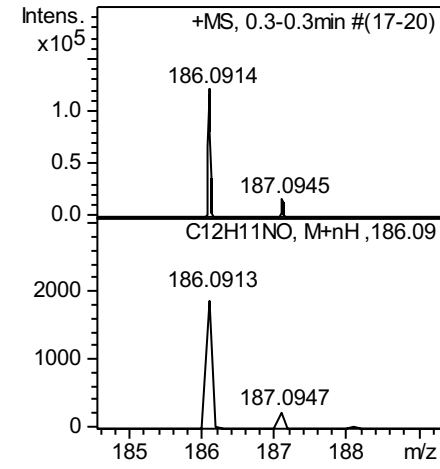
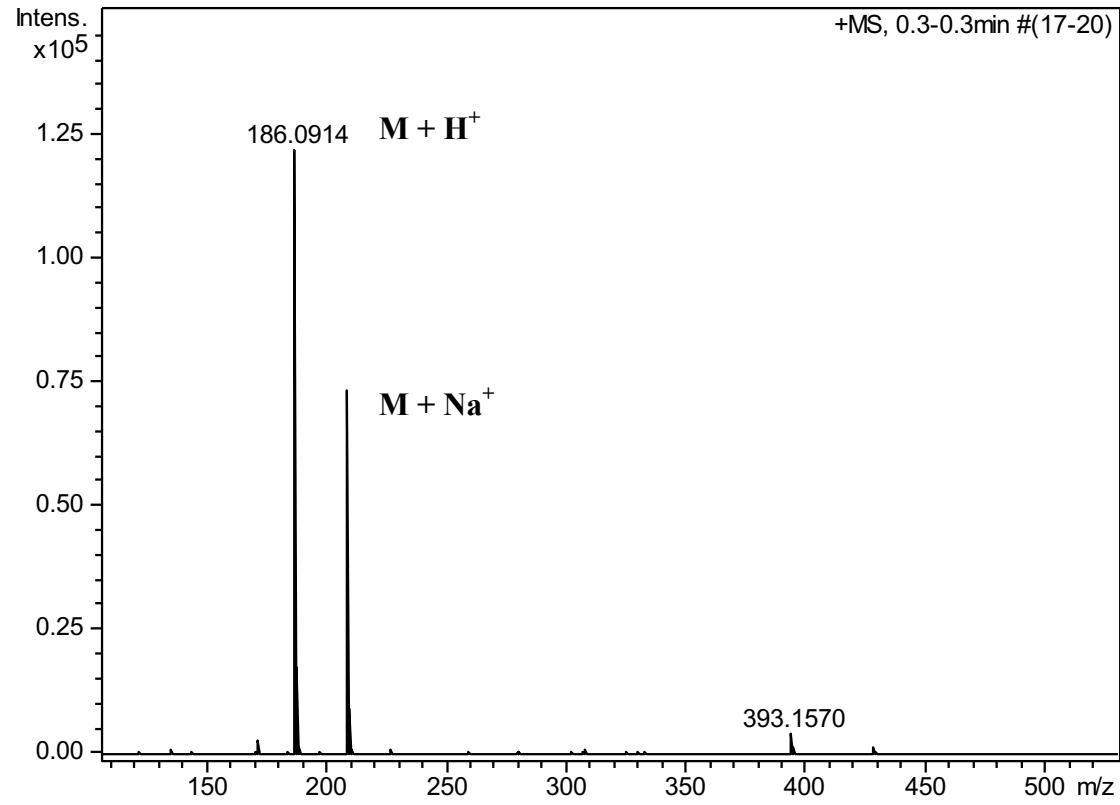
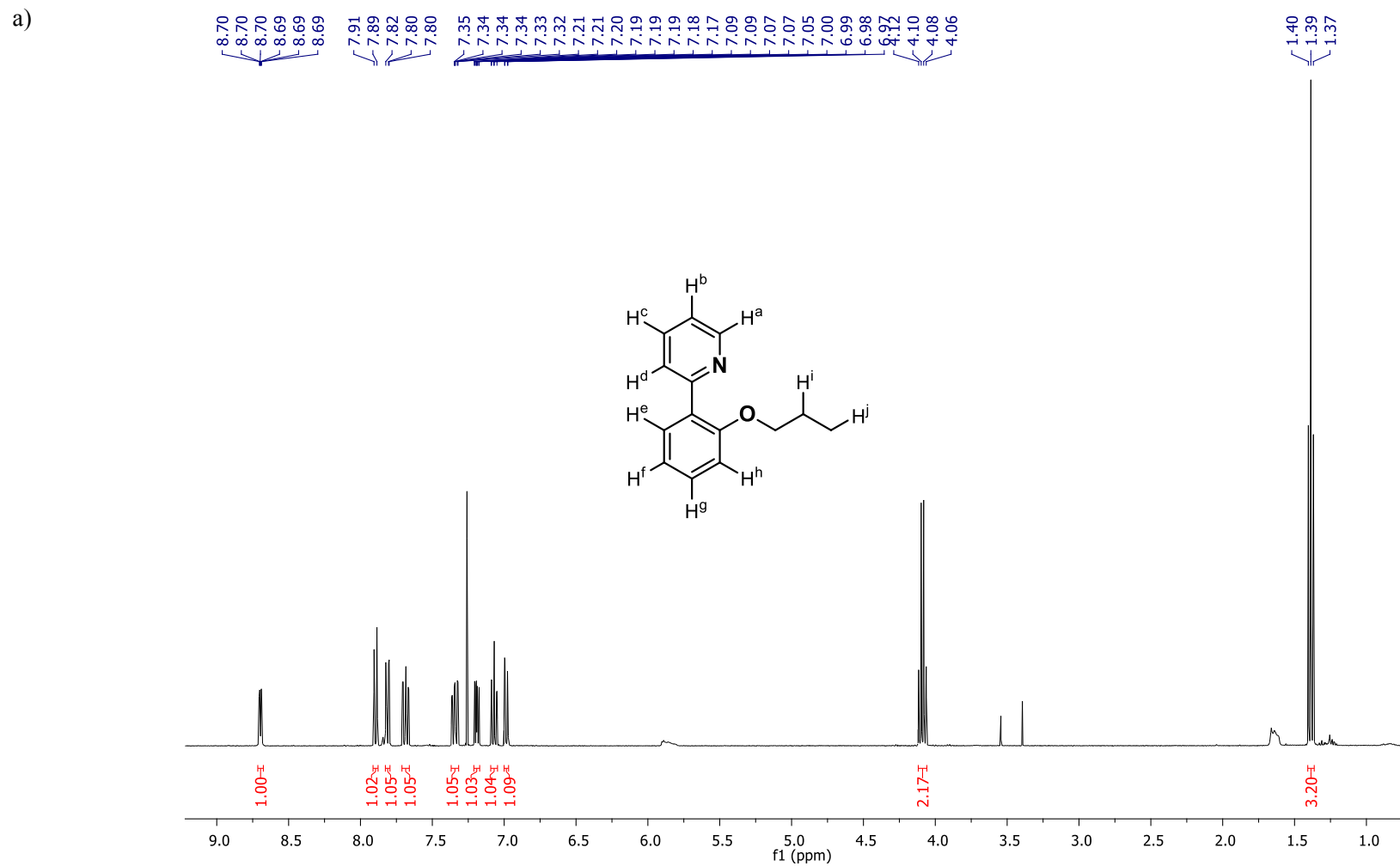


Figure S10. a) ^1H -NMR spectrum of compound **1ac** in CDCl_3 , 400 MHz, at 298 K; b) HRMS (ESI-MS) spectrum (m/z). Observed HRMS (left) with the theoretical isotope prediction (right).



b)

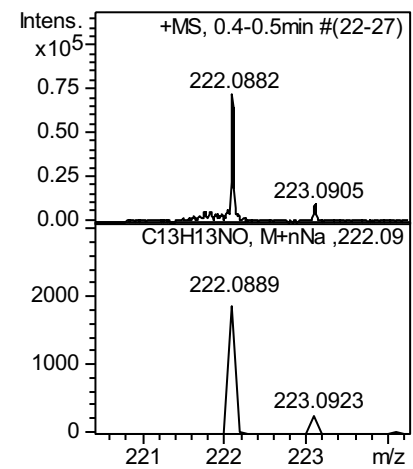
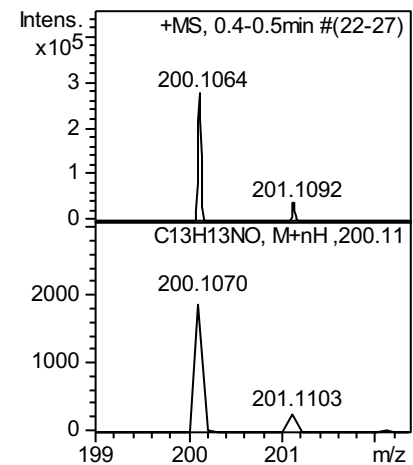
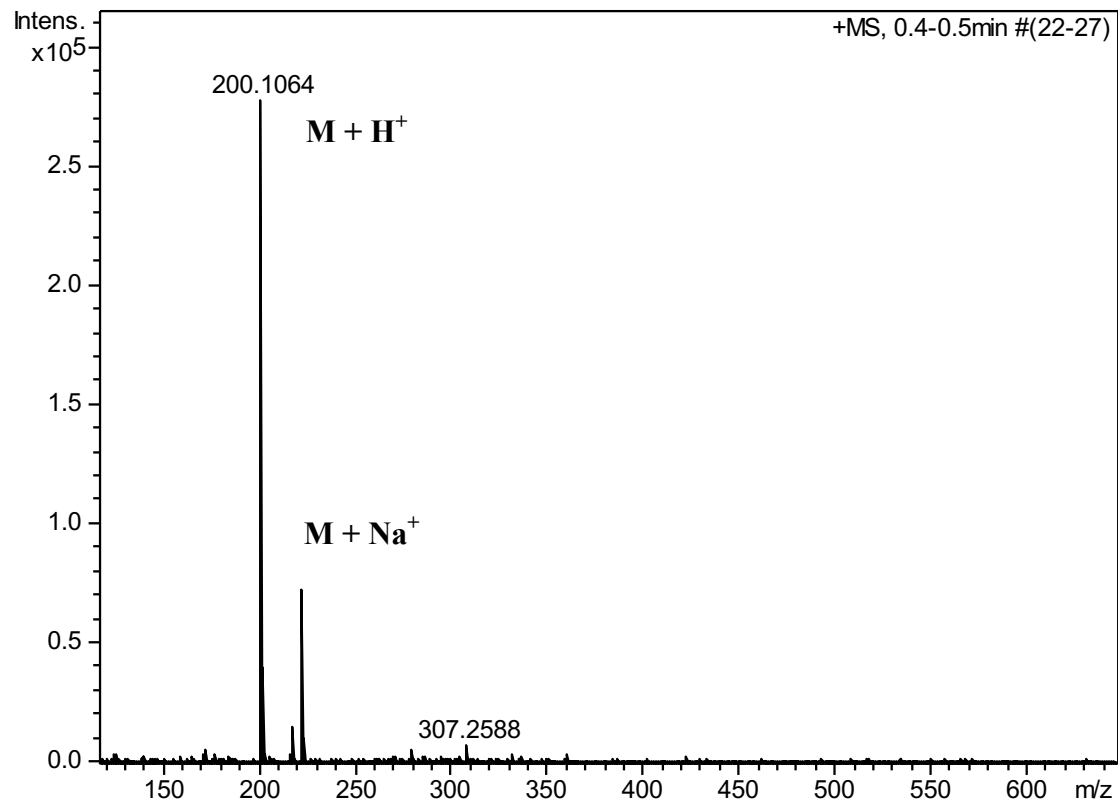
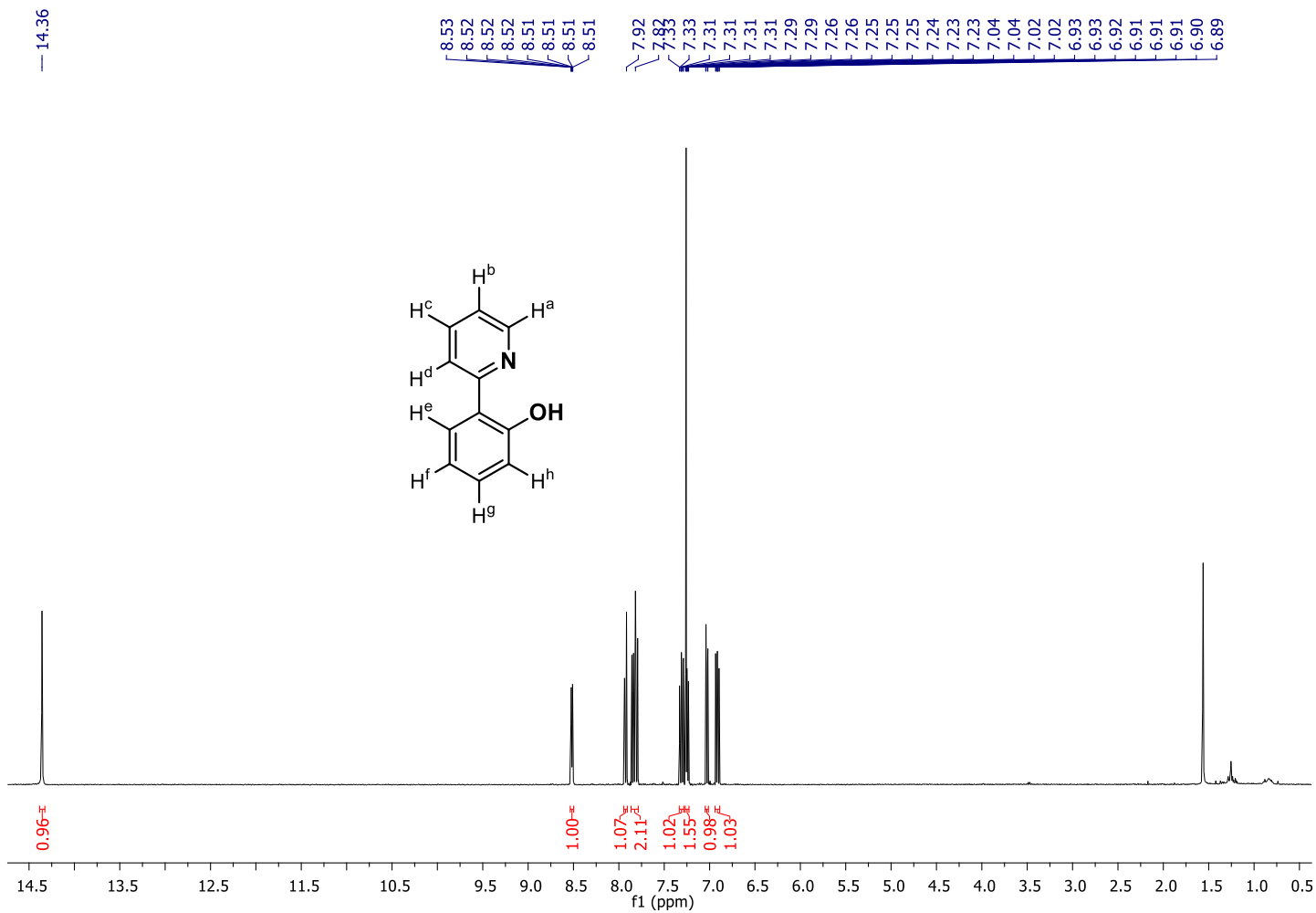


Figure S11. a) $^1\text{H-NMR}$ spectrum of compound **1af** in CDCl_3 , 400 MHz, at 298 K; b) HRMS (ESI-MS) spectrum (m/z). Observed HRMS (left) with the theoretical isotope prediction (right).

a)



b)

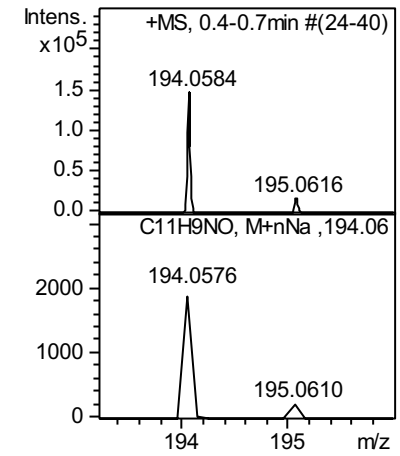
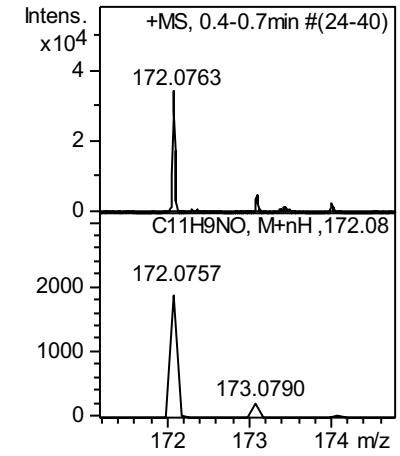
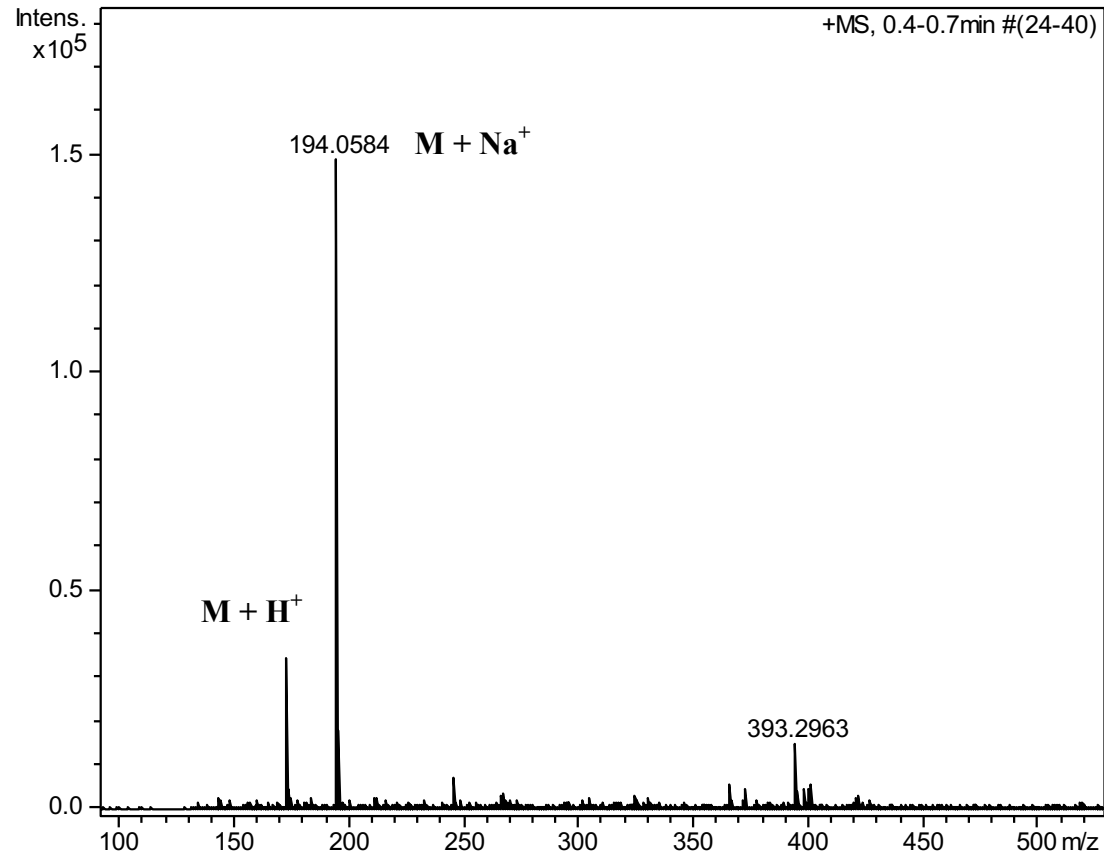
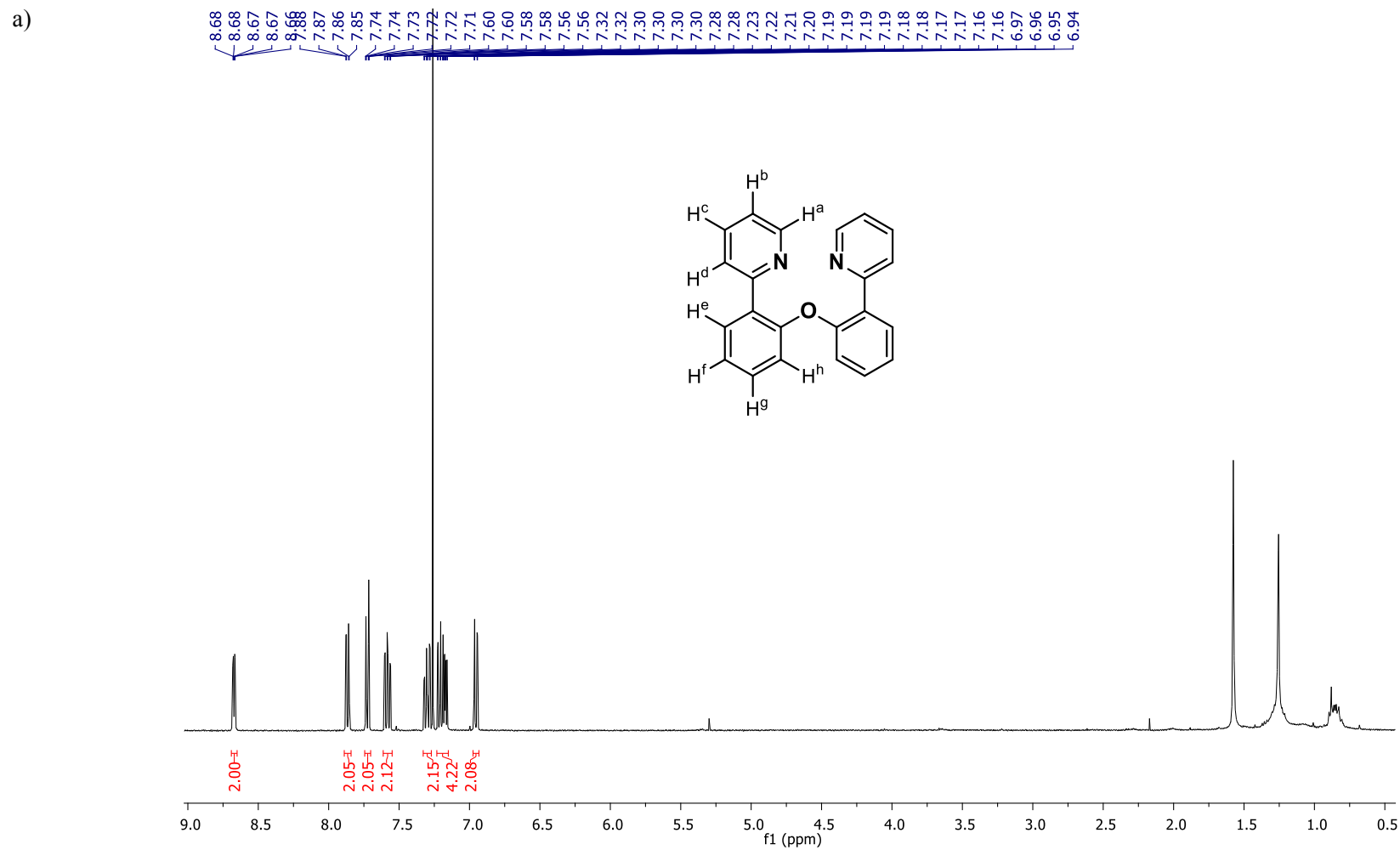
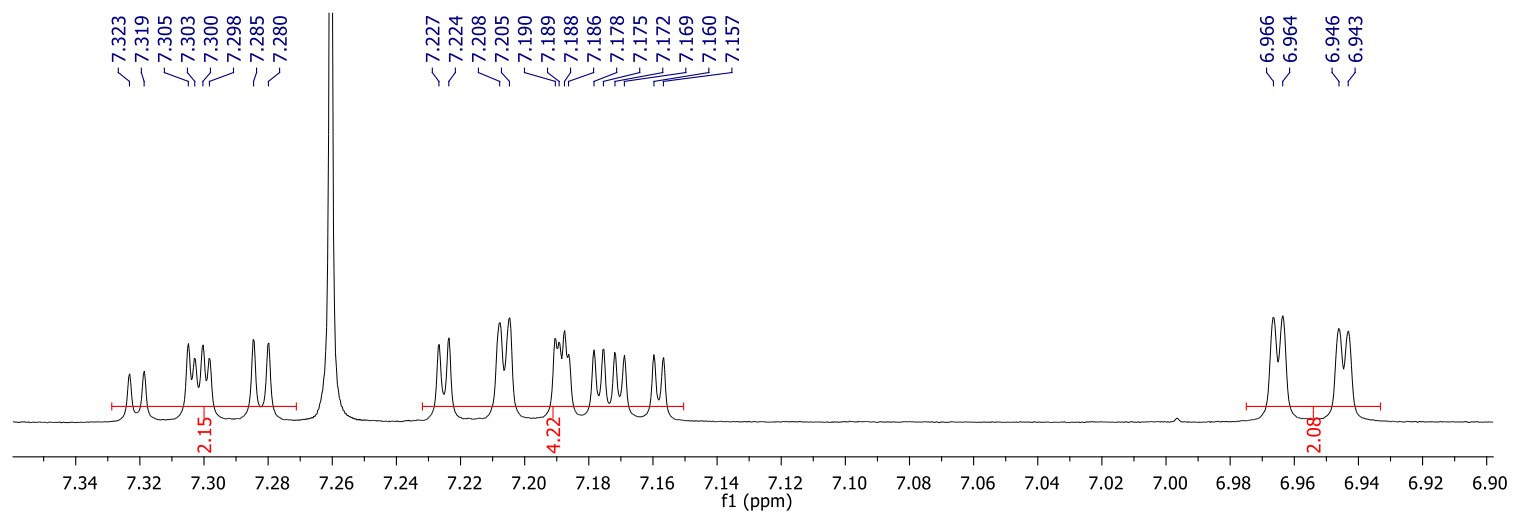
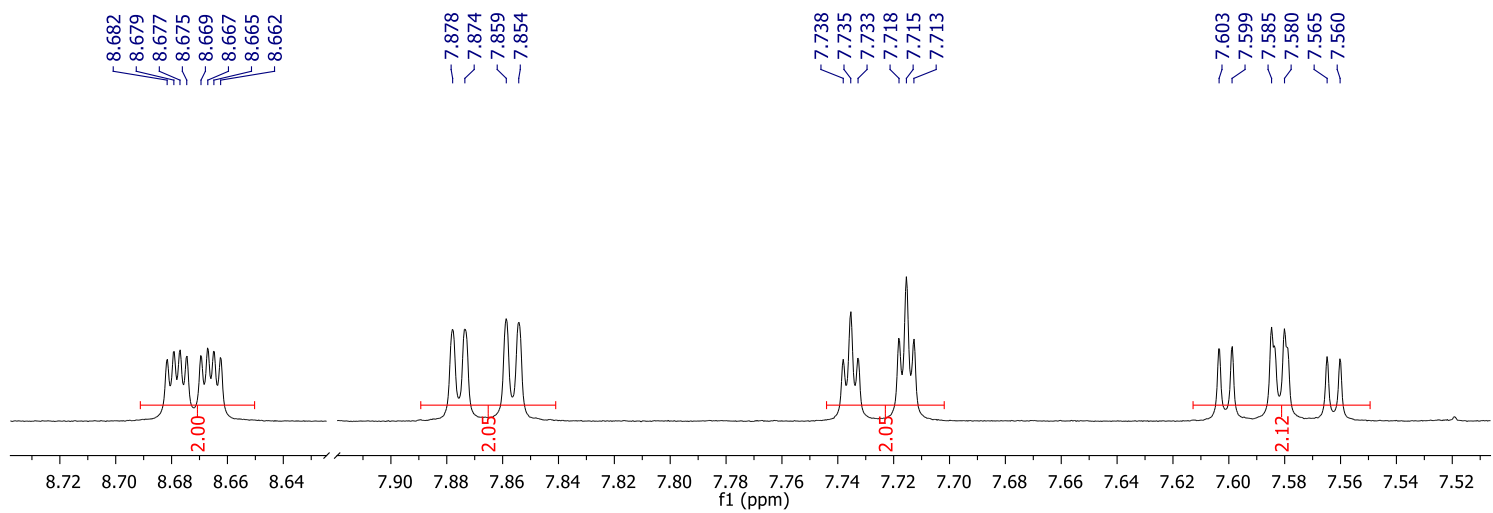


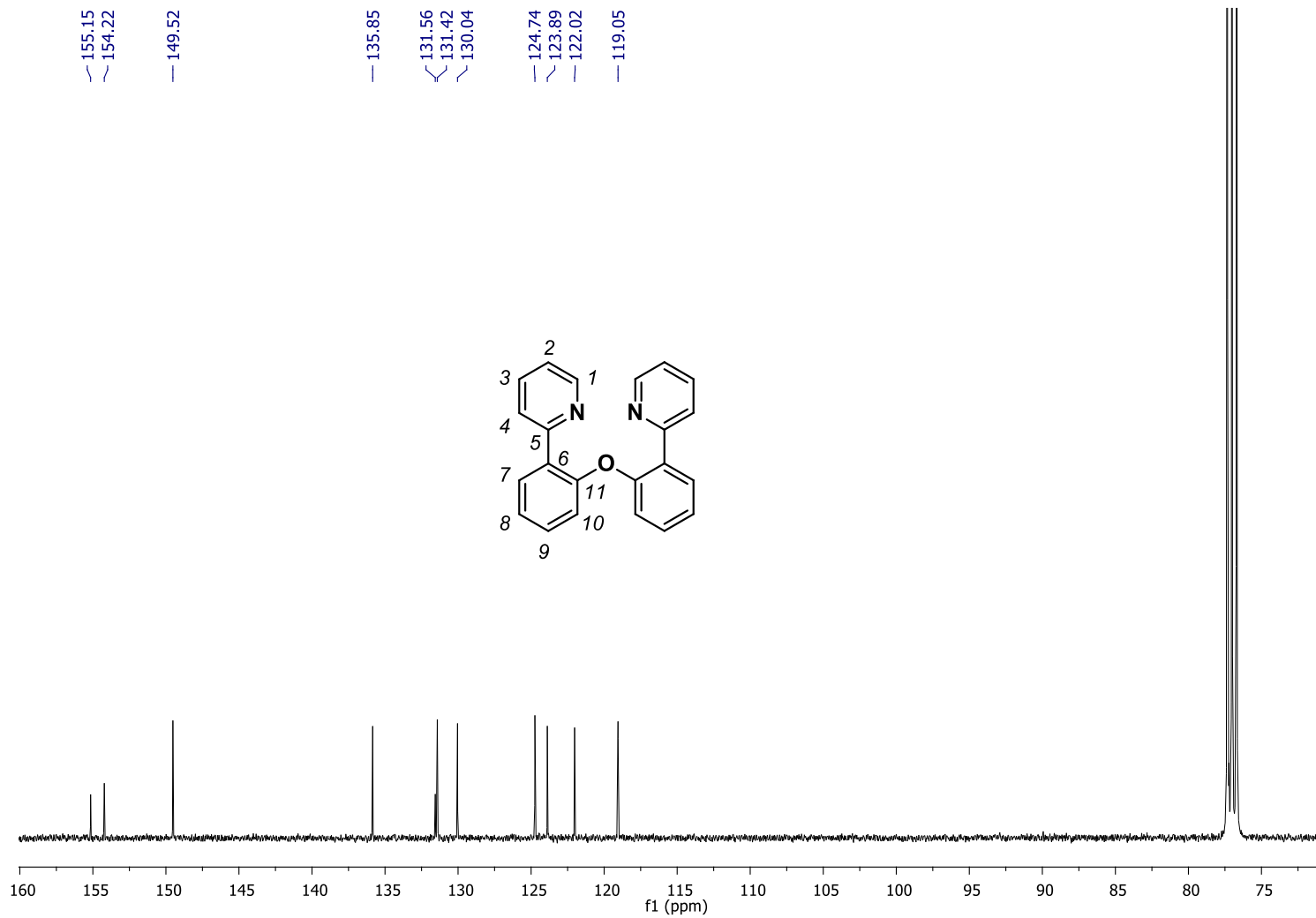
Figure S12. a) ^1H -NMR spectrum of compound **1ag** in CDCl_3 , 400 MHz, at 298 K; b) $^{13}\text{C}\{^1\text{H}\}$ -NMR spectrum (CDCl_3 , 100 MHz, 298 K); c) ^1H - ^1H COSY spectrum (CDCl_3 , 100 MHz, 298 K); d) ^1H - ^{13}C HSQCed spectrum (CDCl_3 , 400 MHz, 298 K); e) ^1H - ^{13}C HMBC spectrum (CDCl_3 , 400 MHz, 298 K); f) HRMS (ESI-MS) spectrum (m/z). Observed HRMS (left) with the theoretical isotope prediction (right).



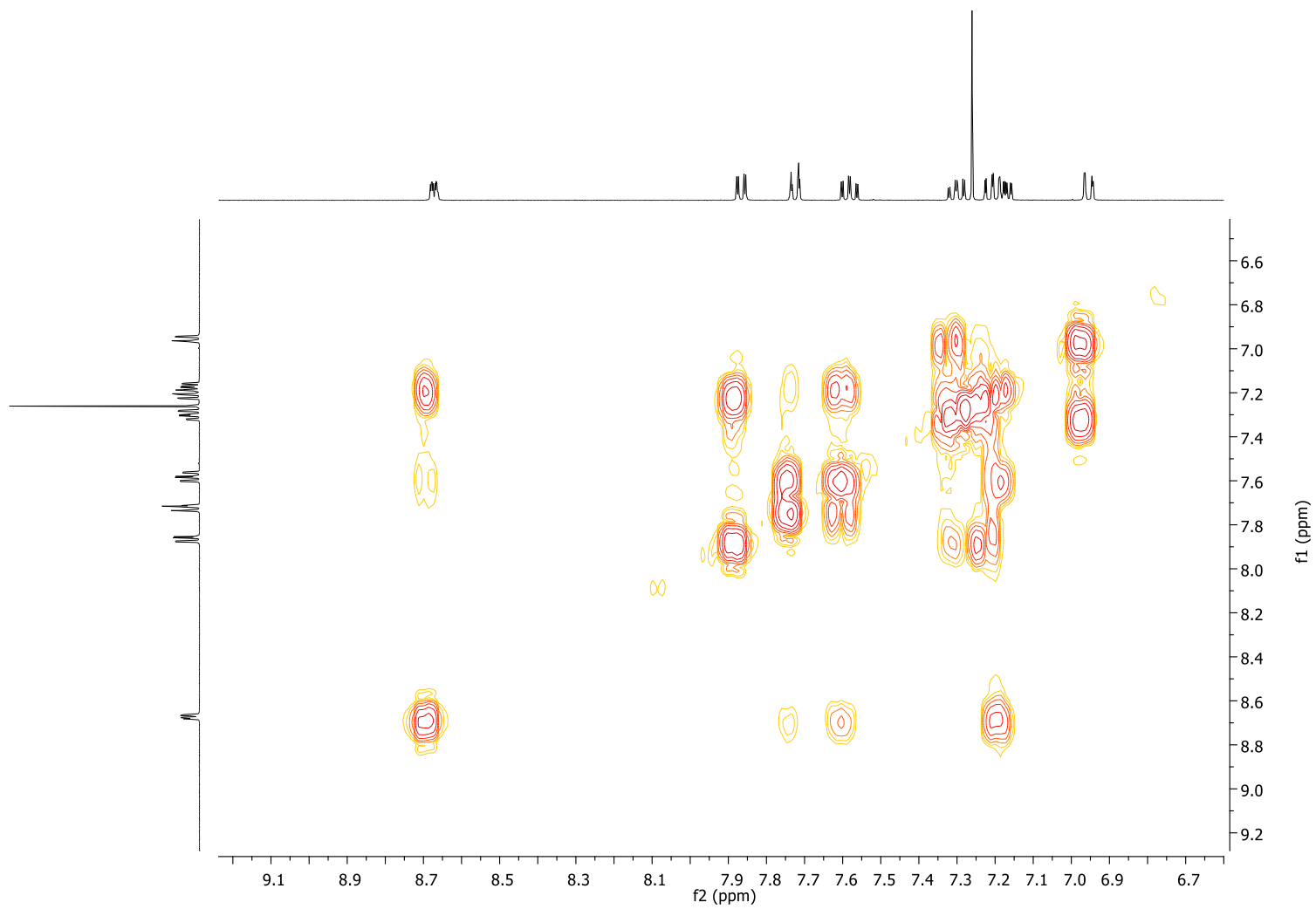


Selected aromatic region

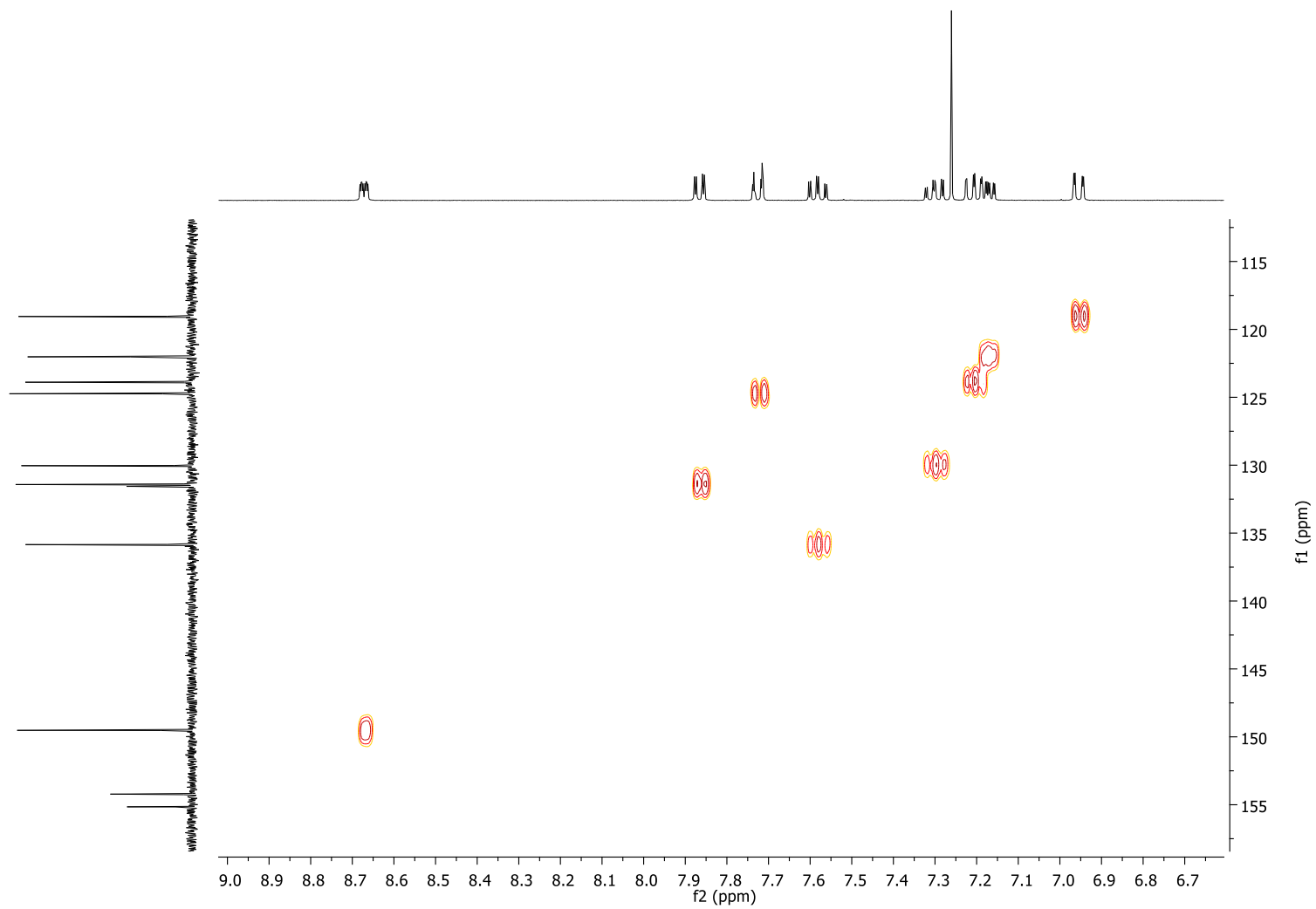
b)



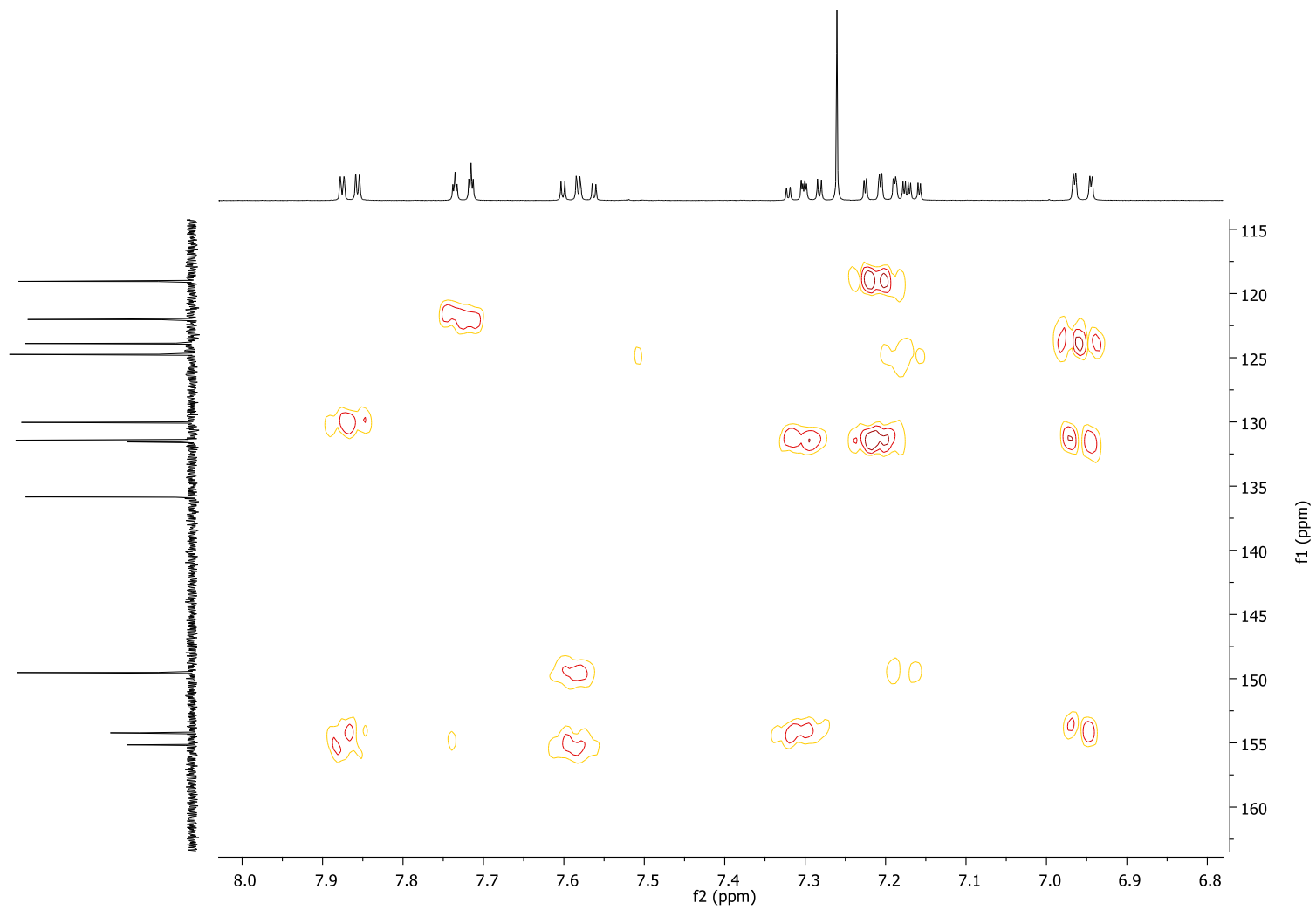
c)



d)



e)



f)

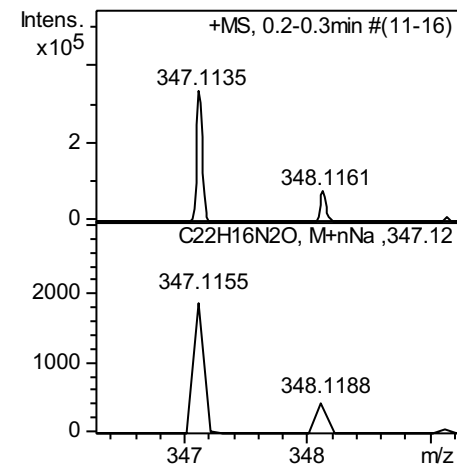
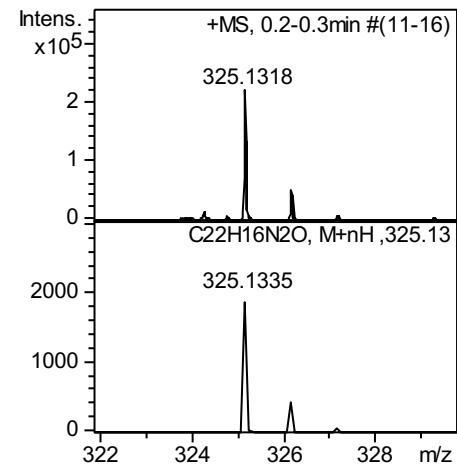
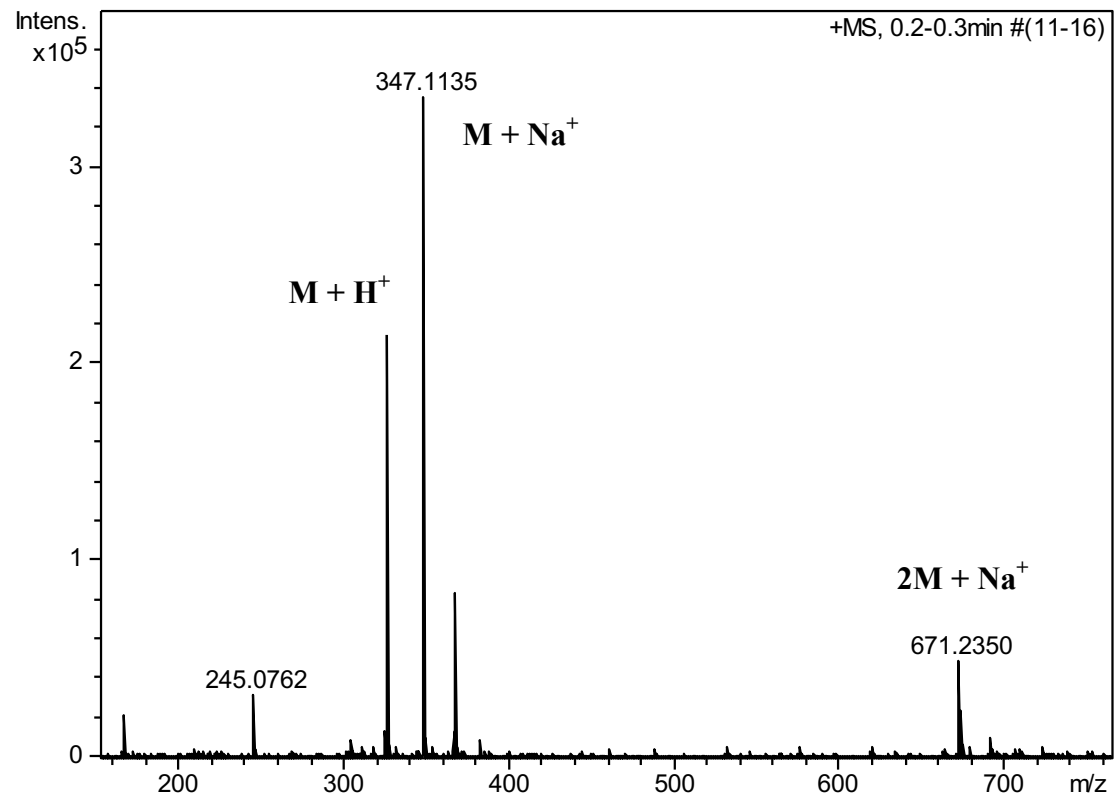
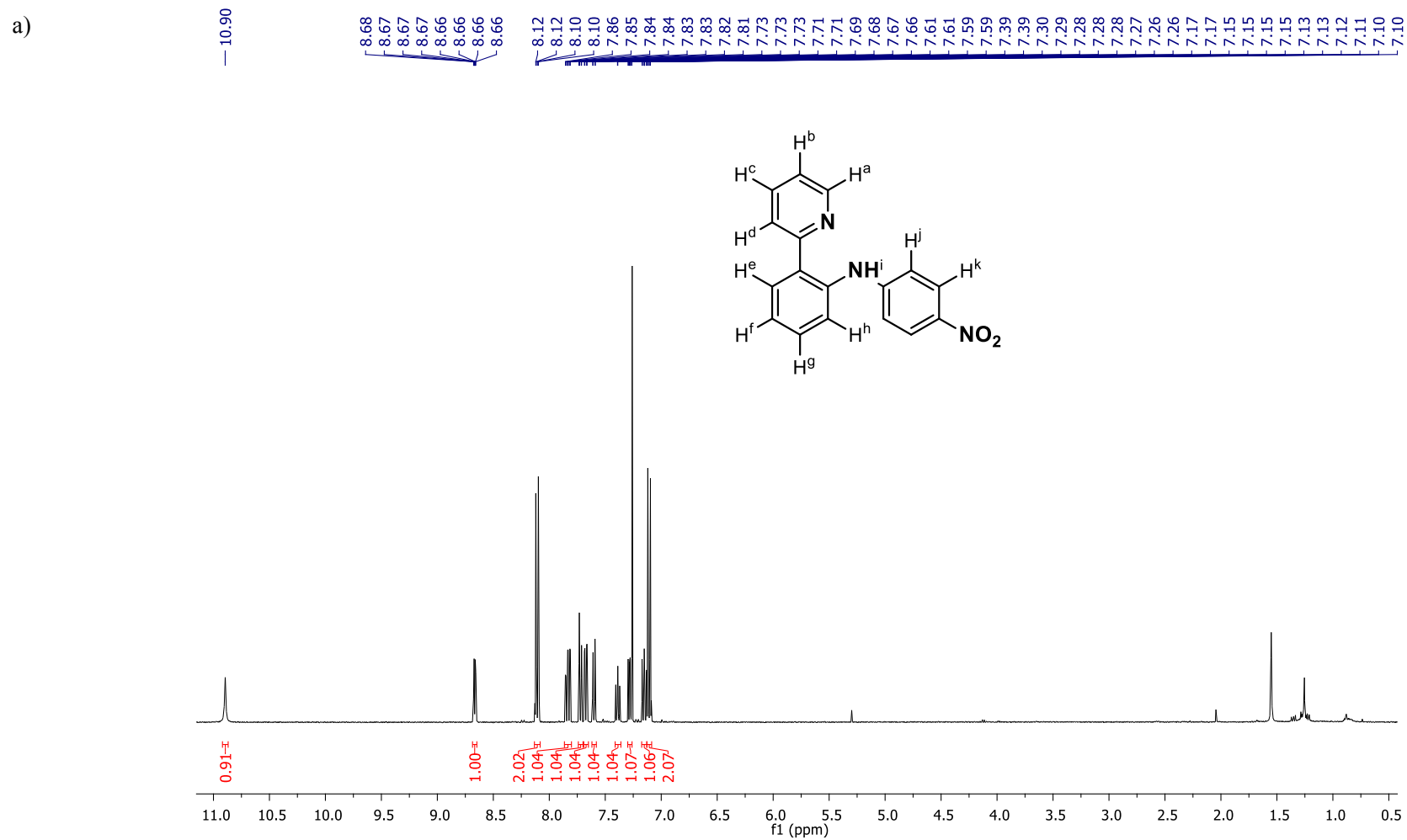
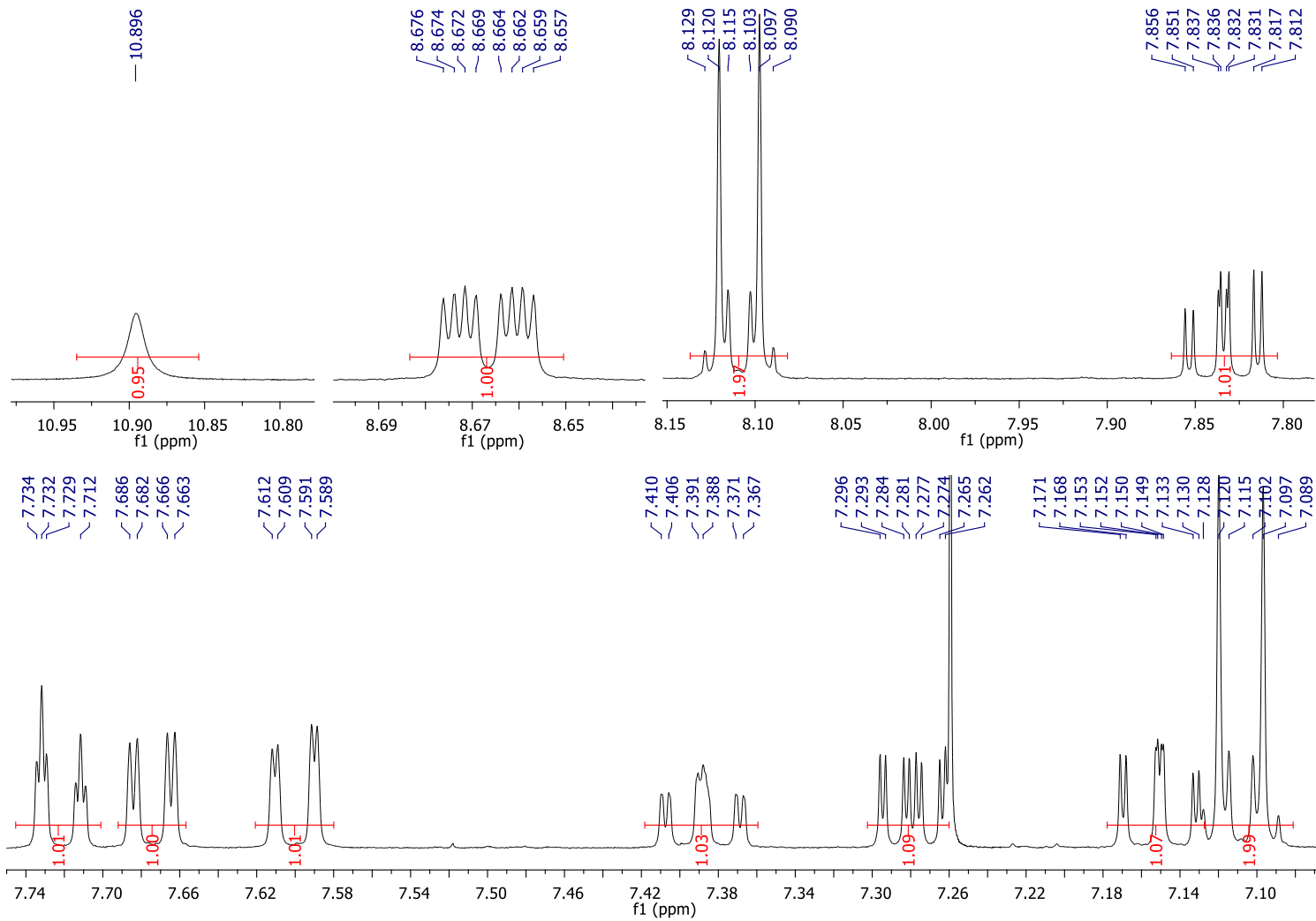


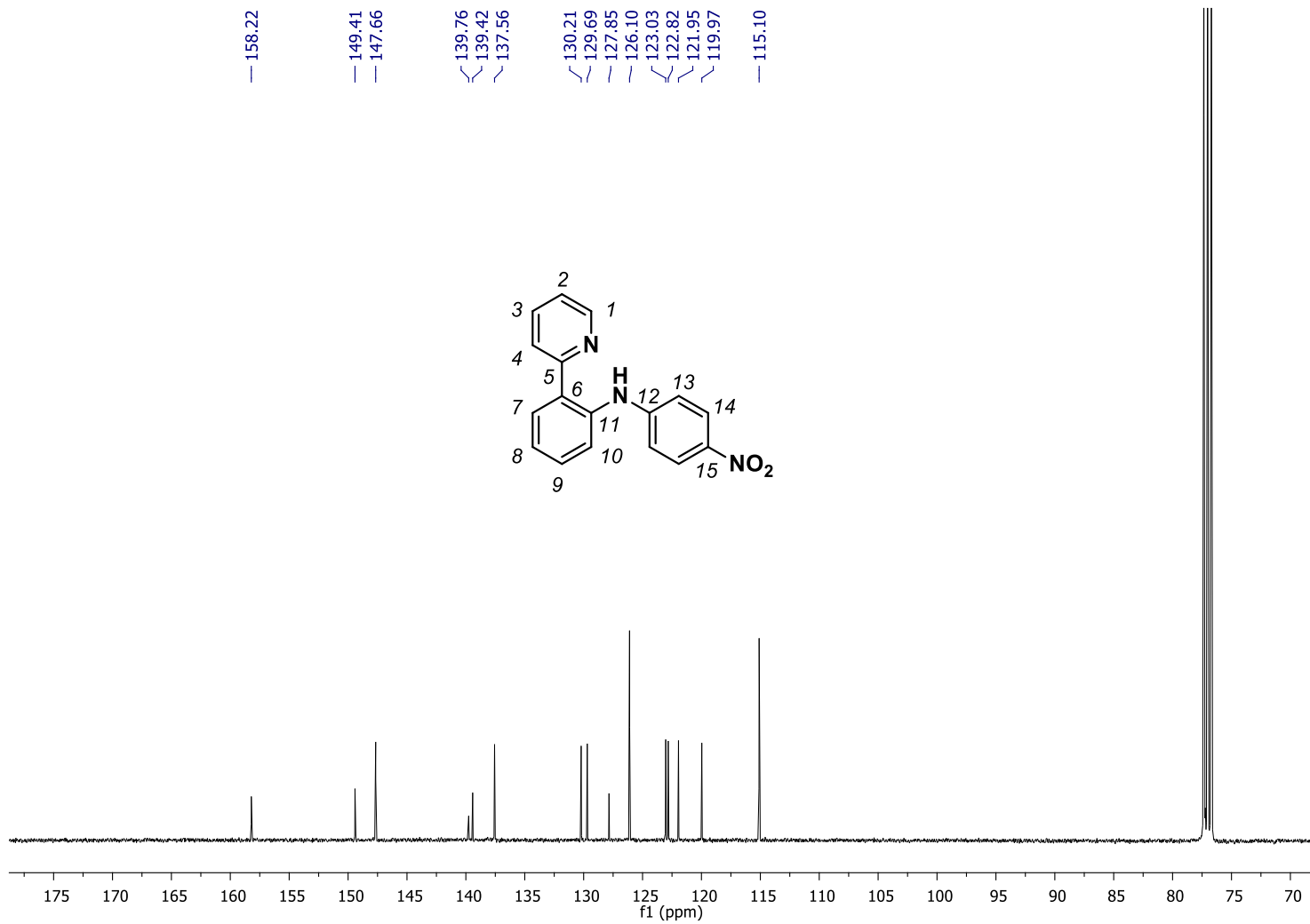
Figure S13. a) ^1H -NMR spectrum of compound **1ah** in CDCl_3 , 400 MHz, at 298 K; b) $^{13}\text{C}\{^1\text{H}\}$ -NMR spectrum (CDCl_3 , 100 MHz, 298 K); c) ^1H - ^1H COSY spectrum (CDCl_3 , 100 MHz, 298 K); d) ^1H - ^{13}C HSQCed spectrum (CDCl_3 , 400 MHz, 298 K); e) ^1H - ^{13}C HMBC spectrum (CDCl_3 , 400 MHz, 298 K); f) HRMS (ESI-MS) spectrum (m/z). Observed HRMS (left) with the theoretical isotope prediction (right).



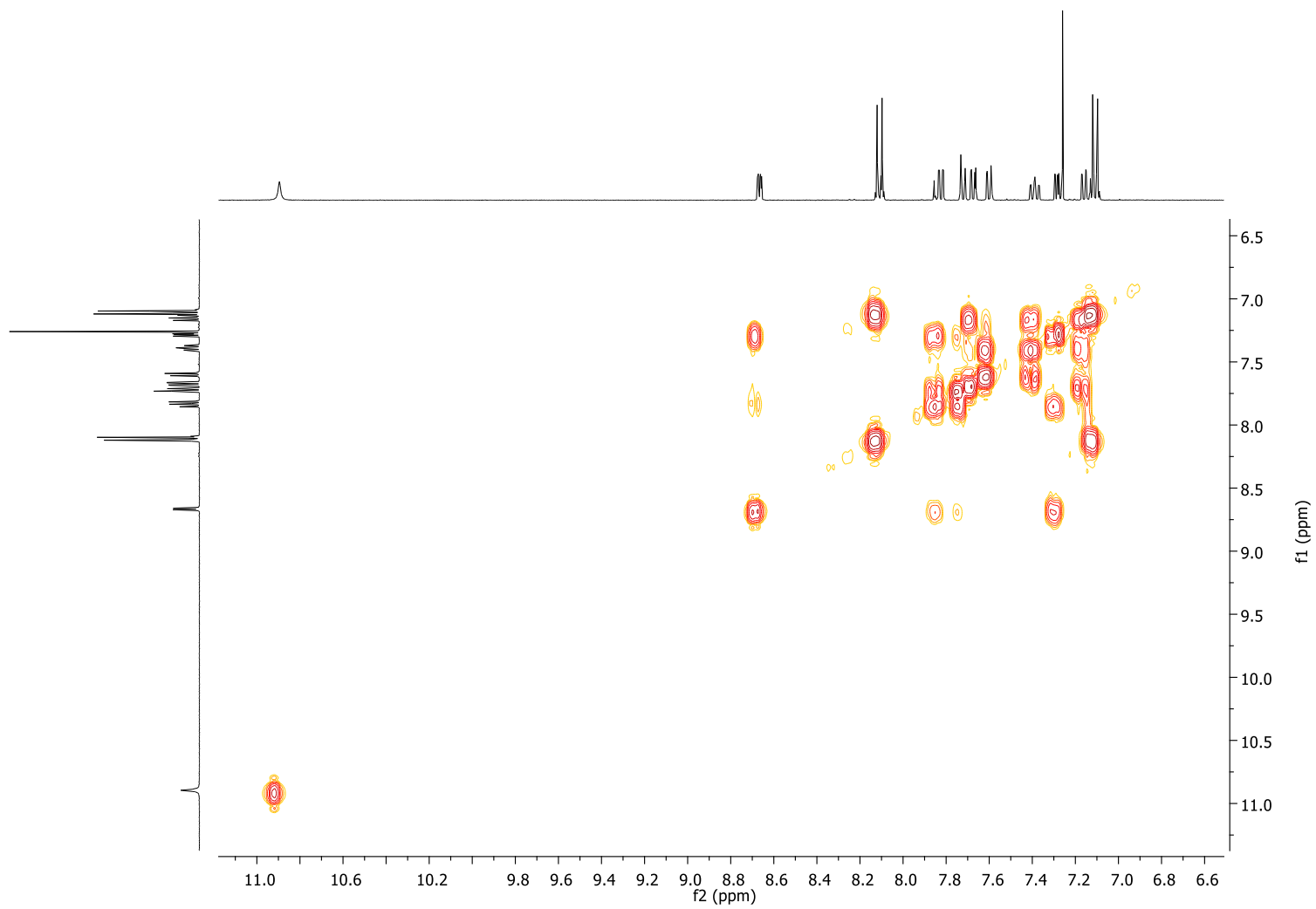


Selected aromatic region

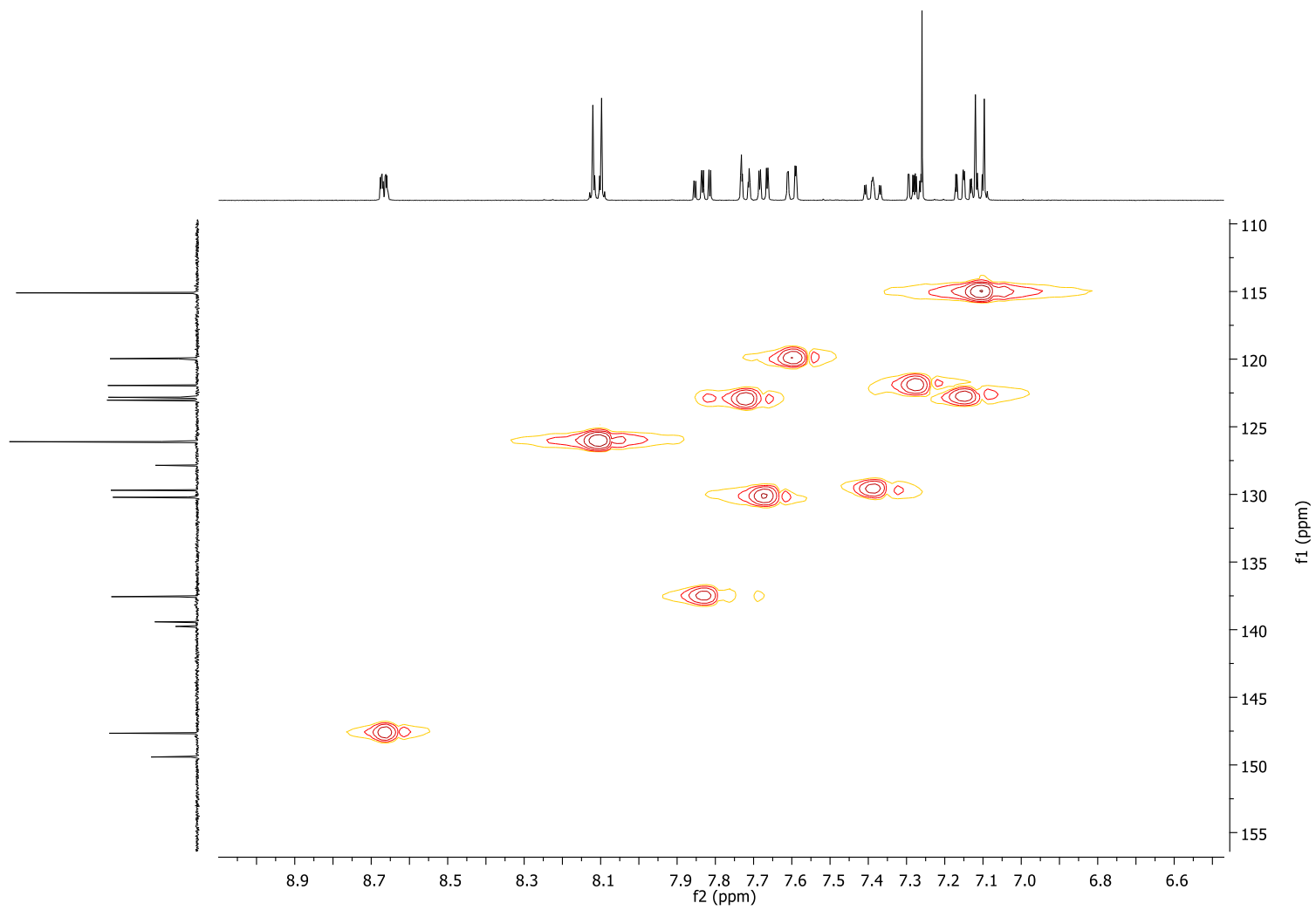
b)



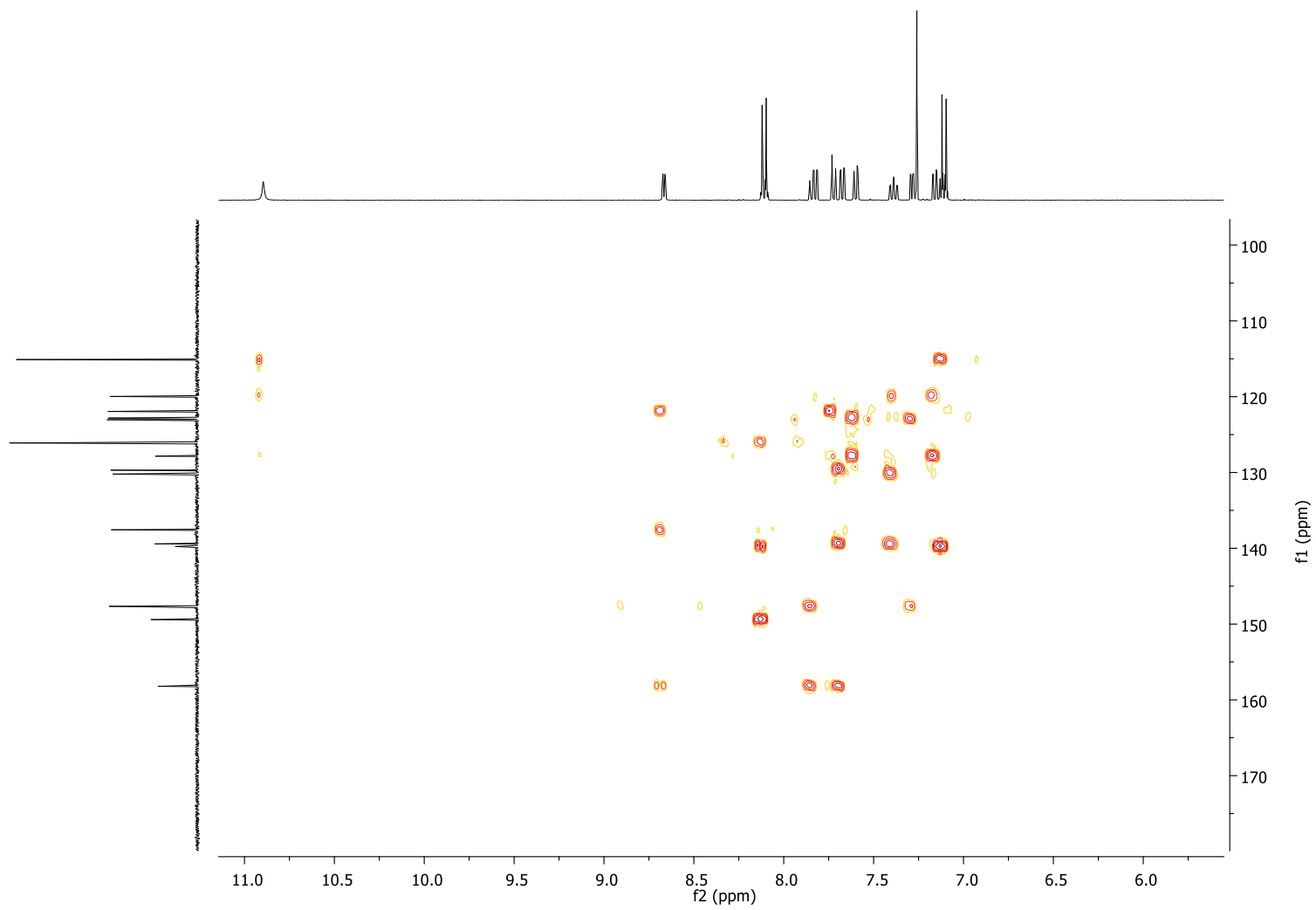
c)



d)



e)



f)

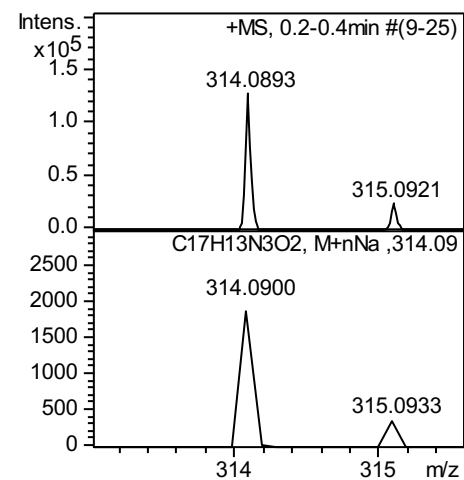
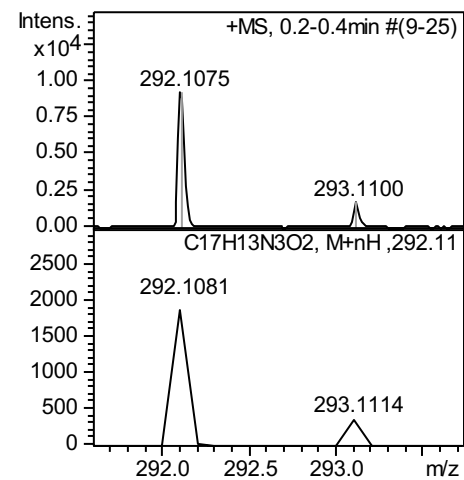
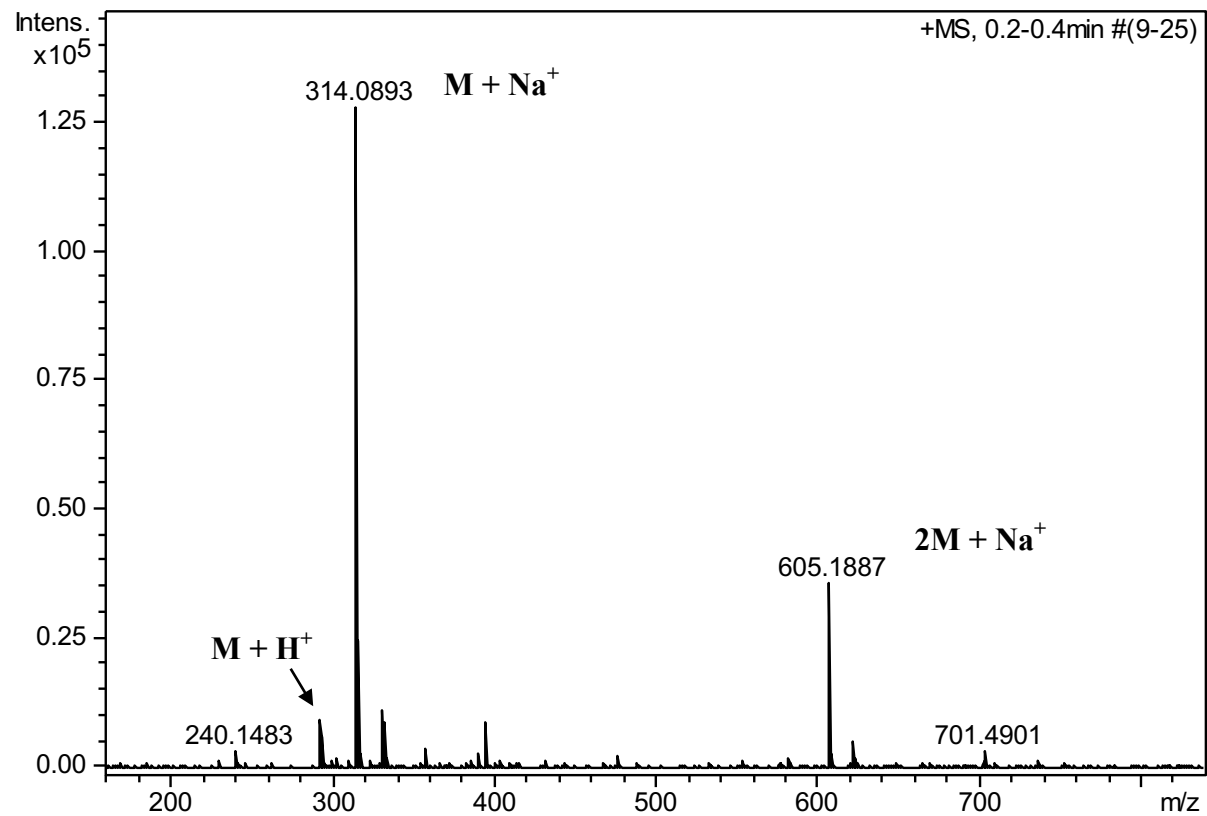
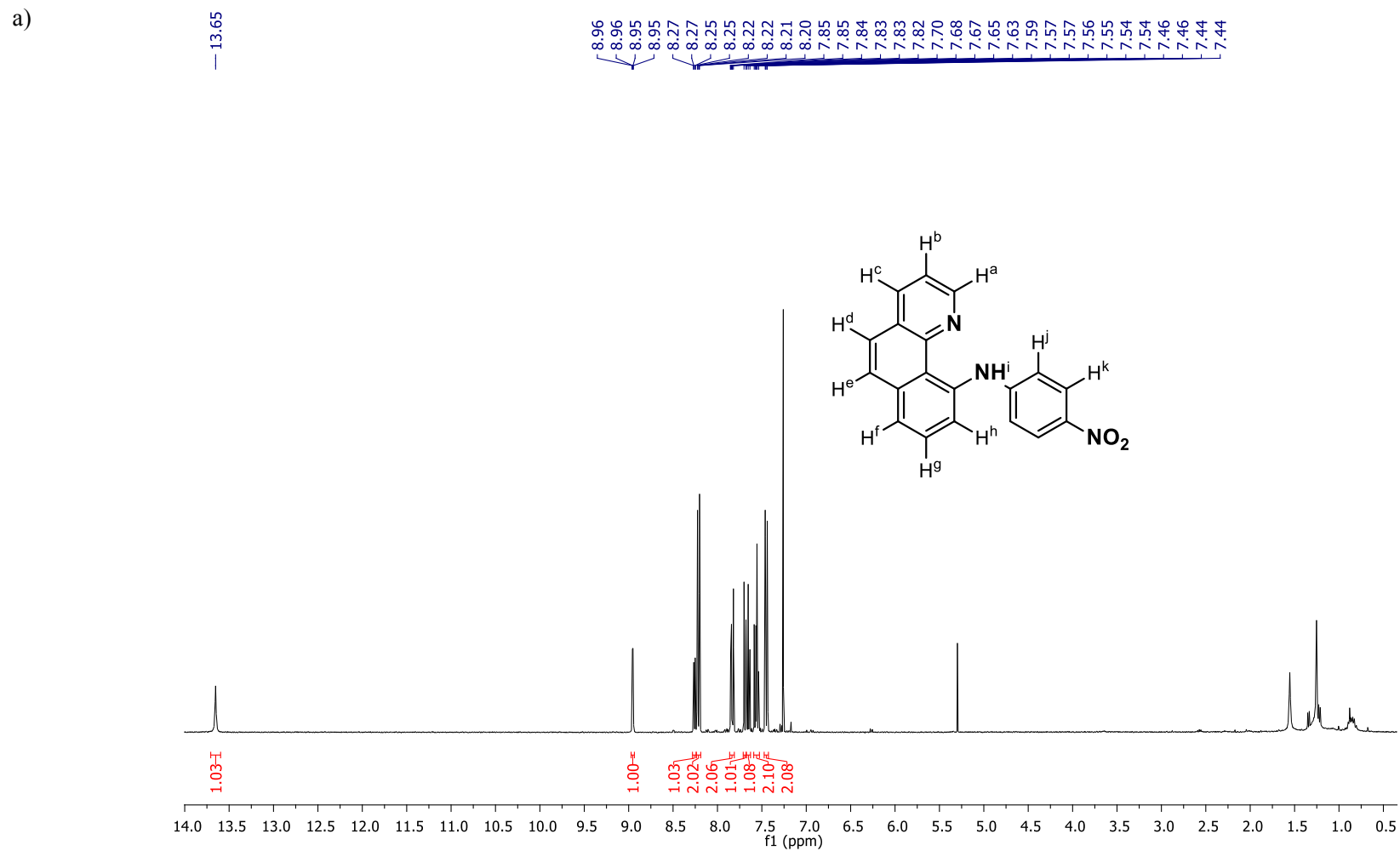
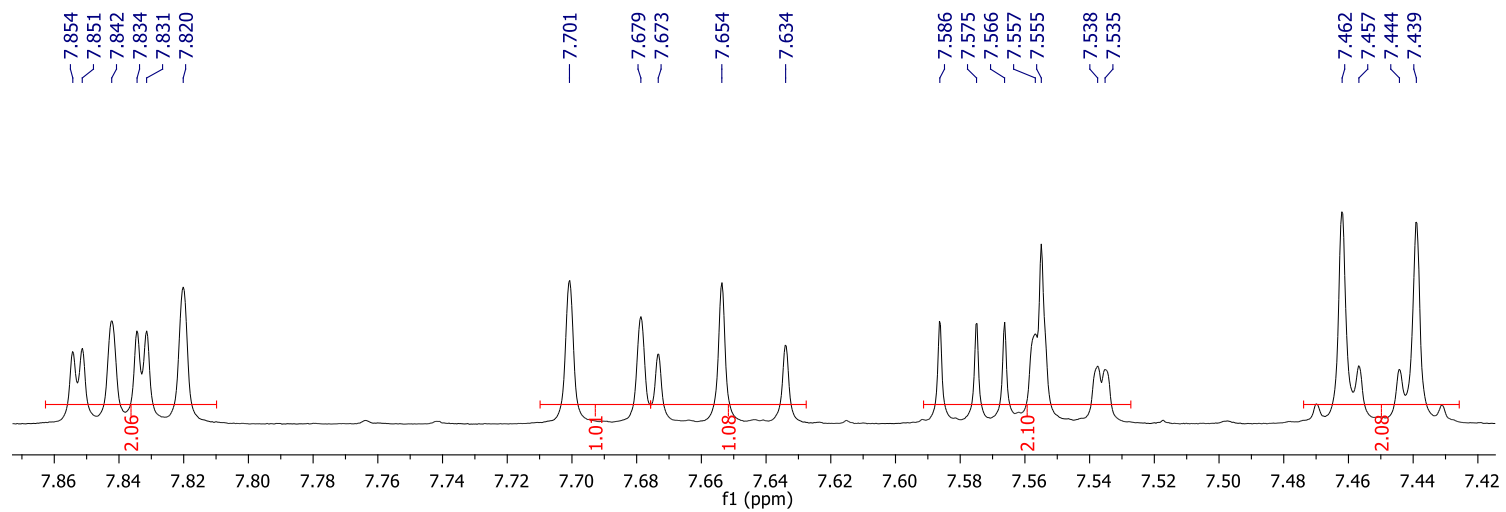
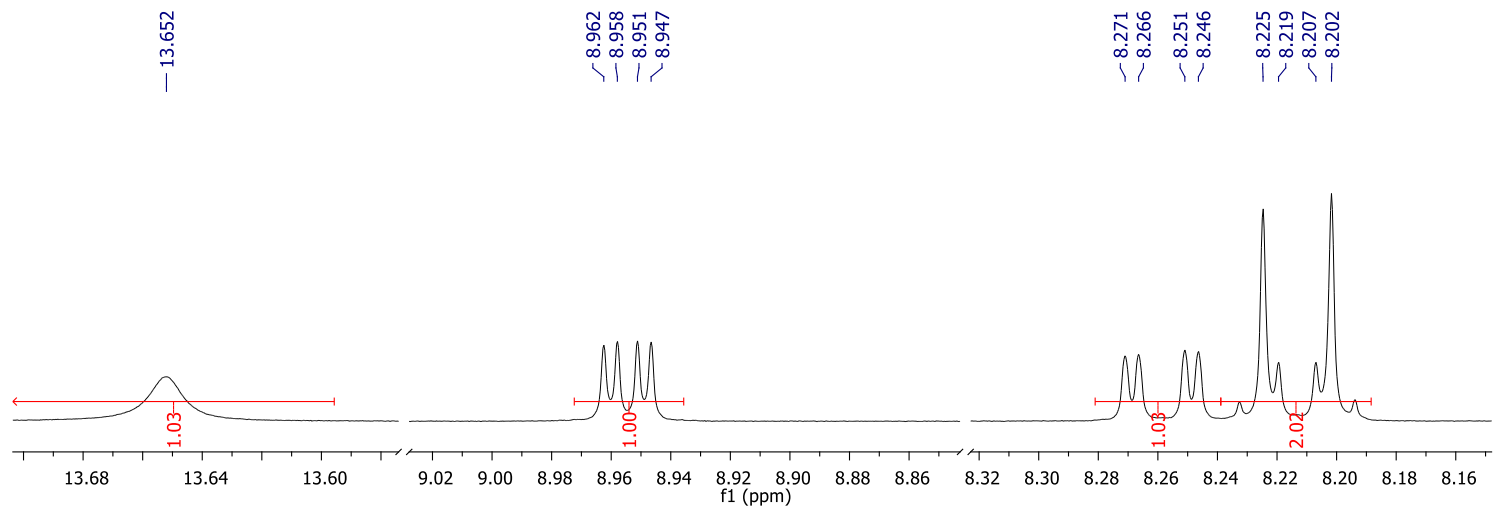


Figure S14. a) ^1H -NMR spectrum of compound **2ah** in CDCl_3 , 400 MHz, at 298 K; b) $^{13}\text{C}\{^1\text{H}\}$ -NMR spectrum (CDCl_3 , 100 MHz, 298 K); c) ^1H - ^1H COSY spectrum (CDCl_3 , 100 MHz, 298 K); d) ^1H - ^{13}C HSQCed spectrum (CDCl_3 , 400 MHz, 298 K); e) ^1H - ^{13}C HMBC spectrum (CDCl_3 , 400 MHz, 298 K); f) HRMS (ESI-MS) spectrum (m/z). Observed HRMS (left) with the theoretical isotope prediction (right).

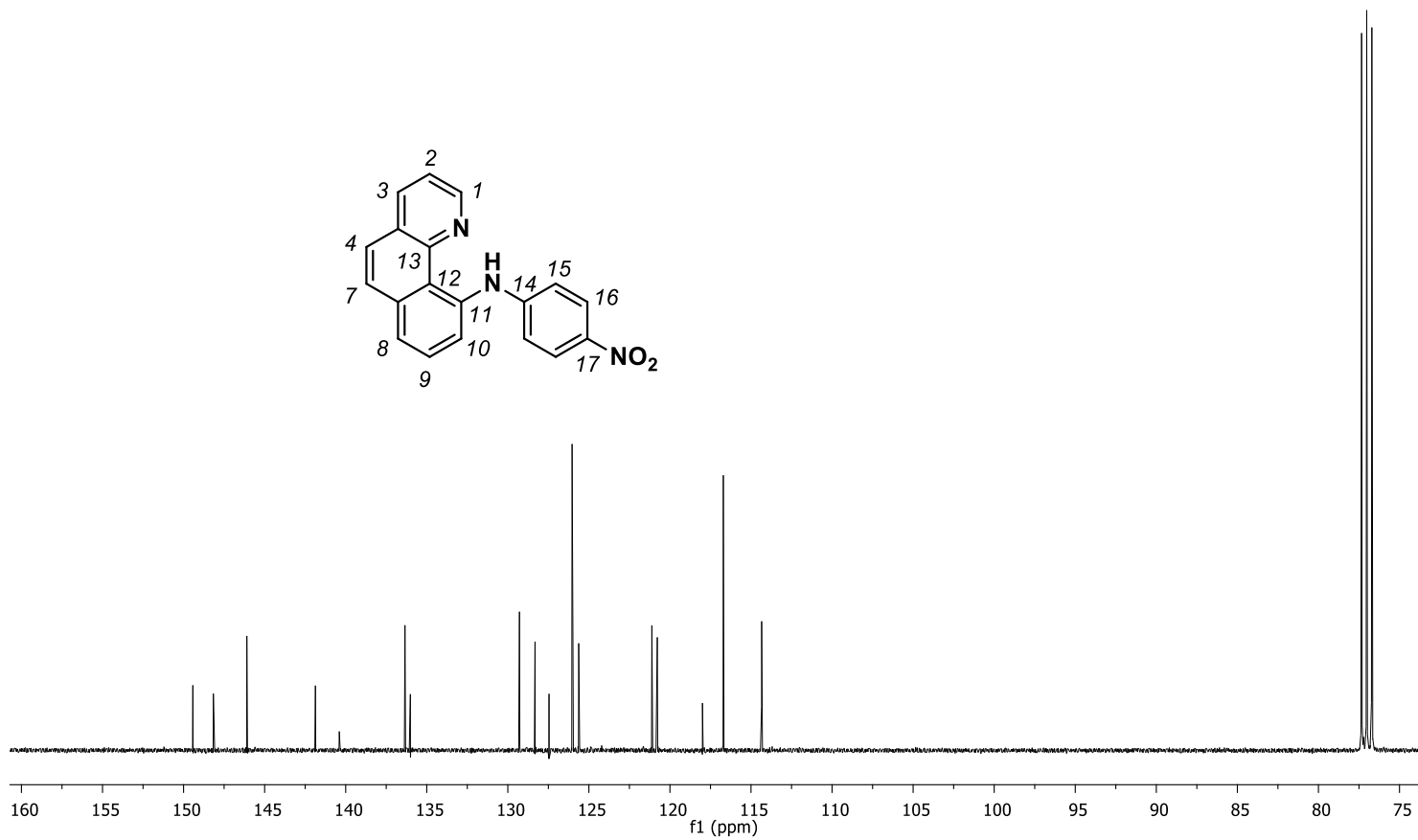
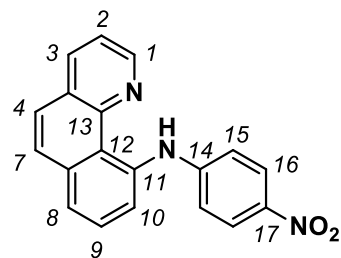




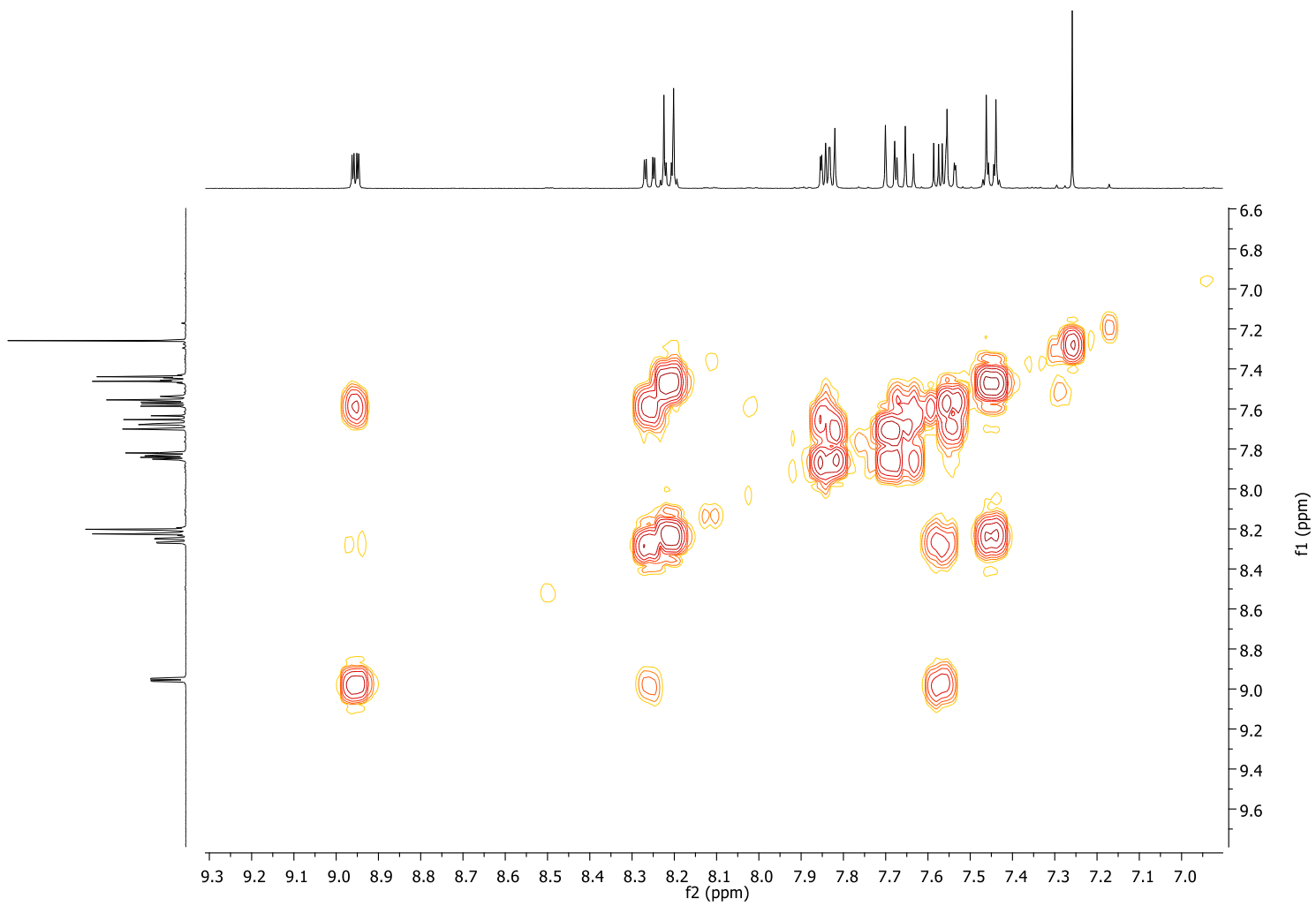
Selected aromatic region

b)

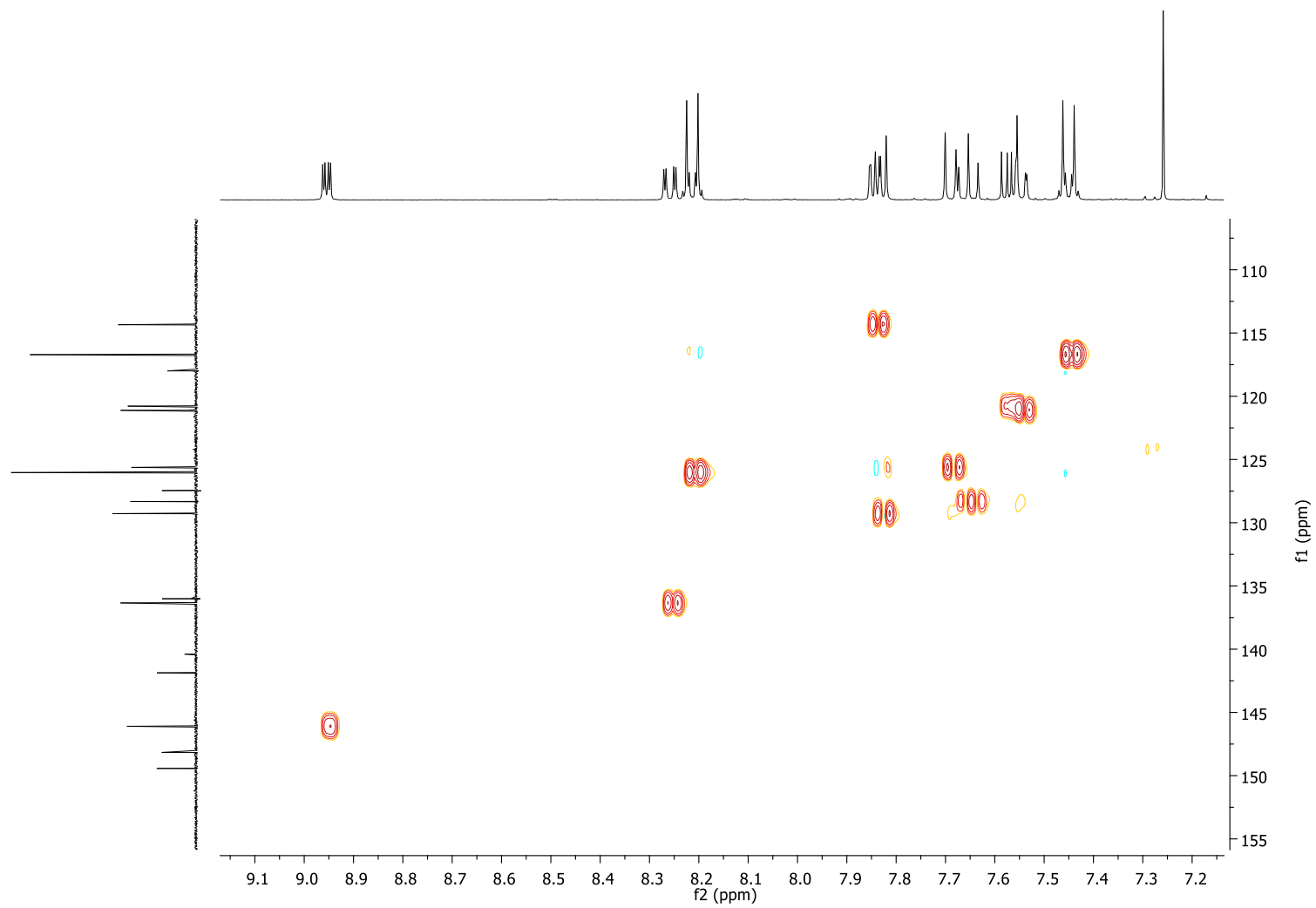
149.43
148.16
146.10
141.87
140.40
136.34
136.01
129.28
128.32
127.46
126.04
125.63
121.12
120.78
117.99
116.71
114.34



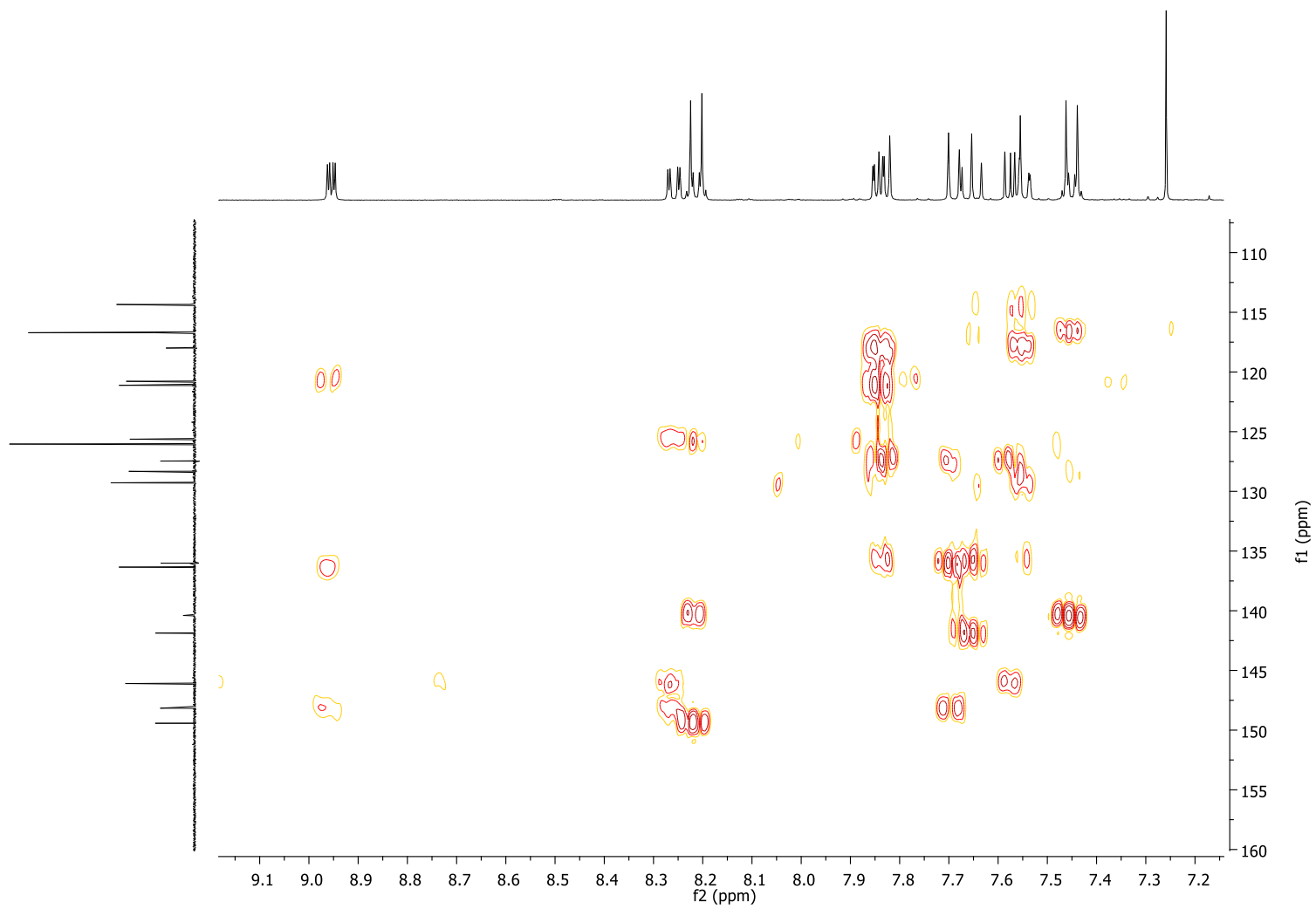
c)



d)



e)



f)

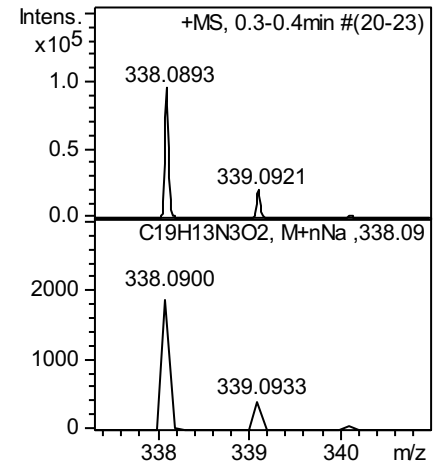
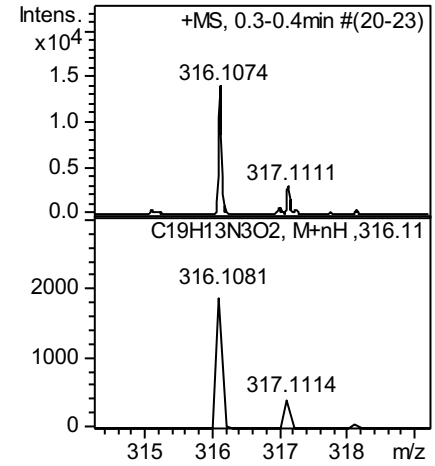
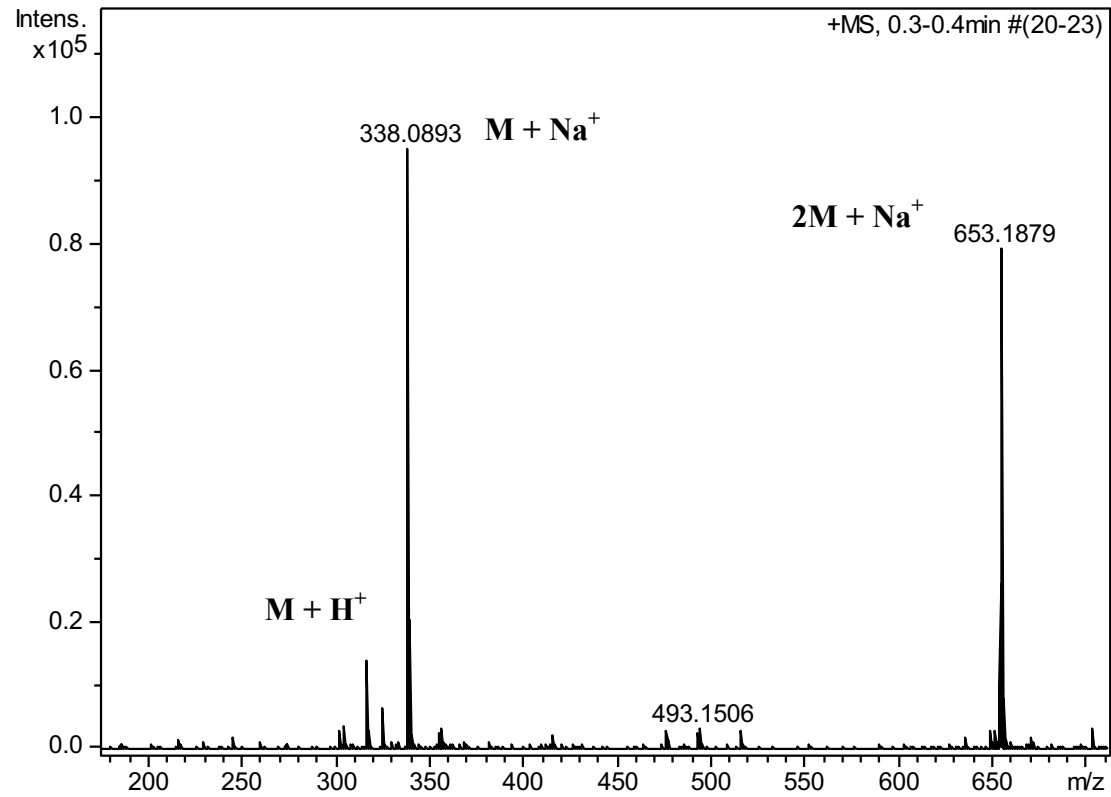
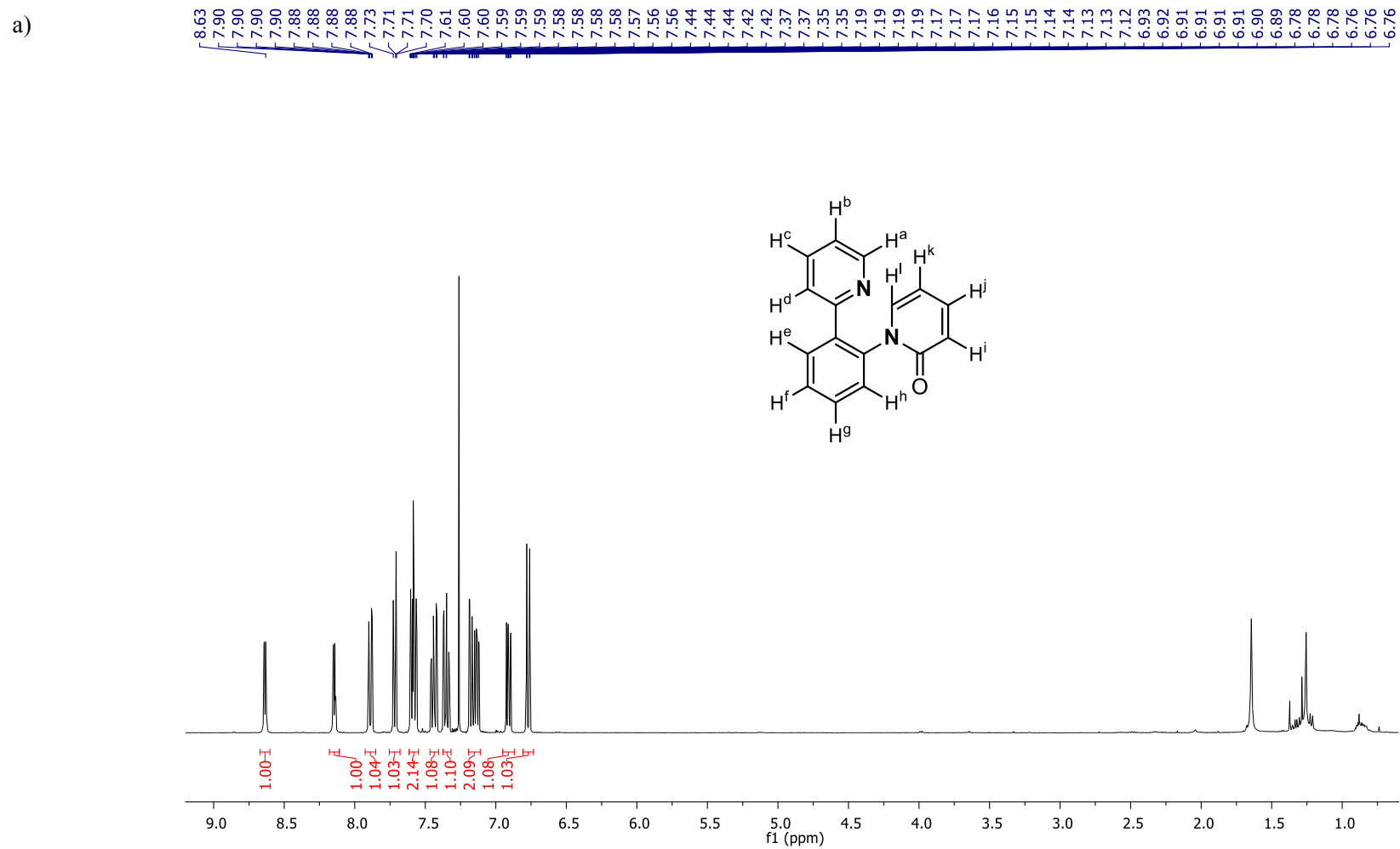
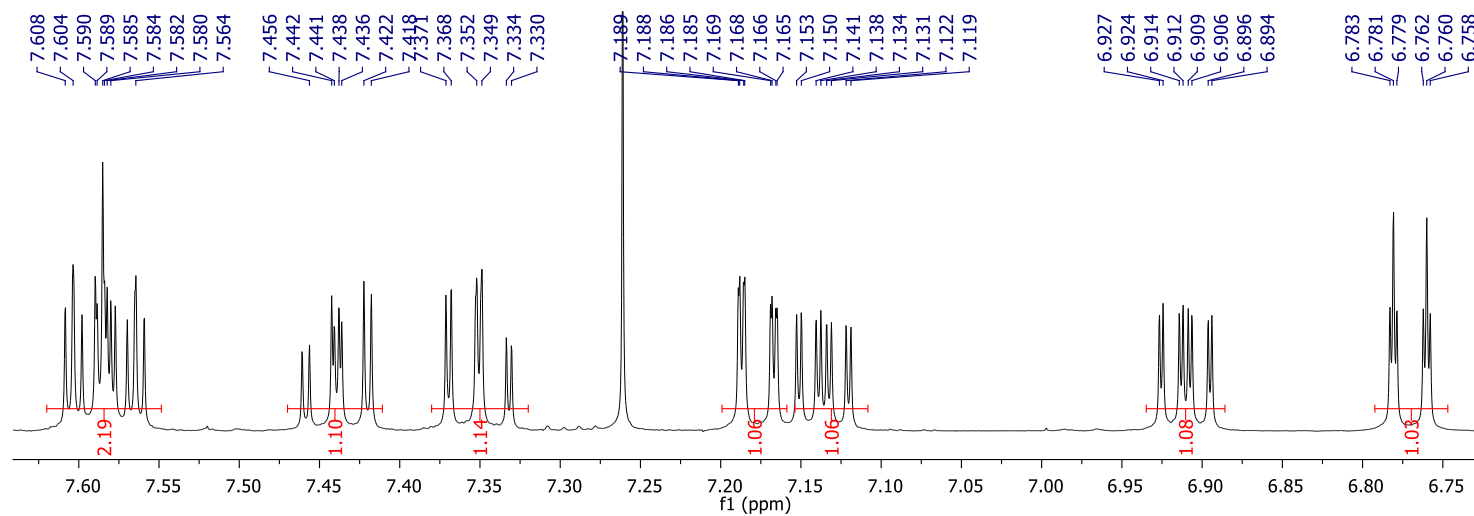
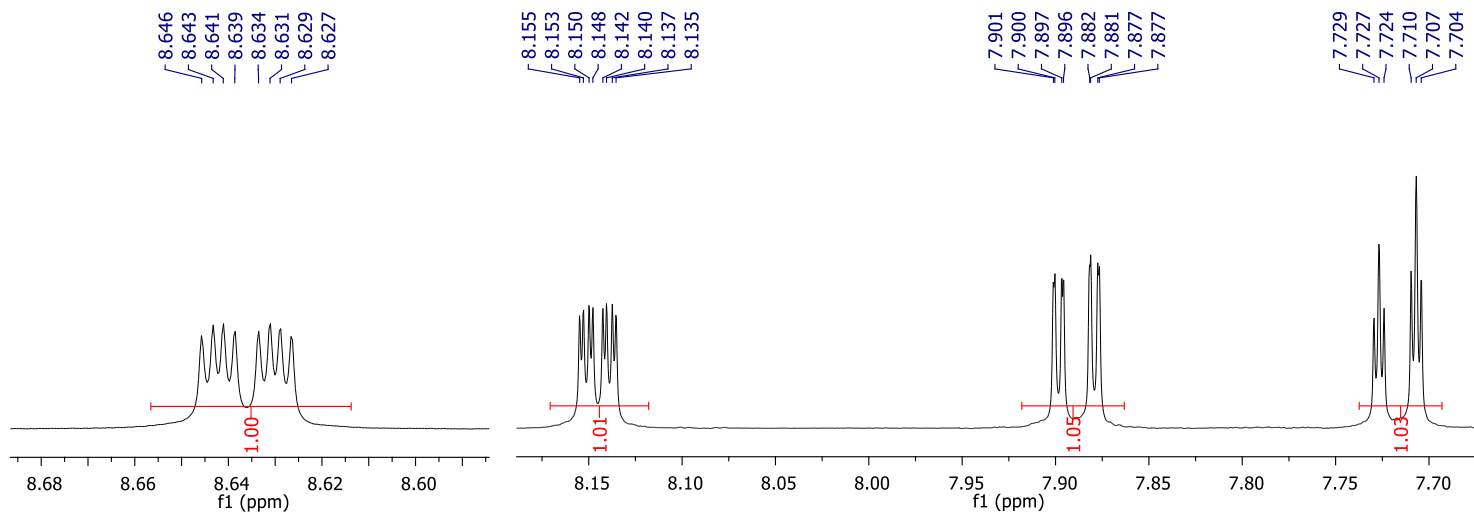


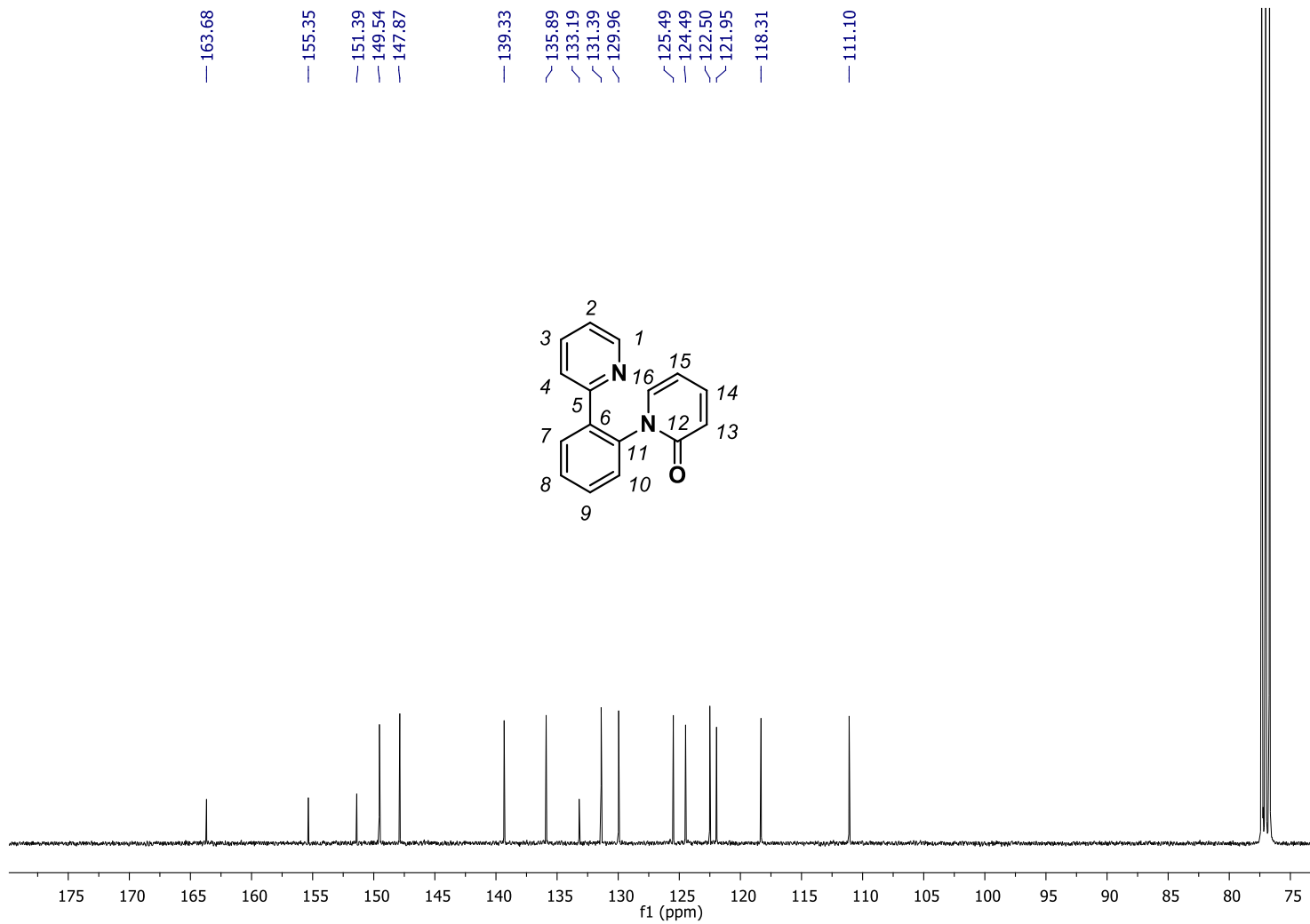
Figure S15. a) ^1H -NMR spectrum of compound **1ai** in CDCl_3 , 400 MHz, at 298 K; b) $^{13}\text{C}\{^1\text{H}\}$ -NMR spectrum (CDCl_3 , 100 MHz, 298 K); c) ^1H - ^1H COSY spectrum (CDCl_3 , 100 MHz, 298 K); d) ^1H - ^{13}C HSQCed spectrum (CDCl_3 , 400 MHz, 298 K); e) ^1H - ^{13}C HMBC spectrum (CDCl_3 , 400 MHz, 298 K); f) HRMS (ESI-MS) spectrum (m/z). Observed HRMS (left) with the theoretical isotope prediction (right).



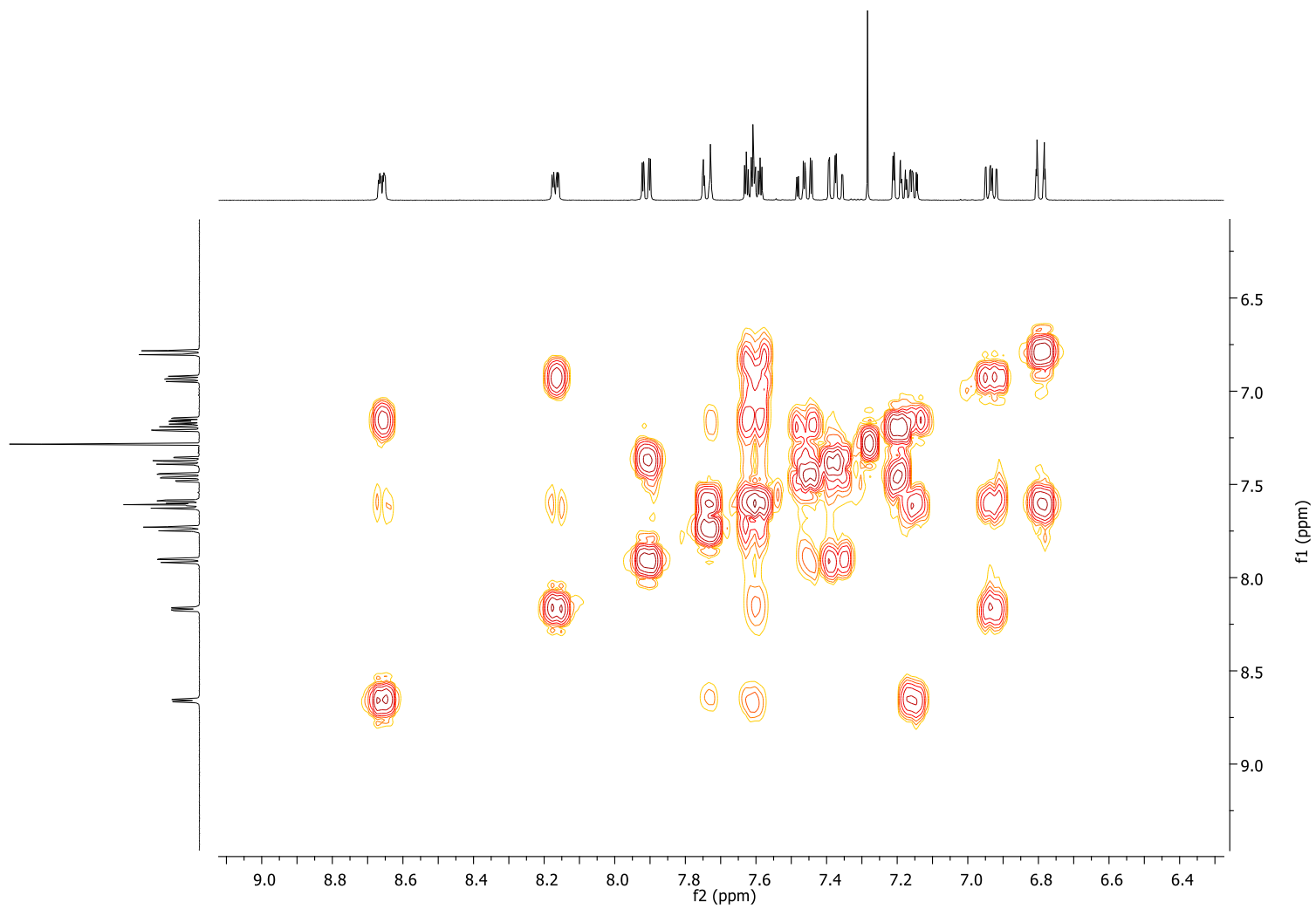


Selected aromatic region

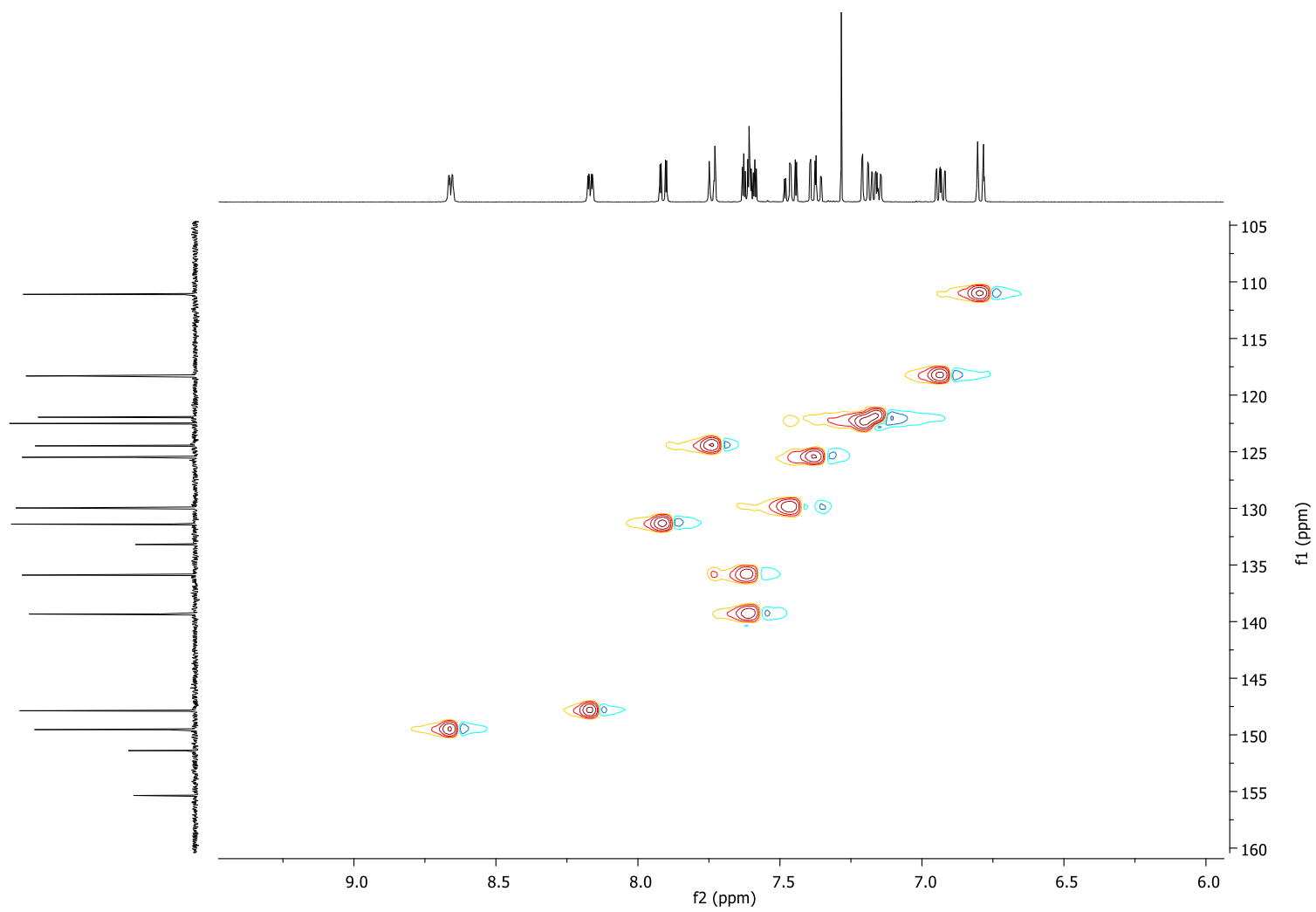
b)



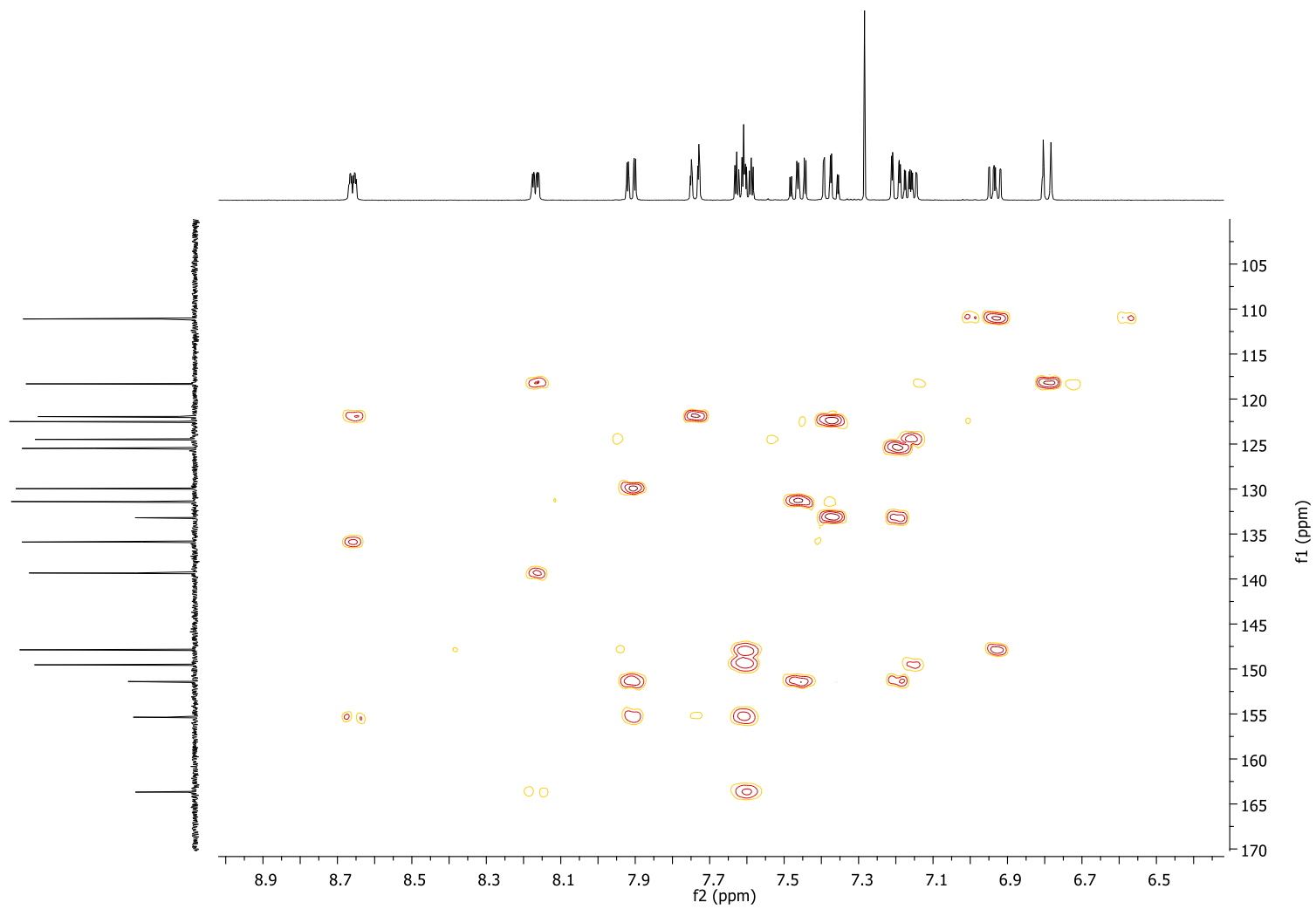
c)



d)



e)



f)

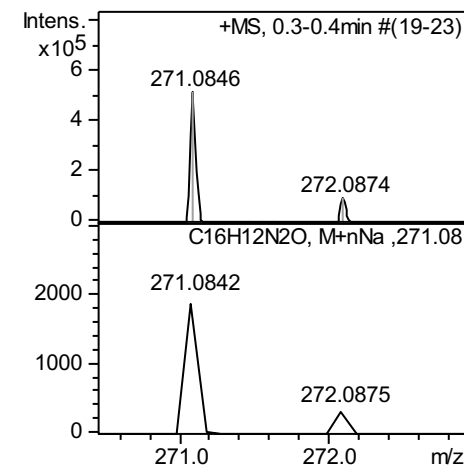
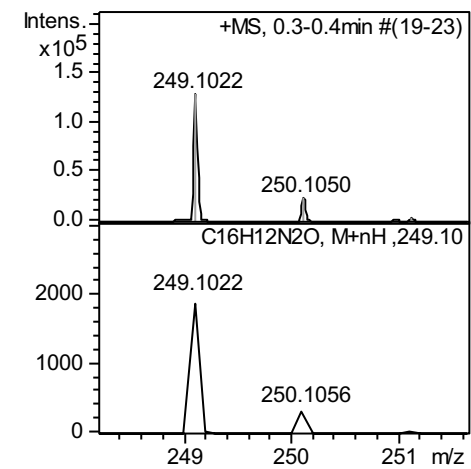
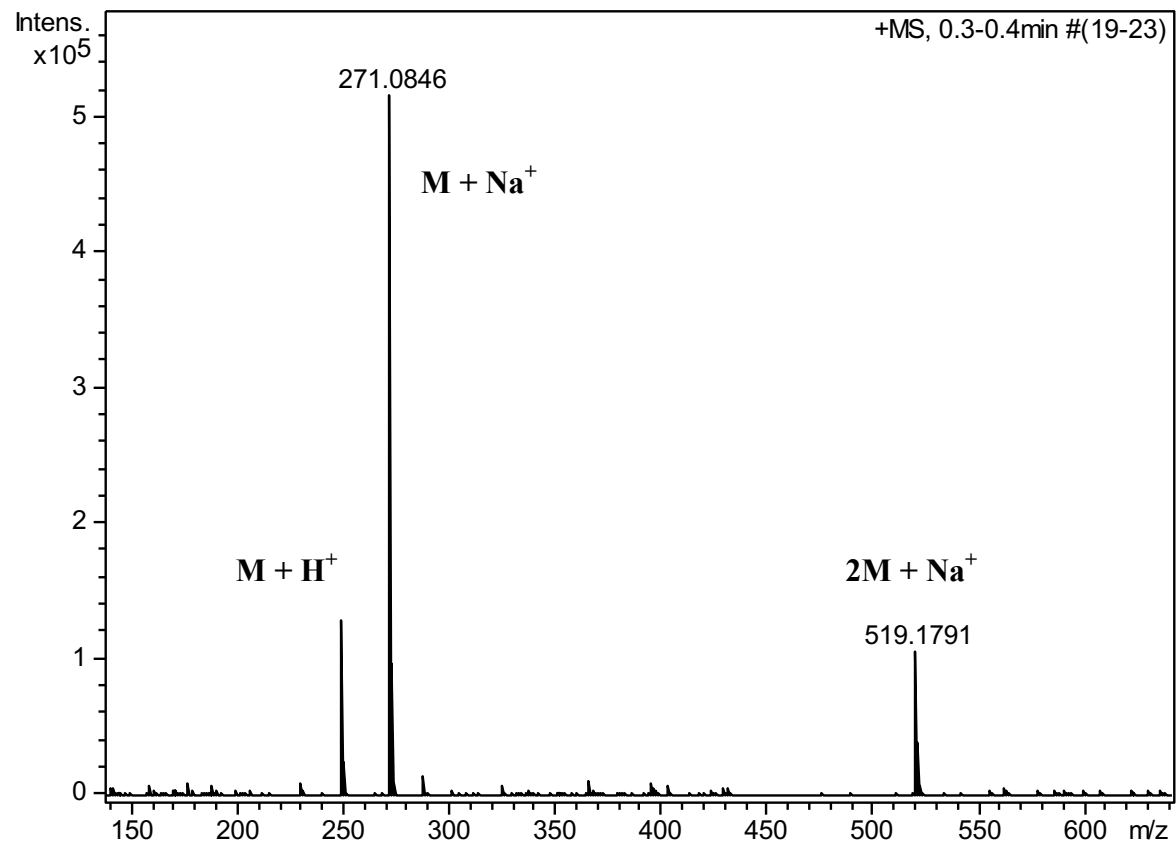
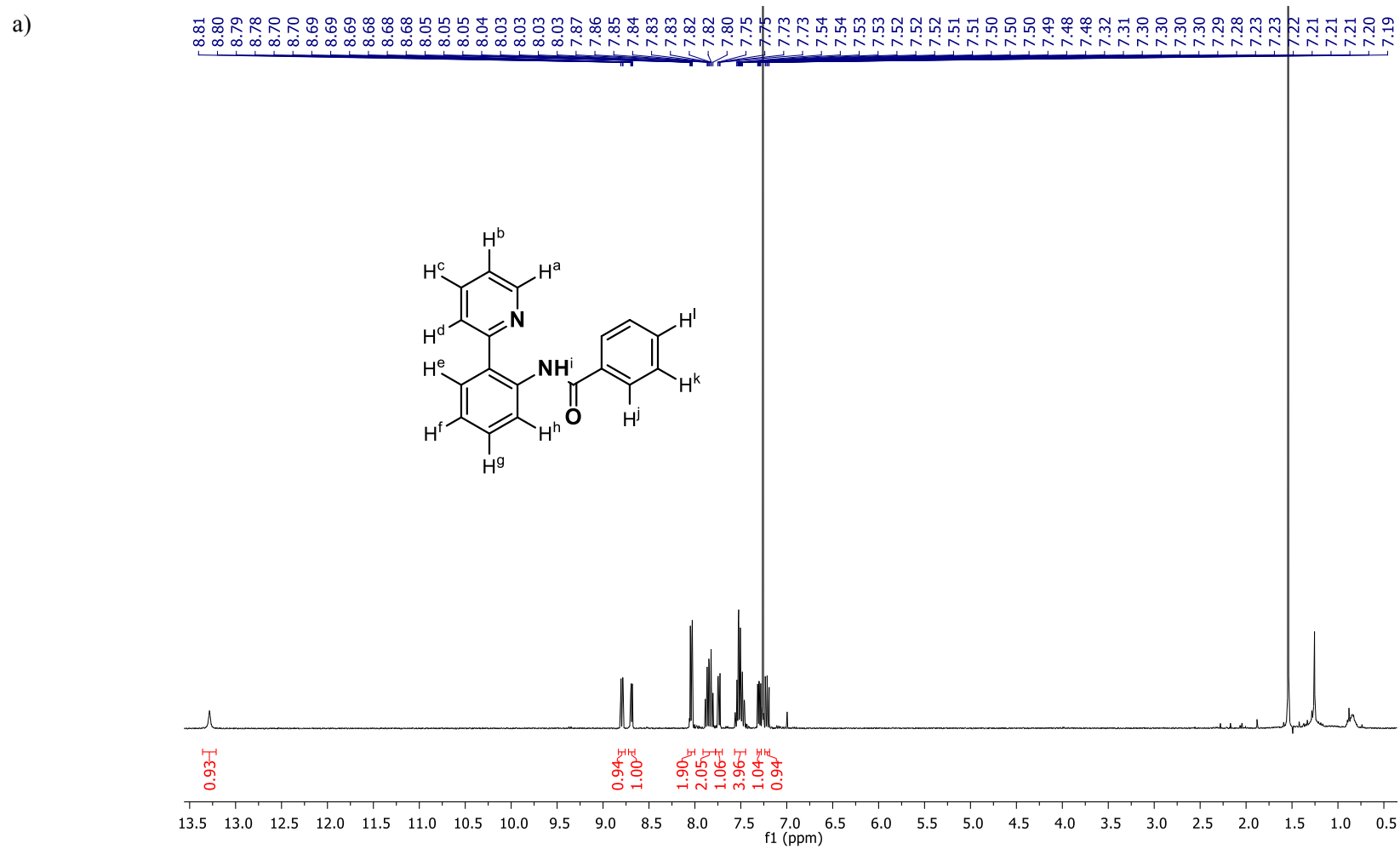
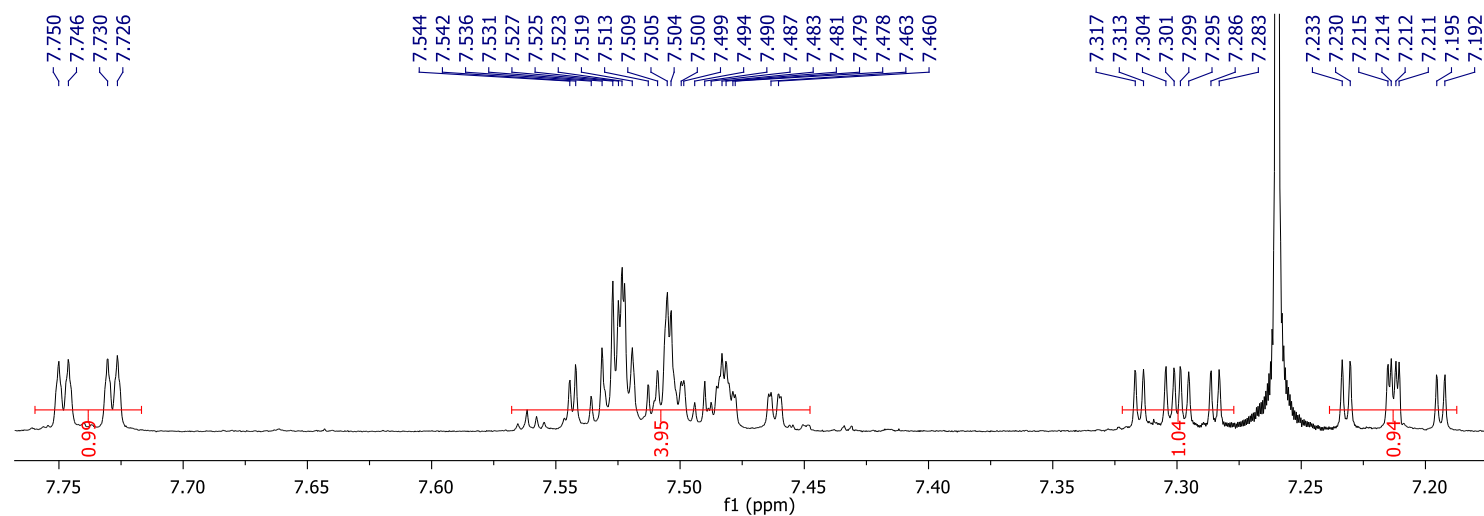
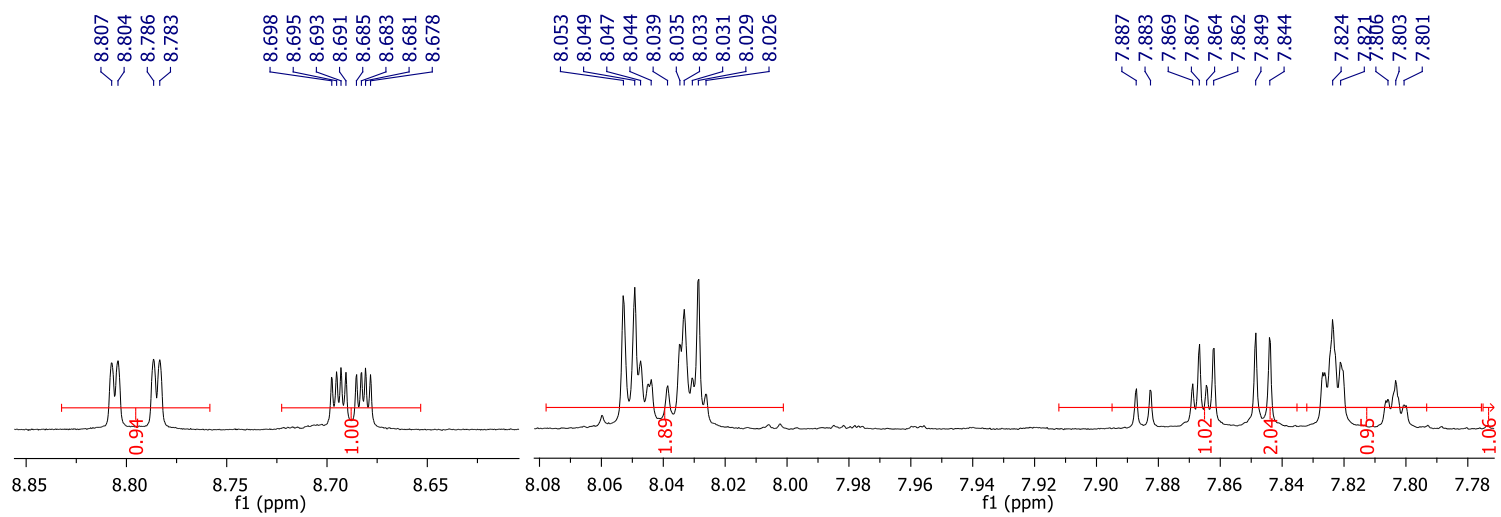


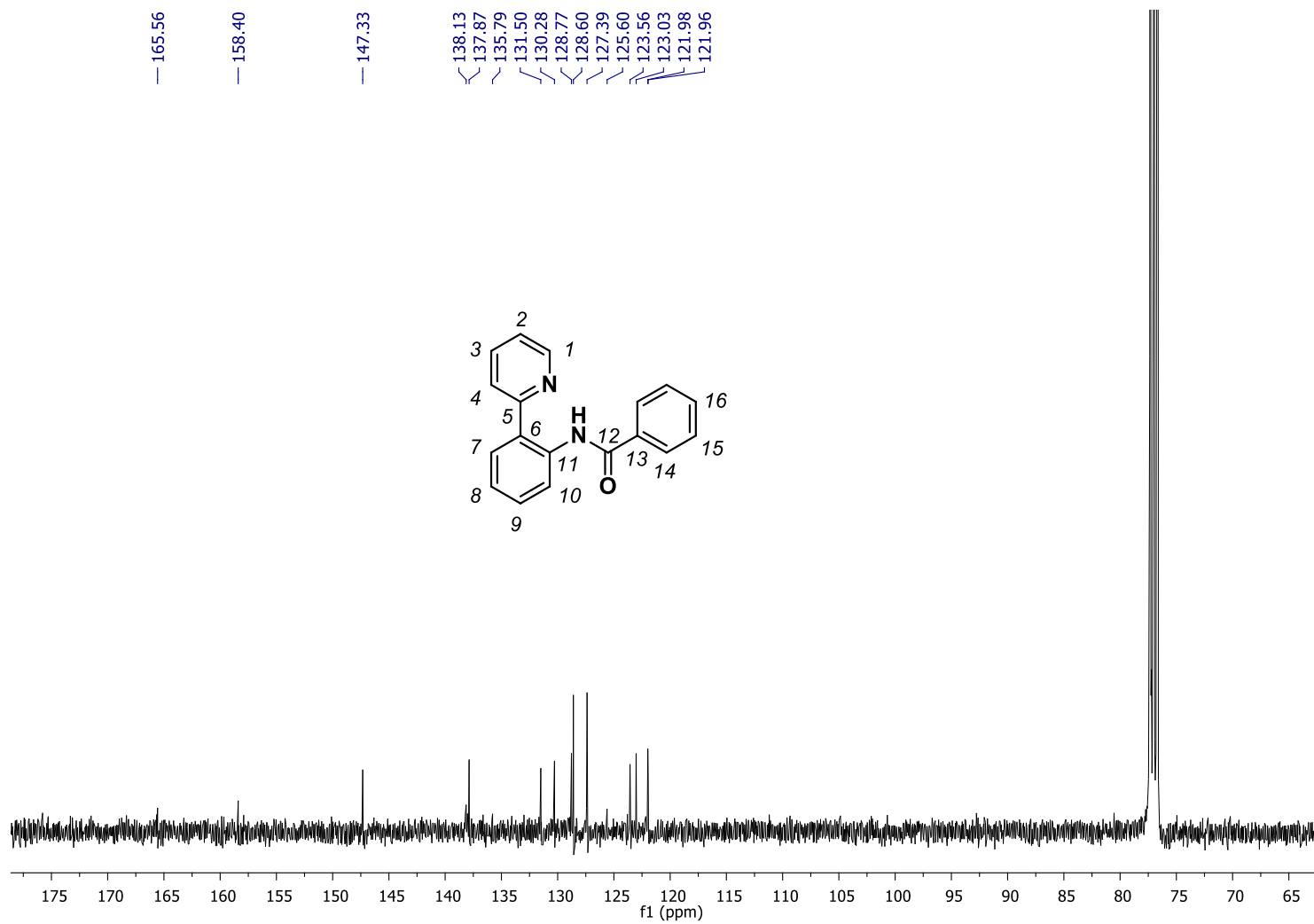
Figure S16. a) ^1H -NMR spectrum of compound **1aj** in CDCl_3 , 400 MHz, at 298 K; b) $^{13}\text{C}\{^1\text{H}\}$ -NMR spectrum (CDCl_3 , 100 MHz, 298 K); c) ^1H - ^1H COSY spectrum (CDCl_3 , 100 MHz, 298 K); d) ^1H - ^{13}C HSQCed spectrum (CDCl_3 , 400 MHz, 298 K); e) ^1H - ^{13}C HMBC spectrum (CDCl_3 , 400 MHz, 298 K); f) HRMS (ESI-MS) spectrum (m/z). Observed HRMS (left) with the theoretical isotope prediction (right).



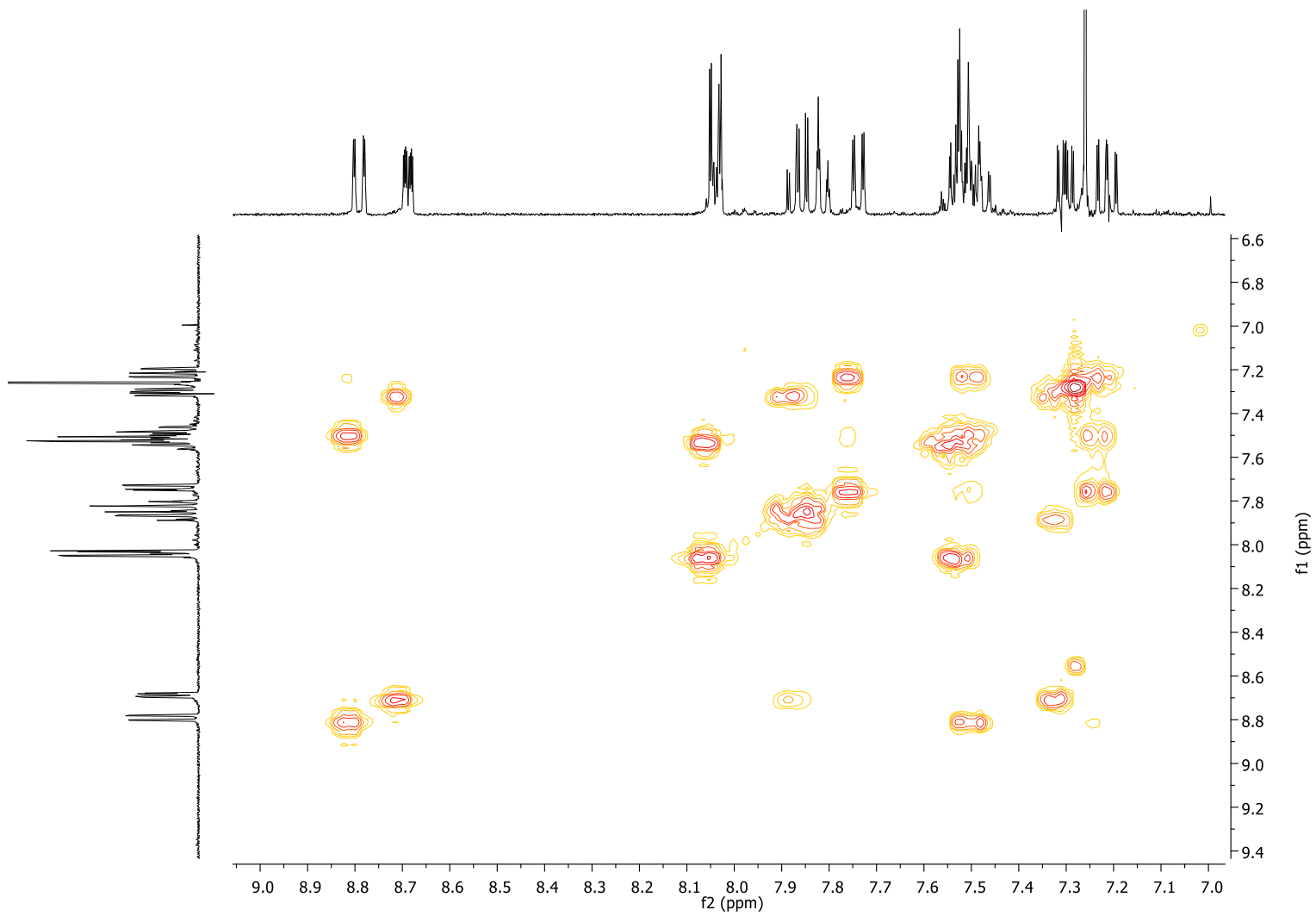


Selected aromatic region

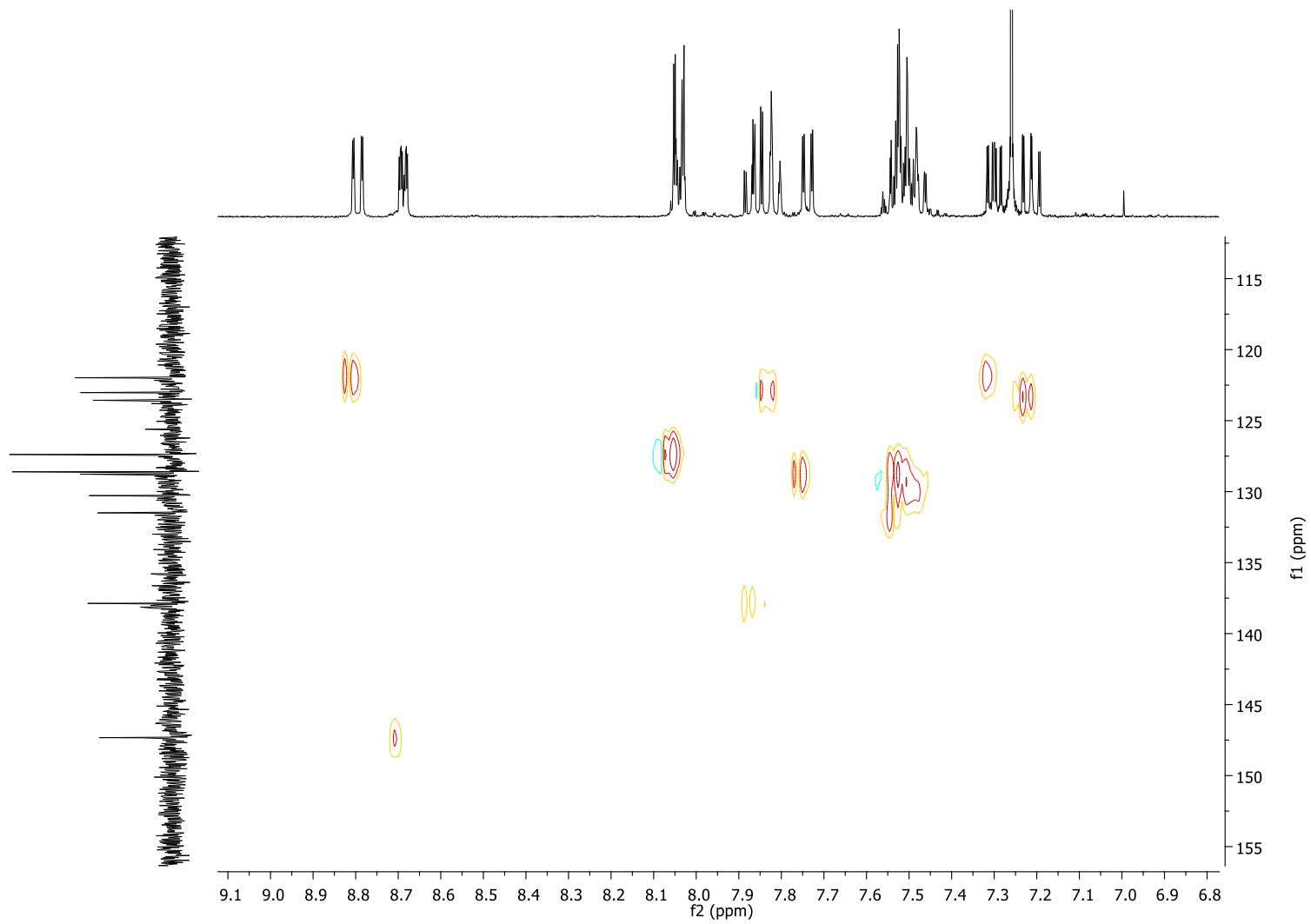
b)



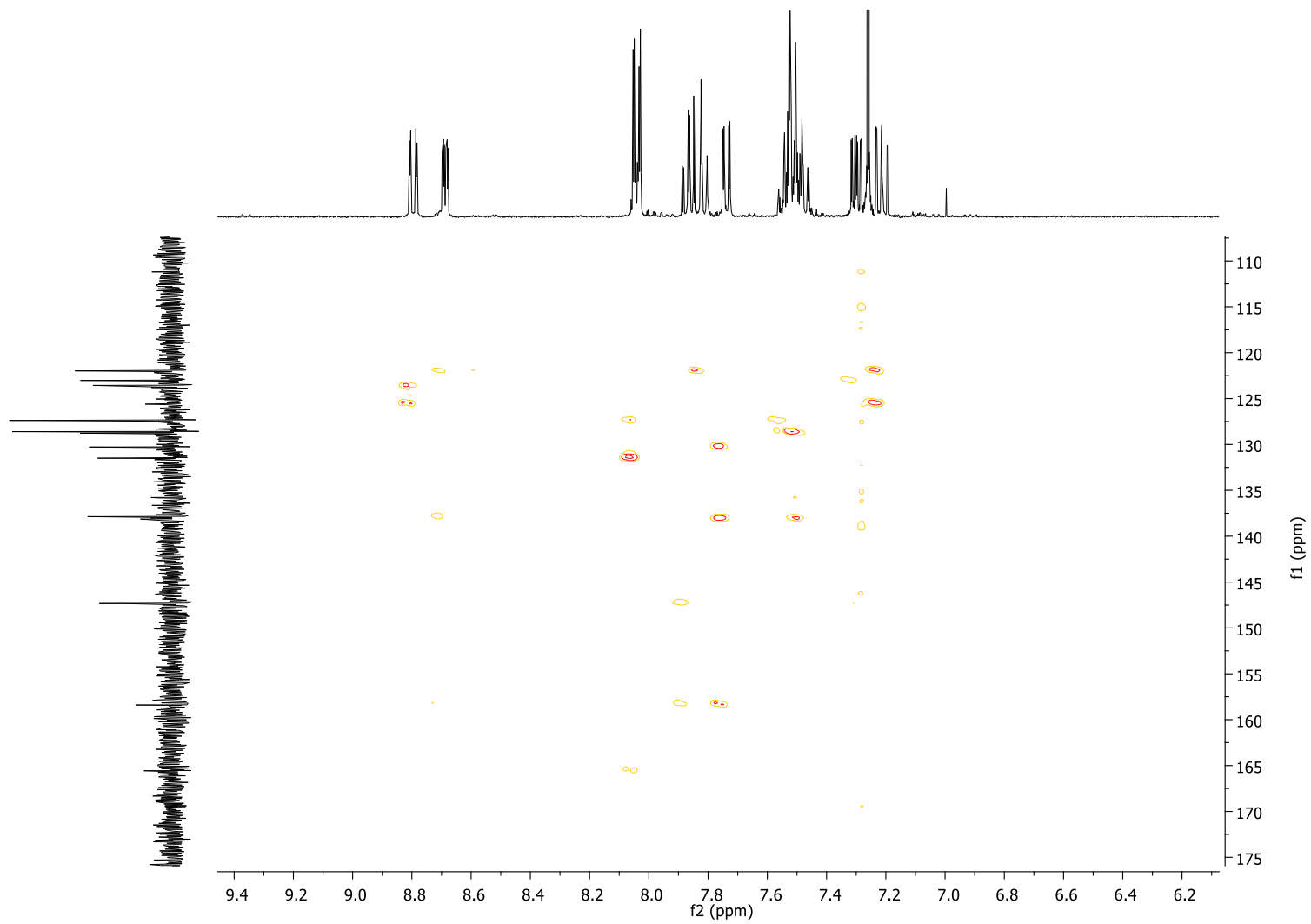
c)



d)



e)



f)

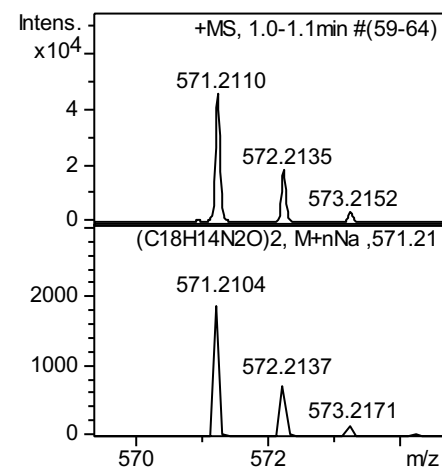
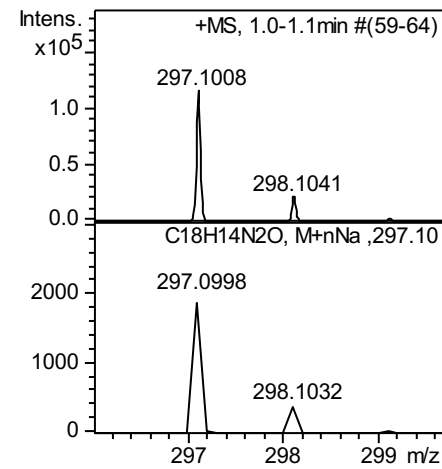
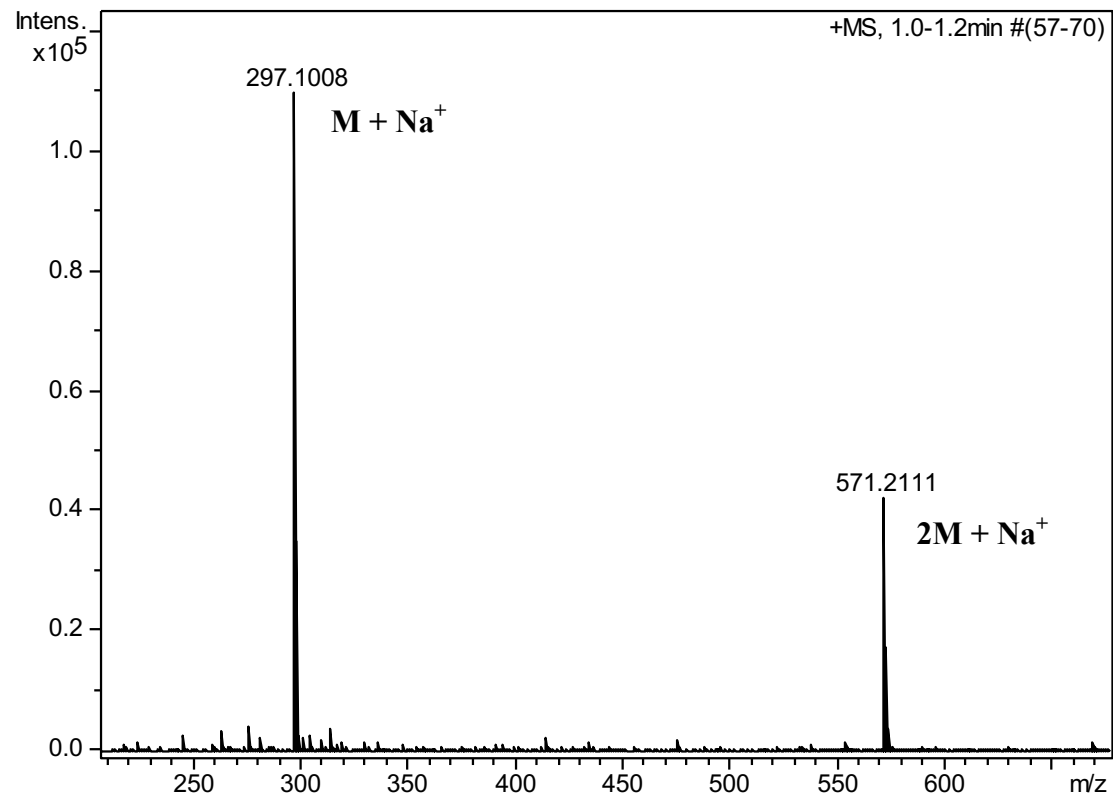
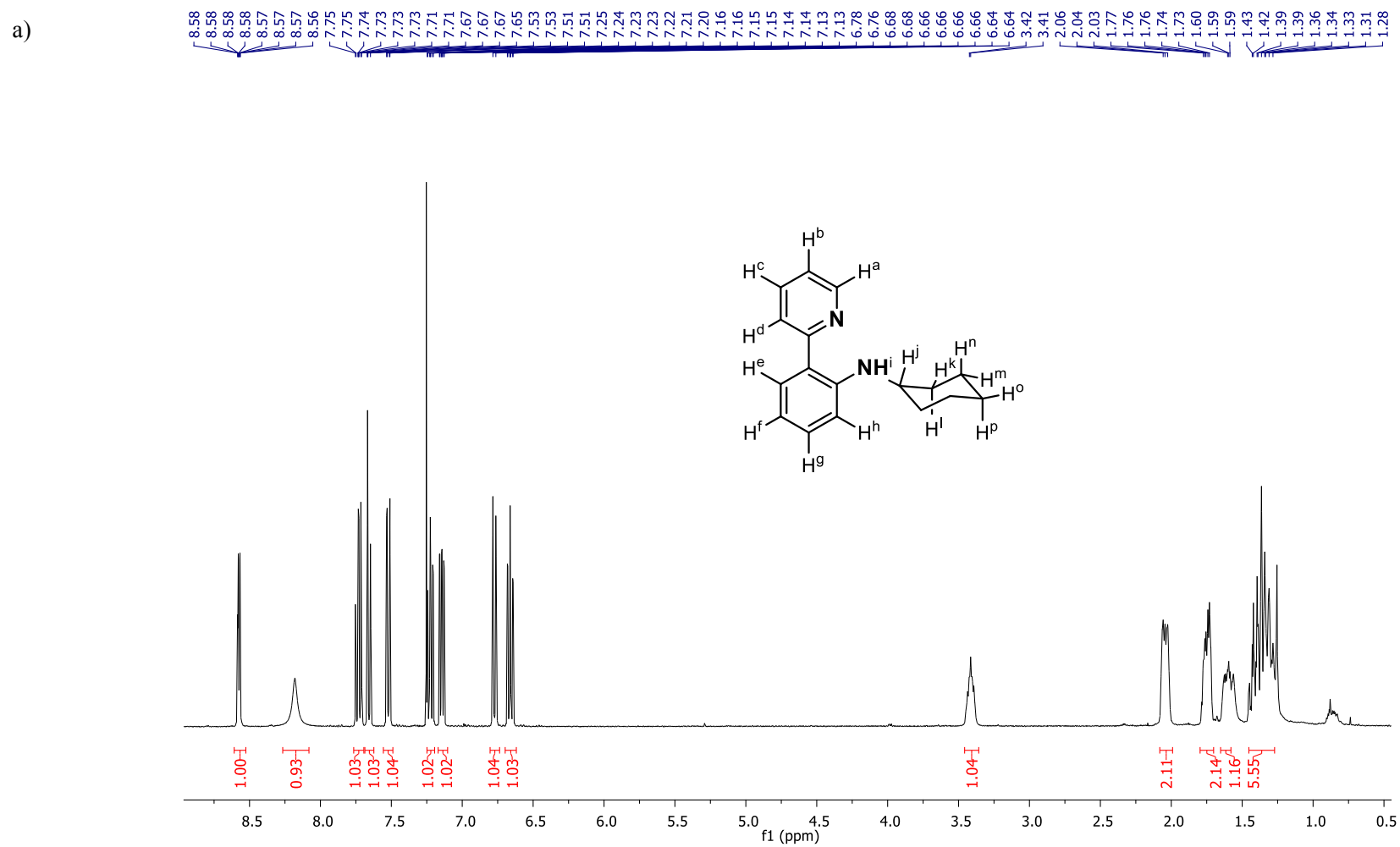
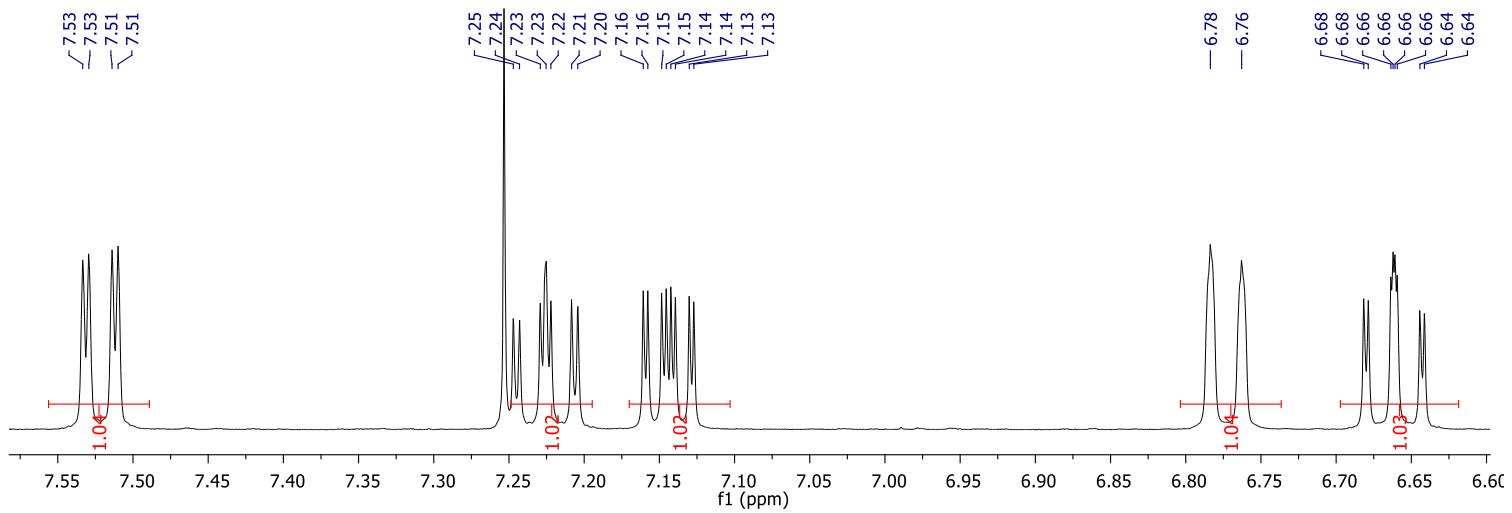
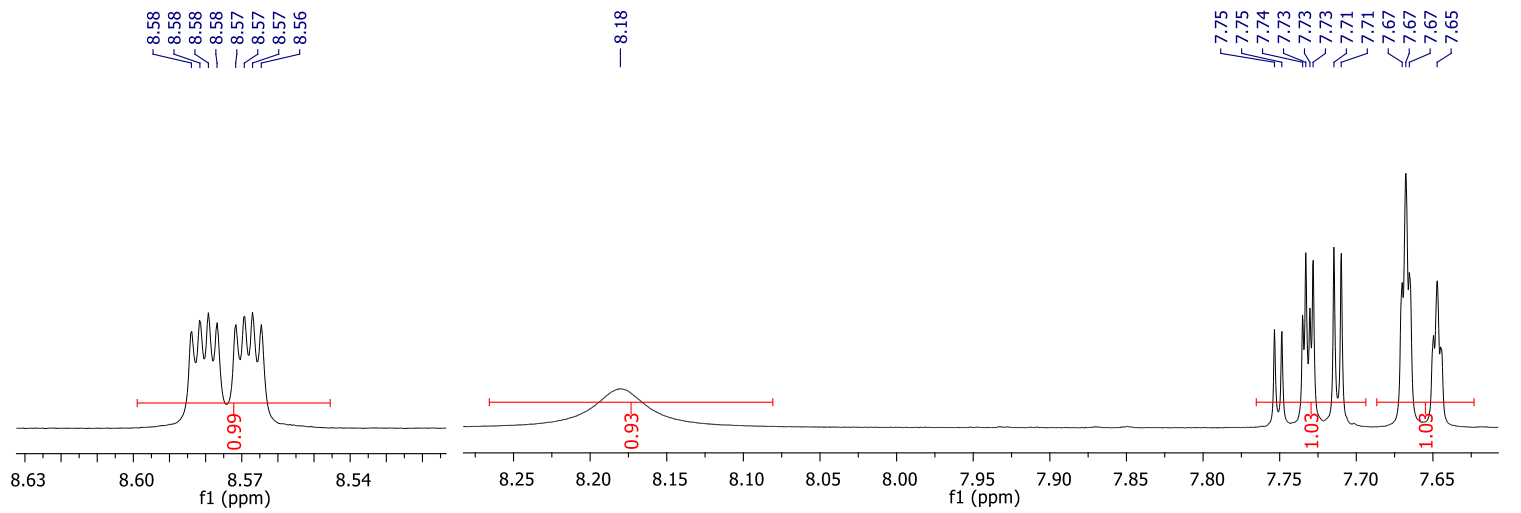


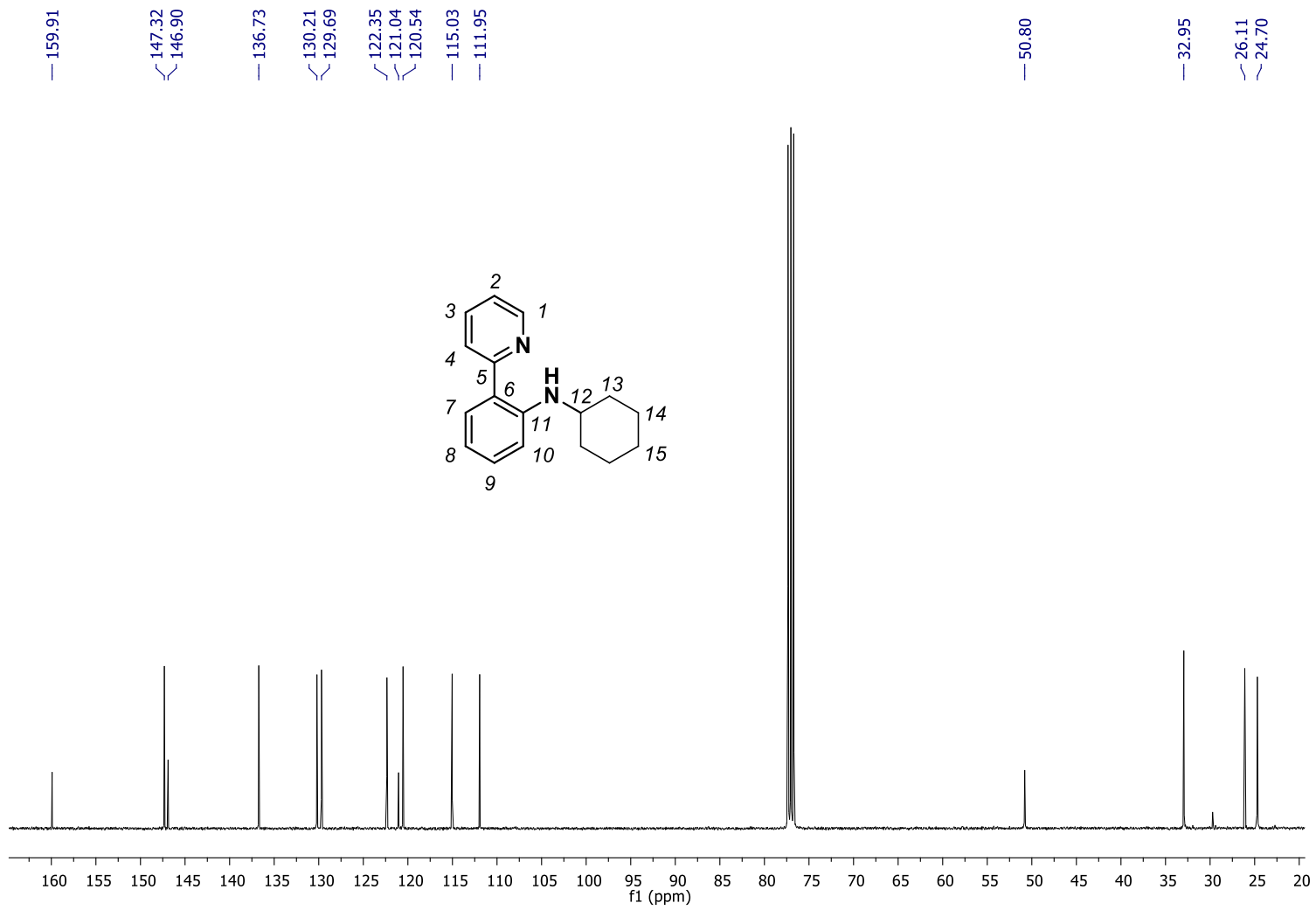
Figure S17. a) ^1H -NMR spectrum of compound **1ak** in CDCl_3 , 400 MHz, at 298 K; b) $^{13}\text{C}\{^1\text{H}\}$ -NMR spectrum (CDCl_3 , 100 MHz, 298 K); c) ^1H - ^1H COSY spectrum (CDCl_3 , 100 MHz, 298 K); d) ^1H - ^{13}C HSQCed spectrum (CDCl_3 , 400 MHz, 298 K); e) ^1H - ^{13}C HMBC spectrum (CDCl_3 , 400 MHz, 298 K); f) HRMS (ESI-MS) spectrum (m/z). Observed HRMS (left) with the theoretical isotope prediction (right).



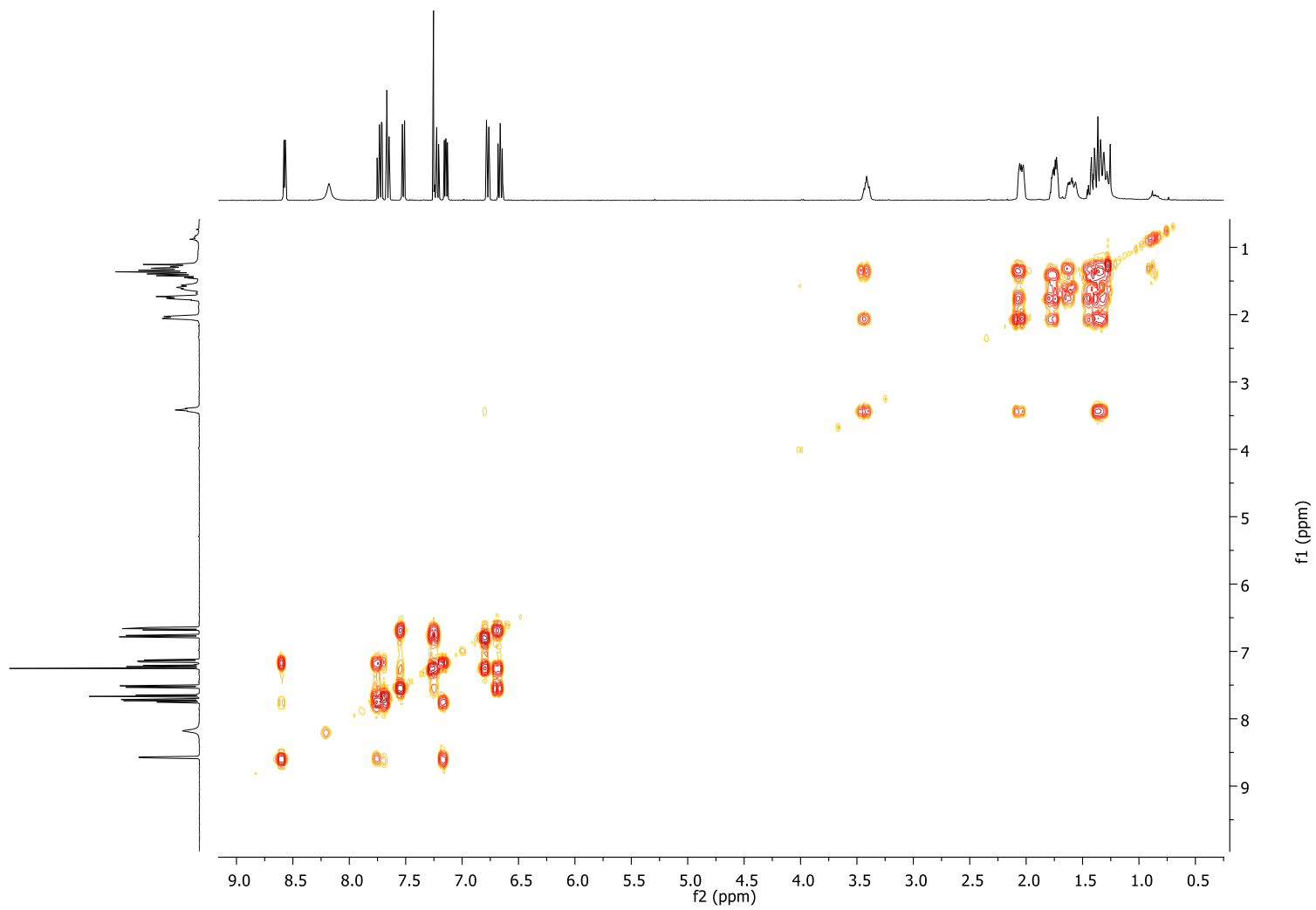


Selected aromatic region

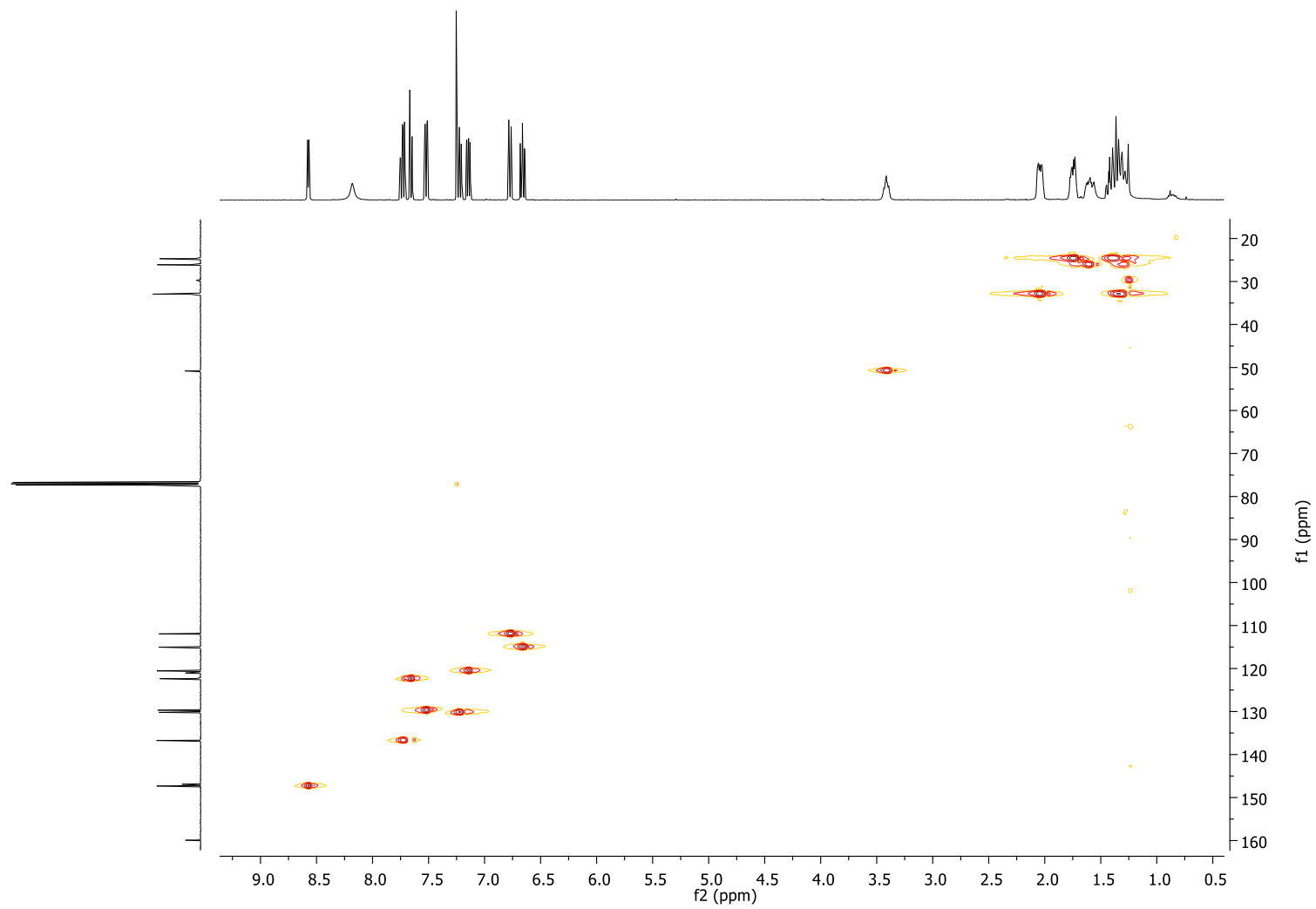
b)



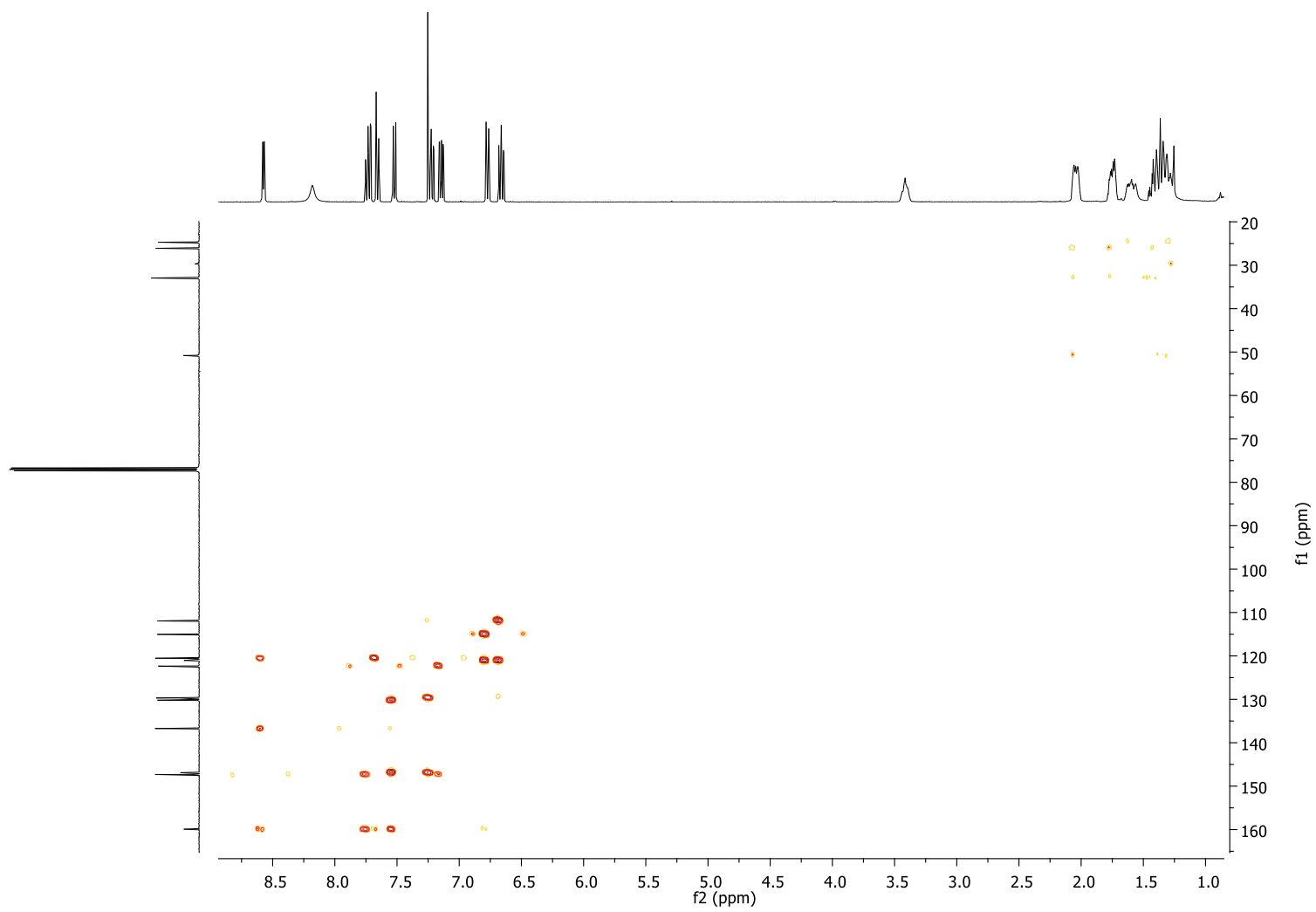
c)



d)



e)



f)

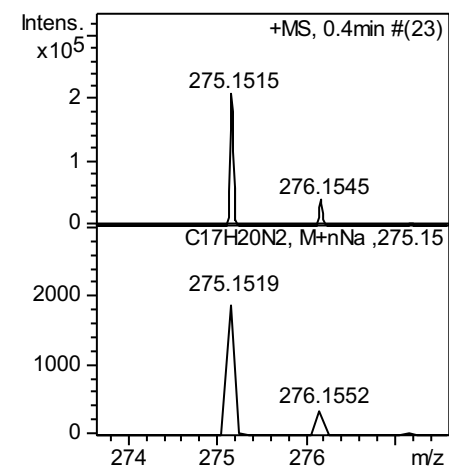
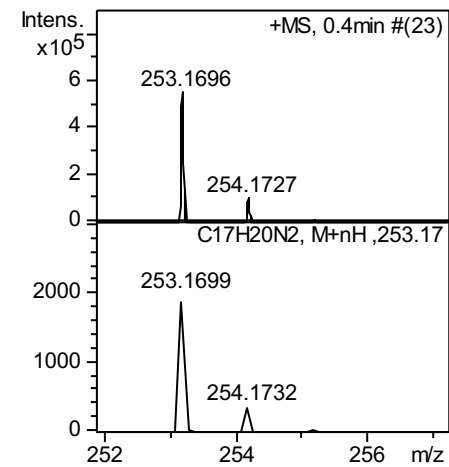
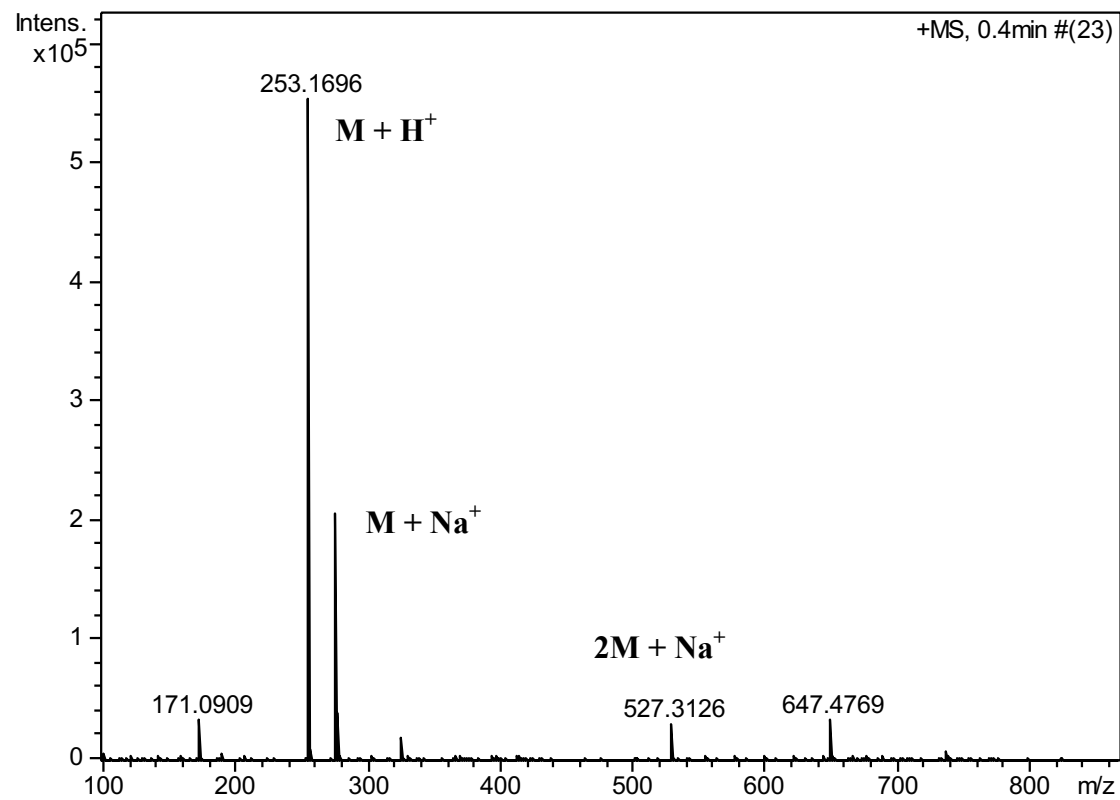
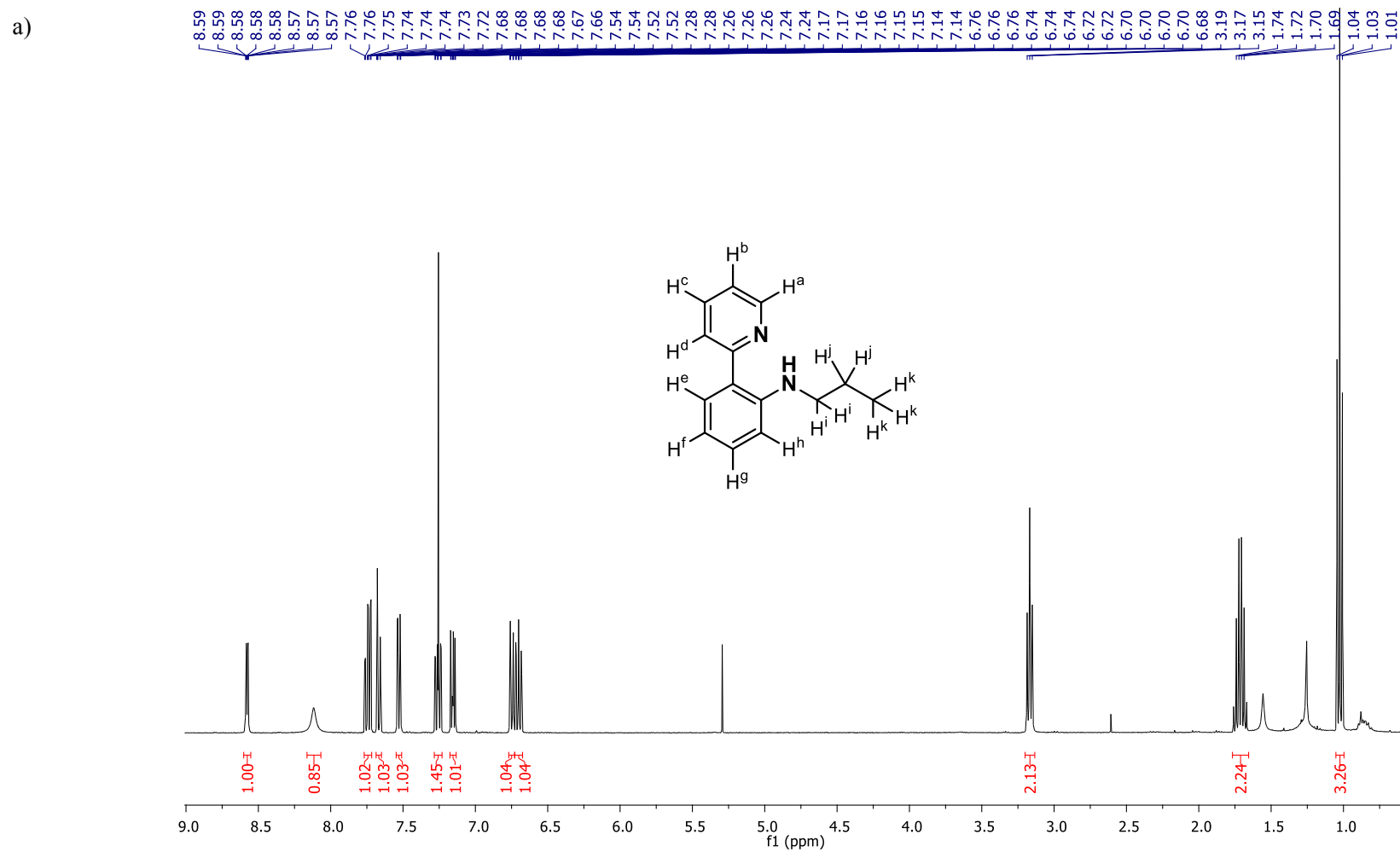
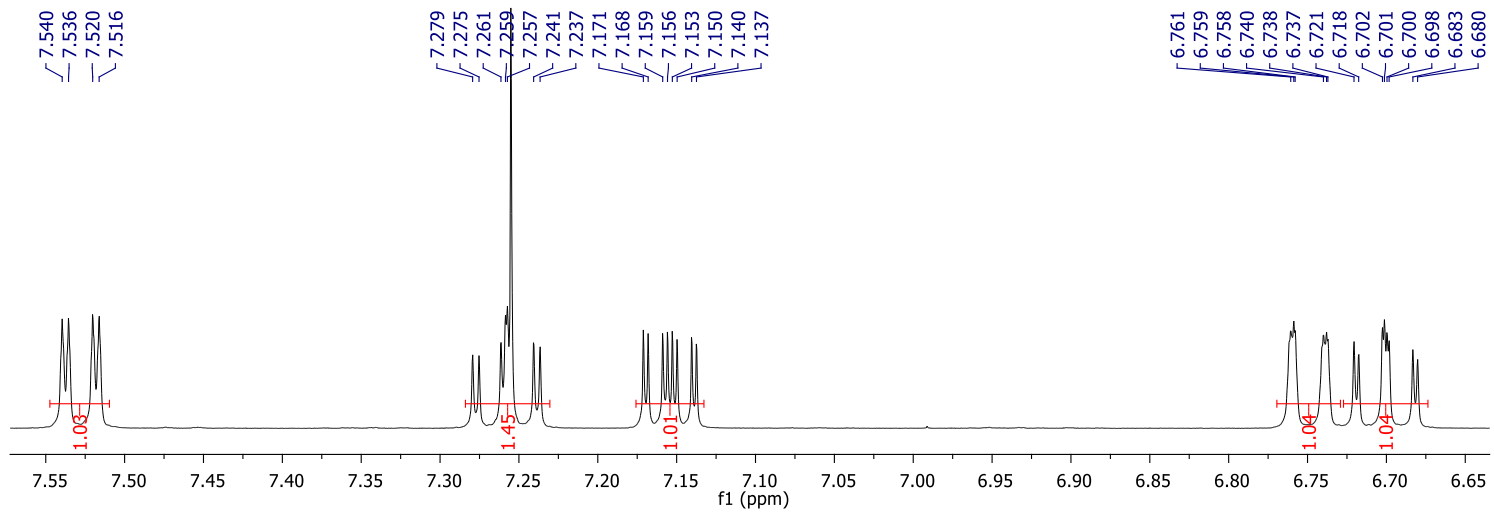
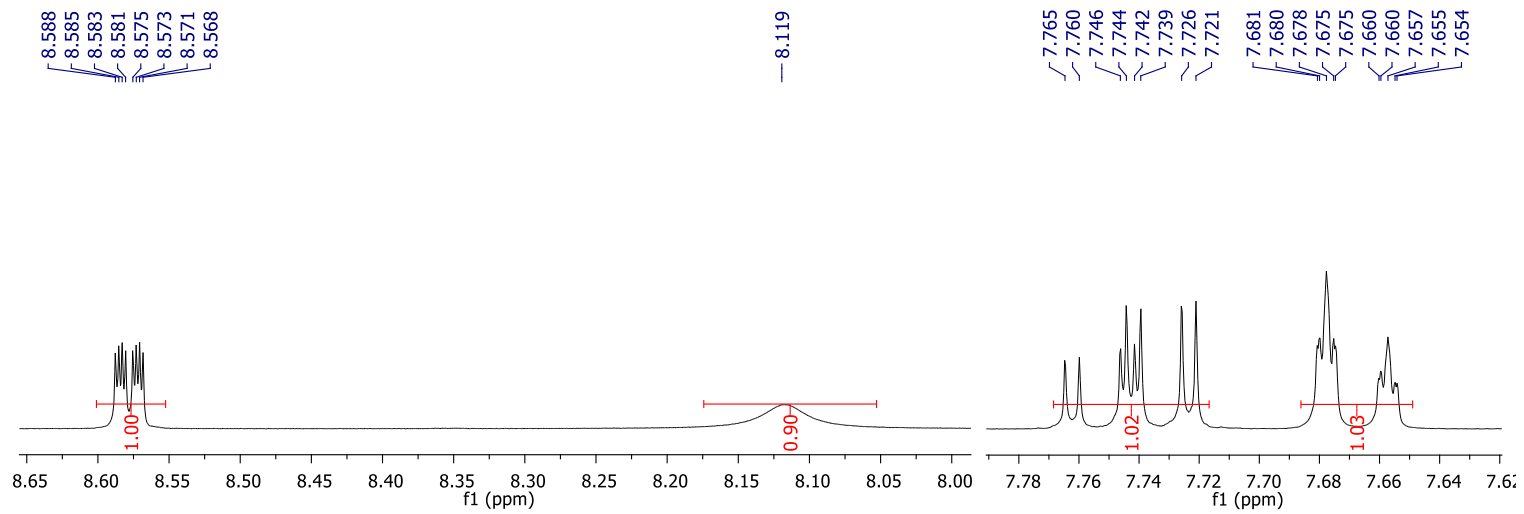


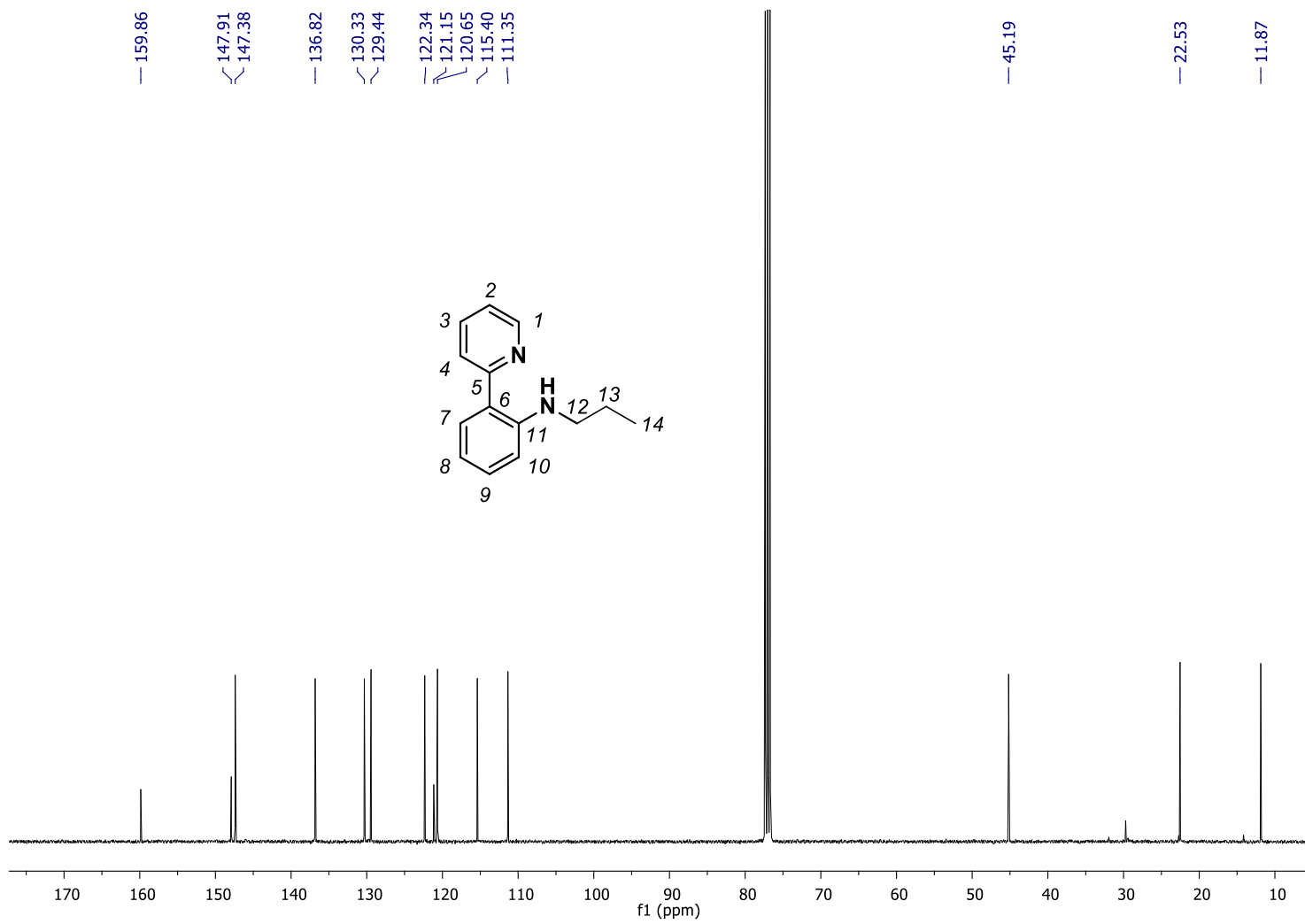
Figure S18. a) ^1H -NMR spectrum of compound **1aI** in CDCl_3 , 400 MHz, at 298 K; b) $^{13}\text{C}\{^1\text{H}\}$ -NMR spectrum (CDCl_3 , 100 MHz, 298 K); c) ^1H - ^1H COSY spectrum (CDCl_3 , 100 MHz, 298 K); d) ^1H - ^{13}C HSQCed spectrum (CDCl_3 , 400 MHz, 298 K); e) ^1H - ^{13}C HMBC spectrum (CDCl_3 , 400 MHz, 298 K); f) HRMS (ESI-MS) spectrum (m/z). Observed HRMS (left) with the theoretical isotope prediction (right).



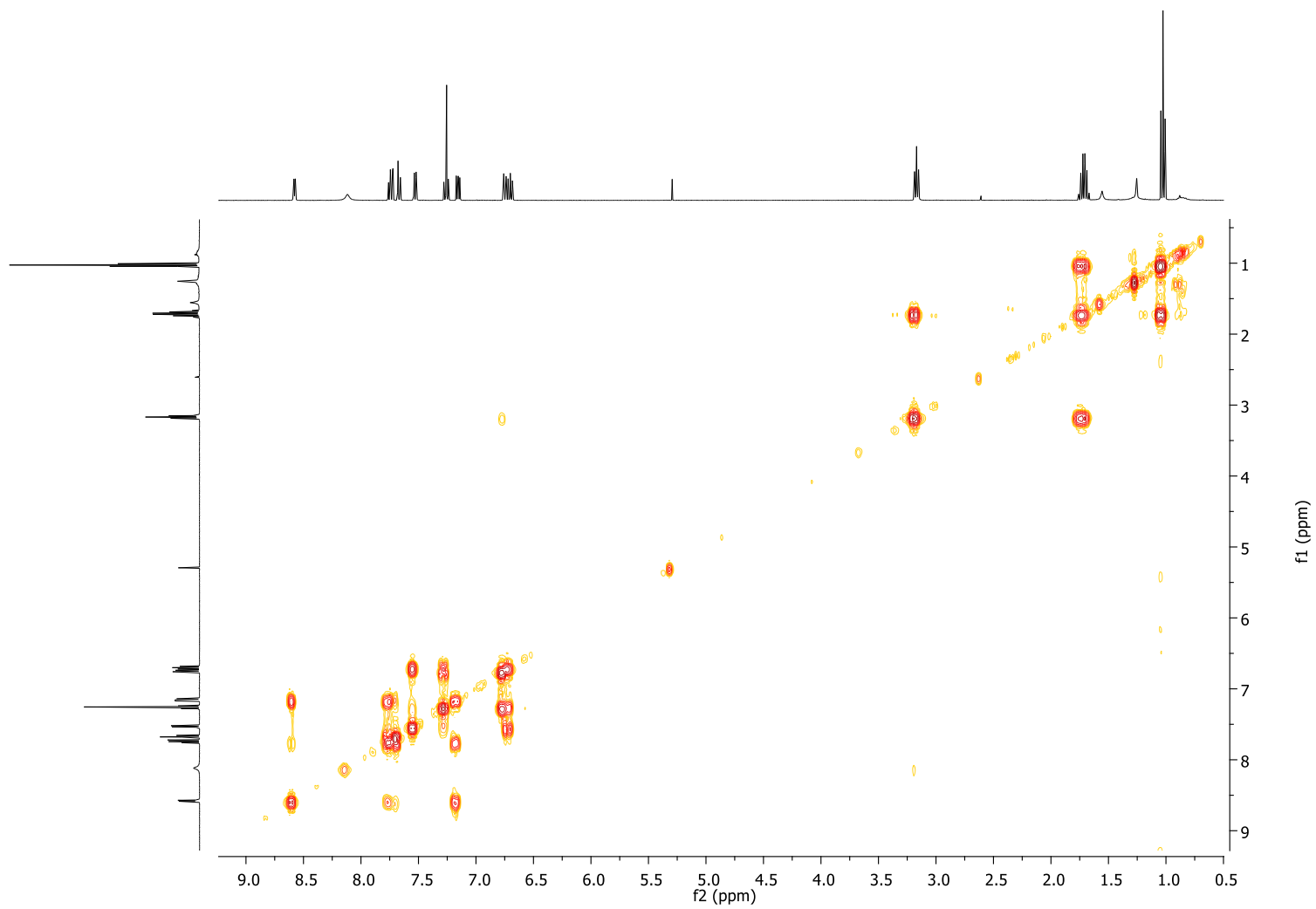


Selected aromatic region

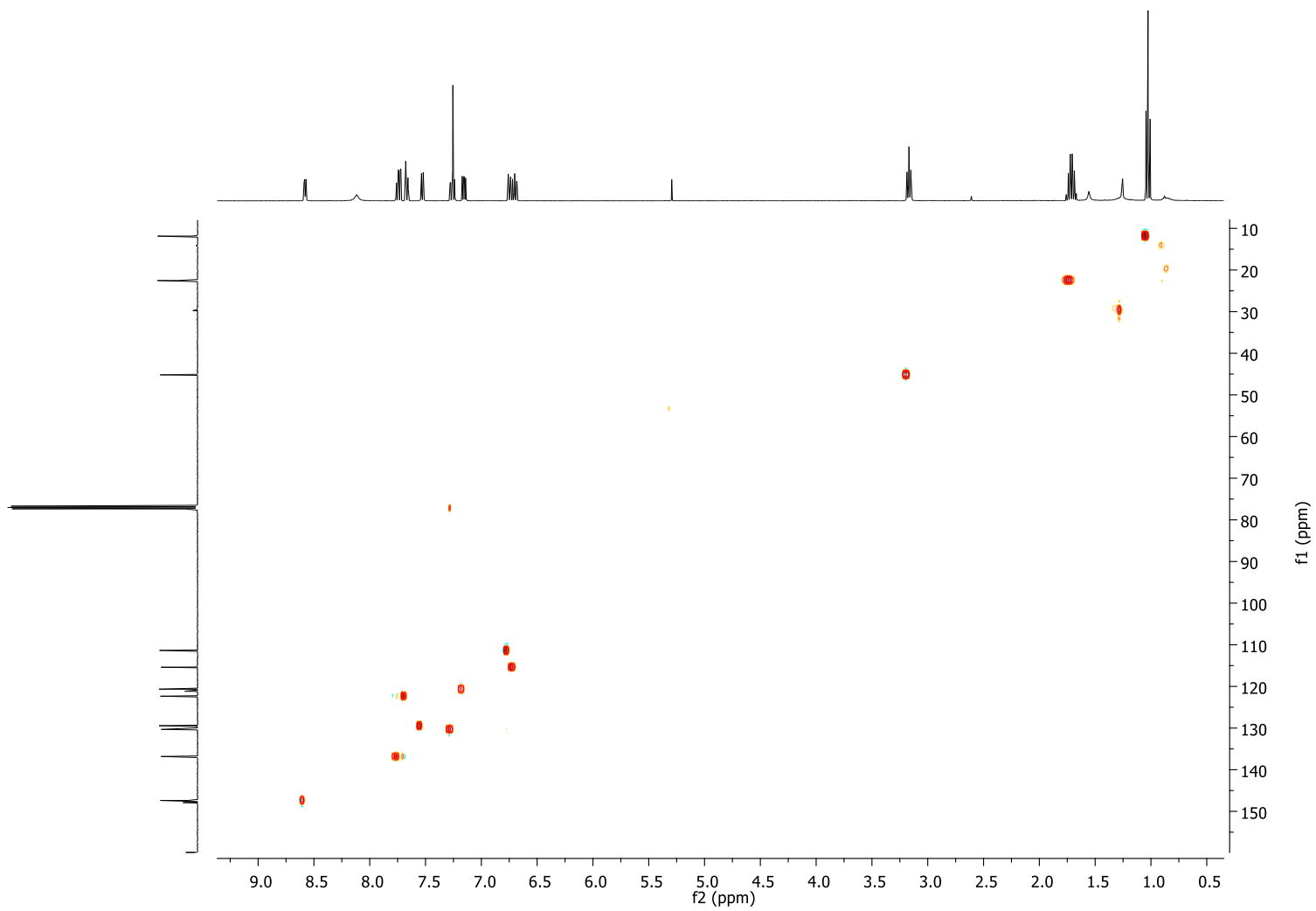
b)



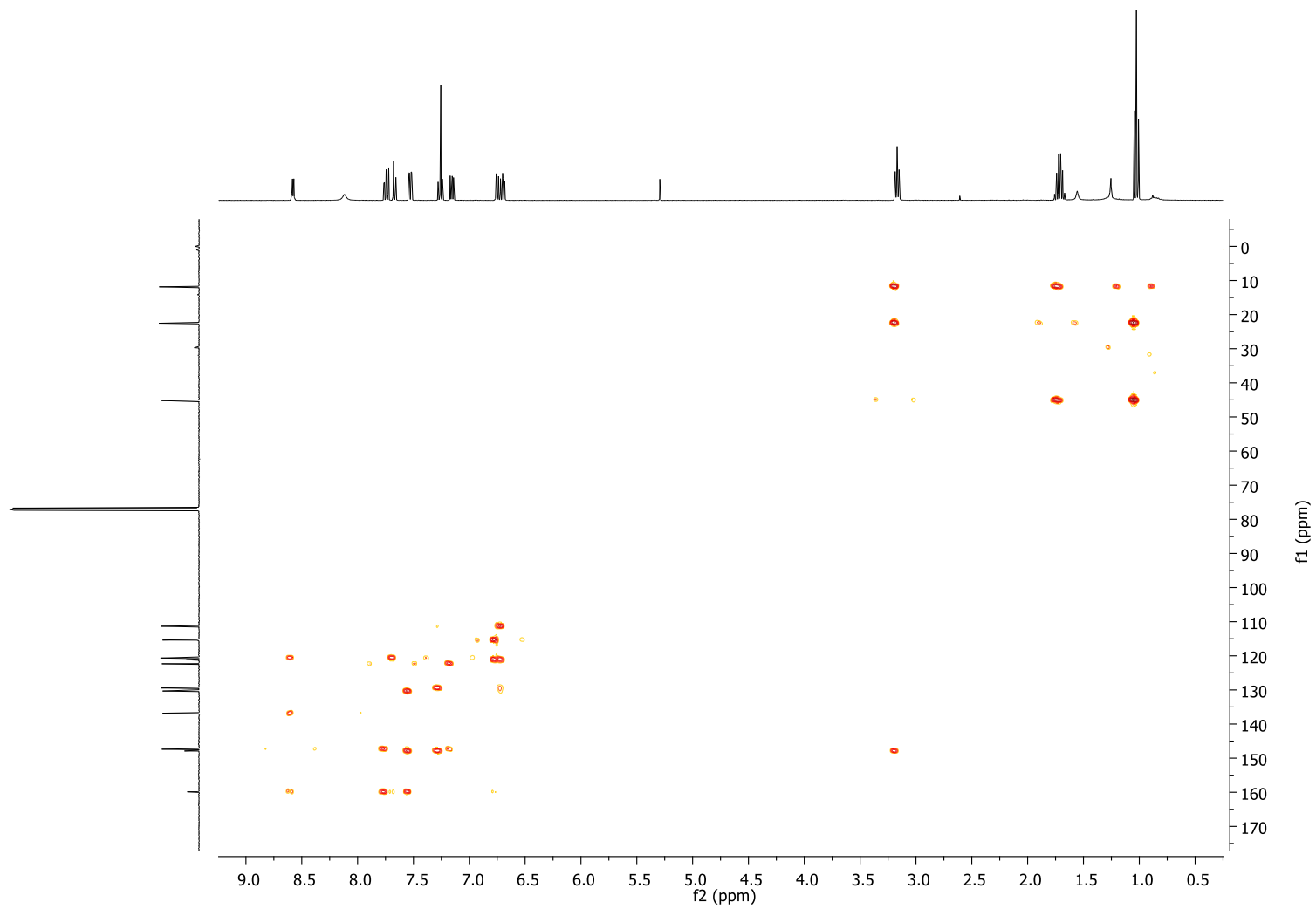
c)



d)



e)



f)

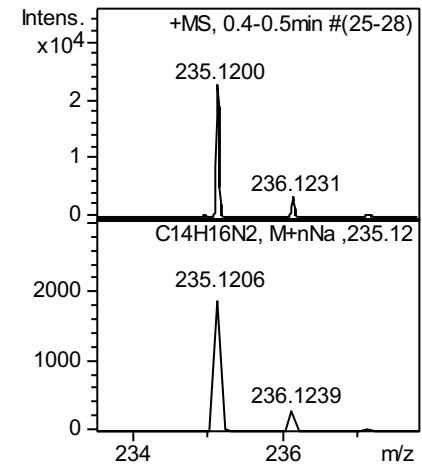
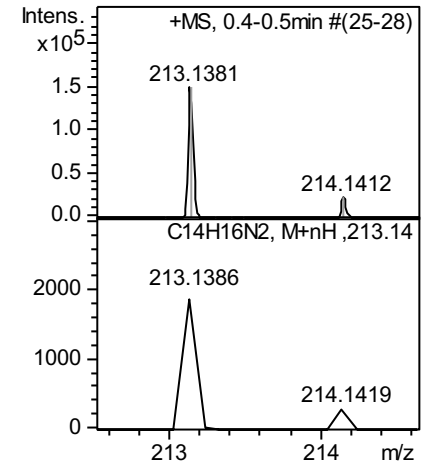
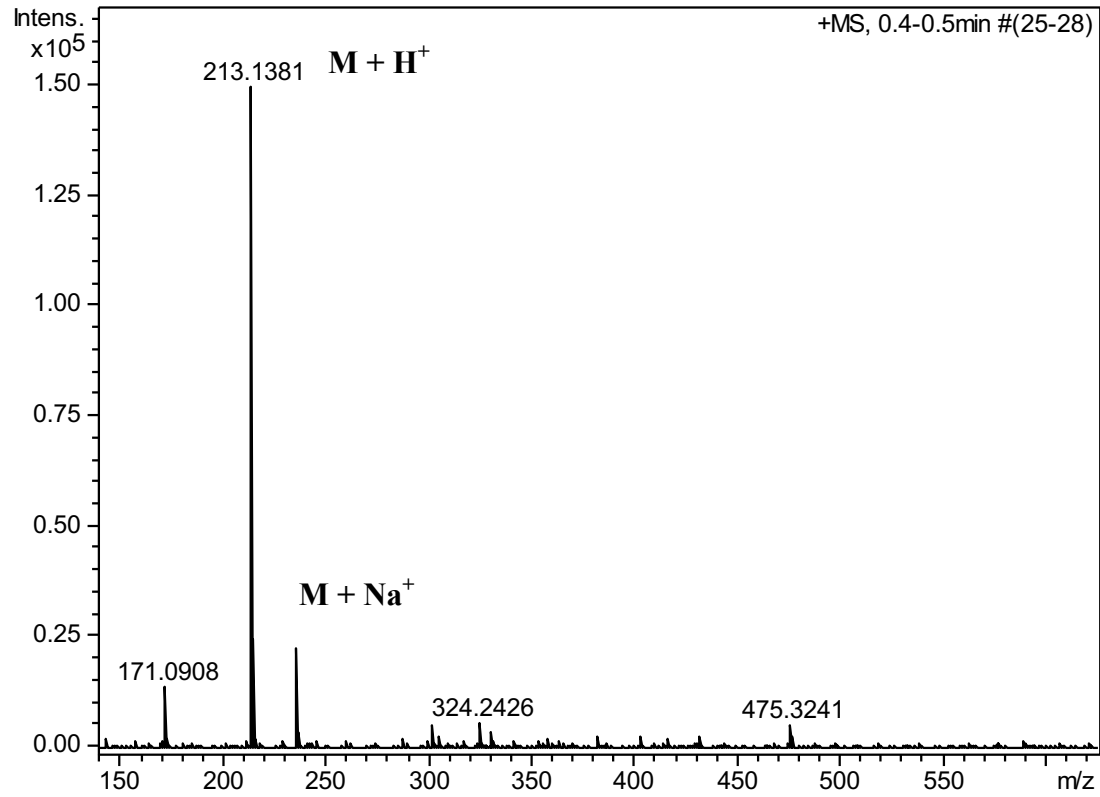
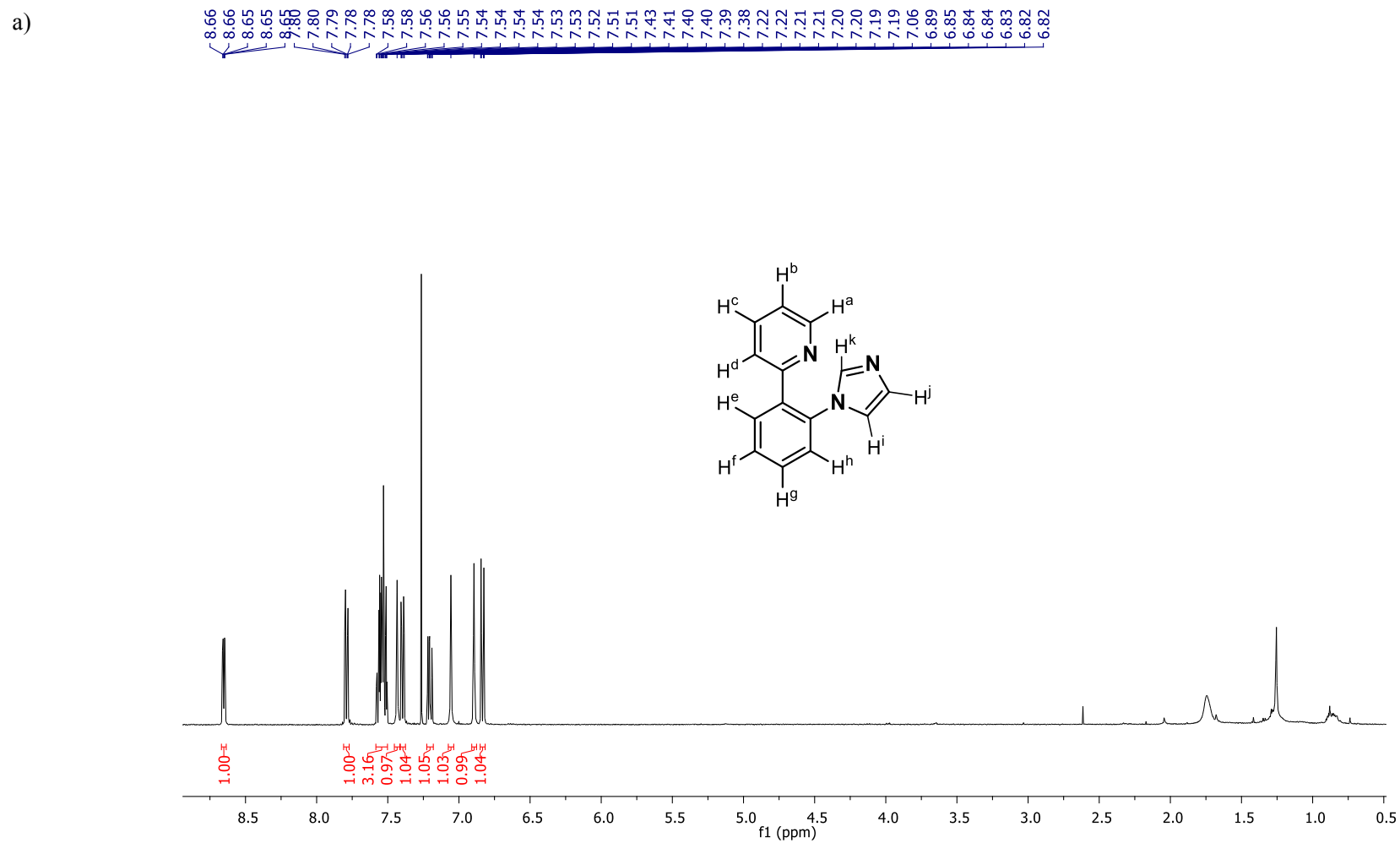
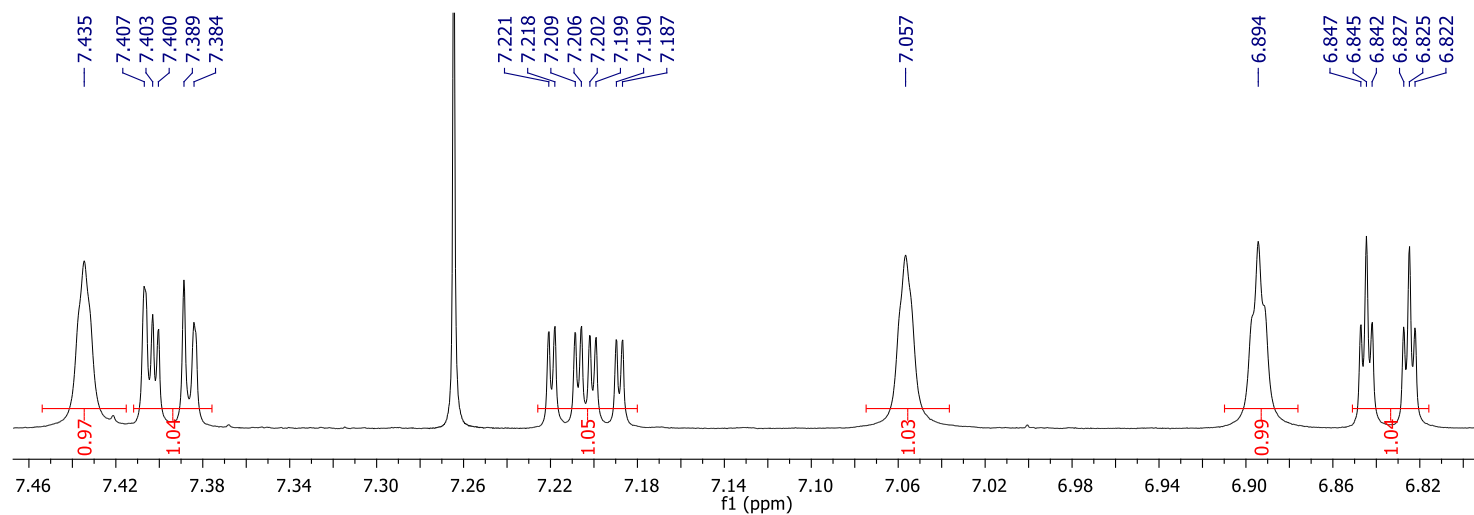
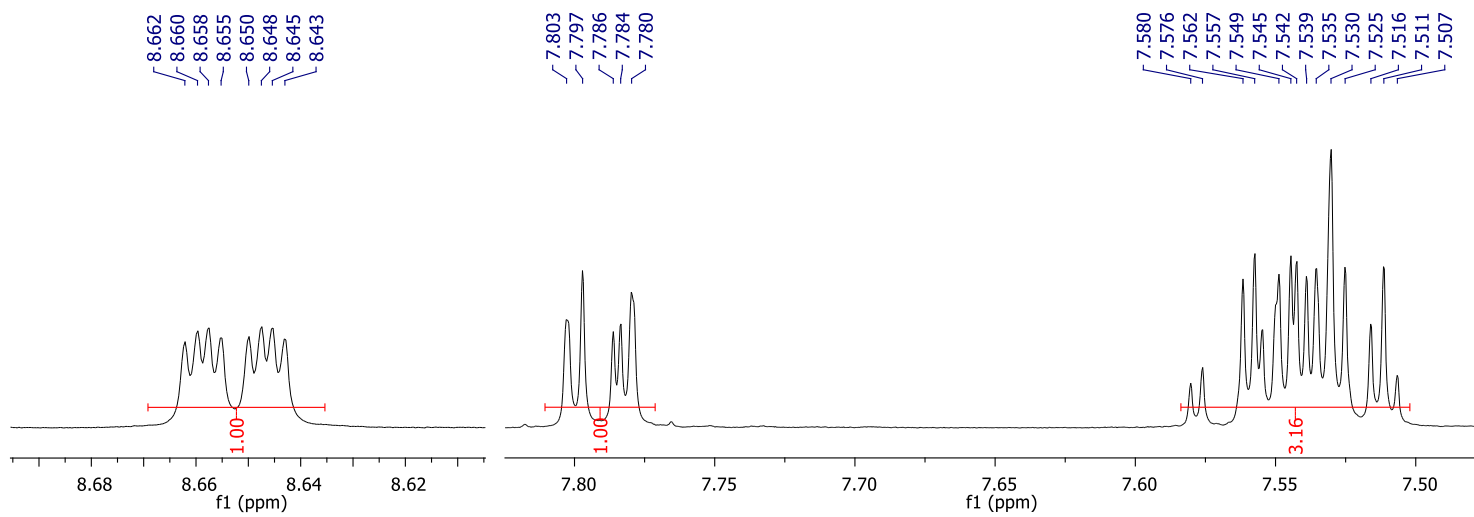


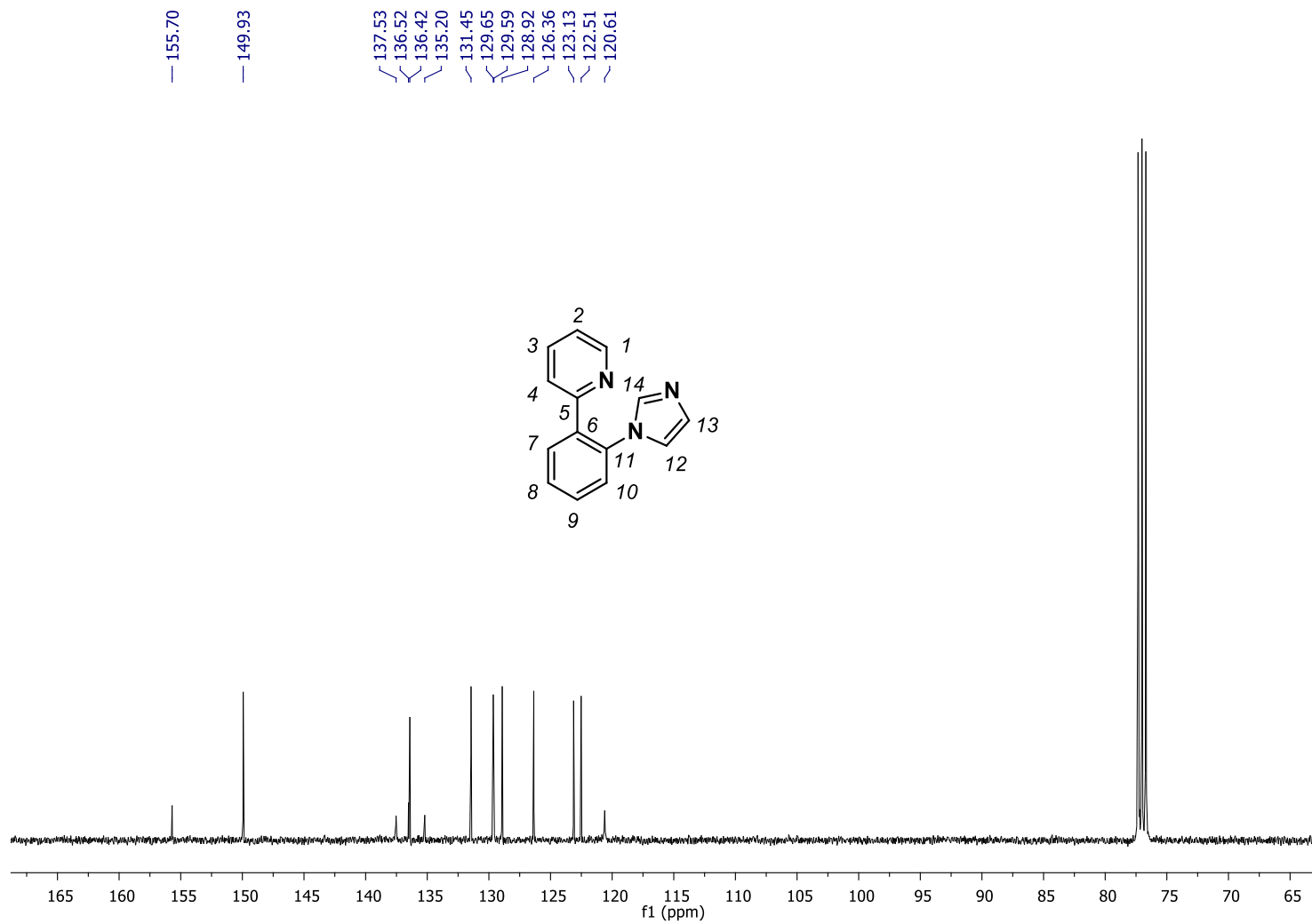
Figure S19. a) ^1H -NMR spectrum of compound **1am** in CDCl_3 , 400 MHz, at 298 K; b) $^{13}\text{C}\{^1\text{H}\}$ -NMR spectrum (CDCl_3 , 100 MHz, 298 K); c) ^1H - ^1H COSY spectrum (CDCl_3 , 100 MHz, 298 K); d) ^1H - ^{13}C HSQCed spectrum (CDCl_3 , 400 MHz, 298 K); e) ^1H - ^{13}C HMBC spectrum (CDCl_3 , 400 MHz, 298 K); f) HRMS (ESI-MS) spectrum (m/z). Observed HRMS (left) with the theoretical isotope prediction (right).



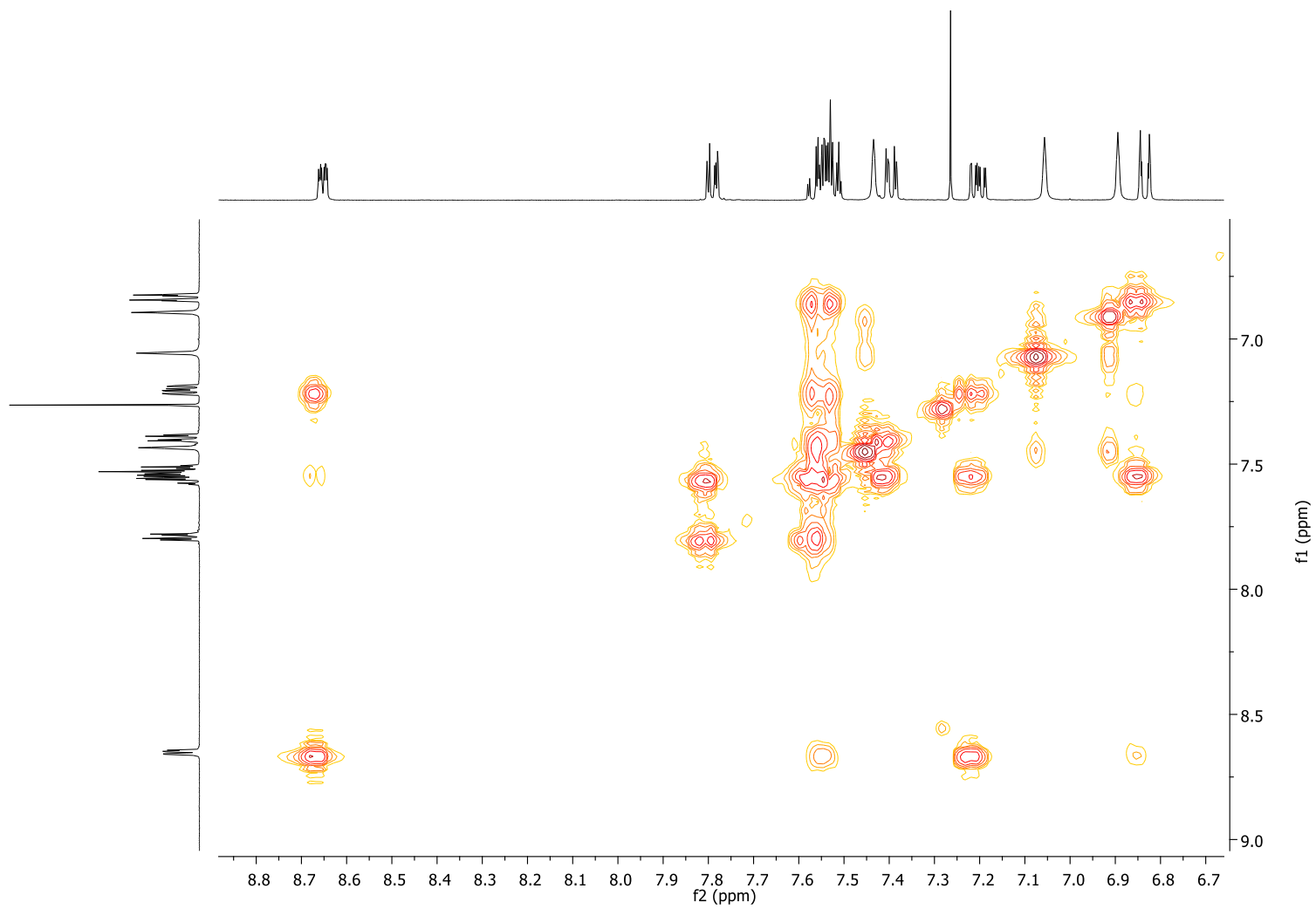


Selected aromatic region

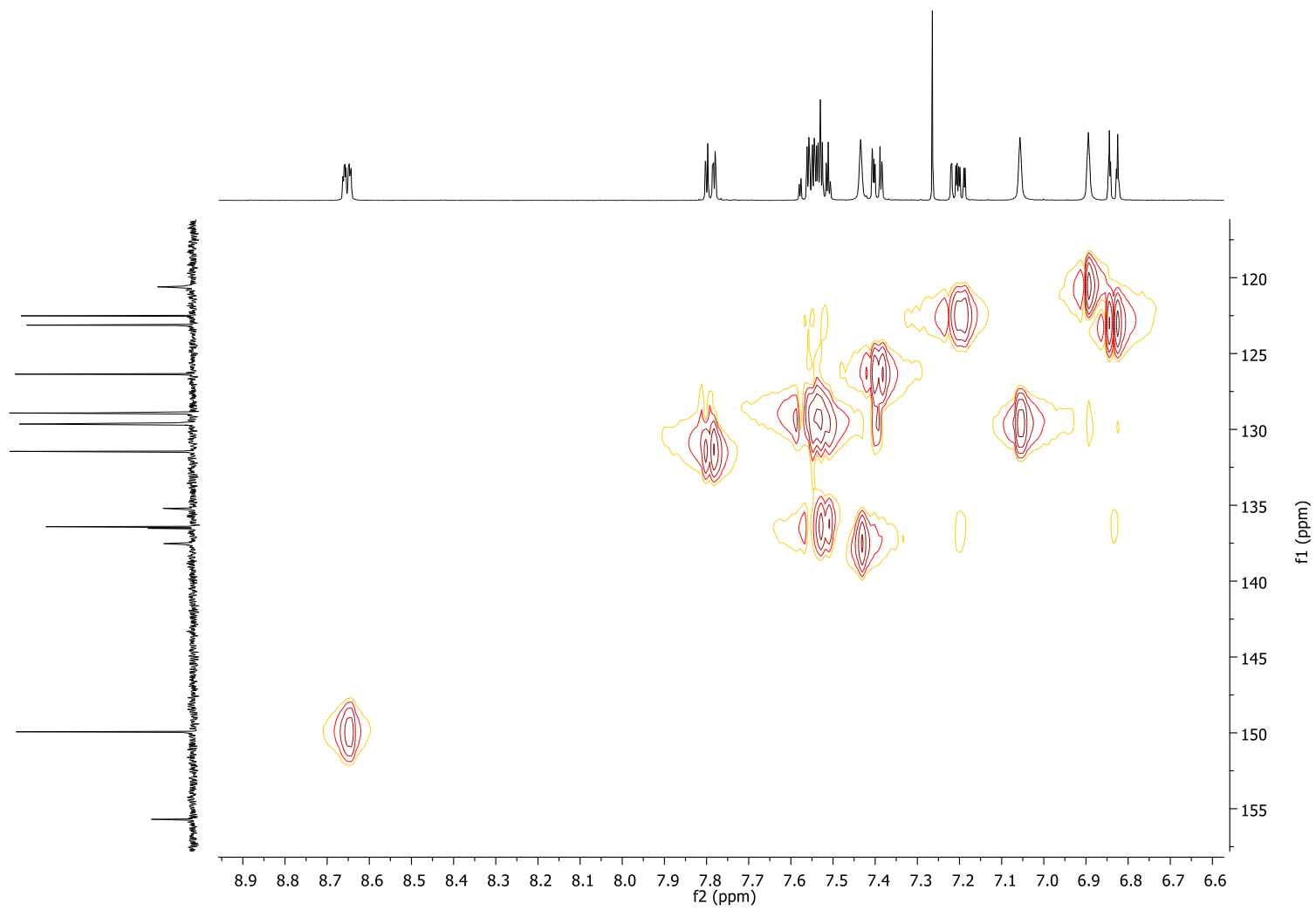
b)



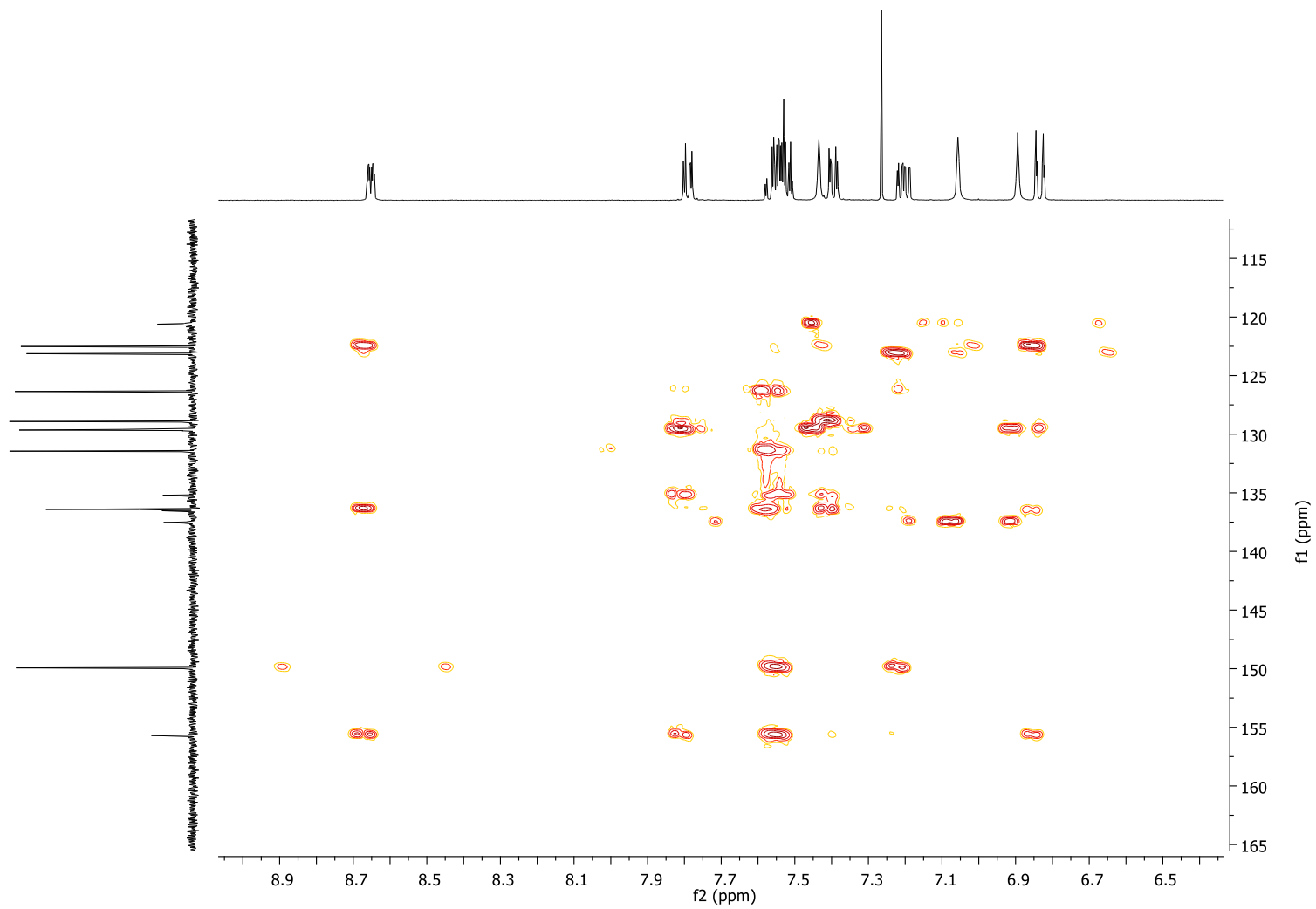
c)



d)



e)



f)

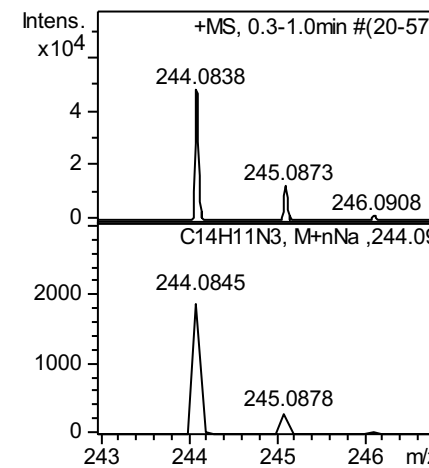
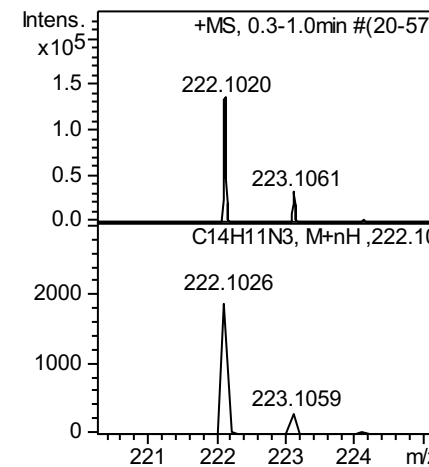
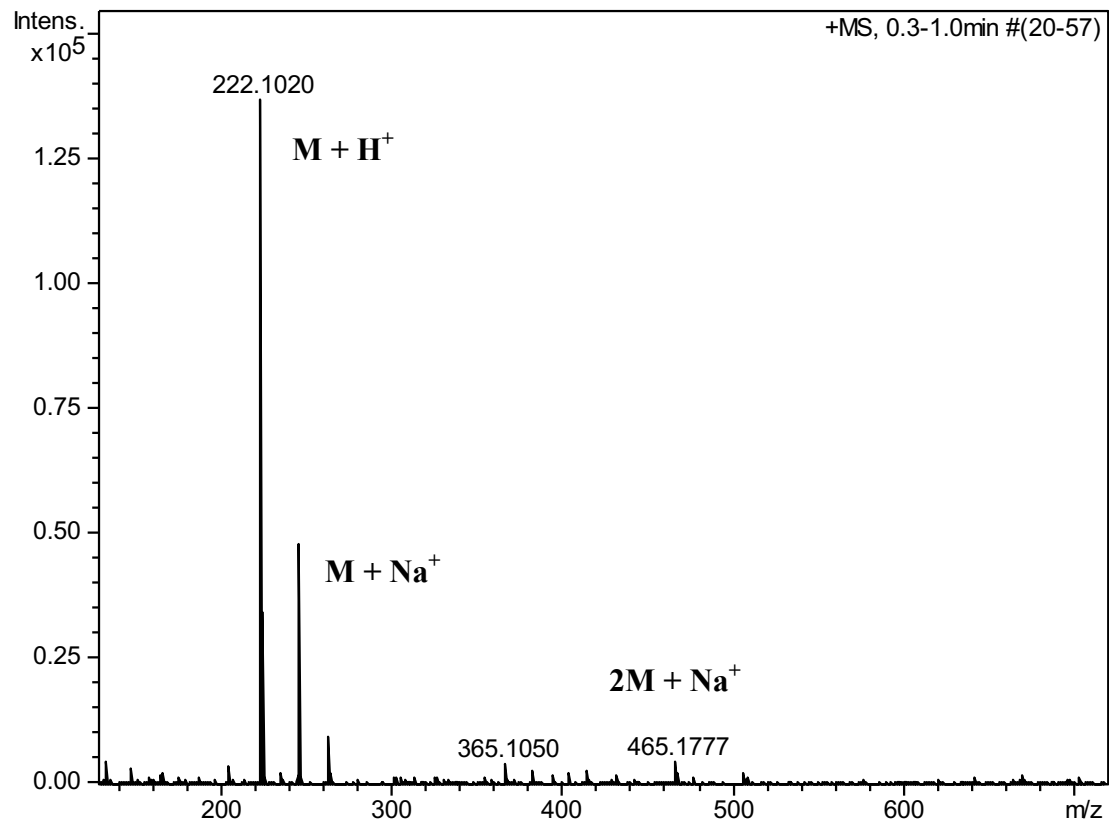
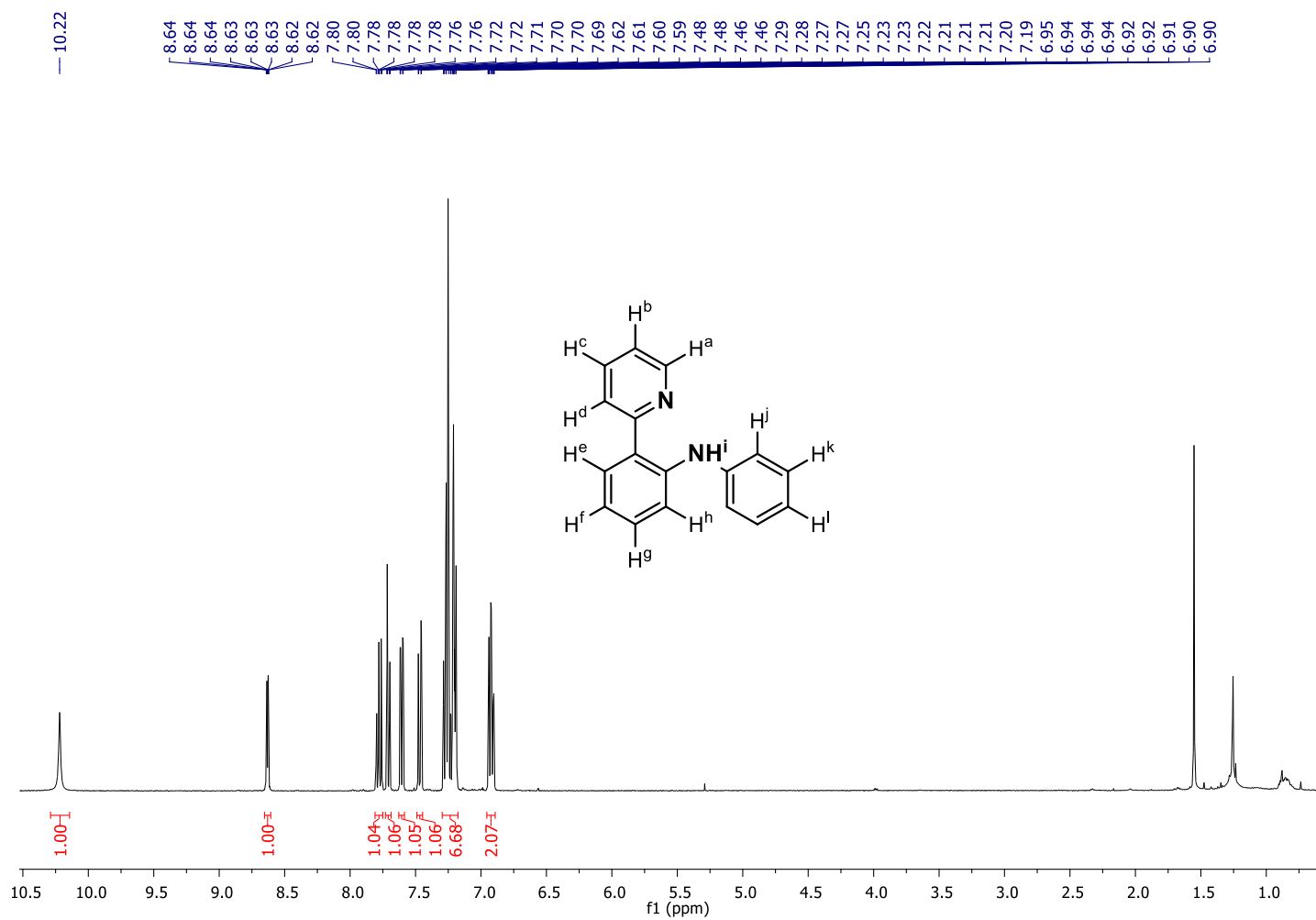


Figure S20. a) $^1\text{H-NMR}$ spectrum of compound **1an** in CDCl_3 , 400 MHz, at 298 K; b) HRMS (ESI-MS) spectrum (m/z). Observed HRMS (left) with the theoretical isotope prediction (right).

a)



b)

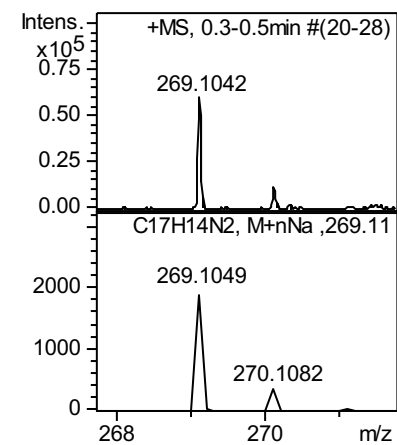
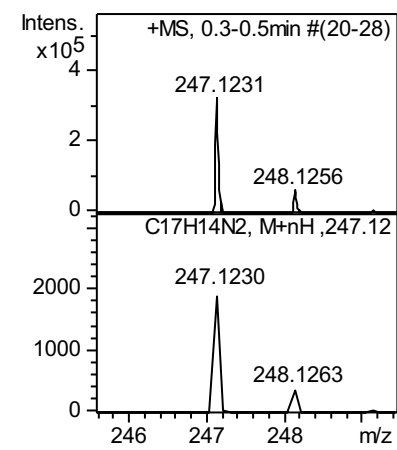
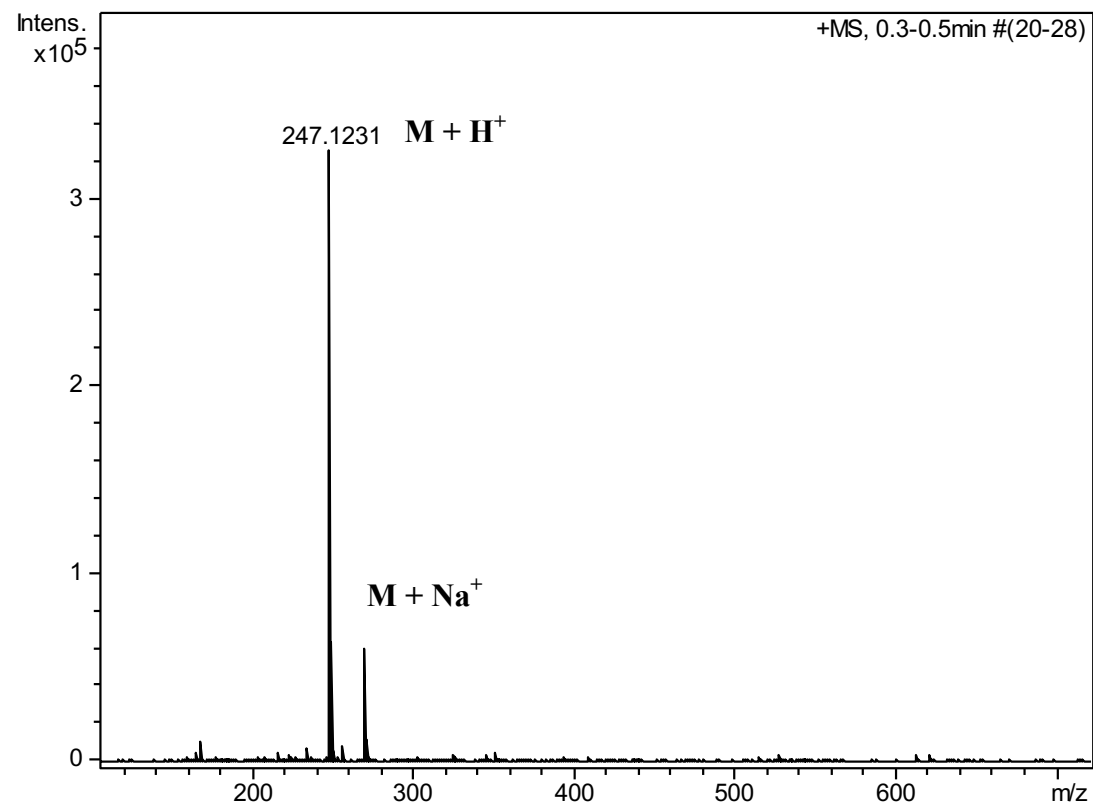
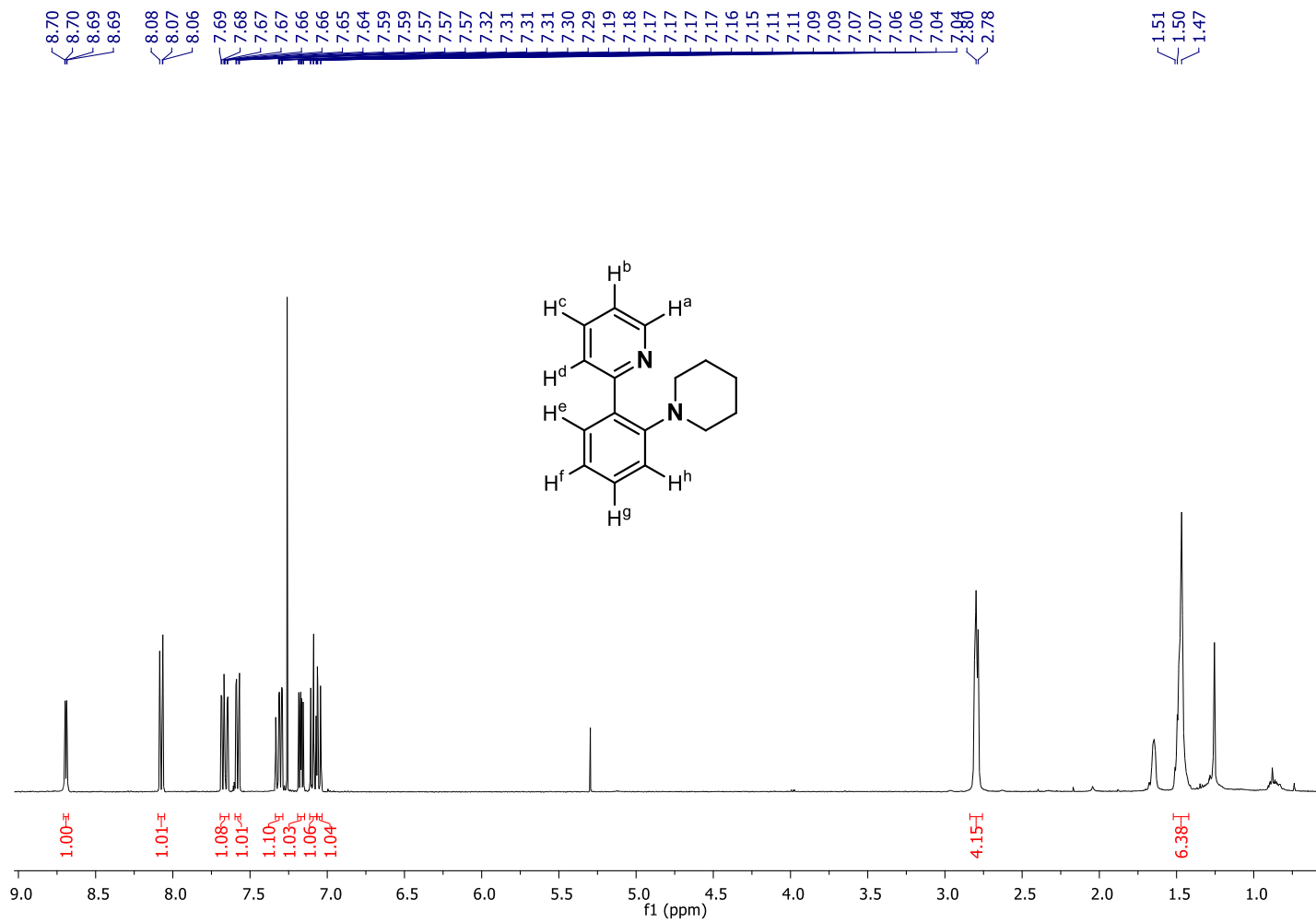


Figure S21. a) ^1H -NMR spectrum of compound **1ap** in CDCl_3 , 400 MHz, at 298 K; b) HRMS (ESI-MS) spectrum (m/z). Observed HRMS (left) with the theoretical isotope prediction (right).

a)



b)

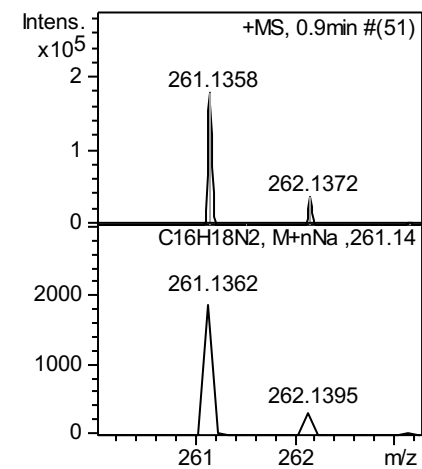
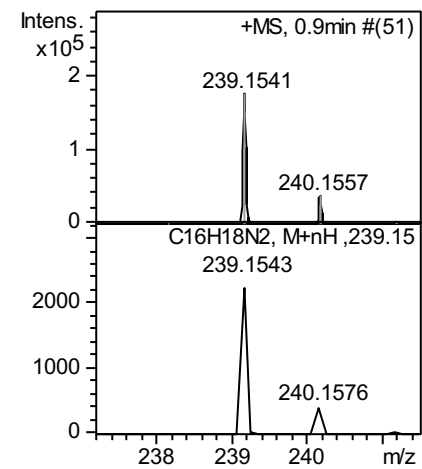
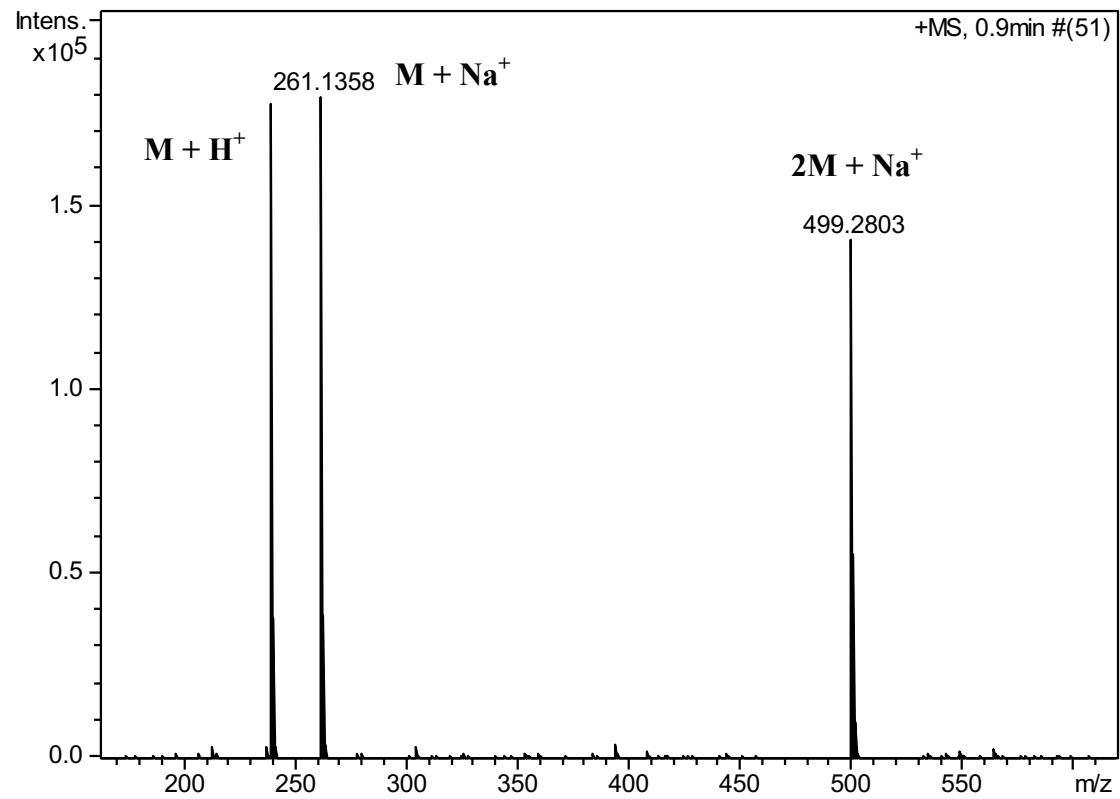
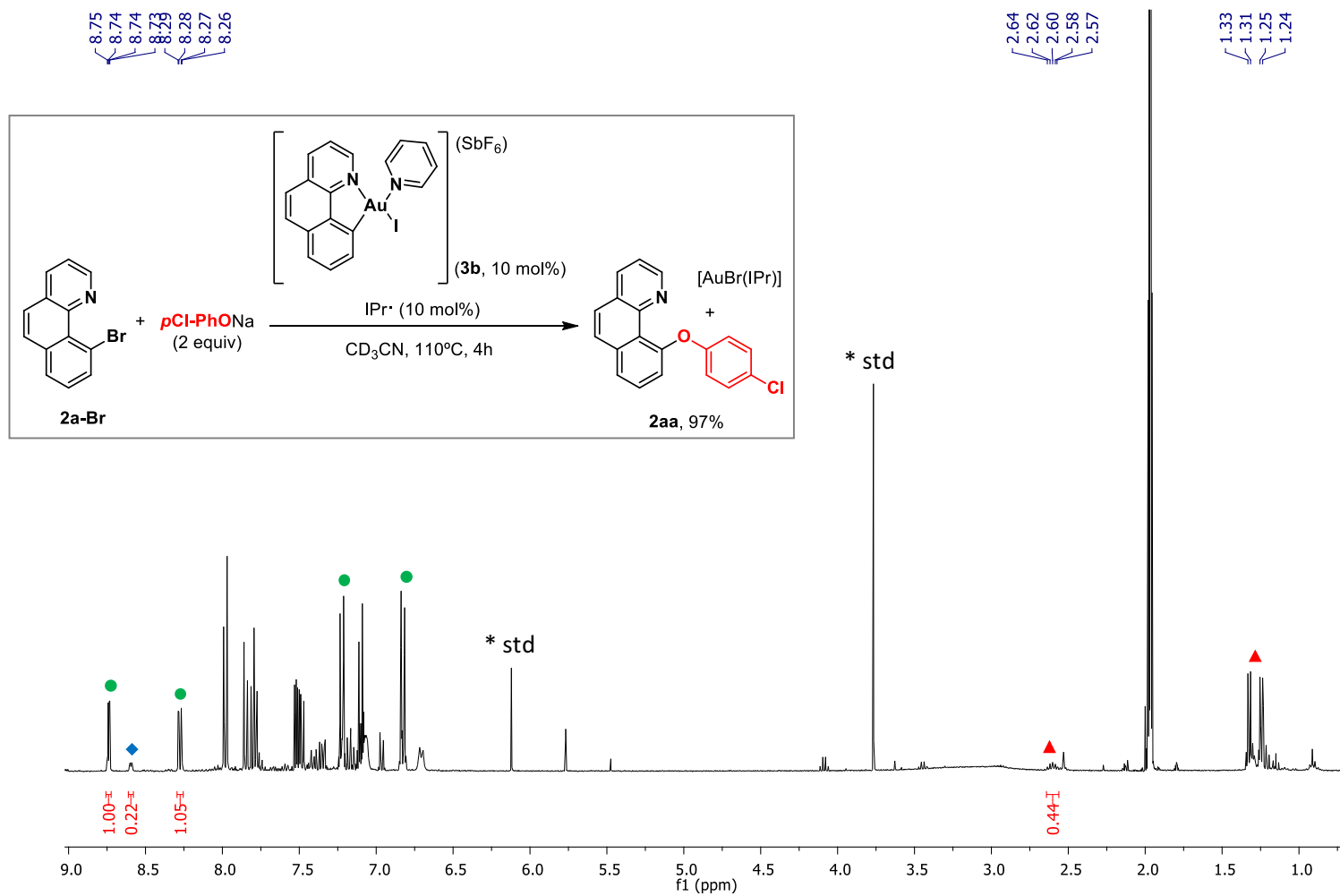


Figure S22. a) $^1\text{H-NMR}$ spectrum (CD_3CN , 298K) of the reaction crude of quantitative *p*-chlorophenolate insertion to **2a-Br** to form **2aa** (●) catalyzed by **3b**, followed by formation of $[\text{Au}(\text{Br})\text{IPr}]$ (▲) and liberation of the pyridine moiety (◆).



3. X-ray crystallography data

Crystallographic data for compound **1ah** (CCDC-1489676) and complexes **3a** (CCDC-1489681) and **3b** (CCDC-1489682) can be obtained free of charge from the Cambridge Crystallographic Data Centre (CCDC) via www.ccdc.cam.ac.uk/data_request/cif.

X-Ray structure of **1ah**:

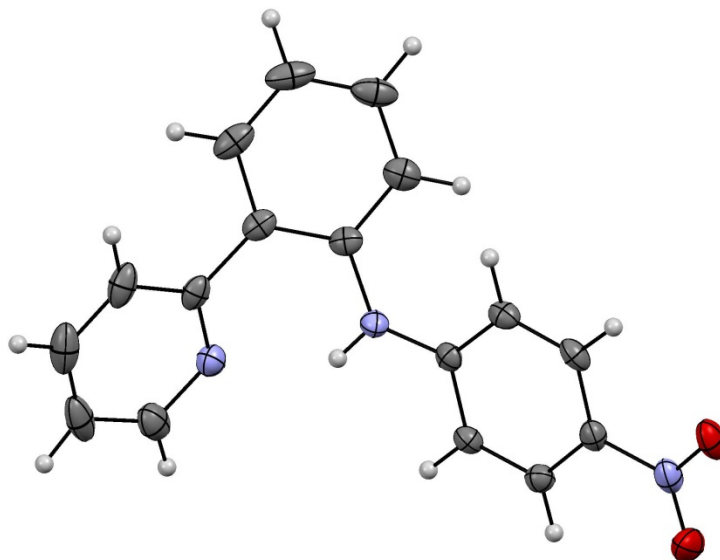


Figure S23. X-Ray structure of compound **1ah** obtained by crystallization from CHCl_3 . Ellipsoids are set at 50% probability.

Yellow crystals were grown from slow evaporation of a CHCl_3 solution of the compound, and used for low temperature (100(2) K) X-ray structure determination. The measurement was carried out on a *BRUKER SMART APEX CCD* diffractometer using graphite-monochromated $\text{Mo } K\alpha$ radiation ($\lambda = 0.71073 \text{ \AA}$) from an x-Ray Tube. The measurements were made in the range 2.144 to 28.317° for θ . Full-sphere data collection was carried out with ω and φ scans. A total of 20282 reflections were collected of which 3428 [$R(\text{int}) = 0.0312$] were unique. Programs used: data collection, *Smart*^[11]; data reduction, *Saint+*^[12]; absorption correction, *SADABS*^[13]. Structure solution and refinement was done using *SHELXTL*^[14].

The structure was solved by direct methods and refined by full-matrix least-squares methods on F^2 . The non-hydrogen atoms were refined anisotropically. The H-atoms were placed in geometrically optimized positions and refined without constraints or restraints.

Chemical formula	C ₁₇ H ₁₃ N ₃ O ₂
fw (g mol⁻¹)	291.30
T (K)	100(2)
Space group	Orthorhombic, P 21/c
a (Å)	13.283(2)
b (Å)	13.585(2)
c (Å)	7.6811(13)
α (deg.)	90
β (deg.)	90
γ (deg.)	90
V (Å³)	1386.0(4)
ρ_{calcd.} (g cm⁻³)	1.396
λ (Å)	0.71073
R₁ [I>2σ(I)]	0.0380
wR₂ [I>2σ(I)]	0.0873

X-Ray structure of 3a:

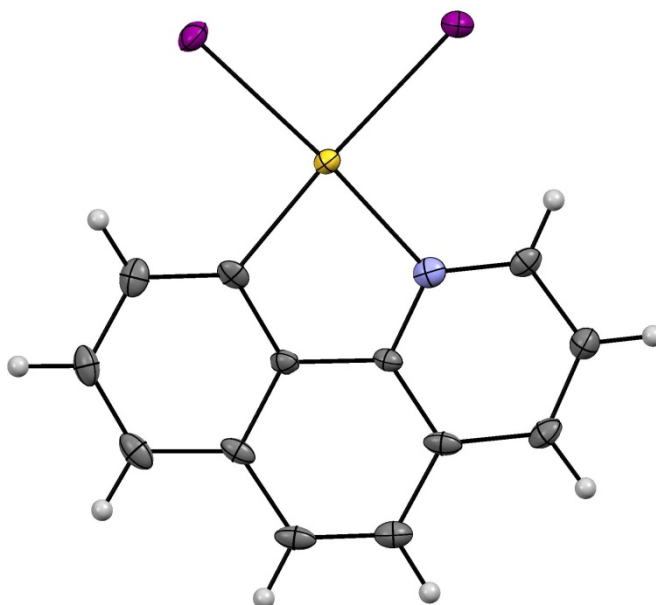


Figure S24. X-Ray structure of compound **3a** obtained by crystallization from CH₂Cl₂. Ellipsoids are set at 50% probability.

Red crystals were grown from CH₂Cl₂, and used for low temperature (100(2) K) X-ray structure determination. The measurement was carried out on a *BRUKER SMART APEX CCD* diffractometer using graphite-monochromated Mo *K*α radiation (λ = 0.71073 Å) from an x-Ray Tube. The measurements were made in the range 2.171 to 28.295° for θ. Full-sphere data collection was carried out with ω and φ scans. A total of 19253 reflections were collected of which 3202 [R(int) = 0.0647] were unique. Programs used: data collection, Smart^[11]; data

reduction, Saint+^[12]; absorption correction, SADABS^[13]. Structure solution and refinement was done using SHELXTL^[14].

The structure was solved by direct methods and refined by full-matrix least-squares methods on F^2 . The non-hydrogen atoms were refined anisotropically. The H-atoms were placed in geometrically optimized positions and forced to ride on the atom to which they are attached.

Chemical formula	C ₁₃ H ₈ AuI ₂ N
fw (g mol⁻¹)	628.97
T (K)	100(2)
Space group	Monoclinic, P 21/c
a (Å)	10.4599(18)
b (Å)	13.687(2)
c (Å)	10.1110(17)
α (deg.)	90
β (deg.)	116.270(3)
γ (deg.)	90
V (Å³)	1298.1(4)
ρ_{calcd.} (g cm⁻³)	3.218
λ (Å)	0.71073
R₁ [I > 2σ(I)]	0.0341
wR₂ [I > 2σ(I)]	0.0849

X-Ray structure of 3b:

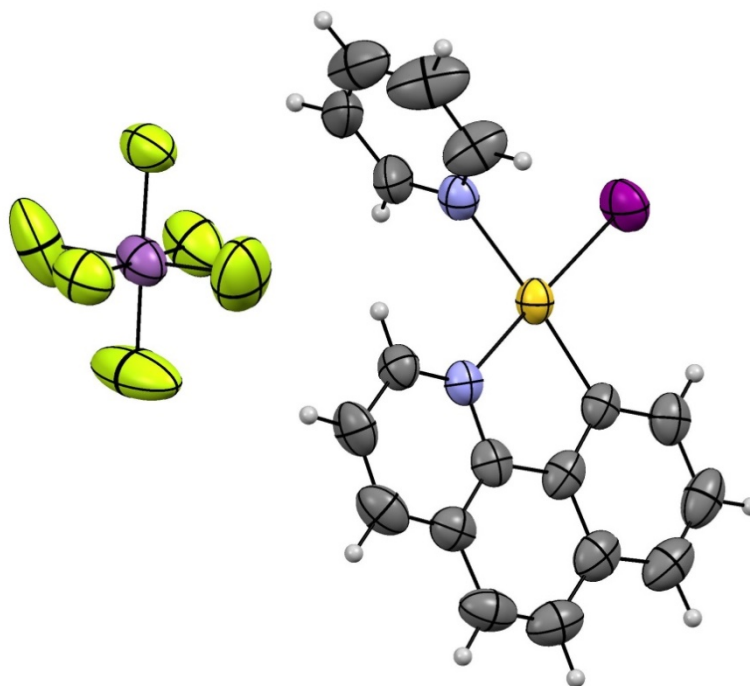


Figure S25. X-Ray structure of compound **3b** obtained by crystallization from CH₃CN and diethyl ether. Ellipsoids are set at 50% probability.

Orange crystals were grown from slow diffusion of diethyl ether in a CH₃CN solution of the compound, and used for low temperature (100(2) K) X-ray structure determination. The measurement was carried out on a *BRUKER SMART APEX CCD* diffractometer using graphite-monochromated Mo *K*α radiation ($\lambda = 0.71073 \text{ \AA}$) from an x-Ray Tube. The measurements were made in the range 2.07 to 28.58° for θ . Full-sphere data collection was carried out with ω and φ scans. A total of 62991 reflections were collected of which 10037 [R(int) = 0.0686] were unique. Programs used: data collection, Smart^[11]; data reduction, Saint+^[12]; absorption correction, SADABS^[13]. Structure solution and refinement was done using SHELXTL^[14].

The structure was solved by direct methods and refined by full-matrix least-squares methods on F^2 . The non-hydrogen atoms were refined anisotropically. The H-atoms were placed in geometrically optimized positions and forced to ride on the atom to which they are attached.

Chemical formula	C ₁₈ H ₁₃ AuIN ₂ F ₆ Sb
fw (g mol⁻¹)	816.92
T (K)	100(2)
Space group	Monoclinic, P 21/c
<i>a</i> (Å)	14.260(9)
<i>b</i> (Å)	20.667(13)
<i>c</i> (Å)	14.033(9)
α (deg.)	90
β (deg.)	104.38(1)
γ (deg.)	90
<i>V</i> (Å³)	4006(4)
$\rho_{\text{calcd.}}$ (g cm⁻³)	2.709
λ (Å)	0.71073
R₁ [I > 2σ(I)]	0.0598
wR₂ [I > 2σ(I)]	0.1587

4. References

- [1] P. de Frémont, N. Marion, S. P. Nolan, *J. Organomet. Chem.*, **2009**, 694, 551.
- [2] X. Mu, H. Zhang, P. Chen, G. Liu, *Chem. Sci.*, **2014**, 5, 275.
- [3] A. Klapars, S. L. Buchwald, *J. Am. Chem. Soc.*, **2002**, 124, 14844.
- [4] J. Serra, C. Whiteoak, F. Acuña-Parés, M. Font, J. M. Luis, J. Lloret-Fillol, X. Ribas, *J. Am. Chem. Soc.*, **2015**, 137, 13389.
- [5] A. R. Dick, K. L. Hull, M. S. Sanford, *J. Am. Chem. Soc.*, **2004**, 126, 2300.
- [6] J. I. Juncosa Jr., M. Hansen, L. A. Bonner, J. P. Cueva, R. Maglathlin, J. D. McCorvy, D. Marona-Lewicka, M. A. Lill, D. E. Nichols, *ACS Chem. Neurosci.*, **2013**, 4, 96.
- [7] T. Vogler, A. Studer, *Org. Lett.*, **2008**, 10, 129.
- [8] X. Chen, X.-S. Hao, C. E. Goodhue, J.-Q. Yu, *J. Am. Chem.*, **2006**, 128, 6790.
- [9] M. A. Ali, X. Yao, G. Li, H. Lu, *Org. Lett.*, **2016**, 18, 1386.
- [10] S. Thapa, A. Kafle, S. K. Gurung, A. Montoya, P. Riedel, R. Giri, *Angew. Chem. Int. Ed.*, **2015**, 54, 8236.
- [11] Bruker Advanced X-ray Solutions. SMART: Version 5.631, **1997-2002**.
- [12] Bruker Advanced X-ray Solutions. SAINT+: Version 6.36A, **2001**.
- [13] G. M. Sheldrick, *Empirical Absorption Correction Program*, Universität Göttingen, **1996**, Bruker Advanced X-ray Solutions. SADABS Version 2.10, **2001**.
- [14] G. M. Sheldrick, *Program for Crystal Structure Refinement*, Universität Göttingen, **1997**, Bruker Advanced X-ray Solutions. SHELXTL Version 6.14, **2000-2003**. SHELXL-2013 (Sheldrick, **2013**).